PIEZOELECTRIC CRYSTAL ATMOSPHERIC POLLUTANT MONITORS: Detection and Determination of Organic Gases by GSC and GLC Coatings.

by

TONY ERNEST EDMONDS, M.Sc., D.I.C.

A thesis submitted for the degree of Doctor of Philosophy of the University of London.

OCTOBER, 1975.

Department of Chemistry,
Imperial College of Science and Technology,
South Kensington,
London, S.W.7.

ABSTRACT

The development of the quartz crystal microbalance and subsequent modification of this device as the piezo-electric detector, is reviewed and discussed, following a brief outline of current methods of organic air pollutant measurement. The fundamental equations relating change in frequency to added mass on the crystal surface are developed according to Lostis, Sauerbrey and Stockbridge. A complete analytical system is described based on 9.0 M Htz AT cut crystals operated in their fundamental mode in a flowing gas stream. The equipment used consists of: oscillating circuits and associated power supplies; a complete oxygen-free-nitrogen gas flow system; detector cell and coated crystal; digital counter for frequency output; digital/analogue converter for voltage readout. The operation of each part of the system is described in detail: equations are given relating detector response to analyte concentration, intrinsic coating parameters, extrinsic coating parameters and equipment parameters, for systems where an equilibrium concentration of vapour in the coating both has, and has not been established. Nine different coatings are used: tri-cresyl phosphate; "Carbowax 20M", silicone gum rubber; β-β-oxydipropionitrile; squalane; di-nonyl phthalate; "Pluronic L64"; ethylene glycol succinate; rubber solution. Seven vapours are determined: chloroform; ethylbenzene; ortho-xylene; acetone; hexane; cyclohexane; heptene. Detectors are

developed that can determine these liquids below their TLVs and methods of improving selectivity are postulated, and some tested experimentally. Application of the detector to air samples is attempted, and detector performance is discussed with reference to the requirements of an atmospheric pollution monitor. 13 tables, 60 figures and 126 references are provided.

ACKNOWLEDGEMENTS

I would like to thank: my supervisor, Professor T.S. West for his help and guidance throughout this work; my wife for her understanding and moral support; the Science Research Council for its financial assistance in the form of a two year maintenance grant.

The research work presented in this thesis was carried out in the Chemistry Department of The Imperial College of Science and Technology from September, 1973 to September, 1975. It is entirely original except where due reference is made. No part of this work previously has been submitted for any other degree.

"It is not truisms which science unveils. Rather, it is part of the greatness and the beauty of science that we can learn, through our own critical investigations, that the world is utterly different from what we ever imagined - until our imagination was fired by the refutation of our earlier theories."

Karl Popper, "The logic of scientific discovery", 1959.

CONTENTS

CHAPTER I AIR POLLUTION

1.1 DEFINITION, DESCRIPTION AND EFFECTS

The variable composition of the earth's atmosphere makes the term atmospheric pollution difficult to define. Attempts to utilize the concept of the presence of extraneous substances founder on the definition and characterization of "normal" atmospheric constituents. The appearance of substances in the atmosphere that injure or degrade the environment, might be another approach to the definition, but this narrower concept runs into problems when compounds are considered that are non-injurious at certain concentrations, but that can be toxic or damaging at others. A universal definition may not be found, and it might be preferable to define atmospheric pollution on a microcosmic scale. Thus, a definition of air pollution should be sought, within the context of a particular situation or geographic locality. Limiting the context of the definition should result in a more meaningful description of the problem. For example, in a city, air pollution may be defined as the presence of certain substances at or above certain toxic or damaging levels, since it is probable that the "normal" atmosphere contains a wide range of these substances at sub-toxic levels. A rural area would not be expected to contain these toxic substances as atmospheric constituents, hence, their very appearance in the atmosphere would be defined as a pollution episode.

The problem of air pollution has been recognised for a considerable time, in England, certainly since the thirteenth century. In 1661, John Evelyn[1] wrote a diatribe on the smoke and fumes derived principally from combustion sources in the City of London.

> "Whilste these (the chimnies of London) belching smoke forth their sooty jaws, the City of London resembles the face rather of Mount Etna ..... That pernicious smoke which ..... tarnishes the plate, gildings and furniture and corroding the very iron bars and hardest stones."

Evelyn described the effects of a pollution, which, although acceptable in earlier times, when men and industry were more disperse, became unbearable as technological advances encouraged increased centralization and urbanization, thus intensifying the local effects of air pollution. This increase in population and concomitant increase in urban population density continues to this day: by-product disposal becomes an increasing problem; the environment is less able to disperse and deactivate this pollution and now pollution effects are being felt on a global scale[2].

Two broad categories of pollution may be defined, associated with specific sources: (i) Combustion of fossil fuels for heat and stationary power sources; (ii) Automobile pollution. Other categories may also be defined: radioactive wastes from energy-producing reactors; toxic chemicals from industrial chemical works; odours from natural degradation of plant and animal matter.

These latter sources usually give rise to isolated localised effects, whereas the combustion and automobile sources cause sufficient number and density of local effects for a national problem to be recognized. Exceptionally, radioactive waste causes widescale problems, as a result of a deliberate release of radioactivity from a nuclear explosion, or accidentally from a disaster at a nuclear reactor, e.g. the "Windscale disaster" in England in the early 1950's. This type of pollution problem is under constant surveillance, and strenuous efforts are being made internationally to limit the number of atmospheric nuclear explosions. Thus, the major sources of pollution on a national basis are those concerned with combustion processes of one form or another.

Classical atmospheric pollution, of the type known for many years, and associated with major urbanized and industrial areas, is due to combustion of fuels for heat, either for domestic or industrial purposes, and stationary power sources. Typically the pollution consists of: gases, such as sulphur dioxide, sulphur trioxide, and the oxides of nitrogen; mists of sulphuric acid; fly ash, a mixture of particulate silica, alumina, iron oxides and carbon. Automobile pollution contributes to the atmosphere such chemicals as carbon monoxide, oxides of nitrogen, hydrocarbons, and particulates of lead compounds and carbon.

Classical smog is produced by the physical and chemical interactions between smoke, sulphur dioxide and fog. More recently a new type of smog has been recognized,

associated with automobile pollution. This smog is caused by photochemical reactions in irradiated pollution to produce noxious compounds such as ozone, peroxyacetyl nitrate, formaldehyde and acrolein.

Evelyn's [1] solution to the smoke and soot problem in the city of London was to dilute and disperse the fumes by the use of taller chimnies. In a situation of increasing industrial centralization and indeed, increasing industrialization this solution is useless: reliance on meteorological and topographical factors for pollution dispersal is an uncertain method. It is not uncommon for "inversions" to occur under certain conditions. An inversion is the presence of a layer of warm air over a layer of cool air; the former acts as a "cap" to the latter, effectively preventing thermal mixing and convection. This phenomenon may take place at any time during the day or night and particularly is associated with valleys or depressions. If no wind is blowing a stagnant volume of air is established, and pollution released into this volume will continue to accrete, thus producing extremely high local levels. Large volumes of static air are also associated with anticyclonic centres. Finally, even if the pollution is dispersed in the atmosphere, it is still chemically reactive, and may cause as much damage at a remote locale as it would have caused at its initial source.

The importance of measuring and controlling pollution is related to its damaging effects: were man and his environment to be left undamaged by pollution,

there would be much less investigation of the subject. Pollution encroaches on man and his environment in four major ways: aesthetic and physical degradation of his environment; damage to his food crops and plant life; damage to his domestic animals; damage to himself. Aesthetic degradation of the environment occurs when the air is pervaded by odours, buildings are blackened, visibility is reduced and plant life is destroyed. Physical destruction of the environment, which also reduces aesthetic qualities, takes place with the corrosion of metals, cracking of paints and synthetic rubbers and the weakening of synthetic and natural fibres. Much literature is available on atmospheric pollutant damage to plant life, since plants are most susceptible to toxic chemicals, due to their poorly developed excretory system. Classical pollutants such as sulphur dioxide, oxidants (e.g. ozone) and fluoride ions cause recognizable lesions in plant material, even at very low concentrations. Thus, economic losses of field and citrus crops have been reported in the U.S.A.[2] as a result of this type of pollution. Similarly, automobile pollution causes damage to plants, with recorded instances of ill-effects up to one hundred miles away from the source. Physical damage to man, as a consequence of air pollution is manifested in a number of ways: exacerbation of chronic disease such as bronchitis; increased susceptibility to bacterial infection; alteration of pulmonary structure, particularly in pulmonary emphysaema; a direct link in the etiology of lung cancer. More subtle effects are also observed, such

as the reduction of mental and physical qualities required for complex problem solving in the presence of sub-lethal levels of carbon monoxide.

1.2 CURRENT METHODS OF POLLUTION MEASUREMENT

The determination of air pollution may be divided into two phases, sampling and analysis: this division is common to many analytical processes. The division may seem spurious when applied to some of the on-site monitoring techniques in current use, but in these cases, the delay between the two processes is reduced to a minimal value. Formal methods of analysis frequently involve some time lag between the sampling stage and analysis of the sample. In terms of the assessment of the real pollution profile, systems where sampling and analysis occur simultaneously, or in very rapid succession, perform better than those systems where a more pronounced time lag occurs. One reason for this, is that the former can produce a more or less instantaneous value for the level of a pollutant, whereas the latter techniques can only produce a retrospective picture.

1.2.1 Sampling

Sampling systems may be of two major types; continuous or discrete. Both types may be associated with continuous on-site monitoring systems; the latter also is associated with measurement systems where a relatively long time lag intervenes between the two stages, sampling and analysis. Discrete sampling systems may be

subdivided further, depending on whether or not a pre-concentrative or pretreatment step is required to bring the sample within the analytical capabilities of the method.

The sampling procedure for air pollution can be a complex and difficult task. West[125] has emphasized this point, "in conclusion it appears that much of the effort that is put into pollution analysis by analytical chemists, may be wasted or vitiated by poor sampling at source". Hendrickson[3] has defined a number of parameters for consideration in the design of sampling systems: (i) Sample size; this requires a knowledge of the minimum pollution level, and the analytical range of the measurement method; (ii) Sampling rate; an optimum rate of sample uptake must be found to ensure efficient sampling; (iii) Sampling duration; this depends on the sampling rate and on the variation of pollution with time; (iv) Collection efficiency; although one hundred per cent efficiency is not required, a fairly high and reproducible efficiency must be attained, for reliable results; (v) Alteration of constituents, this may either occur as a result of the sampling procedure, or as an effect of storage of the sample.

Methods of sample collection are quite varied, grab sampling techniques being the most simple. These techniques usually employ a container of an inert material which is filled with the polluted air, either by drawing or pumping the sample into a flexible container, or by breaking open the seal on an evacuated bottle or flask.

Grab sampling is one hundred per cent efficient, but sample size is restricted. Larger samples may be collected by using some form of preconcentrative method, that accumulates the compound of interest, and passes all others. Adsorption techniques are extremely efficient representatives of this class of sampling technique. The pollutant of interest is adsorbed onto the surface of a highly porous solid, until all the available sites for adsorption are used up: analysis is carried out on the pollutant when it is expelled from the solid. Occasionally an indicator may be added to the adsorbate, and a quantitative analysis carried out in situ. Absorption is frequently used for collecting gases: a soluble component is dissolved in a liquid or hygroscopic solid. The sampling devices employing this method are specifically designed to provide maximum contact between absorbant and absorbate, e.g., impingers, fritted-glass scrubbers, countercurrent scrubbers and packed columns. Another preconcentrative technique is the cold trap, this may simply be a U-tube packed round with an ice/salt mixture ($-21^{\circ}C$), or a complex stainless steel apparatus operated at $-196^{\circ}C$ in liquid nitrogen. The advantage of a cold trap is that judicious alteration of the temperature can lead to a distillation of the various compounds in the liquid mixture, and a well-designed series of traps operating at a number of different temperatures can cause quite effective separation of pollutants. A disadvantage of the cold trap is that a certain amount of pollutant loss can occur, particularly when water is frozen out, since some compounds are carried down with the water.

1.2.2 Analysis

The analysis of organic gaseous pollutants in the atmosphere may proceed at a number of definitive levels. Total organic pollutant analysis was attempted in 1949 by Shephard et al.[4], using mass spectrometry, (MS). Atmospheric samples of 100 to 200 litres were collected in liquid-oxygen freeze-out traps: exhaust emission samples were collected by grab-sampling using two-litre evacuated glass bulbs. Rounds et al.[5] also employed mass spectrometry for car exhaust gases, and found good agreements with the results from alternative analytical methods for total hydrocarbons, but rather poorer results for the elucidation of the individual hydrocarbons. These results were similar to those obtained by Shephard. Infra red spectrometry (IR) has been applied to total hydrocarbon determination. Samples were usually collected by freeze-out techniques, then expanded into a 1 to 10 metre path length cell. Dispersive systems generally measured the transmittance of the sample at 3.45 μm for a variety of pollution sources. Problems occurred due to the lower response of methane and unsaturated hydrocarbons, when compared with saturated hydrocarbons, and often it was necessary to correct the transmittance at 3.45 μm after determination of these less sensitive constituents at other wavelengths. Non-dispersive infra red spectrometry (NDIR) employing hexane-sensitized cells has been used for the determination of total organics in automobile exhausts. This method has been adopted as a standard method by some states in the U.S.A. This type of system

responds to the amount of light absorbed by molecules whose absorption bands overlap with the n-hexane bands. The results are variable with respect to carbon atom. content, and are interfered with by carbon dioxide and water. A more uniform response can be obtained from this system, but the sensitivity is reduced. The application of the flame-ionization detector (FID) to gas chromatography (GC) systems was quickly followed by the use of this device as a non-specific organic compound detector. Andreatch and Feinland[6] demonstrated that the detector's response reached significant values for a wide range of compounds, and that the response was proportional to the number of carbon atoms in the sample. The operating conditions were shown to notably affect the sensitivity of the device, particularly for similar atoms bonded in different ways: the effects of interferents were also influenced by changes in operating conditions. Some problems were experienced with reduced sensitivity when carbon atoms were directly linked to hetero atoms, in some compounds. However, the detector displayed a rapid and sensitive response to many compounds, and had a large linear range. NDIR and the FID are the most useful of the current methods for total organic pollutant level determination.

The determination of specific groups of organic compounds may be achieved by a variety of analytical techniques, some of general application, others more specific. Each of the major groups of polluting organic compounds will be considered in turn.

Alkanes. In general these compounds have low to negligible reactivity, both in classical chemistry, and in the photochemistry of smog formation. The common methods of determining alkanes employ subtraction techniques: the reactive compounds are preferentially removed, and the residual unreactive compounds (assumed to be alkanes) are determined by MS, FID or GC. Thus, unwanted reactive hydrocarbons and oxygenated compound may be removed by passing the air through mercury perchlorate tubes. Alternatively freeze-traps may be employed, but these tend to give lower methane and ethane values. The best technique for alkane analysis is GC, where a large number of stationary phases are available to give good separation of alkanes, e.g., molecular sieves, silica gels, squalane. Subtractive techniques may be used before or after the column. Infra red spectrometry (IR) has limited value due to the large number of interferences; methane may be determined at 7.6 μm.

Alkenes. Alkenes are more reactive than their saturated counterparts, and contribute significantly to photochemical pollution. A number of spectrophotometric and titrimetric techniques are available for the determination of these compounds. Reaction of alkenes with phosphomolybdate species produces a compound that absorbs light at 680 nm. Prior to application of this test to atmospheric samples, the contaminated air is passed through ascarite to remove acidic gases, and then a liquid oxygen freeze-out trap. Care must be taken to eliminate carbon monoxide and hydrogen from the sample, since these are the main interferents. The product of

para-dimethylaminobenzaldehyde with alkenes absorbs at 500 nm, but this reaction is subject to interference from aromatic hydrocarbons, alcohols, aldehydes and phenols. Titrimetric and coulometric techniques have been developed around bromination-type reactions.

Instrumental techniques, such as MS and IR are not particularly favourable for the determination of alkenes; the former gives incomplete qualitative and quantitative analysis of alkenes; and the latter, although more useful, is insensitive without long path lengths, and can only identify ethylene as an individual hydrocarbon with any degree of accuracy. GC is a powerful technique, good separations are possible on single or multicolumn systems, with stationary phases such as "Carbowax 20M", β-β-oxydipropionitrile and dibutylmaleate. A FID is used as the system's detector, and small volumes (3-10 ml.) of the polluted air may be used.

Alkynes. A colorimetric test is available for the alkynes, in which ammoniacal cuprous chloride reagent gives red copper acetylide. Hydrogen sulphide is a major interferent, and instrumental methods are preferred. MS requires a freeze-trap prior to analysis to ensure adequate sensitivity: IR is applicable at 13.7 μm, but carbon dioxide interferes, particularly in the long path lengths (100 metres) required for atmospheric analysis. GC offers the most useful analyses, good separations are achieved of the alkynes from other atmospheric constituents, with stationary phases such as silica gel, "carbowax" and alumina.

Aromatic Compounds. The substituted benzenes, particularly the meta isomers, and tri-methyl benzene, are as reactive as the alkenes in photochemical smog formation. Generally these compounds are present in the atmosphere as a result of unburnt components of fuel, and alkyl benzenes with more than ten carbon atoms have been identified. Mainly instrumental methods are used to measure these compounds: IR has limited applications at 3 to 4 μm, but, again, GC with an FID is most useful. Compounds containing six to eleven carbon atoms can be determined in the 0.1 to 1 p.p.m. range, with no freeze-out or preconcentrative step.

Aliphatic Oxygen-Containing Compounds. Instrumental analyses are less well developed for this class of compounds, and wet-chemical techniques predominate: titrimetric and colorimetric procedures are both available for determination of total carbonyl compounds. One of these is the bisulphite addition procedure, in which excess bisulphite is reacted with the sample to form an addition complex between the bisulphite ion and carbonyl compound: residual bisulphite is destroyed, the addition complex broken down, and the bisulphite titrated. A colorimetric method measures the absorbance at 420 nm, due to the compound formed between carbonyls and 2-4 dinitrophenyl-hydrazine. Paper chromatography has been used to determine individual aldehydes and ketones.

IR and MS have not generally successfully been applied to oxygen-containing compounds, one major problem being the collection of these substances for instrumental

analysis, since they can be lost, either by solution in water, or by condensation in water in collecting traps. Organic acids are determined by titrimetry: IR is used for formic acid at 9.05 μm. Alcohols may be determined by MS, after a previous preconcentration procedure.

An oxygenated compound of extremely toxic nature is acrolein, which is formed in photochemical smogs. Polarography, GC and paper chromatography have been used to determine acrolein, but are not generally applied to atmospheric pollution. A sensitive and selective colorimetric method has been developed around a mixture of tryptophan, phlorogyl-ucinol and 4-hexylresorcinol.

Sulphur Compounds. The manufacture of sulphates and the commercial pulping process give rise to sulphur-containing air pollutants, such as: mercaptans; dimethyl sulphide; dimethyl disulphide. GC is used for the detection and determination of these compounds, but the lack of sensitivity of the method requires that prior preconcentration of the sample is carried out.

Halogenated Compounds. MS, GC and IR may all be used for the determination of chlorine-containing compounds in the air, but with poor sensitivity and selectivity. Neutron activation analysis has been attempted on chlorinated hydrocarbons sorbed onto charcoal. The electron capture detector (ECD) is both sensitive and selective for compounds such as trichloroethylene, tetrachloroethylene and carbon tetrachloride. Compounds such as sulphur hexafluoride, trifluoro-bromo methane,

and octafluoro-cyclobutane also are detected. The last two compounds are not normally present as air pollutants, but are often introduced as tracers for meteorological or pollution studies.

Aliphatic Nitrogen-Containing Compounds. Few techniques are available for these less-common pollutants: low molecular weight amines have been determined by MS following freeze-out; paper-chromatography and autoradiation have been used to determine carbon - fourteen labelled benzamides of methyl- and ethyl-amine.

An important pollutant class of nitrogen compounds that have been detected by IR in photochemical smogs, are the peroxyacyl nitrates. These compounds absorb at several IR wavelengths: 5.4, 7.7, 8.6 and 12.6 μm, the last two being most commonly used. GC with an ECD provides an analytical method for these compounds with sensitivities of 1 p.p.b.

1.2.3 Monitoring Systems

An important concept in air pollution is the threshold limit value (TLV). This is a concentration value of a pollutant that can be tolerated by humans during a working day, with no long or short term health effects: the TLV of a compound is determined from clinical data. This value represents a maximum level for the concentration of a given compound, and a pollution-time profile that exceeds this value at any point must be considered dangerous. As a result of this type of concept, there is an increasing need to continuously measure

pollution values, not only for the early detection of dangerous episodes so that remedial action may be taken, but also as a valuable contribution to the knowledge of pollutant distribution and movement, enabling more effective solutions to be applied to the problem of pollution disposal. These attitudes to air-pollution require measurement techniques that are capable of continuous on-site analysis which can rapidly produce accurate representations of the concentration/time profile of the pollutant. Thus, consider the pollution profile depicted in figure 1a. A technique for measuring the pollution that employs a discrete sampling step of fairly long duration will give a pollution/time profile of the type shown in figure 1b. In this figure, it has been assumed that a half-hour sample preconcentration is followed by relatively rapid analysis and data output. A consequence of this type of sampling in the monitoring system is that the peaks at 1 and 2 in figure 1a, where the pollutant concentration exceeds the TLV, are completely missed, i.e.: a time averaged histogram is produced rather than a true profile. In spite of this problem, monitoring systems have been constructed using preconcentrative sampling. Narain et al[7] have described the GC determination of air pollutants after preconcentration of the compounds of interest in a liquid oxygen cryogenic freeze-trap, through which was drawn fifty to one hundred litres of the contaminated air. Simmons[8] has described a mobile analytical system for the determination of organic solvents in factory atmospheres, which is another example of a discrete

FIGURE 1a

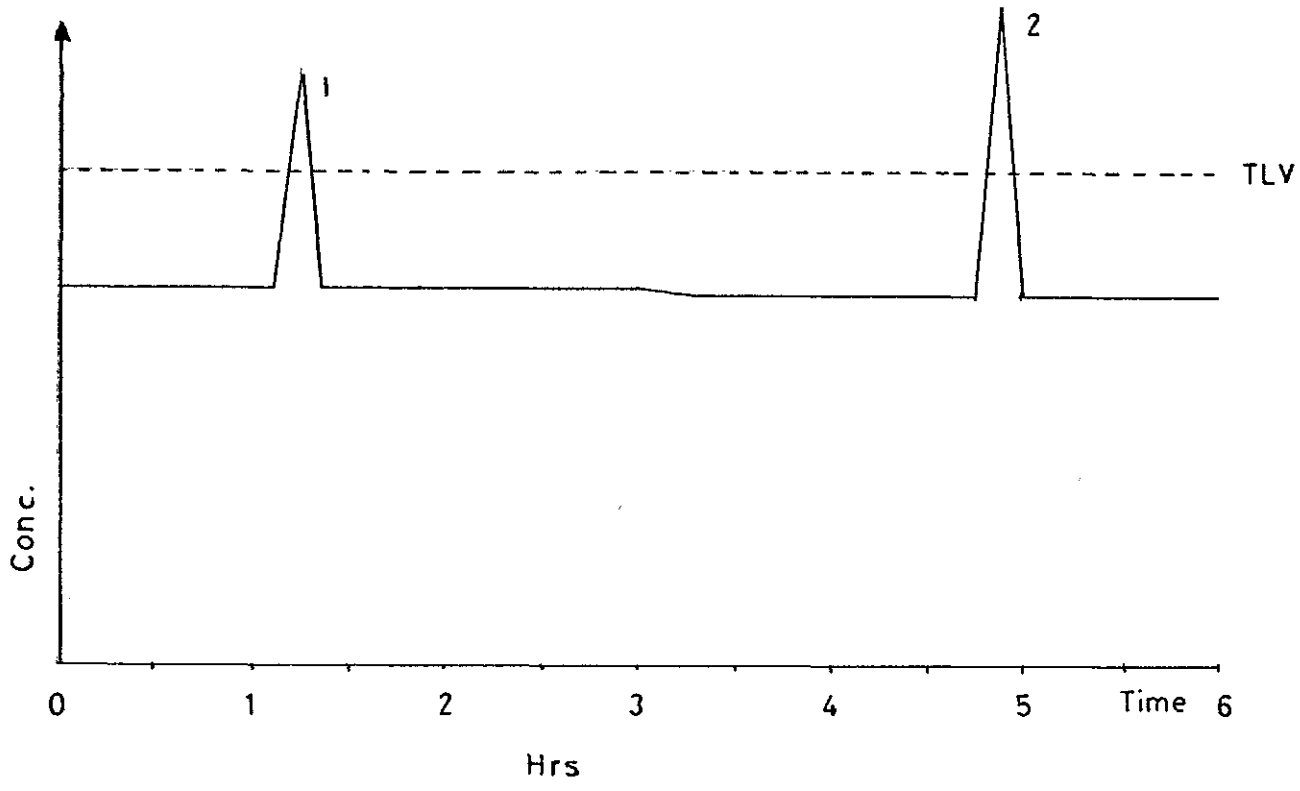

FIGURE 1b

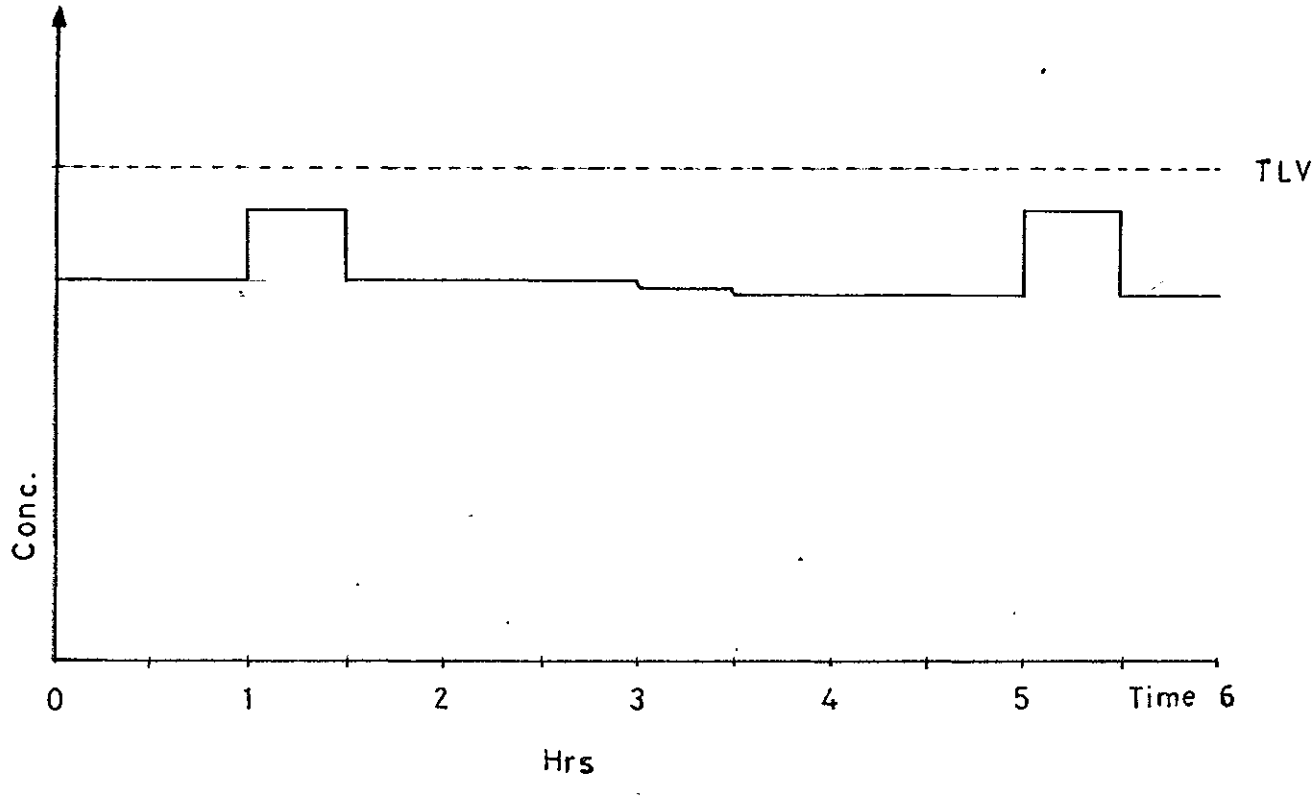

sampling, on-site monitor. The device consisted of a complete GC system mounted on a substantial trolley: the equipment consisted of sampling valves, gas cylinders, GC column and oven, FID, chart recorder, compressor and standard atmosphere apparatus. Grab sampling and pre-concentration sampling methods were used. H.M. Factory Inspectorate[9] employ the "Simmons" type of system, as well as sampling/detector devices of the chemical indicator type. Discrete sampling methods were used in a recent national survey of sulphur dioxide and smoke pollution in Britain[10]. The majority of the sampling was carried out by manual methods, although one fully automatic sulphur dioxide measuring system was employed. Fairly simple techniques were used: smoke was measured by the degree of darkening of a filter through which the sample air was drawn; sulphur dioxide was measured by acid-base titrimetry.

A pollution monitoring device where continuous on-site sampling and fully automatic data output was achieved, has been described by the Phillips company[11]. The device measured inorganic pollutants, sulphur dioxide, nitrogen dioxide, nitric oxide, carbon monoxide, hydrogen sulphide and ozone. The latter compound was determined by chemiluminescence, the former compounds by electrolytic methods. The entire system required for analysis, calibration, and control of the sampling procedures was housed in a single cabinet. The air sample was drawn through to the analysis module via a range of dust filters. Results were displayed on a chart recorder, or transmitted

to a remote location by landline, using either a frequency multiplex system, or a time division multiplex system. No systems of this type have yet been developed for organic pollutants, although suitable detectors are available which can carry out sampling and analysis of organics in rapid succession, e.g. NDIR and FID. Several portable commercial NDIR spectrometers are available, with gas handling equipment incorporated into the instrument design. Selection of the desired frequency range is achieved by optical filters or by gas-filled tubes, which are placed in the instrument's light path. Thus, if an interferent is to be suppressed, a dual-beam system is used, with a high concentration of interferent gas in the reference side. Similarly, the FID of Andreatch and Feinland[6] is available as a non-specific hydrocarbon detector from commercial companies.

An attractive method for the remote monitoring of pollution is the interaction of electromagnetic radiation with the contaminants of interest: light sources may be aimed at, or through, a target volume of air, and various detector configurations can measure scattered, absorbed or fluoresced light. A review[12] of this type of photometry has discussed the three signal types available. Rayleigh scattering was not favoured, since it was insignificant, when compared with back-scattering obtained from particulates in the air. IR absorption and fluorescence were considered to be of sufficient magnitude to provide information about air pollutants, in spite of the necessity for close measurement of atmospheric temperature profiles. Traditional IR sources were

considered suitable for absorption processes only, with the concomitant limitation that results achieved by this system were average concentration values for the path length, and gave no information about the variation of pollutant concentration along the path length.

The use of lasers should give more information for shorter path lengths, as well as opening the door to fluorescence techniques for both IR and UV. Robinson and Dake[13] have reviewed the use of laser-induced IR fluorescence for the measurement of air pollution: the authors considered the method an attractive technique. The envisaged equipment configuration is depicted in figure 2; the telescope mirror could be ranged along the length of the laser beam, in order to measure the distribution of pollutant in the light path. The use of lasers for air pollution measurement is still at an early stage, tuneable IR lasers under development, and laboratory systems are under investigation[14]. It will be some time before the full impact is felt on air pollution monitoring of these systems and systems incorporating tuneable dye UV lasers.

It may be seen that organic pollutant monitoring systems are at an embryonic stage of development. There is a growing need for continuous on-site monitoring systems, on a small scale, such as in laboratories, factories or mining situations, and on a large scale, for instance, in urban or national pollution surveys. It is against this background of unfulfilled demand, that the piezoelectric crystal detector was investigated, in order to

FIGURE 2

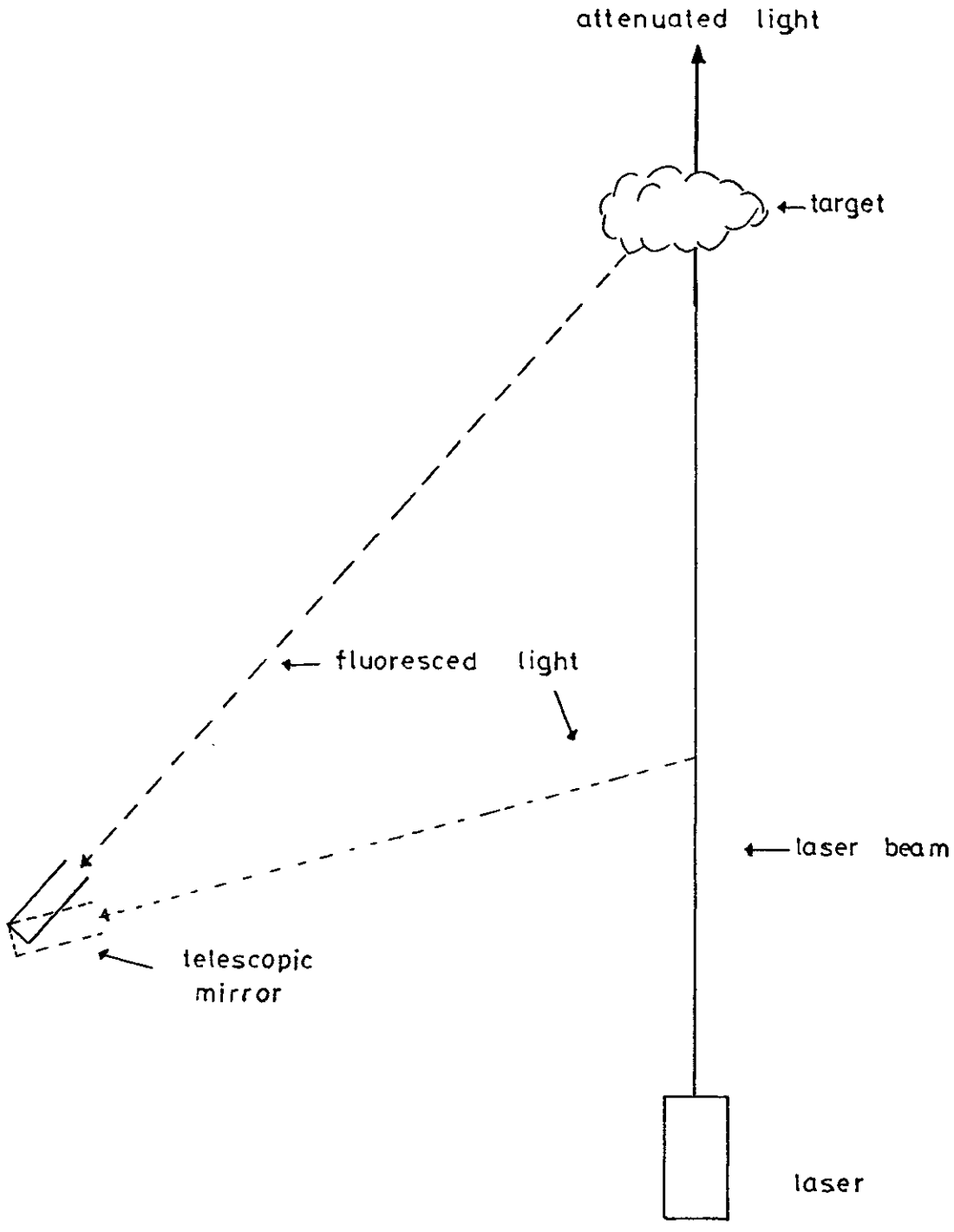

LASER MONITOR FOR AIR POLLUTION

establish its potential as an atmospheric pollutant monitor for organic gases.

CHAPTER II THE PIEZOELECTRIC DETECTOR

The piezoelectric detector is a simple sensitive device developed from the quartz crystal microbalance (QCM). The QCM consists of an AT cut quartz crystal slab operated at its fundamental frequency, typically 3.0 to 15.0 MHz This device measures mass, and a review of the development of the detector must include a discussion of its predecessor. The terminology in use is rather loose at present, the term piezoelectric detector or monitor being adopted by workers in the atmospheric pollution or gas chromatography field: the term QCM is usually reserved for non-analytical-chemical applications, where the crystal surface has not been coated with a specific sorbant. This practice will be followed in the subsequent review.

2.1 THEORY

The theory behind the operation of the piezoelectric detector may be conveniently divided into three sections: the theory of piezoelectricity; the properties and cuts of quartz crystals, with reference to the desirable properties for the piezoelectric detector; derivation of equations relating the change in frequency of a resonating quartz slab, to mass added to the surface of the slab. Each division will be considered in subsequent sections of this chapter.

2.1.1 Piezoelectricity.

Piezoelectricity is the electrical phenomenon exhibited by certain crystal classes, and other materials, whereby an electrical potential is developed between two parts of the material, as a result of a deforming stress. If the direction of the deforming stress is reversed, the polarity reverses: the converse effect, deformation of the substance, by an applied electric field is also observed. The effect was first noticed in quartz and other materials in 1880 by the Curie brothers, Jacques and Pierre, but remained a scientific curiosity for thirty years. Research on piezoelectricity recommenced in 1910, and received added impetus during the war years, when Langevin employed the electromechanical transducing properties of quartz and Rochelle salt for depth-sounding equipment on submarines. Significant work on the practical use of piezoelectric materials was also undertaken by Cady[75], who, in 1923 reported on the performance of electronic resonators, and oscillators controlled by these quartz resonators. The circuits described had far superior stability to the electronic oscillators of the day, and could be used for accurate frequency measurement or standardisation. Cady's circuits were modified by Pierce, and from 1923 to 1929 significant improvements were made both in circuitry, and in the methods of holding, clamping and delivering the electric field to quartz crystals. In 1927, Marrison's discovery[91] of a low temperature coefficient quartz crystal cut inspired research and development of a whole new range of quartz

crystal cuts, with varying properties useful to workers in the field of quartz crystal applications[92].

The piezoelectric effect arises when pressure on a material deforms the crystal lattice and causes a separation of the centres of gravity of oppositely charged species; a dipole moment is produced in each molecule. The coupling of this field to an electrical circuit can be seen from figure 3. The diagram shows a section through an imaginary piezoelectric resonator; usually this is a thin slab or rod of the material of interest. The electrodes are applied to the two faces normal to the direction of charge separation. If the electrodes are short circuited, and a stress applied to the material that causes a separation of the centres of gravity of the charges, negative charges will flow down the wire to the electrode in the direction of positive charge separation. Similarly, surplus negative charges will flow along the other wire, from the electrode in the direction of negative charge separation. The overall effect is that a pulse of electricity flows in the circuit, rendering the crystal electrically neutral to any external tests. Releasing the deforming stress causes a similar pulse to occur, but in the opposite direction. An alternating wave form applied to the electrodes will produce the converse effect, but due to the mechanical qualities of quartz, stable oscillation will only occur at the resonant frequency of the slab; the quartz plate thus becomes the frequency determining element.

FIGURE 3

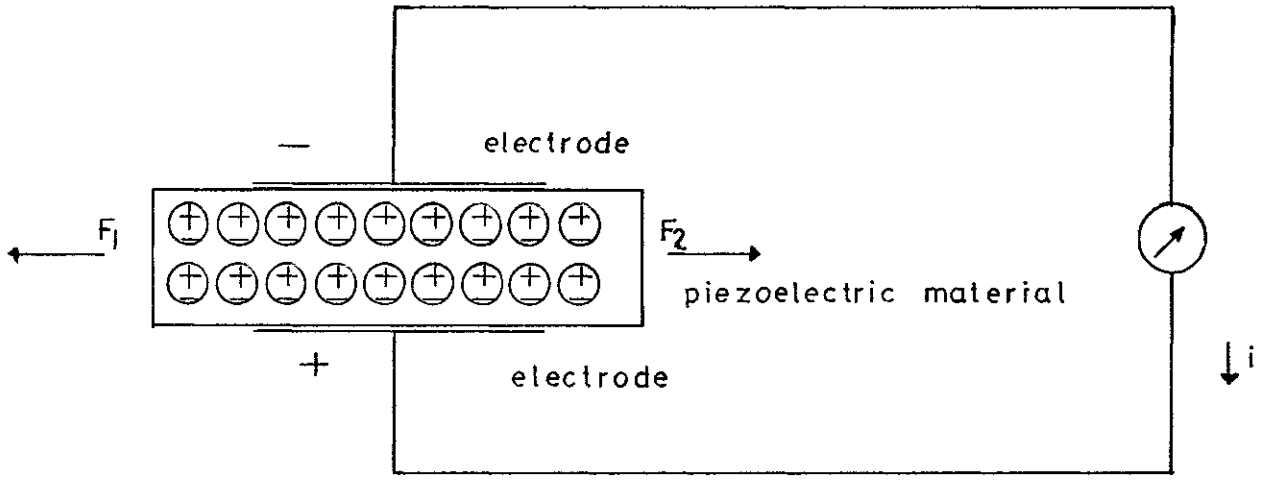

Diagram of coupling between a thin slab of piezoelectric material under stress, and an electric circuit.

Only those stresses applied to the crystal lattice whose deformations cause charge separation will give rise to piezoelectric effects. This directional effect is clearly exhibited, in that most of the crystal classes that give rise to piezoelectricity, will only do so, if the deforming stress bears certain well defined, angular relationships to the crystal axes. The asymmetric triclinic class is the exception to this, in that a deformation in any direction will cause piezoelectricity. The piezoelectric crystal is an electromechanical transducer: elastic constants of the crystal are related to the electric constants of the piezoelectric effect by the piezoelectric coefficients. A complete description of this phenomenon is quite complex; such a description may be found in Cady[93].

2.1.2 The Quartz Resonator

The rigidity of quartz and its mechanical stability, coupled with the high frequency constants and desirable properties obtained by specifically orientated crystal cuts, have caused it to assume a major role in the production of frequency controlling devices for oscillating circuits. Alpha quartz is a crystalline mineral of silicon dioxide, forming hexagonal prisms with pyramidal terminations. The crystal displays one axis of three-fold symmetry, and three axes of two-fold symmetry: the two-fold axes are in a plane normal to the three-fold axis, and at an angle of 120° to each other. See figure 4. Quartz crystals exist in two enantiomorphic forms, the right-handed form is illustrated in figure 5.

FIGURE 4

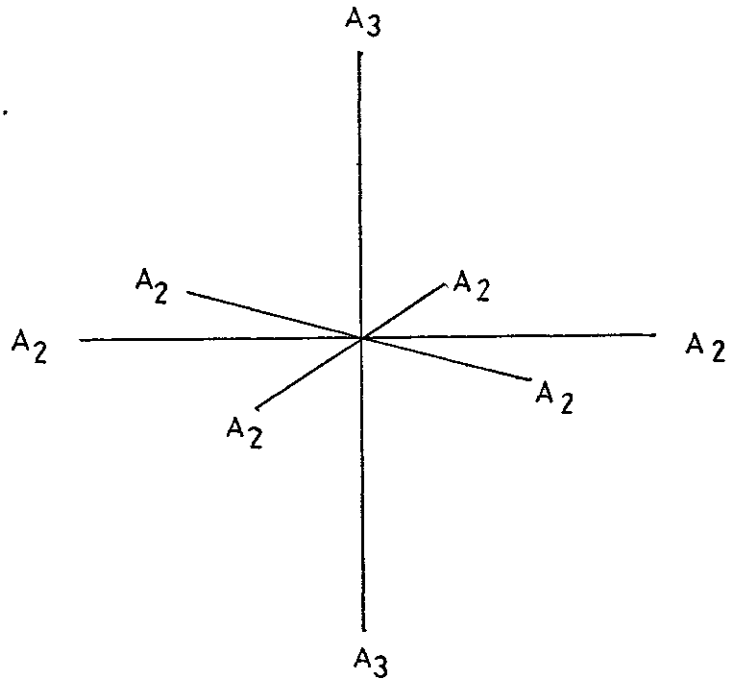

Symmetry axes in Quartz

FIGURE 5

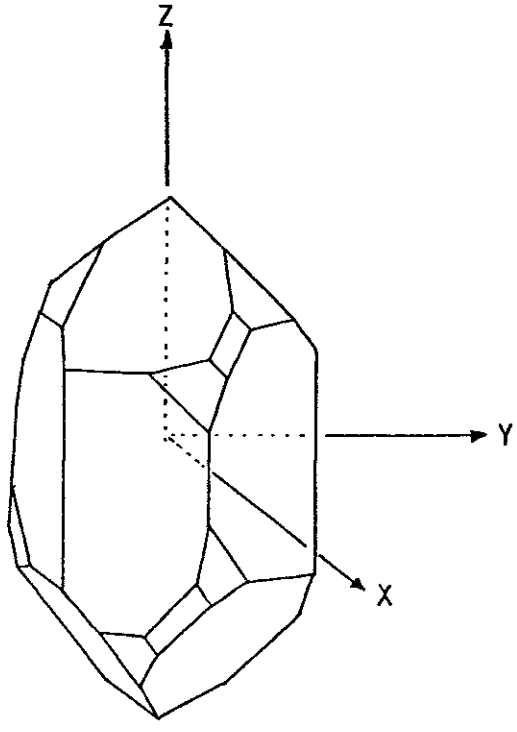

Right-handed Quartz

The X, Y and Z axes in figure 5 have been defined for right-hand quartz, and information based on these axes can be applied to left-hand quartz by changing the sign of the electrical, (X), axis. A thin slab of quartz, cut from a crystal at a specific angle, invariably produces a plate, whose resonance, mode of deformation, and electric, elastic and piezoelectric constants are predictable. The first specific crystal cuts to be examined for piezoelectric work, were the X, Y and Z cuts; see figure 6. Later work involved the examination of rotated cuts based on these three archetypal orientations. The selection of a particular crystal cut for a given purpose, depends on a number of different factors. (i) The frequency constant of the plate obtained must be of sufficient magnitude to permit the manufacture of reasonably robust slabs of manageable dimensions at the desired resonant frequency. (ii) The predominant mode of vibration should ensure that the frequency-controlling dimension of the plate or rod is of sufficient magnitude to permit a pure mode of oscillation at the desired frequency. Poorly dimensioned plates have noisy frequency spectra caused by coupling between the three modes of vibration, flexural, extensional and shear. (iii) The value of the temperature coefficient of the plate should be suitable for the operating temperature, and desired frequency stability of the device incorporating the quartz plate.

The selection of a suitable plate for the piezoelectric detector or QCM has received considerable attention, from Sauerbrey[20, 94], Warner and Stockbridge[22] and

FIGURE 6

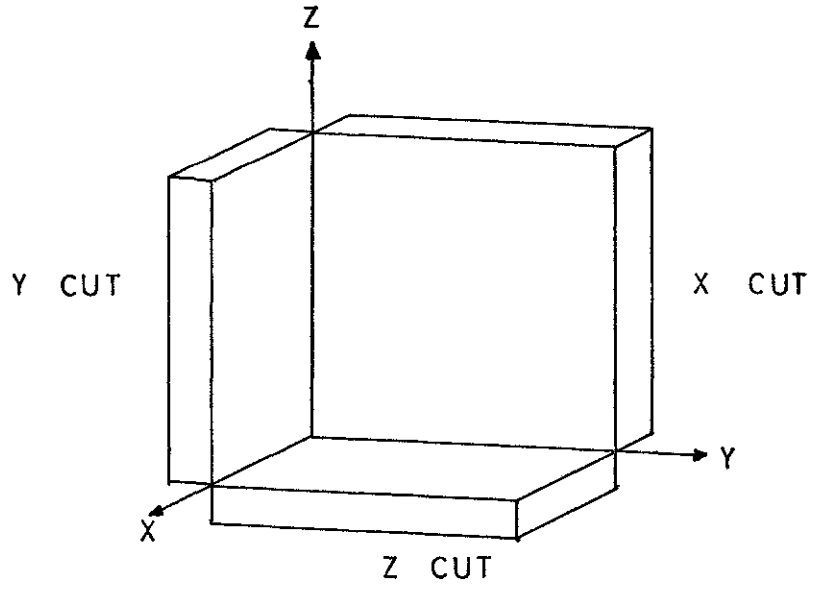

Archetypal Quartz Crystal Cuts

Khan[26]. The requirements of a quartz plate for this purpose, drawn from these and other sources are:-

(i) A quartz cut with a high frequency constant must be used, to ensure manageable plates of high frequency. The requirement for high-frequency plates will be explained in section 2.1.3., where it will be shown that mass sensitivity is proportional to frequency.

(ii) The crystal plate will undergo a degree of handling, hence a robust slab is needed in order to provide a durable detector.

(iii) The frequency-controlling dimension of the crystal plate should be the thickness, so that added mass can be placed on the surface of the plate, rather than the edge, thus facilitating coating procedures.

(iv) The plate should resonate in one mode only, with little or no tendency to couple to other modes. The particular dimensions of the plate that are selected for the detector should be proportioned to allow a certain latitude in the precise ratios, so that increase in the thickness of the plate, by added mass, does not cause coupling and hence anomalous frequency changes.

(v) A crystal cut should be chosen with a very low temperature coefficient in the temperature region in which the detector is to be operated. This requirement not only limits the temperature drift of frequency, but also reduces error due to the heating or cooling effects that can occur on the plate surface as a result of chemical or physical interactions between analyte species and the coating.

(vi) The electromechanical qualities of the plate must be suitable. A low electromechanical coupling constant, and high capacitance ratio help to reduce the dielectric constant correction, thus minimising the alteration of the constant when coatings and vapour are present on the surface of the slab. Hence, any change in the resonant frequency on coating the plate is due to the mass effect on the surface, and not to alterations in the electrical properties of the quartz.

(vii) The elastic constants must be relatively insensitive to damping and viscous retardation, thus ensuring that the crystal plate will continue to vibrate, even when substantial masses of coatings are present on the surface.

The quartz plate that satisfies many of these desiderata is derived from the AT cut. The AT is one of a family of crystal cuts obtained by rotating the Y cut around the X axis. Its main vibration mode is the thickness shear, and the electric field is applied along the Y axis. See figure 7. The crystal cut produces plates with a high frequency constant, low temperature coefficient at or around 27°C, and which are strongly driven by the correct circuitry, to give stable resonators. Care must be taken in the dimensioning of plates obtained from the AT cut, to avoid coupling to high, even order, flexural modes of vibration. Most manufacturers ensure that the low values of the length to thickness ratio which give rise to coupling (typically 8 - 20) are avoided,

FIGURE 7

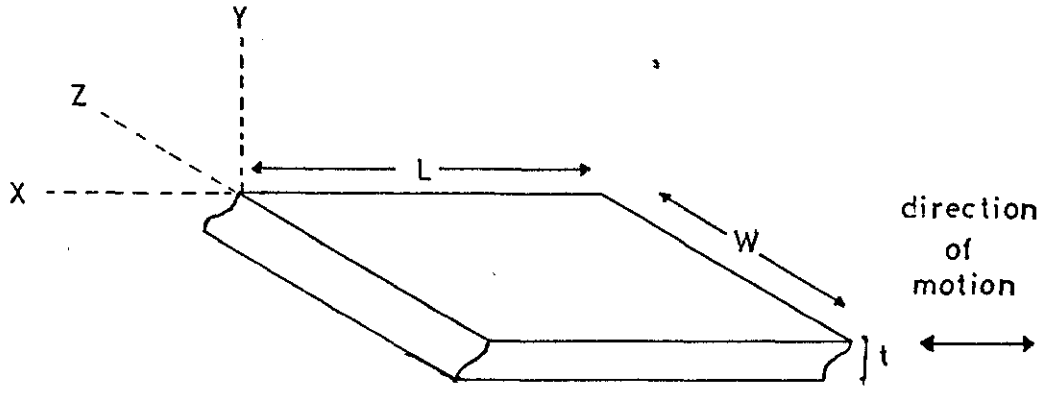

Thickness-shear vibration in an AT cut crystal

FIGURE 8

FIGURE 9

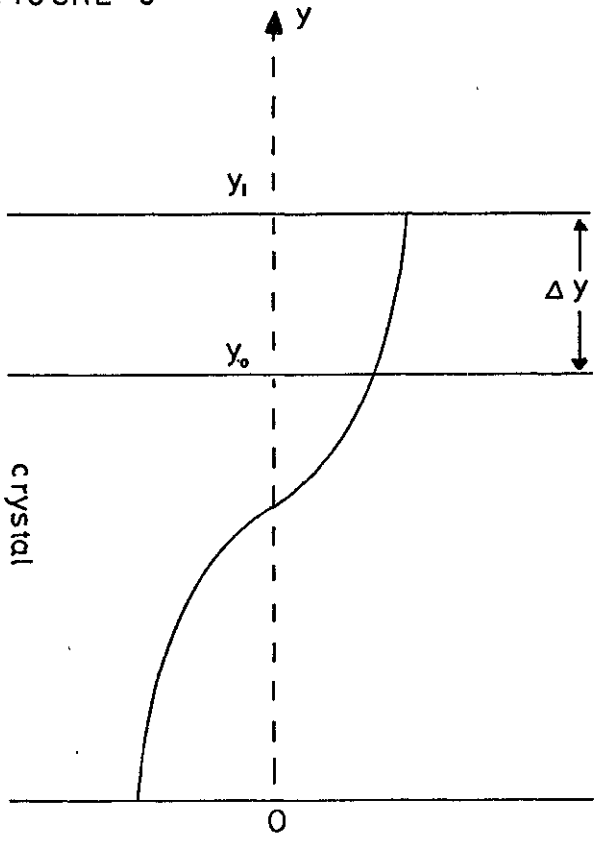

and the plates so produced have a clean frequency spectrum.

Section 2.2 reviews the development of the piezoelectric detector, and it is significant that a large majority of workers have used the AT cut plate. Occasional use of other rotated Y cuts has been reported, but the AT cut has been preferred.

Both the scientific literature and manufacturer's literature indulge in synecdoche, the term crystal being frequently used to represent both the whole crystal, and a thin plate of the crystal. This terminology is well established, and will be used subsequently in this study.

2.1.3. Equations Relating Frequency Change to added mass.

The essential property of the piezoelectric detector is that there is a well defined and reproducible relationship between the change in fundamental frequency of the resonating plate, and addition of mass to the face. Three distinct derivations for the equation expressing this relationship have been made, but before passing on to these a brief consideration should be made of the fundamental equations for the frequency of a vibrating plate.

The wave velocity V_r for an isotropic body vibrating in thickness shear mode, can be shown to be:

$$V_r = \sqrt{\frac{n}{r}} \qquad \ldots\ldots\ldots\ldots \quad 2.1$$

where

r = the density of the body

n = $(c - z)/2$

n,c,z = isotropic elastic constants.

Cady[93] has demonstrated that the velocity of a shear wave in an anisotropic body is given by:

$$V_r = \sqrt{\frac{q_m}{r}} \quad \ldots\ldots\ldots\ldots \quad 2.2$$

where q_m = the stiffness factor or elastic coefficient in the direction of wave propagation.

In figure 8 it can be seen, that for a plate resonating in thickness shear mode:

$$t = \frac{w}{2} \quad \ldots\ldots\ldots\ldots \quad 2.3$$

where

t = thickness of the plate

w = wavelength of the propagated wave.

Since the frequency (F) of a vibration is given by:

$$F = \frac{V_r}{w} \quad \ldots\ldots\ldots\ldots \quad 2.4$$

combining 2.2, 2.3 and 2.4.

$$F = \frac{n}{2t} \sqrt{\frac{q_m}{r}} \quad \ldots\ldots\ldots\ldots \quad 2.5$$

where n = 1,2,3 .... etc., depending on the overtone.

For a quartz crystal vibrating in thickness shear, Mason[95] has demonstrated that:

$$F = \frac{1}{2t} \cdot \sqrt{\frac{e}{r}} \quad \ldots\ldots\ldots\ldots \quad 2.6$$

where e = the contour elastic constant of the crystal.

Similarly, McSkimmin[96] has shown that for a

very large quartz plate:

$$o = \frac{\pi}{t}\sqrt{\frac{e}{r}} \qquad \ldots\ldots\ldots\ldots \quad 2.7$$

where o = the angular velocity of the transverse wave,

but $o = 2\pi F$, therefore equation 2.7 = equation 2.6.

For a smaller plate, McSkimmin[96] has derived an equation that takes account of the effect of other shear modes in the plate:

$$F = \tfrac{1}{2} \cdot \sqrt{\frac{1}{r}} \cdot \sqrt{\frac{e_1 n^2}{L^2} + \frac{em^2}{t^2} + \frac{e_2 p^2}{W^2}} \qquad \ldots\ldots \quad 2.8$$

where L = length of the plate

W = width of the plate

t = thickness of the plate.

n,m,p are integers.

$e_1 = c_{11}$

$e = c_{66}$ Elastic constants of quartz.

$e_2 = c_{55}$

Sykes[97] found that the higher modes predicted by equation 2.8 were given more accurately by an empirical expression:

$$F = \tfrac{1}{2}\sqrt{\frac{e}{r}} \sqrt{\frac{m^2}{t^2} + \frac{kn^2}{L^2} + \frac{k_1(r-1)^2}{W^2}} \qquad \ldots\ldots \quad 2.9$$

where k and k_1 are experimentally determined constants.

If $L \gg t$ and $W \gg t$, equations 2.8 and 2.9 reduce to 2.6.

The earliest derivation of the relationship between frequency change, ΔF and change in mass Δm on a

crystal plate was carried out by Lostis[18,19]. His method involved a consideration of the displacements of coated and uncoated crystals. Figure 9 is a detailed representation of the shear motion of a coated and uncoated quartz, AT cut plate.

The basic equation for the displacement (u_1) of any point in the wave path at a distance y from the origin O at time 't is given by:

$$u_1 = A_1 \cos \frac{o_1 y}{V_1} , \sin o_1 't \qquad \ldots\ldots\ldots \qquad 2.10$$

where

o_1 = angular velocity of an uncoated crystal.

$V_1 = \sqrt{\frac{e}{r}}$ = velocity of a transverse wave through the quartz.

A_1 = peak amplitude of the wave motion in the crystal.

Similarly, the displacement of any point in the crystal coating at a distance y_1 from y at time 't is given by:

$$u_2 = A_2 \cos \frac{o_2(y_1-y)}{V_2}, \sin o_2 't \qquad \ldots\ldots \qquad 2.11$$

where

u_2 = displacement in the layer

A_2 = peak amplitude of the wave in the layer.

$V_2 = \sqrt{\frac{e_2}{r_2}}$ = velocity of a transverse wave through the coating

e_2 = elastic coefficient of the coating

r_2 = density of the coating

o_2 = angular velocity of a particle in the coating.

At the point y_o, the displacements are the same, therefore:

$u_1 = u_2 = u$ and $o_1 = o_2 = o$. Let $\Delta y = (y_1 - y)$.

Thus combining 2.10 and 2.11:-

$$A_1 \cos \frac{o y_o}{V_1} = A_2 \cos \frac{o \Delta y}{V_2} \quad \ldots\ldots\ldots \quad 2.12$$

At y_o, the crystal plate, and coating at each instant are in equilibrium such that the following stress equality could be made:-

$$e \frac{du_1}{dy} = e_2 \frac{du_2}{dy} \quad \ldots\ldots\ldots \quad 2.13$$

Thus equation 2.12 may be rewritten in terms of equation 2.13:-

$$- \frac{o}{V_1} \cdot e A_1 \sin \frac{o y_o}{V_1} = - \frac{o}{V_2} \cdot e_2 A_2 \sin \frac{o \Delta y}{V_2} \quad 2.14$$

Divide 2.14 by 2.12

$$\frac{e}{V_1} \tan \frac{o y_o}{V_1} = \frac{e_2}{V_2} \tan \frac{o \Delta y}{V_2} \quad \ldots\ldots\ldots \quad 2.15$$

Since $o = o_1 + \Delta o$

Then, $\frac{o y_o}{V_1} = \frac{o_1 y_o}{V_1} + \frac{\Delta o y_o}{V_1} = \pi + \frac{\Delta o y_o}{V_1}$

$$\therefore \quad \tan o \frac{y_o}{V_1} = \frac{y_o \Delta o}{V_1} \quad \ldots\ldots\ldots \quad 2.16$$

Similarly it can be shown that:

$$\tan \frac{o \Delta y}{V_2} = \frac{o_1 \Delta y}{V_2} \quad \ldots\ldots\ldots \quad 2.17$$

Substitute 2.16 and 2.17 in 2.15

$$\frac{e_1}{V_1^2} \cdot y_o \Delta o = \frac{e_2}{V_2^2} \cdot o_1 \Delta y \quad \ldots\ldots\ldots \quad 2.18$$

Now, $V = \sqrt{\frac{e}{r}}$

Thus:

$$\frac{\Delta y}{y_o} = \frac{r_1}{r_2} \frac{\Delta o}{o_1} \qquad \ldots\ldots\ldots\ldots \quad 2.19$$

Since $o = \pi 2 F$, where F = the frequency of the wavemotion, equation 2.19 becomes

$$\frac{\Delta F}{F_o} = \frac{r_2}{r_1} \cdot \frac{\Delta y}{y_o} \qquad \ldots\ldots\ldots\ldots \quad 2.20$$

Now, if the area of the coating = $'A$, and the mass of coating applied to the face of the crystal plate = Δm, then:

$$\Delta m = \Delta y \cdot r_2 \cdot {}'A$$

and

$$\frac{\Delta F}{F_o} = \frac{\Delta m}{{}'A} \cdot \frac{1}{r_1 y_o} \qquad \ldots\ldots\ldots\ldots \quad 2.21$$

The Lostis derivation required no knowledge of the elastic constants of the mass added to the surface. However, the important point in the derivation at equation 2.13 required that very thin even layers were present on the surface of the resonating plate in order that the layer could be considered as an extension of the crystal plates' surface.

The derivation for ΔF and Δm due to Sauerbrey[20] commenced with equation 2.19. Sauerbrey made the assumption that $L, W >> t$, and reduced the equation to a form similar to equation 2.6.

Let $$N = \frac{V_r}{2} \qquad \ldots\ldots\ldots\ldots \quad 2.22$$

Then substitute 2.22 in 2.6, given that $V_r = \sqrt{\frac{e}{r_1}}$:-

$$F = \frac{N}{t} \qquad \ldots\ldots\ldots\ldots \quad 2.23$$

Differentiate 2.23

$$\frac{dF}{dt} = -\frac{N}{t^2} \qquad \ldots\ldots\ldots\ldots \quad 2.24$$

÷ 2.24 by 2.23, and let $dF = \Delta F$ and $dt = \Delta t$.

$$\frac{\Delta F}{F} = -\frac{\Delta t}{t} \qquad \ldots\ldots\ldots \quad 2.25$$

This equation resembles equation 2.20, save that the factor r_2/r_1 appears in the equation due to Lostis. Sauerbrey continued to make the assumption that the increase in thickness Δt of the quartz crystal was brought about by a substance which had identical properties to quartz, including density, i.e. $r_1 = r_2$.

Thus $\Delta t = \frac{\Delta m}{{}^{1}_{A} r_1}$

where:- Δm = mass of coating added to the crystal.

Then:-

$$\frac{\Delta F}{F} = -\frac{\Delta m}{{}^{1}_{A}} \cdot \frac{1}{r_1 t} \qquad \ldots\ldots\ldots \quad 2.26$$

Again, the validity of the derivation depended upon the application of a thin film to the crystal surface. Sauerbrey's derivation introduced a negative sign into the ΔF, Δm relationship, and certainly the experience of all workers with thin film coatings on quartz crystal plates has supported this equation.

Similar derivations have been carried out by Eschback and Kriudhof[36], Lawson[98], Hartigan[68] and Janghorbani[87]. A completely different derivation has been carried out by Stockbridge[25] who used Rayleigh perturbation analysis.

Rayleigh[99] showed that a small change in the inertia or elastic stiffness of a mechanically vibrating system perturbs the resonant frequency of the system according to:-

$$'F_n^2 = \frac{c_n + \Delta c_{nn}}{a_n + \Delta a_{nn}}$$

$$'F_n^2 = F_n^2 \frac{1 + (\Delta c_{nn}/c_n)}{1 + (\Delta a_{nn}/a_n} \qquad \ldots\ldots\ldots \quad 2.27$$

where

F_n = resonant frequency of system vibrating in mode n.

$'F_n$ = perturbed frequency of the system vibrating in mode n.

c and a = coefficients in a quadratic expression for the potential and kinetic energies of the vibrating system.

The equation for the perturbation caused by the addition of a small mass (with respect to the mass of the vibrating system) onto a resonating plate may be derived from equation 2.27. The mass is considered as being added onto an antinode of the system, and stores no potential energy during the vibration cycle. Stockbridge showed that for this situation:

$\Delta c_{nn} = o$ (Zero potential energy stored during vibration cycle.)

$$a_n = \frac{r_1}{2} \int_v U^2 dV$$

$$\Delta a_{nn} = \tfrac{1}{2} \int_{'A} s[U \tfrac{t}{2}]^2 \, d'A$$

Where:- s = mass added/unit area

t = thickness of plate

r_1 = density of plate (quartz in this case)

$'A$ = plate area

U = velocity of plate at any point

V = volume of the plate in motion.

Hence
$$'F_n^2 = F_n^2 \frac{1}{1 + \dfrac{\left(\int_{'A} s[U(t/2)]^2 \, d'A\right)}{r_1 \int_V U^2 \, dV}} \quad \ldots\ldots \quad 2.28$$

In practice, the values of the integrals in equation 2.28 may not be found, for three major reasons.

(i) The mass may not be added uniformly over the antinodal surface, i.e. s is variable over $'A$.

(ii) Area A_a where mass is added, may not coincide with A_1, the area of the antinodal surface in motion.

(iii) The variation of displacement across the area perpendicular to the thickness coordinate may itself vary as an unknown function of the thickness coordinate.

Stockbridge introduced factors k_1, k_2 and k_3 to account for the parts of the integrations that could not be performed due to the lack of complete information about the exact node shapes and mass distribution.

Hence equation 2.28 becomes:

$$'F_n^2 = F_n^2 \frac{1}{1 + k_1 \dfrac{m}{'A_a} \cdot \dfrac{k_2 k_3}{r_1 \frac{t}{2}}} \quad \ldots\ldots\ldots \quad 2.29$$

2.29 may be reduced thus:-

$$\frac{|\Delta F|}{F_n} = \frac{k_1 k_2 k_3 m}{r_1 t\, {}'A_a} \qquad \ldots\ldots\ldots \quad 2.30$$

Where m is the total mass added over A_a.

Let $k_1 \cdot k_2 \cdot k_3 = K$

$$\frac{|\Delta F|}{F_n} = K \cdot \frac{m}{{}'A_a} \cdot \frac{1}{r_1 t} \qquad \ldots\ldots\ldots \quad 2.31$$

Stockbridge indicated that k_1 would be less than unity for quartz plates, where the centres were more sensitive than the periphery, and that k_1 would increase, where the added mass per area value was greater at the centre than at the periphery. Similarly he showed that:

$k_2 < 1$ when ${}'A_a < {}'A$

$k_2 = 1$ when ${}'A_a = {}'A$

k_3 varies with surface curvature.

Stockbridge felt that the derivation utilizing perturbation analysis would be more useful than Sauerbrey's derivation, particularly for small values of added mass.

Equation 2.31 resembles equation 2.26, save that the negative sign of Sauerbrey's equation is replaced by a $|\Delta F|$ value. Stockbridge's assumptions were less drastic than Sauerbrey's, and certainly the full evaluation of k_1, k_2 and k_3 would give a very accurate value for the frequency change on added mass. For most practical purposes, it has been found sufficient to assume that K equals unity, and to reduce equation 2.31 to equation 2.26. The similarity of equations 2.31, 2.26

and 2.21, bears witness, by virtue of intersecting evidence to the validity of the differing assumptions made in their derivations. All workers have reported the experimental validity of these equations providing that thin, even films of coating have been applied. Unpublished work[100] has indicated that for irregular coatings, or high mass coatings, the frequency decrease of Sauerbrey's equation did not obtain, instead an increase in frequency was reported. The further elucidation of this phenomenon may shed light on the small, but significant differences between the three equations, i.e. the difference in sign for the predicted frequency change.

2.2 REVIEW OF THE DEVELOPMENT OF THE QCM AND PIEZOELECTRIC DETECTOR.

The decrease in frequency of a resonating quartz plate on the addition of further material to the electrode (or even by marking the crystal with a pencil) has been observed and used by radio engineers for some time[15-17]. The first deliberate attempt to utilize this phenomenon for mass measurement, and to develop equations relating the frequency change to added mass, was reported by Lostis[18] in 1958. A subsequent paper[19] in 1959 described the system, in which a quartz crystal was used as a reference monitor for film thickness measurement. In the same year, Sauerbrey[20] reported a more thorough study of this phenomenon, and gave an alternative derivation

for the frequency change relationship. The paper included a description of the oscillating circuits used for the study, estimation of frequency constants and proof of the equations, as well as a demonstration of the device in its capacity as a microbalance. Lostis' results were checked by Bruyere[21] using 5.0 MHz crystals. Linear curves for film thickness of cobalt, silver and gold, were obtained and checked against results obtained from multiple-beam interferometry. The QCM described by Sauerbrey and Bruyere received detailed attention from Warner and Stockbridge[22,23]. These authors developed circuitry capable of detecting frequency changes of the order of 1 part per 10^{10}. The effective mass sensitivity of this device was one to ten picogrammes: this figure was obtained by careful cell design and close temperature control ($\pm$ 0.01°C). The microbalance was designed for operation under vacuum. An ultra high vacuum environment for the QCM was employed by Haller and White[24], who stressed the simplicity of the basic QCM system. Further attention was given by Stockbridge[25] to the relationship between frequency change and added mass on the crystal surface, using Rayleigh perturbation analysis. Gold films were used by Stockbridge to determine the constants generated in the derivation, and the accuracy of the relationship was examined. Consideration of the fundamental design of the QCM received attention from Khan[26] as recently as 1972. The selection of the correct crystal cut for the resonating plate was critically examined in this paper.

Since its inception by Lostis in 1959, the QCM has been considered a useful tool for film thickness monitoring. In 1960, Lins and Kukuk[32] gave the details of a thin-film thickness monitor employing 5.0 and 3.6 MHtz AT cut crystals driven by Colpitts oscillators. The crystal was mounted on a water-cooled block in order to suppress undesired heating effects. Similar precautions were taken in a monitor described by Pulker[33]. Hillecke et al,[34,35] and Eschback[36] et al, have described film thickness monitors based on the designs of the previous papers. Edgecumbe[37] and Wolter[38] have reported the measurement of metallic film densities with the QCM. The QCM can not only measure the total amount of deposit on its surface, but can also measure the rate of accretion of the deposit. Thus Oberg and Lingensjo[27] designed a system for monitoring the rate of deposition of metallic films produced by vacuum evaporation. A basic QCM system was used, and 3.5 MHz AT cut crystal operated in their fundamental mode acted as the deposition-rate detectors. Behrndt[28] and Love took this concept a stage further in a QCM device that not only monitored the deposition rate, but also controlled it by the use of feed-back mechanisms. Results showed that the total rate of deposition could be kept within ± 1% of a desired value with this system. The implications of this work were realised by Riegert[30], for process control of the thickness of vacuum deposited films. Riegert developed a system for monitoring the rate of deposition, and composition, of alloys laid down by vacuum deposition techniques. Hartman[29] determined the

density of thin aluminium films evaporated onto the QCM. Langer and Patton[31] have described a QCM thin-film-thickness monitor for operation at elevated temperature.

The QCM has been used for weighing partial monolayers of gas adsorbed onto the surface of the resonating quartz plate. Slutsky and Wade[39,40] determined the approximate adsorption isotherms for hexane, argon and water vapor on quartz, in this way. The frequency changes caused by the admission to the QCM of various gases at room temperature and atmospheric pressure have been followed in detail by Stockbridge[41]. Partial monolayers of gas physically adsorbed onto the gold electrodes were determined, and relationships between frequency change and gas pressure derived. A later paper by the same author[42] described the determination of further frequency/pressure relationships, by the accurate determination of the pressure derivatives of the elastic module. Wade and Allen[43] have measured the chemisorption of oxygen on aluminium films with the QCM.

Electrogravimetric determination of metals at the micromolar level by the QCM has been described by Mieure[44] and Mieure and Jones[45,46]. The gold electrodes of AT cut quartz crystals were used as cathodes in a controlled-potential electrodeposition circuit. The frequency of the clean crystal was determined, the metal of interest electro-deposited from solution, the crystal dried, and the new frequency of the crystal determined. Linear calibration curves were established for nickel, indium, zinc, lead and cadmium. The range over which

the cadmium curve was obtained extended from 5.0×10^{-8}M to 5.0×10^{-4}M. Precision was achieved of 0.47% at the 5.0×10^{-4}M level, and 8% at the 5.0×10^{-8}M level. The authors felt that the technique could have been expanded to include other metals by the use of platinum electrodes instead of gold.

The versatility of the QCM has been instrumental in its application to a wide range of research fields, where small changes in mass need to be measured. Examples of a few diverse applications are: McKeown[47] measured sputtering rates with the QCM; Littler[48] has determined the corrosion rates of metals vacuum deposited onto the crystal electrode; Fischer and King[49] painted or pipetted solutions of various elastomers onto the crystal surfaces, and then followed the oxidation rates of these compounds at elevated temperatures in the presence of U.V. light; Bonds[50] studied the sorption of low molecular weight alkanes on a series of cholesteryl esters that were coated on a QCM; Hillecke and Mayer[51] determined the intensity of a rubidium atom beam by the use of a QCM operated at 180°K; Van Dyke[52,53] has designed a dew-point measurement system based on the QCM; King et al.[56] have investigated the application of the QCM to differential thermal analysis; King and Corbett[57] used a QCM coated with asphalt to determine the oxygen uptake of asphalt.

The development of the piezoelectric detector from the QCM commenced in 1963 with the work of King[54,55]. King reported the preparation and use of a moisture analyser based on a QCM coated with specific water-sorbing

substances. Molecular-sieves, polymers and silica gels were used to fabricate selective detectors capable of measuring 0.1 to 33,000 ppm of water. The later paper[55] contained a more complete description of the detector, and included a discussion and evaluation of the Sauerbrey equation. King suggested that the QCM could be coated with a range of different compounds to give detectors sensitive to many different analytes. Some GC coatings were examined briefly, and King demonstrated that the piezoelectric detector responded rapidly and linearly with no dependence on the carrier gas used in the system. The work on the piezoelectric detector, particularly with respect to the determination of moisture, was made the subject of three United States patents[58,59,60], and two British patents[61,62]. Improvements in the moisture detector were related in the patents, generally by the use of different coatings. Thus, the original coating of water-soluble non-cross-linked high molecular weight sulphonated polystyrene polymer, was replaced with coatings of deliquescent salts such as lithium and calcium chlorides. The lithium chloride coatings were preferred, since they showed greater sensitivity than the polymer, and none of the hysteresis problems of the calcium chloride. The moisture detector was further modified by King et al.[63] to include gas-stream switching, so that alternate dry and moist air passed over the coated crystal. The pulse type of signal obtained from this system was amplified, clipped to a square wave, fed to an RC differentiation circuit, rectified, and the voltage output displayed on a

meter or chart recorder. The commercial Du Pont moisture analyser[64] employed this final design save that the crystals were equipped with integral heaters, thus replacing the need for gas switching. Two linear ranges were provided from 0-250 and 0-10,000 ppm of water.

King[65] employed the moisture detector in order to measure hydrogen, methane and other hydrocarbons in the atmosphere. The air sample was thoroughly dried, and then passed over a platinum wire combustor, where the analyte of interest was selectively combusted to water, depending on the temperature of the platinum wire. The water vapour was measured by the moisture detector, and the concentration of analyte obtained from the stoichiometry of the combustion process. The range of this detector was putatively extended by King, in review articles[66,67], to the determination of carbon dioxide and the oxides of sulphur.

The detection and determination of sulphur dioxide has received attention from a number of workers in the piezoelectric detector field. Hartigan[68] attempted the determination of sulphur dioxide by the use of amine coatings: the analyte was injected into a helium carrier gas stream. Detection limits of 1×10^{-8} moles of sulphur dioxide were reported, although considerable difficulty was experienced with the rapid bleed of amines from the crystal surface. Lopez-Roman and Guilbault[69,70] used sodium tetrachlormercuriate and "Carbowax 20M" to determine sulphur dioxide. The coatings were sprayed, in solution, onto the masked crystals: 0-100 ppm sulphur dioxide gave

a linear response. A detection limit of 5 ppm sulphur dioxide has been reported by Frechette et al[71] for a crystal coated with "SDM polymer" (Uniroyal Ltd.). Tridodecyl- and tripropyl-amines were more sensitive, but excessive bleed rates and hysteresis problems rendered these coatings far less suitable. The most successful coating for sulphur dioxide determination was developed by Karmarker and Guilbault[72]. Triethanolamine coated crystals determined sulphur dioxide concentrations as low as 1 ppb.

The piezoelectric detector has been used for the determination of organophosphorus compounds in the atmosphere. Guilbault[73] carried out a preliminary study into the reaction of diisopropyl-methylphosphonate (DIMP) with the halides of mercury and other heavy metals. The coated crystals were maintained in an environment of high-vacuum, whilst partial pressures of DIMP (10^{-6} to 10^{-4}torr) were introduced. Linear response for the sorption of DIMP in this range was shown, and desorption of the compound occurred, under high vacuum. Scheide[74] used ferric chloride coatings for DIMP, and examined the chemisorption process between analyte and coating by both UV and IR. Static and flowing systems were investigated for the introduction of the sample to the detector. The former was preferred, due to the slow reaction rate and rapid diffusion of the analyte. Modification of the systems used in references[73,74] was carried out by Scheide and Guilbault[76], Shackleford and Guilbault[77] prepared a sensitive detector for organophosphorus compounds from

an organophosphorus-doped oxime-cobalt complex. Initially two different oximes were investigated, isonitrilobenzoylacetone (IBA) and 2-Pyridylaldoxime methiodide (2-PAM). The IBA gave the more sensitive coating, demonstrating a fast reversible reaction with the model organophosphorus compound, dimethyl-dichlorovinyl phosphonate. Addition of a small quantity of another organophosphorus compound, diethyl p-nitrophenylphosphonate, to the coating, stabilized the cobalt oxime complex, and slowed down the rapid loss in sensitivity due to bleed of the coating. A detection limit of 10 ppb was obtained for the organophosphorus analyte.

The piezoelectric detector has been adapted for the determination of a number of other analytes: Guilbault et al[78] determined mono-, di- and trimethylamines by heavy metal halide coatings; Bristow[79] used baked-out crystals for the determination of mercury in soil gases by amalgamation of the analyte with the clean gold electrodes; Karmarker and Guilbault[80] employed GC coatings for the determination of nitrogen dioxide and ammonia.

By 1973, Mueller and Kothny considered that sufficient work had been carried out on the piezoelectric detector for it to be regarded as a potentially useful pollution monitor[81].

An important parameter of polluted air is the size and distribution of particulate matter. The piezoelectric detector has been applied to this problem by two groups of workers: Chuan[82] employed a crystal coated with adhesive material, the peaks caused by discrete impacts

being converted to a voltage and differentiated to give the rate of mass change at the crystal surface; Olin et al[83,84,85] developed a system with uncoated crystals, an impactor being used to bring the particles to the crystal face in one system, and in another system electrostatics were used. This latter detector measured particle concentrations in the range 1 - 200,000 microgrammes/m^3, for particle sizes between 0.01 to 20 μm.

The operation of the piezoelectric detector with coatings whose major mode of analyte accretion was dissolution has been studied by Earp[86]. The relationship between response and retention volume, and log response and the reciprocal of temperature for GC coatings was demonstrated experimentally. Janghorbani[87] considered the linking of a partitioning-liquid coated crystal detector to a digital computer for rapid data-acquisition. Later, Janghorbani and Freund[88] developed equations for the behaviour of a detector coated with a partitioning liquid, and tested these experimentally. The detector was applied to the determination of sulphur compounds eluting from a GC column in an on-line data-acquisition system for measuring effluents from a pulp-mill. The performance of a GC detector based on GC stationary-phase coated crystals has been investigated by Karasak et al[89,90]. The detector generally employed the same stationary phase as the preceding column, a configuration which minimised problems due to bleed, both from the column and from the detector. Detector response linearity with respect to peak area, sample size and carrier gas flow rate was

examined, and "Carbowax 400" suggested as a useful general purpose detector.

Much of the work carried out on the piezoelectric detector is at a very early stage. The fundamental equations relating frequency change to added mass have been extensively tested, and upheld, yet little is known of the parameters for optimum detector cell design. Similarly, although equations relating response to sample size, flow rate, peak area, etc. have been developed, they have not yet been tested under the conditions for which they were derived, viz. equilibrium concentrations of analyte in the partition-liquid coating. Most applications of the detector in a system with a flowing carrier gas have utilized short slugs of sample gas, such that equilibrium analyte concentrations have not been attained in the crystal coatings: no equations have been developed to describe the effects of flow rate and other parameters in this situation. A restricted number of atmospheric pollutants have been investigated; very little attention has been given to the wide range of organic pollutants that occur in industrial and domestic situations. Finally, none of the papers have described the use of the detector for real atmospheric samples.

The purpose of this study is to elucidate the behaviour of partition-liquid coated piezoelectric detectors, in both equilibrium and non-equilibrium situations; discuss and illustrate detector cell design; demonstrate the detection and determination of a number of organic gases by the detector; indicate methods of detector

design, for a selected application; establish the potential of the detector as a monitor for atmospheric pollution.

CHAPTER III THE EXPERIMENTAL SYSTEM

The piezoelectric detector requires two distinctly different systems of equipment in order to operate. One system is completely electronic, being concerned with the circuitry for driving the crystal at its resonant frequency, and the subsequent signal handling and display. The other system involves the introduction of the analyte to the detector, and consists of gas handling equipment, sample introduction area and detector cell. These two systems may be considered separately as far as experimental technique is concerned, since very few techniques simultaneously involve both systems. A third area of technique and experimentation may be defined: the preparation and optimization of coated crystals. Each of these three areas will be considered in turn.

3.1 ELECTRONIC CIRCUITRY : SIGNAL HANDLING AND DISPLAY

3.1.1 Theory

The basic requirements of an electronic system associated with the piezoelectric detector are simple, viz.: oscillator circuits to drive the crystal, and some form of scalar or counter to display the frequency signal from the crystal. Both sides of the system, electronic circuitry or signal handling, are capable of further complexity, depending on the desired performance of the system.

Many different circuits have been designed to drive the quartz crystal, their operation depends on the

maintenance of an alternating voltage in the circuit of the same frequency as the slab of quartz employed. Van Dyke[101] showed that at or near its resonant frequency, the crystal can be represented by the equivalent electrical circuit shown in figure 10. This is a series resonant circuit, with capacitance paralleling, which exhibits both phenomena, series resonance and parallel resonance. Measurements made on crystals indicate that the value of the inductance is of the order of 10^5 Henries, and the capacitance less than 10^{-12} farads. The oscillator circuit usually contains the crystal, as the frequency determining element, an amplifier with feedback from output to input, and an amplitude limiter to prevent amplifier overload. One of the simplest is the Colpitts oscillator which drives the crystal at a frequency between its series and parallel value, see figure 11a. The crystal resonates with the series combination of capacitors, and the circuit stability is determined by the stability of the two capacitors, the voltage source and the output loading. Good design of the circuit gives a very stable oscillator. Another simple oscillator is the Pierce type shown in figure 11b, where the crystal is directly in the feedback path of the npn transistor. A less stable circuit, but one which can readily drive high frequency crystals at their fundamental series resonance, or at overtones, is the common-base oscillator shown in figure 12 . The instability is introduced to the circuit by virtue of the tuning components. Butler[102] has described a range of useful transistor oscillators based on these designs.

FIGURE 10

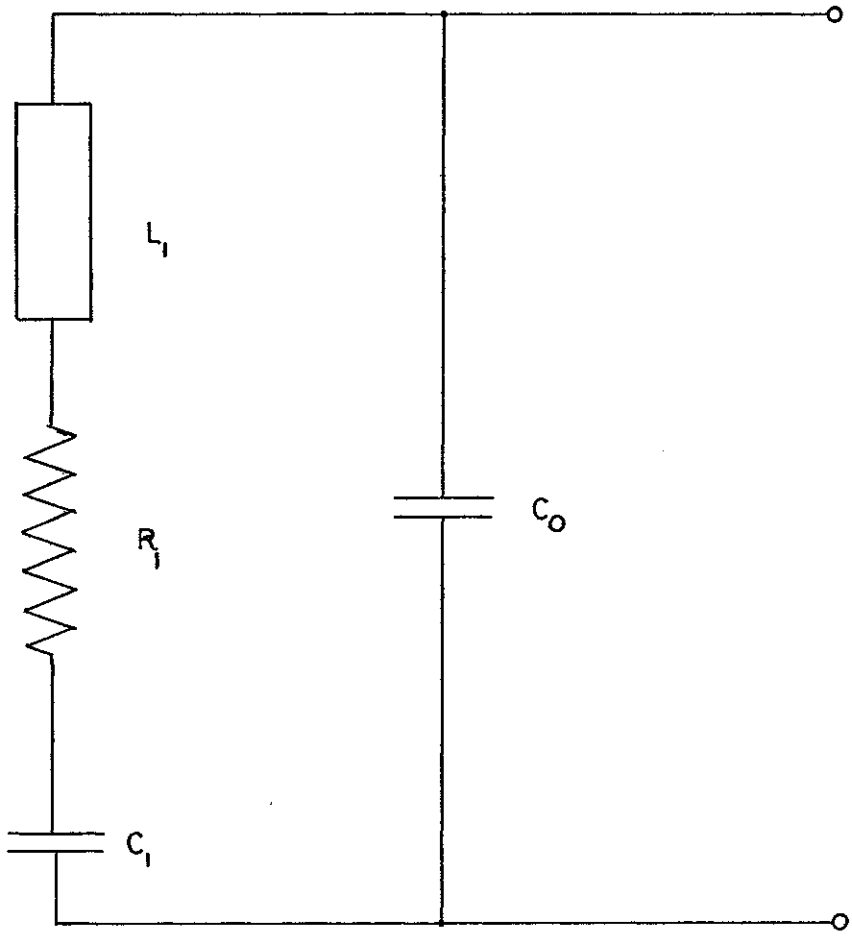

Equivalent electrical circuit of a quartz crystal at or near resonance

FIGURE 11a

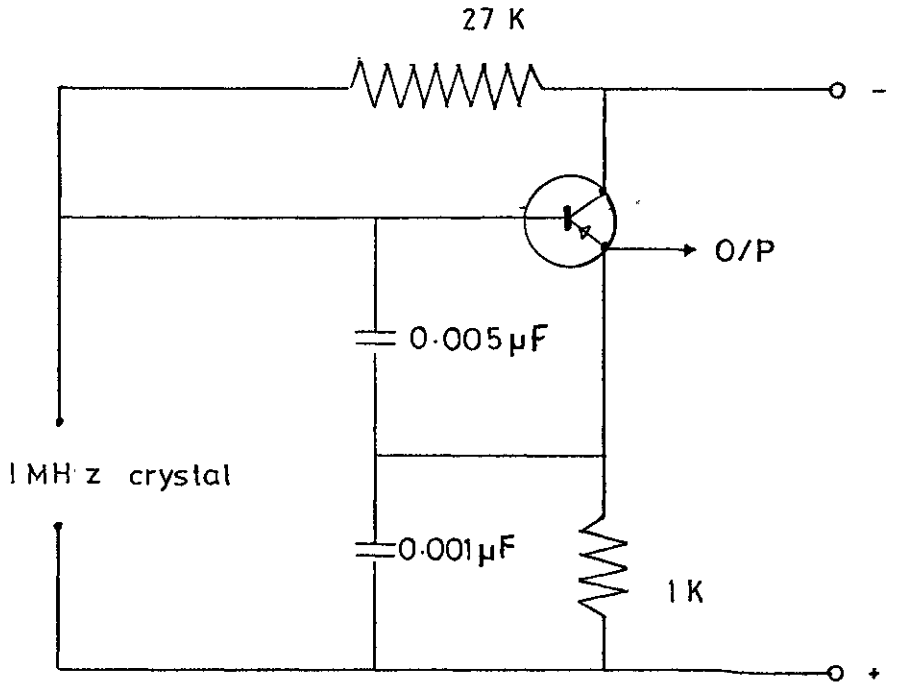

COLPITTS OSCILLATOR

FIGURE 11b

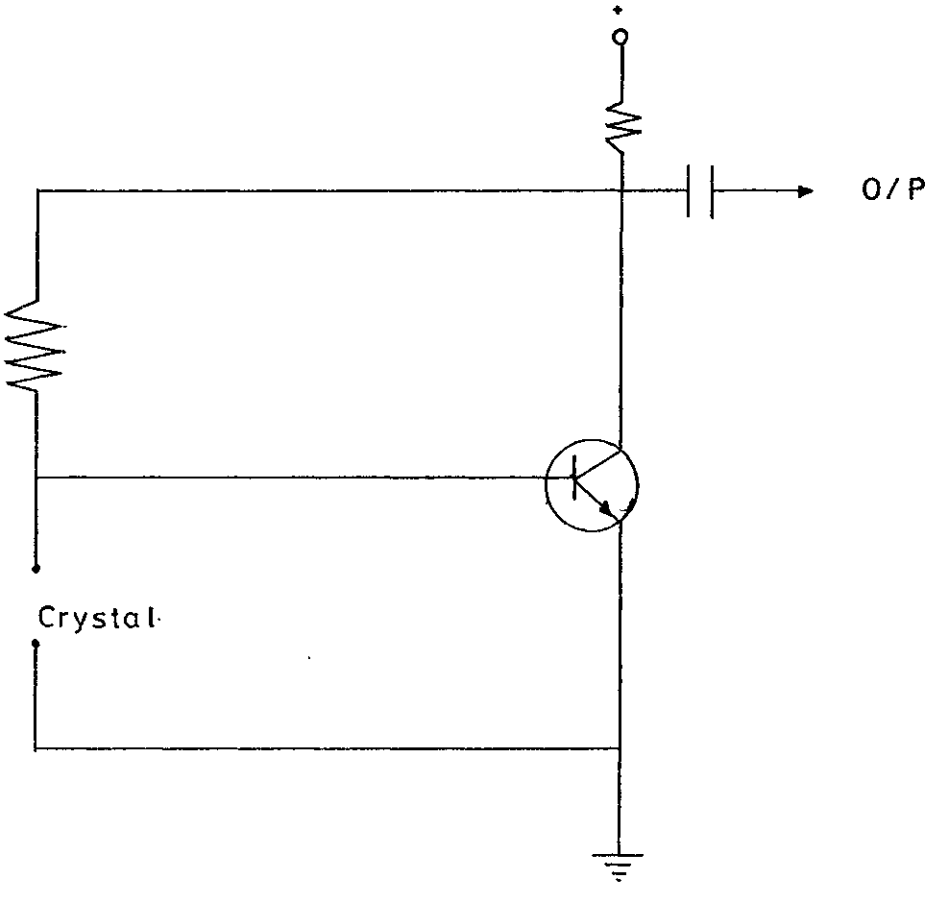

PIERCE OSCILLATOR

FIGURE 12

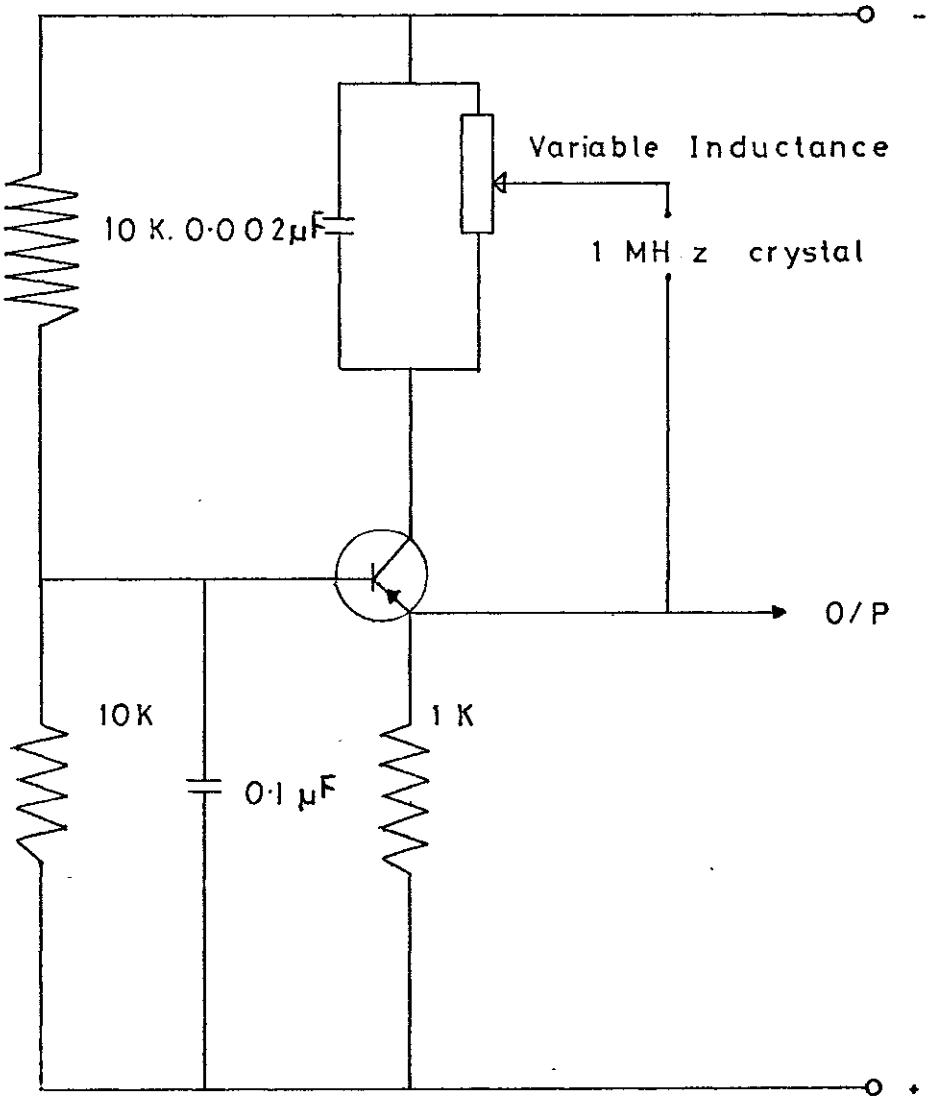

COMMON—BASE OSCILLATOR

The frequency output from the oscillator may be handled in three different ways: the frequency may go direct to a counter; another frequency may be combined with the first signal, and the resultant signal counted, or converted to an analogue form; direct conversion of the frequency to an analogue form. The least complex system involves the use of scalers; these are circuits which count the number of incoming pulses for a preset time. This approach was used by Earp[86]. The scalers were set to count the background from the detector, then reset to count, over the same period, the pulses from the monitor as analyte gas was introduced. The first reading was subtracted from the second, and the difference between the two signals obtained represented the signal due to the analyte gas. More usually a frequency meter is employed, which is, in effect, a more flexible scaler. A quartz crystal oscillator provides a stable reference frequency, which is used to control the opening and closing of a counting gate. Thus, a selector switch may be set, so that for "n" pulses derived from the standard frequency source, the counting gate is open. A frequency signal applied to the input of the meter enters the gate until, on the "n'th" pulse from the internal standard frequency source, the gate is closed. The number of pulses held inside the gate, due to the input frequency is counted, and displayed on some form of visible indicator. The stability of the standard frequency source is critical for the accurate and precise determination of incoming frequencies. At the completion of the counting cycle,

the gate is emptied, reset and the cycle repeated.

Direct conversion of the high frequency signal to a voltage may be accomplished by the previous encoding of the frequency into some form of binary signal. Usually, the value of each decimal column of the frequency is represented by a four-bit binary code, the conversion to this code is often carried out within the frequency meter. Conversion of the encoded frequency is carried out by a digital/analogue converter, which initially stores each binary coded decimal in an array of four transistor flip-flops (for four-bit codes). The output of each flip-flop is weighted, according to whether it is the least significant digit (LSD) of the frequency, or the second LSD or the third LSD, etc. Each of the storage decades containing the flip-flops is summed, to produce a voltage that is proportional to the incoming digital signal. The conversion of high frequency signals to voltages is quite difficult, and a number of workers have described the digital/analogue conversion of the audio frequency component of a heterodyne system, e.g.: Bruyere[21], Crawford[63], Lins[32] and Warner[23]. The diode mixer is the most common method of heterodyning. The mixer circuit receives two similar input frequencies, f_1 and f_2, and outputs four frequencies, $f_1 - f_2$, $f_1 + f_2$, f_1 and f_2. A low-pass filter selects the difference frequency, which is subsequently amplified: suitable operational amplifiers will combine these two functions. The two crystals selected for use in a mixer circuit are chosen to be as similar as possible, in cut, temperature coefficient and frequency.

The QCM application of heterodyning usually maintained one crystal in a carefully controlled environment to provide a stable reference, so that variation in the output signal was due only to variation in the sample crystal. In the piezoelectric detector, the reference crystal is usually maintained in the same environment as the sample crystal, in order to compensate for fluctuations in the ambient temperature, gas flow rate and other detector-environment alterations.

The effect of the diode mixer may be described algebraically.

Let f_1 = frequency of the sample crystal

f_2 = frequency of the reference crystal.

From the mixer circuit:-

$$|{}^1f_a| = f_1 - f_2 \quad \ldots\ldots\ldots \quad 3.1$$

Suppose that a sample is admitted to the detector, and the frequency f_1 is altered thus:- $f_3 = f_1 - \Delta f$ 3.2

The mixer will now put out a new audio frequency:-

$$|{}^2f_a| = f_1 - f_3 \quad \ldots\ldots\ldots \quad 3.3$$

substitute 3.2 in 3.3

$$|{}^2f_a| = f_1 - f_2 - \Delta f \quad \ldots\ldots\ldots \quad 3.4$$

Substitute 3.1 in 3.4

$$|{}^2f_a| = |{}^1f_a| - \Delta f \quad \ldots\ldots\ldots \quad 3.5$$

Thus, the mixer output follows directly the change in frequency of the sample crystal.

Assume now, that in a piezoelectric detector system, the initial frequencies, f_1 and f_2 are altered to new frequencies f_3 and f_4, by the alteration of an environmental

parameter by x units, where the coefficient is "a" Hertz per unit (i.e., independent of the frequency value of the crystal).

Then $f_3 = f_1 + ax$ 3.6

$f_4 = f_2 + ax$ 3.7

Now, let $f_1 - f_2 = |f_a|$ 3.8

Then $f_3 - f_4 = (f_1 + ax) - (f_2 + ax)$

$f_3 - f_4 = f_1 - f_2$ 3.9

Substitute 3.8 in 3.9

$$f_3 - f_4 = |f_a|$$

Hence this type of variation may be directly compensated.

Suppose the same situation occurs, but this time the coefficient of the parameter that alters is a function of the frequency.

Thus $f_3 = f_1(1 + ax)$ 3.10

$f_4 = f_2(1 + ax)$ 3.11

Conbining 3.10 and 3.11 :-

$$f_3 - f_4 = (f_1 - f_2) + ax(f_1 - f_2) \quad . . . . \quad 3.12$$

Substitute 3.8 in 3.12

$$f_3 - f_4 = |f_a| (1 + ax) \quad . . . . . \quad 3.13$$

Hence variations of this type cannot be directly compensated for by mixer techniques.

A problem associated with the mixer type of circuit is "lock-on", where, if the frequencies of the two circuits are similar, one of the oscillators appears to control the other. This difficulty was experienced

by Bruyere[21], who found that frequency changes of 100 Hz or less were unreadable. This effect usually can be eliminated, by placing each oscillator in an earthed Faraday cage, and by introducing low pass filters into the oscillator power lines, if a common power source is used.

The conversion of the digital signal from the mixer is preceded by amplification of the signal, and clipping of the sinusoidal wave form to a square wave, by a Schmitt trigger. In the simplest system, the square waves are summed at a capacitor to give the analogue output: more complex systems use differentiator circuits followed by rectification. The recent introduction of single-chip phase-locked loop (PLL) circuits has provided an alternative method for digital/analogue conversion. In the PLL, the audio frequency of a free-running oscillator is tuned to coincide with the input frequency. Alteration of the input frequency causes the PLL to adjust the free-running frequency so that it follows the input. The voltage required to maintain this similarity is proportional to the difference between the start and finish frequency, and hence a voltage signal is obtained for a digital input. The two frequencies may only be maintained similar within a ± 10% range of the value of the audio frequency from the free-running oscillator.

The use of the mixer circuit for compensation of some forms of frequency drift is not the only method of achieving this end. The frequency division facility, available on a number of digital counters or frequency

meters, may also be used to overcome some problems of drift. In this configuration, the internal standard reference crystal of the meter or counter is replaced by an external frequency standard which can be one of a pair of crystals in a piezoelectric detector system. If the frequency of the external source is f_1 Hz, and the number of pulses derived from this source for operation of the gate is n, the gating time is given by $\frac{n}{f_1}$ seconds. If a frequency source, f_2, applied to the input permits c pulses to enter the counting gate, during the gating period, the value of f_2 may be determined from:

$$f_2 = \frac{c}{n} \cdot f_1$$

Hence the displayed number, $c = \frac{f_2}{f_1} \cdot n$ 3.14

Since n is constant, the effect is of frequency division. Consider the situation described for equations 3.10 to 3.13. Thus:-

$$f_3 = f_1 (1 + ax) \quad \ldots\ldots\ldots \quad 3.15$$

$$f_4 = f_2 (1 + ax) \quad \ldots\ldots\ldots \quad 3.16$$

For the gating period applied to equation 3.14

$$'c = n\frac{f_3}{f_4} = n\frac{f_1}{f_2} \cdot \frac{(1 + ax)}{(1 + ax)} \quad \ldots\ldots \quad 3.17$$

Substitute 3.14 in 3.17

$$'c = c$$

Thus, this type of drift may be directly compensated for. Applying the same reasoning to the conditions described by equations 3.6 to 3.9:-

$$f_3 = f_1 + ax \quad \ldots\ldots\ldots \quad 3.18$$

$$f_4 = f_2 + ax \quad \ldots\ldots\ldots \quad 3.19$$

Then

$$'c = n\frac{f_3}{f_4} = n\frac{f_1 + ax}{f_2 + ax} \quad \ldots\ldots\ldots \quad 3.20$$

Hence $'c \neq c$

The drift caused by addition of an increment to the frequency, independent of the frequencies' magnitude, cannot be directly compensated by this method.

Finally, consider the case where one frequency stays constant, and the other alters by an amount, ΔF, due to the introduction of analyte to the detector.

f_1 stays constant.

$$f_3 = f_2 + |\Delta f| \qquad \ldots\ldots\ldots\ldots \quad 3.21$$

The original frequency divide value is given by equation 3.14; $c = \frac{f_2}{f_1} n$.

The final frequency divide value is:-

$$c' = n\frac{f_3}{f_1} = n\frac{f_2 + |\Delta f|}{f_1} \qquad \ldots\ldots\ldots \quad 3.22$$

Hence the change in reading on the frequency meter is given by 3.14 - 3.22:

$$c - c' = \Delta c = n\frac{f_2}{f_1} - n\frac{f_2 + |\Delta f|}{f_1} \qquad \ldots\ldots \quad 3.23$$

$$\Delta c = \frac{|\Delta f|}{f_1} n \qquad \ldots\ldots\ldots\ldots \quad 3.24$$

Now, since n and f_1 are constants, it can be seen that Δc is proportional to $|\Delta f|$, and may be directly calculated if required.

The full advantages of using either system for drift compensation will obviously depend on the nature of the drift: a frequency independent drift will be dealt with efficiently by the mixer system, whereas the divider system will reduce frequency dependent drift. It is likely that in a given situation both types of drift will occur, and the selection of compensation method

will depend on the relative proportions of each type.

Both systems require that the crystals be closely matched in order to obtain drift elimination. This condition may be difficult to achieve, since for some parameters, minute alterations in the angle of cut can radically alter the effect on the frequency due to an alteration in that parameter. Thus, Warner and Stockbridge[23] have shown, that for a one minute change in the angle of cut for an AT crystal, the temperature at which the zero temperature coefficient obtains, alters by 30°C. Similarly for a range of AT cut crystals, the temperature coefficient at 27°C varied from less than1 ppm/°C, to greater than 10 ppm/°C.

3.1.2 Practice

The crystals used in this study were AT cut quartz, resonating at 9.0 MHz, in their fundamental thickness-shear mode. Each one consisted of a one centimetre square slab of quartz, 0.1 mm thick, with a vacuum deposited gold electrode on each surface of the plate. The crystals were mounted in phosphor-bronze clips attached to an HC6/U holder. See figure 13. These units were supplied by the Quartz Crystal Company. The crystals were not cemented into the clips, nor were the protective metal caps sealed onto the base of the holder. The crystals were driven at their fundamental resonant frequency by oscillator circuits of the Pierce type. The circuits were fabricated from kits supplied by the Amtron International Company, and were designed to provide a

FIGURE 13

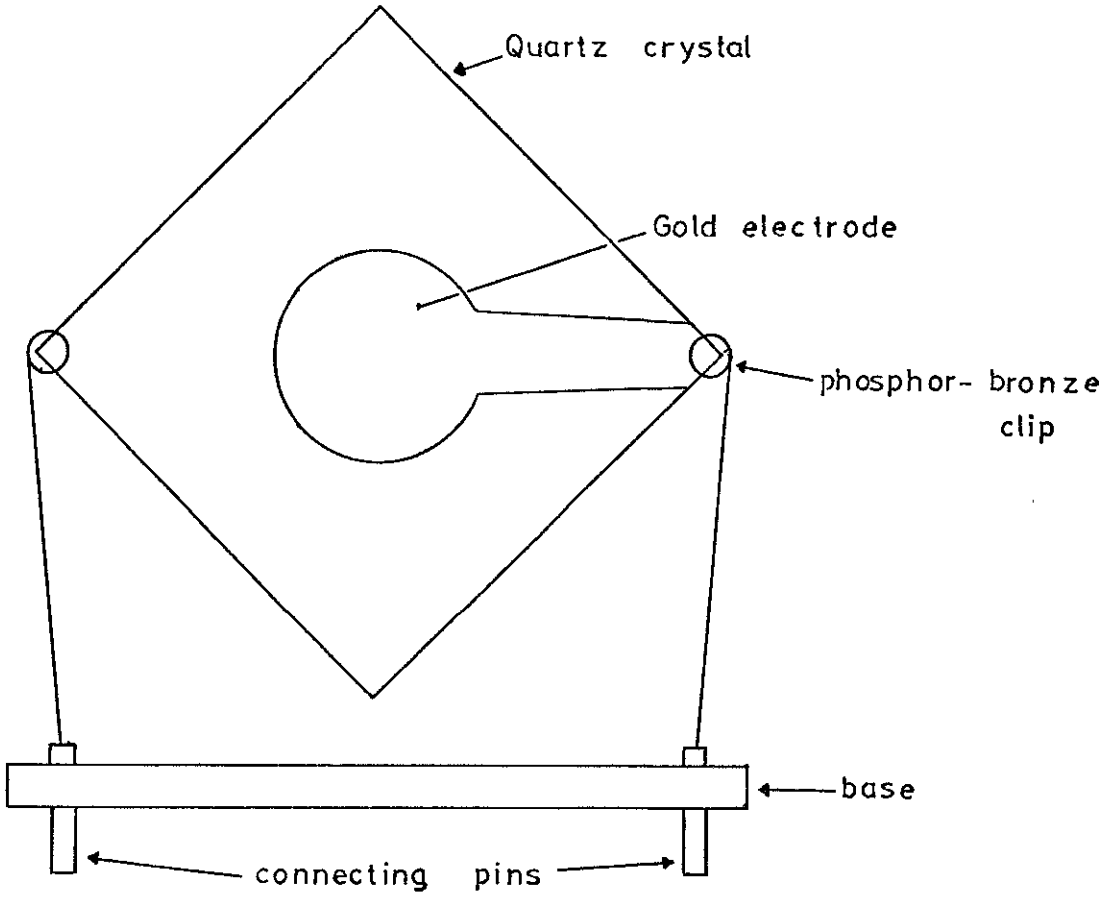

FIGURE 14

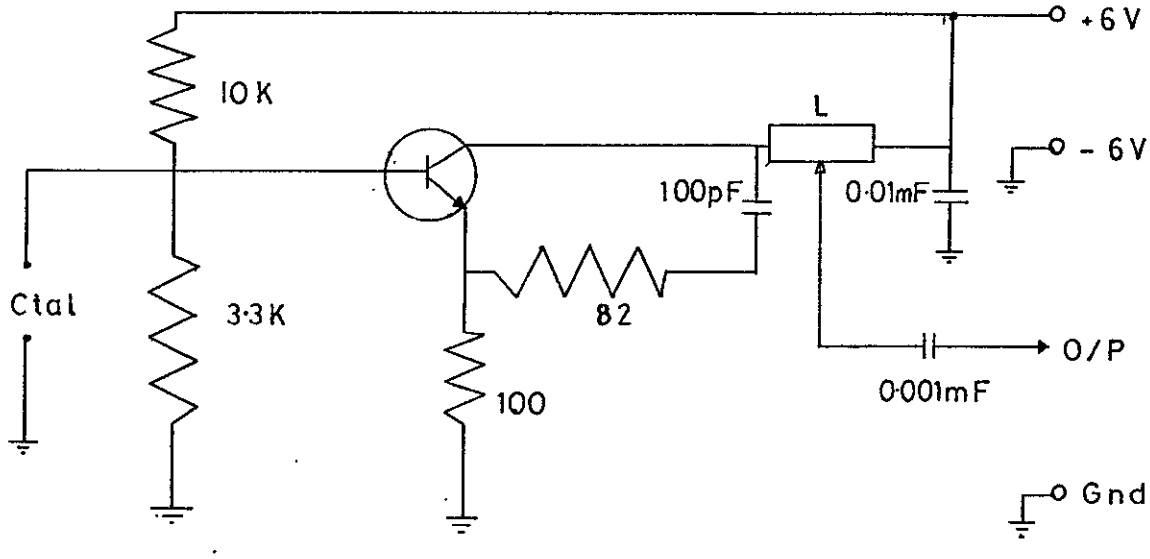

Ctal = 6·0 - 9·0 MHz crystal

Oscillator circuit used in this study

broad-tuned circuit capable of driving a crystal within the frequency range 6.0 to 10.0 MHz. The output signal amplitude was 200 mV RMS across a 50 ohm load, and the frequency was within 0.02% of nominal. The circuit's power requirement was 4 to 9 V at 20 mA, and a one volt alteration in supply caused a 0.001% change in the frequency. The power supply was accomplished by a Coutant Electronics LM 50/30 power-pack. This device could deliver 0 to 30 V at 0 to 0.5 A, with a voltage variation of 0.001% at 9V. A 10% change in mains voltage altered the output value by one mV, thus causing a frequency change of 0.1 Hz for a 9 MHz crystal. When two oscillators were in use, they were both powered by the same unit, in a parallel conformation, with a low pass filter incorporated into one set of leads. Each oscillator was housed separately in an earthed metal box, in order to screen each from the other, and from other sources of high frequency. The digital outputs from the oscillators were taken to digital counters via coaxial leads with BNC plug terminations. The counters used throughout this study were model number 7737 from the AMF Venner company. Option Z was selected, so that the parallel 1 - 2 - 4 - 8 BCD output could be interfaced with a Hewlett Packard 580A/003 digital/analogue converter. Voltage signals from the latter source were displayed on a Servoscribe RE 541.20 potentimetric flat-bed recorder. The layout of the electronic system may be seen from figure 15.

The principal source of data was the digital counter, whose operation previously has been described

FIGURE 15

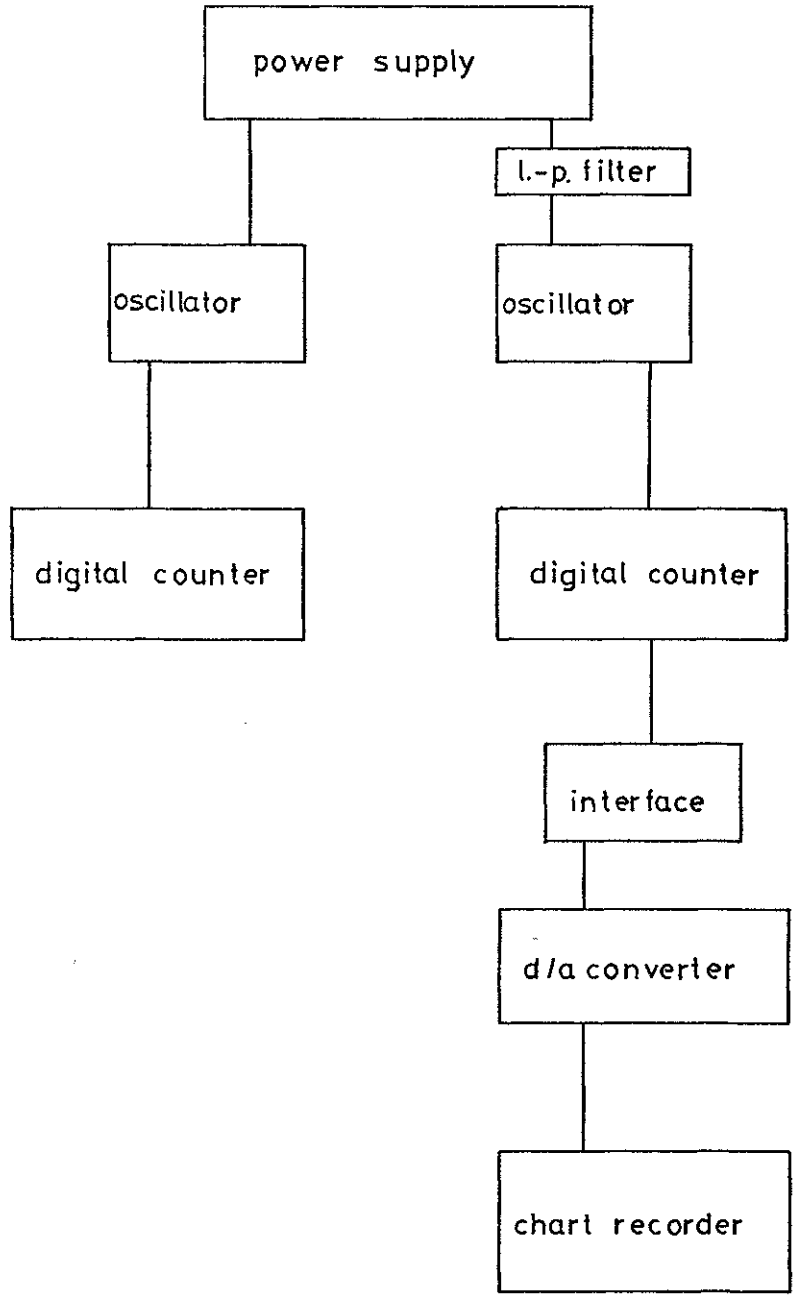

Electronic system used in this study

(Section 3.1.1). The one second gating period was used most often, so that the frequency of the input signal was directly displayed. A potentiometer on the front of the counter permitted selection of varying time intervals between successive counts, from 0.1 to 5 seconds. A three position switch selected the correct shape of input waveform, in this case a sine wave, and the trigger was set to count leading edges of pulses. The minimum input sensitivity was 10 mV for a sine wave and frequencies from 10 Hz to 50 MHz could be counted, with an accuracy of ± 1 in the least significant digit. Gating time could be adjusted in decade steps, from 0.1 microsecond to 10 seconds, and the counter could be used with an external reference crystal.

Stability and Drift of the Electrical System

A single oscillator was set up with a sealed AT cut, 10.0 MHz crystal. The system was operated at room temperature, and readings were taken using the one second gating time, at 5 second, 5 minute and 30 minute intervals. Prior to the experiment, all the equipment had been permitted a thirty minute warming-up period. The results were plotted as frequency versus time. See figure 16.

Drift versus Temperature: Single Oscillator.

A single oscillator was set up with an unsealed 9.0 MHz crystal at room temperature. The frequency of the crystal was read from the counter and temperature from a 0 to 50°C thermometer every five minutes. The results were plotted as frequency versus temperature, see figure 17a, and frequency and temperature versus time, see figure 17b.

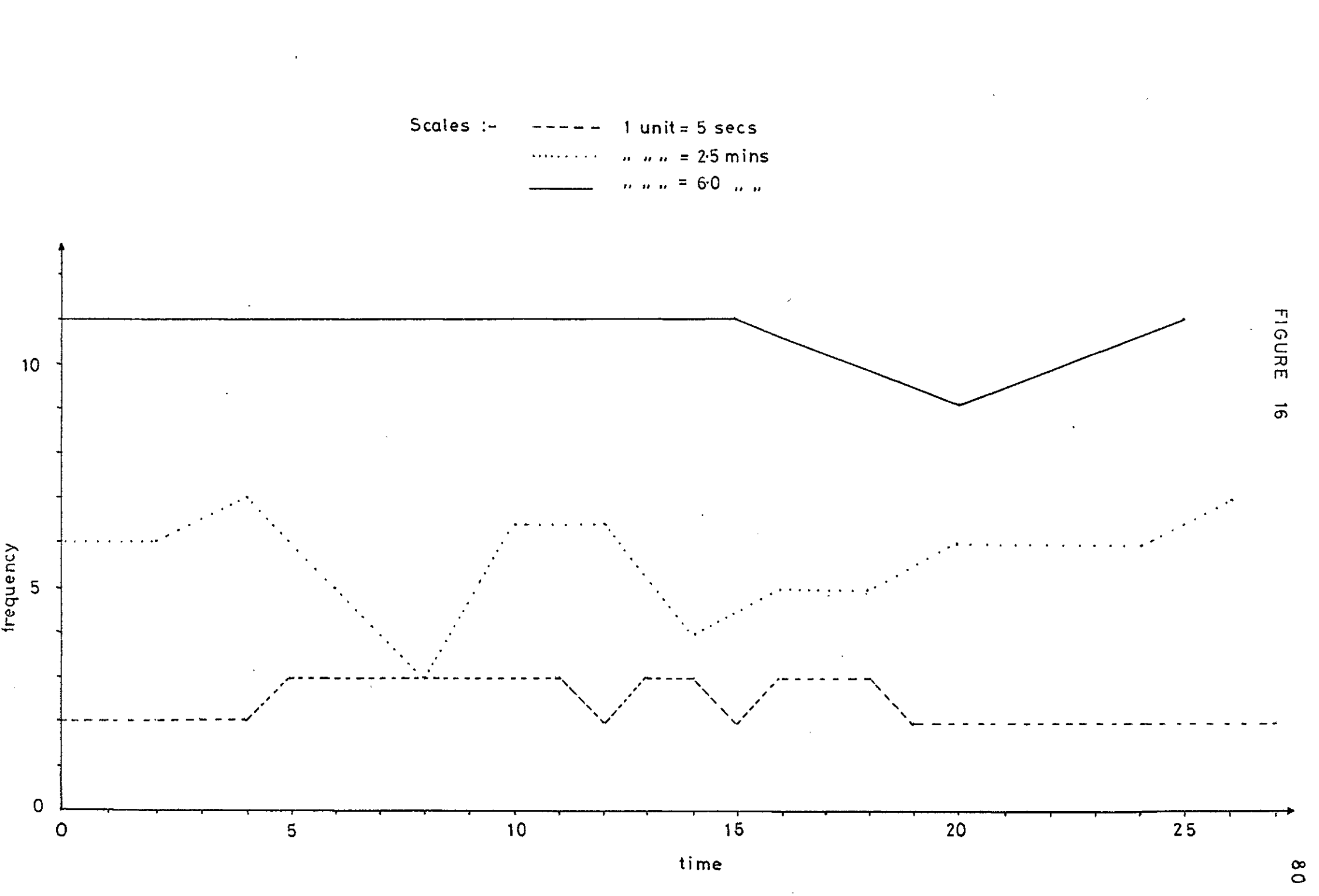
Scales :- ----- 1 unit = 5 secs
..... " " " = 2·5 mins
——— " " " = 6·0 " "
10
5
0
frequency
0
5
10
15
20
25
time

FIGURE 16

FIGURE 17a

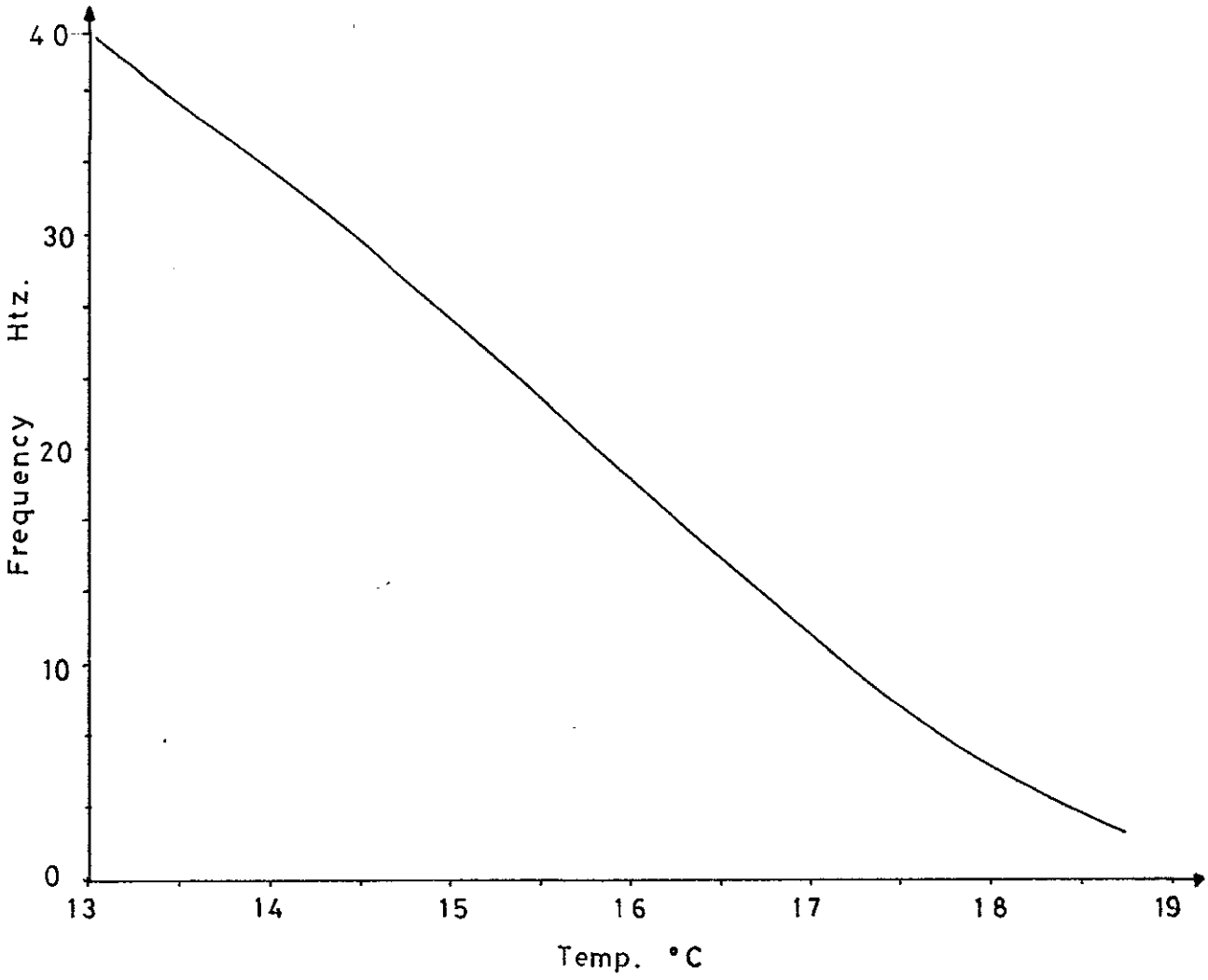

FIGURE 17 b

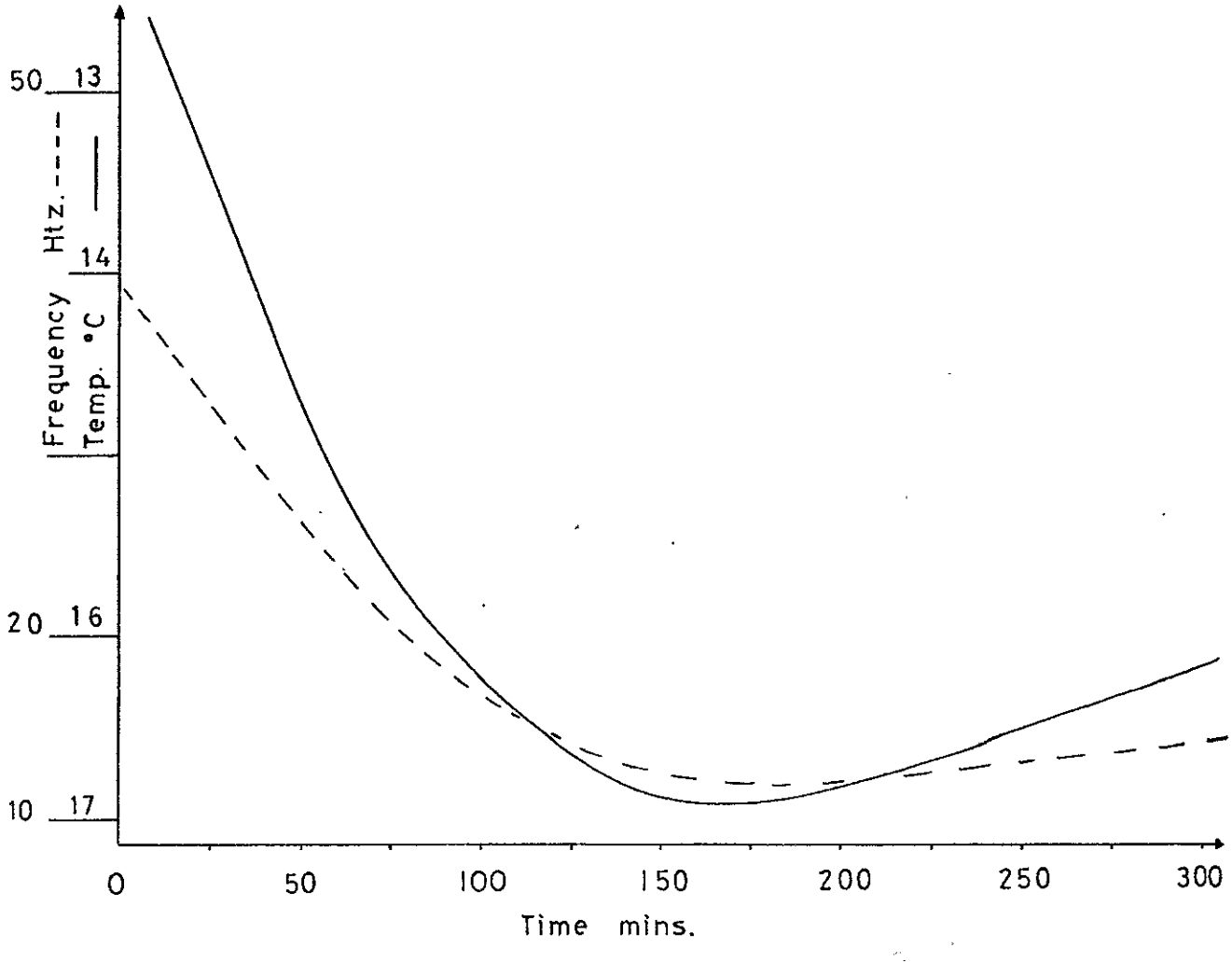

Drift versus Temperature: Frequency Dividing

Two oscillators were set up, each with a 9.0 MHz crystal: the crystals were located in the high volume impinger detector cell described in Section 3.2.2, but no gas flow was switched in. The output from one oscillator was taken to the external frequency standard socket of the counter, and the output from the other oscillator was taken to the input socket of the counter in the normal way. A toggle switch on the counter could select either the internal or the external frequency standard, and by switching from one to the other readings of the input frequency could be taken with and without frequency dividing. The two readings were taken every five minutes, along with the temperature, and the results plotted as frequency, and divided frequency, against temperature. See figure 18.

Drift versus temperature: coated crystal; no thermostatting.

A single oscillator was set up with a 9.0 MHz crystal coated with 20 microgrammes per side "Apiezon M" wax. The crystal was located in a glass, static detector cell (see Section 3.2.2), and equilibrated at room temperature. The frequency of the crystal, and temperature of the ambient air were recorded simultaneously every five minutes. The frequency versus temperature was plotted, see figure 19a, and frequency versus time, see figure 19b.

Drift versus time: coated crystal, thermostatted temperature.

A 9.0 MHz crystal, coated with 200 microgrammes

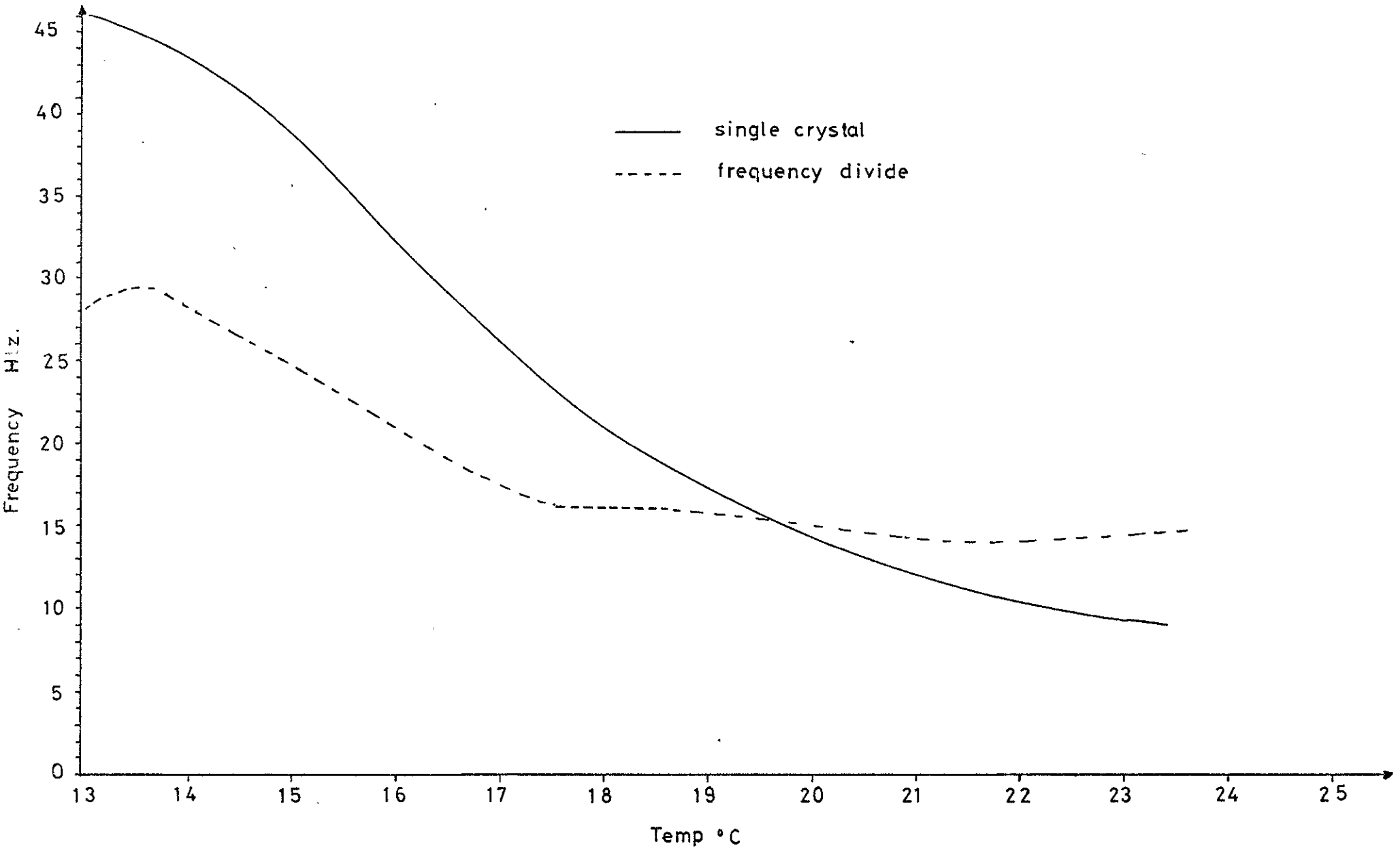
45
40
35
30
25
20
15
10
5
0
Frequency Hz.
single crystal
frequency divide
13
14
15
16
17
18
19
20
21
22
23
24
25
Temp °C

FIGURE 18

FIGURE 19a

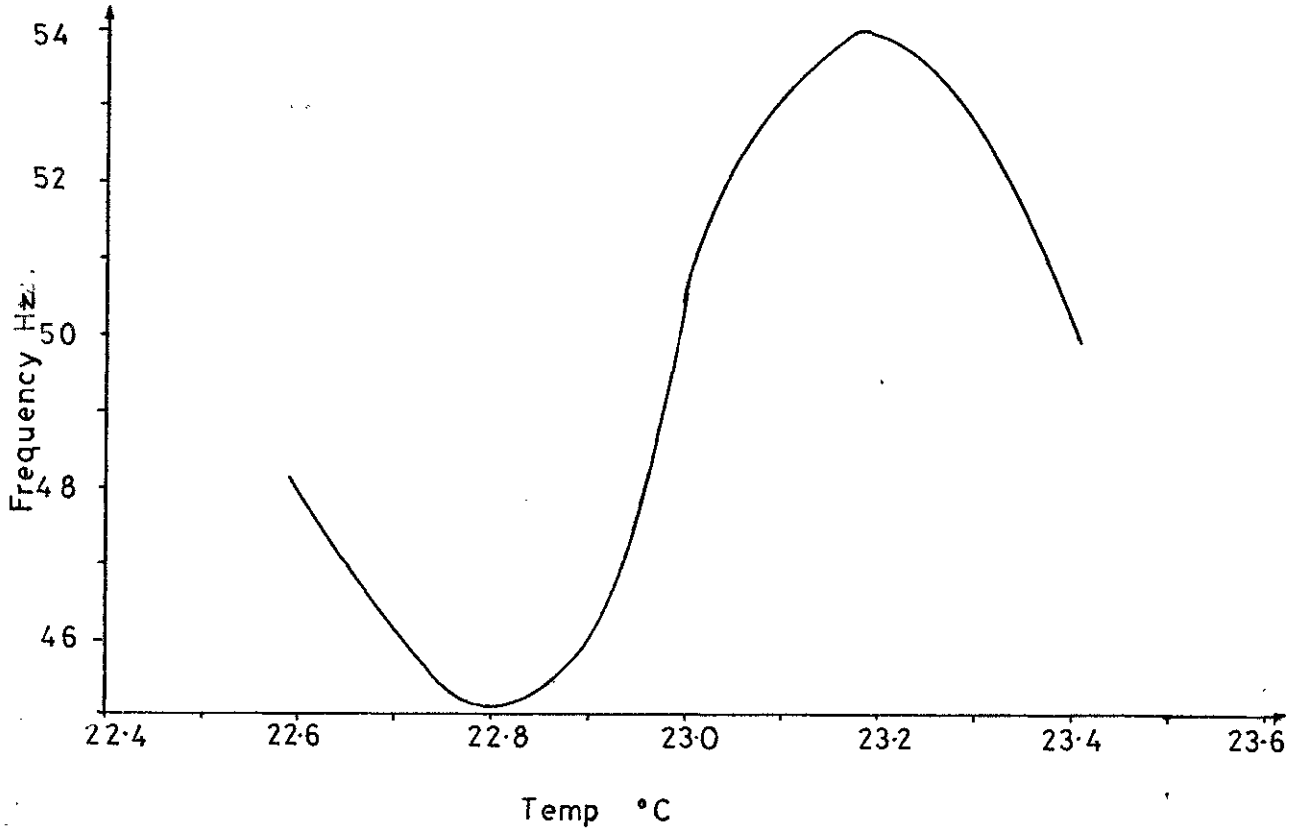

FIGURE 19b

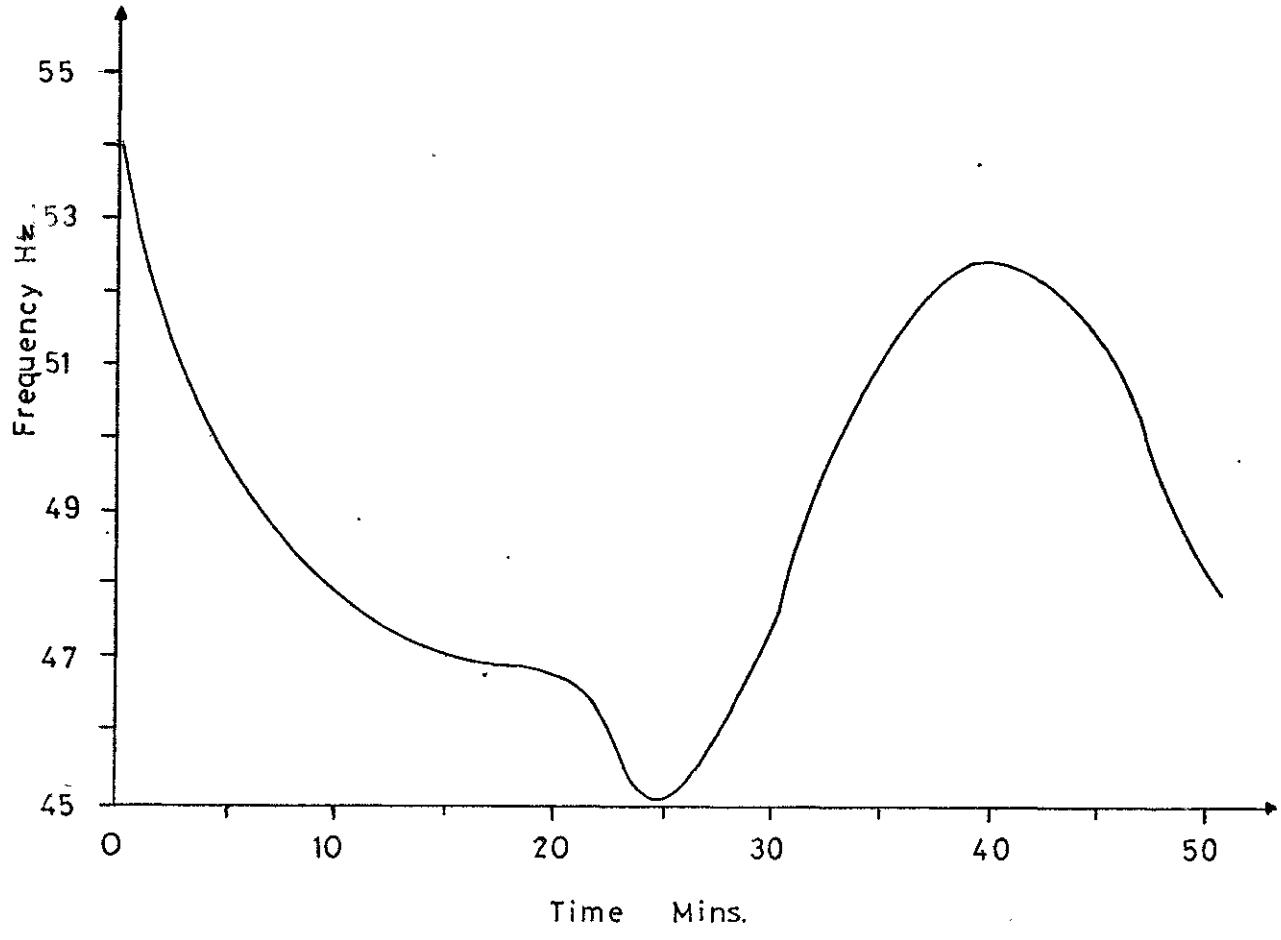

per side of "Carbowax 20M" was placed in a low volume impinger detector cell (see Section 3.2.2). The cell was immersed in a Grant Instruments water bath at 31.5°C ± 0.1°C. No gas flow was used, and the frequency readings were taken over a 110 minute period. The results were plotted as frequency versus time. See figure 20.

It may be seen from this series of experiments that the major cause of drift in simple systems, utilizing both coated and uncoated crystals, was due to temperature fluctuation. From figures 17a and b, the effect of temperature change on frequency clearly may be seen. Comparison of graphs 19b and 20 demonstrates the marked effect on frequency drift of eliminating temperature fluctuations by thermostatting. Care must be taken in the interpretation of drift data from coated crystals, since these crystals have a lower Q value than their uncoated counterparts. The Q value of a crystal is a measure of its electrical quality in the circuit, and the lower the value of Q the more susceptible the crystal becomes to alterations in circuit parameters. Thus, it is possible to argue that the frequency drift with temperature of graphs 19a and 19b was due to alterations in circuit parameters, and not to a change in the fundamental frequency of the quartz plate. This argument may be defeated, by comparing graphs 19b and 20, and by noting two important points. The crystal used to obtain graph 20 was coated with ten times the material present on the surface of the crystal used for graph 19b, hence the Q value would be expected to be lower, and greater drift

FIGURE 20

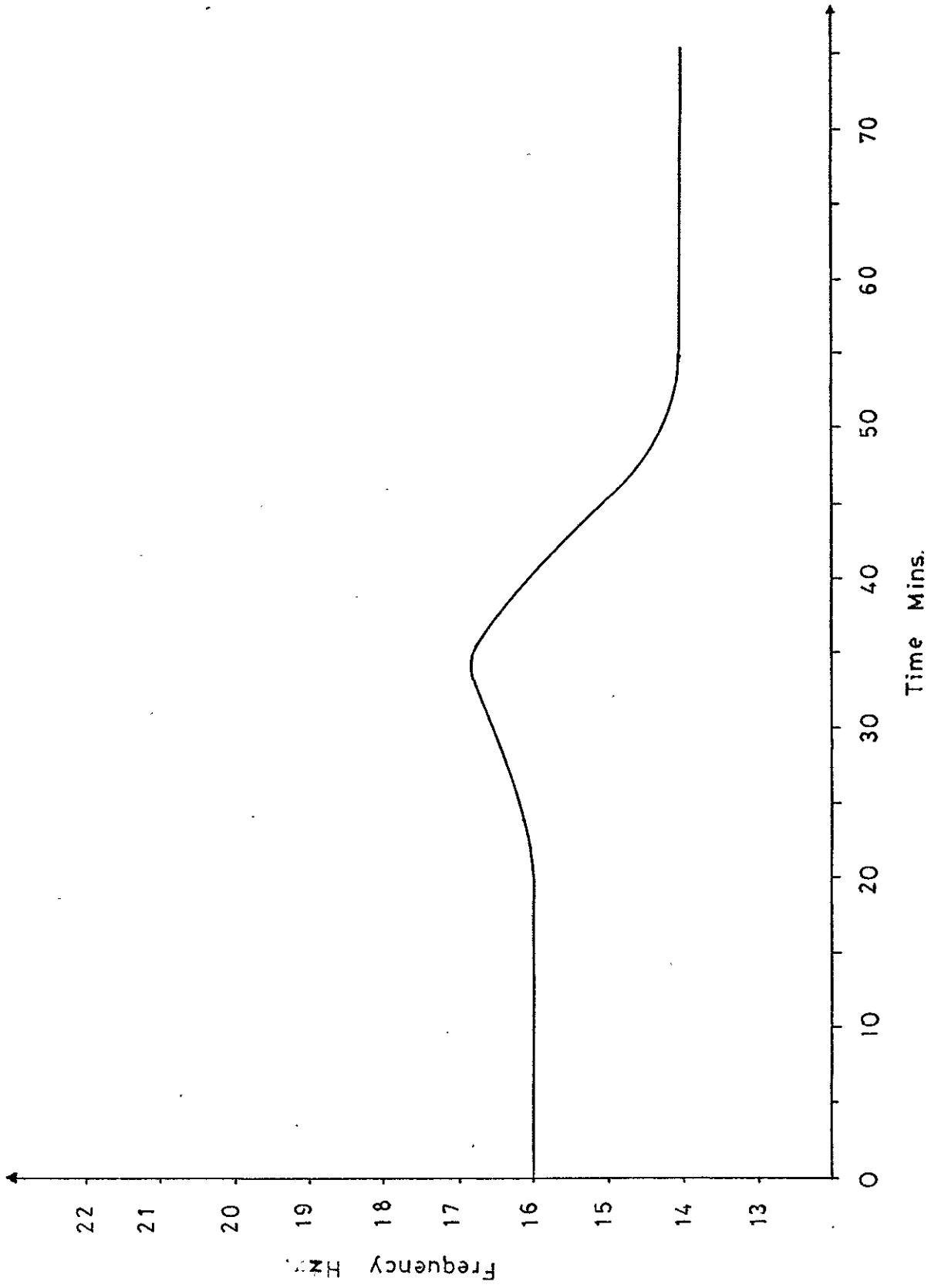
Frequency Hz.
22
21
20
19
18
17
16
15
14
13
0
10
20
30
40
50
60
70
Time Mins.

would be seen in figure 20 than in figure 19b, were the "Q value" argument to be correct. The validity of this first point is reinforced, when it is understood that the ambient temperature drift, to which the oscillators were subject was approximately the same in both experiments, since it was only the crystal in its detector housing that was held at a fixed temperature. Another possible source of drift, was that the frequency of the internal frequency standard of the digital counter was altering with the fluctuations in ambient temperature. Certainly this is to be expected, since the counter used had no oven for maintaining the internal crystal at a steady temperature. It may be surmised that this drift contribution was small, for the majority of the drift was eliminated simply by thermostatting the sample crystal, no special effort being made to maintain the internal crystal at a fixed temperature.

In figure 18, the effect on drift of frequency dividing may be seen. The drift was reduced by using an external reference crystal, and over the 17.5 to 18.5°C temperature range a plateau region was reached by the frequency divide readings. The incomplete compensation for drift by the frequency divide configuration may be explained by the variability of the value of the temperature coefficient of AT cut crystals described by Warner and Stockbridge[23]. Thus, the two crystals used for this system were not specifically selected for their closeness of match with regard to temperature coefficient variation, and hence, the only partial elimination of drift over most

of the temperature range. The plateau region in the frequency dividing graph can be surmised to be due to the similarity between the temperature coefficients of the two crystals in the 17.5 to 18.5°C range.

The frequency dividing system, although compensating in part for some frequency drift due to temperature alteration, was not considered as effective nor as flexible as thermostatting the crystals. The use of a closely controlled temperature environment gave a superior elimination of drift, could be operated at any selected temperature and required only a single oscillator and crystal set-up. This latter consideration would be of great importance in a system employing more than one type of coated detector, for the frequency dividing method would require duplicates, not only of the oscillators, but also of the coated crystals, thus doubling the complexity of the completed system. The frequency dividing configuration had one major advantage, unassociated with its performance in eliminating drift. The ease with which the digital counter could be switched from internal to external reference, effectively meant that two oscillators could be read simultaneously by one frequency meter, without the need for frequent plugging-in and unplugging of coaxial leads, or the use of a switchable junction box, which could lead to "lock-on" problems.

Short term noise: uncoated crystal.

The short term noise of the system may be seen from figure 16. Figure 21 shows the results of a similar experiment, in that a single oscillator was set up with

FIGURE 21

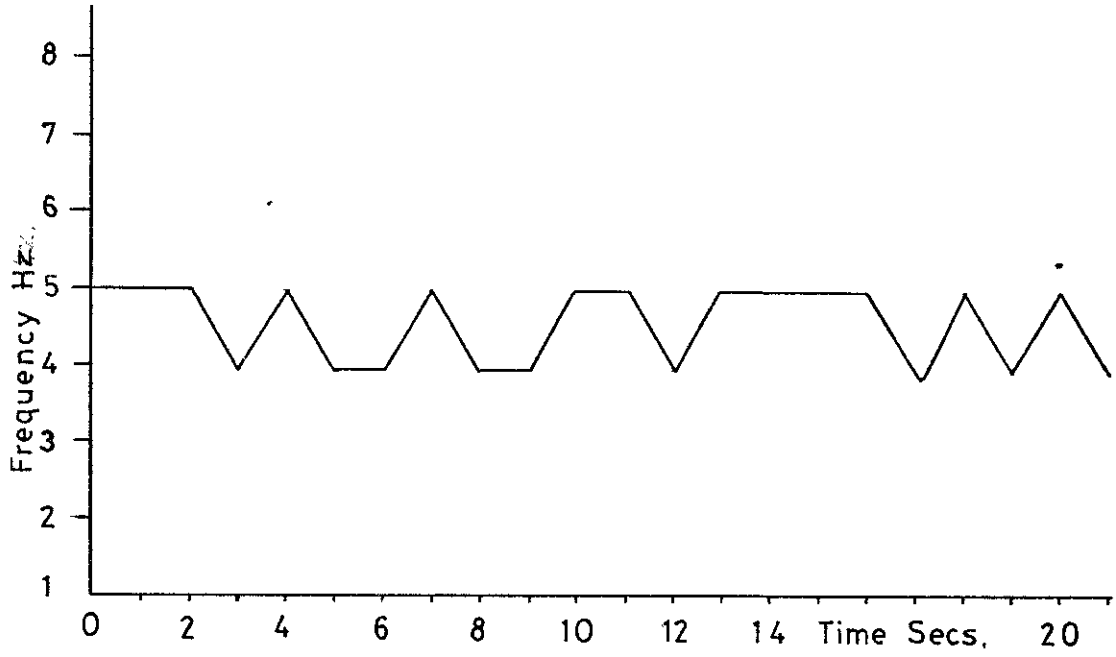

FIGURE 22a

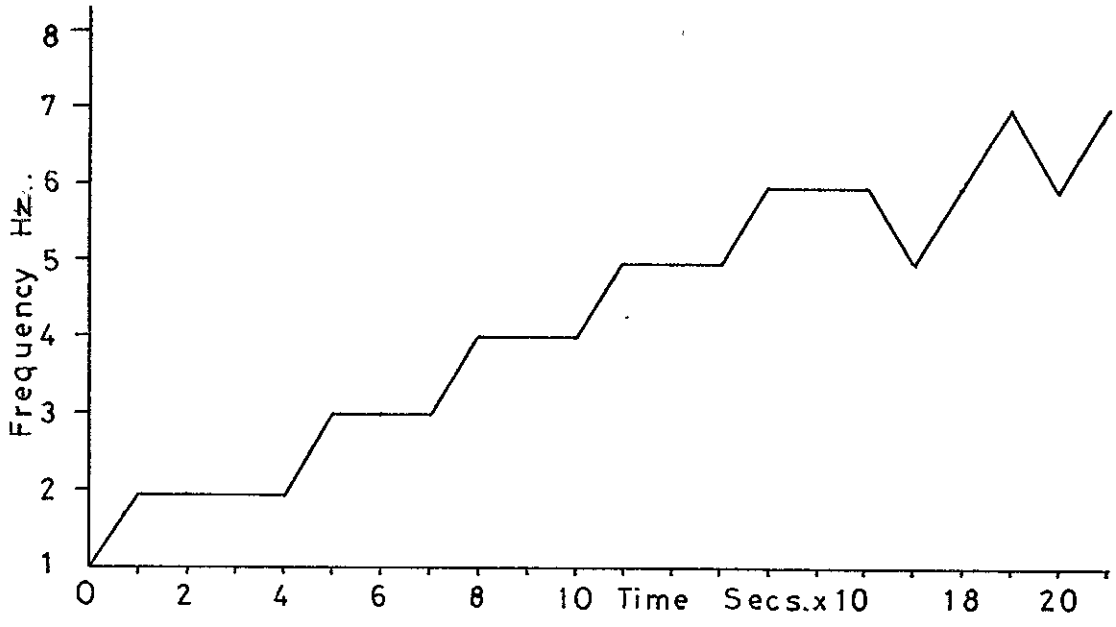

FIGURE 22b

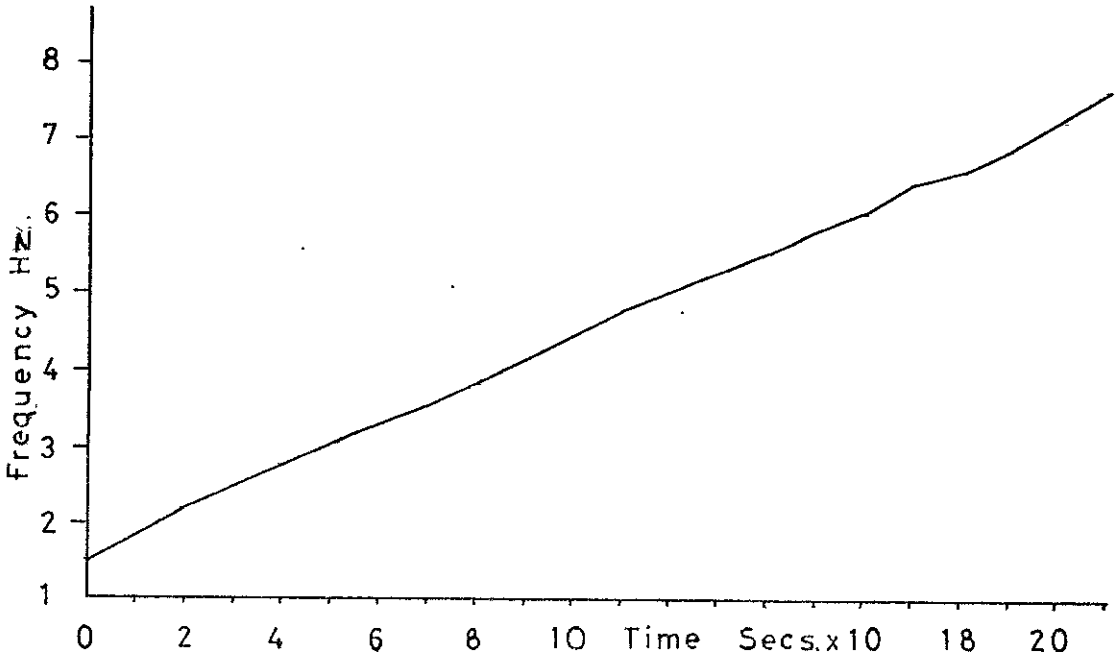

an uncoated crystal in a high volume impinger detector cell at ambient temperatures. Readings of the frequency were taken every second, and a graph drawn of frequency versus time.

Short term noise: coated crystal

A single oscillator was set up with a crystal coated with 20 microgrammes per side of "Apiezon M". One second readings of the frequency were taken every 10 seconds and the results plotted against time. See figure 22a. Simultaneously, readings of the frequency for the same system were taken, using the ten second gating time, by switching from the one second to the 10 second position on the gating-time selector switch. Thus, once every 10 seconds the total count for that period was displayed. The results were plotted as frequency versus time. See figure 22b.

The results from these experiments indicate that for both coated and uncoated crystals a small amount of noise occurs in the base-line frequency. This noise is an inherent property of the digital counter, the accuracy of which is always ± 1 in the last digit. The reason for this uncertainty may be seen from figure 23, where, for the given frequency and time interval (gating period), two different values for the number of peaks counted in that interval may be achieved, depending on the positioning of the time interval. The difference in number is always one, whatever the frequency or time interval. The effect of noise due to electronic or mechanical instability would manifest itself as differences between two successive

FIGURE 23

FREQUENCY READING NO. 1

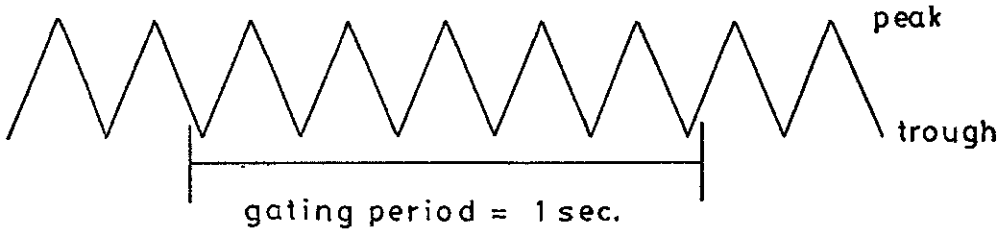

FREQUENCY READING NO. 2

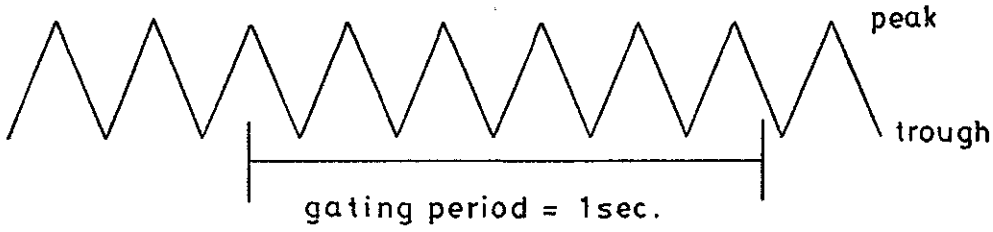

For a counter set to trigger on each wave's trough, reading 1 gives 6 Hz and reading 2, 5 Hz, for identical input signals, depending on the positioning of the gating period.

base-line readings of values greater than one, assuming that, at that point the drift of the crystal was small with respect to random noise. In the situation examined, (figure 21), this phenomenon did not arise, and indeed was not observed throughout the entire study, indicating that the electronic and mechanical short-term noise contributions, if any were present, were negligible.

The effect of using the 10 second gate apparently was to eliminate the ± 1 uncertainty, see figure 22b. This is not so, the noise is still there, but has become less distinguishable against the drift in frequency.

The measurement of the peaks obtained from a piezoelectric detector may be carried out by several different methods, with respect to the peak shape, and by a range of methods with respect to signal handling techniques. The application of different methods of peak measurement concerned with the shape of the peak will be discussed in Section 3.2. The subject of this section is the signal handling aspect of peak and base-line measurement. It should be noted that the signal obtained from the detector is a frequency depression rather than a peak. However, it is convenient to refer to the signal as a peak, and this terminology will generally be used.

Factors affecting estimation of the base-line frequency.

The results of the experiment whose results are illustrated in figures 22a and b were recorded in tabular form and statistical analyses carried out on them, see Table 1a. A single oscillator was set up with a squalane coated crystal located in the low volume impinger detector

TABLE 1a

All readings presented as 3 least significant digits of frequency expressed to one decimal place.

1 SECOND MODE READINGS	10 SECOND MODE READINGS
2.0	1.5
3.0	1.8
3.0	2.2
3.0	2.5
3.0	2.8
4.0	3.1
4.0	3.3
4.0	3.5
5.0	3.8
5.0	4.1
5.0	4.4
6.0	4.7
6.0	5.0
6.0	5.2
7.0	5.5
7.0	5.7
7.0	6.0
6.0	6.3
7.0	6.5
8.0	6.8
8.0	7.2
9.0	7.6
Mean = 5.363 S.D. = 1.896 R.S.D.= 35.35%	Mean = 4.522 S.D. = 1.763 R.S.D.= 38.99%

TABLE 1b

10 SECOND MODE READINGS	100 SECOND MODE READINGS
71.0	68.1
76.0	73.8
77.0	76.9
79.0	77.9
79.0	79.1
78.0	79.1
80.0	78.8
83.0	81.4
84.0	83.1
82.0	83.2
82.0	82.1
75.0	78.9
67.0	70.0
62.0	64.7
59.0	58.8
Mean = 75.46 S.D= 7.94 R.S.D=10.5%	Mean = 75.73 S.D. = 7.24 R.S.D.= 9.6%

cell, there was no gas flow, and the cell was maintained at the ambient temperature. Frequency readings were taken using a 10 seconds gating time and a 100 seconds gating time. The latter was achieved by using a one MHz external reference source. Thus, when the internal reference (10 MHz) was used, and a 10 second gating time selected, the entire frequency count over that 10 second period was displayed: by switching from the internal reference to the external reference a 100 second gating time was employed. The 10 second and 100 second readings were taken alternately. The results were tabulated and statistically analysed in the same way as the one second and ten seconds results. See Table 1b.

The results were treated as an estimation of the value of the base-line frequency. Inspection of both sets of figures indicates that frequency drift was experienced over the two measurement periods. Comparison of the relative standard deviations for the one second and ten seconds mode, and for the ten seconds and one hundred seconds mode shows that there is very little difference in the precision achieved by either the shorter or the longer periods of frequency counting. In some respects, this is an unexpected result. In both experiments the two series of measurements, one with a shorter gating period, the other with a ten times longer gating period, were taken over the same time period, and represented estimations of the same base-line frequency. The difference between the individuals of each pair of measurements was purely the length of time taken to amass the total count. In this respect, the difference could be regarded

thus: the one second result represented a one point determination of the base-line frequency; the ten seconds result represented a time-averaged account of the base line, equivalent to the average of ten successive readings. It would be expected therefore, that the uncertainty arising in the least significant digit would tend to be averaged out in the longer gating time, and that for the gating time a decade larger in each pair of results, a lower relative standard deviation should occur. This expectation was not fulfilled. The results from Table 1a were corrected for base-line drift, and statistical calculations carried out on these results, see Table 2. It can be seen that when base-line correction is made, the relative standard deviations of the two results differ widely: a "t" test carried out on the results showed that the difference between the standard deviations was significant at the 99% certainty level. These results fulfil the expectation that longer gating periods should give a more precise account of the base-line frequency. The failure of the other data in tables 1a and 1b to demonstrate this result can be attributed to the drift in the values, causing an apparent scatter of results that swamped the scatter due to the ± 1 uncertainty in the least significant digit.

The measurement of peaks arising from the piezoelectric monitor, whether by peak height or peak area, can only be implemented if the value of the base line is also known. The general measurement procedure should be: assess the base line prior to the peak; assess the desired

TABLE 2

All readings presented as last 3 digits of the frequency, including one decimal place.

1 SECOND MODE READINGS	10 SECOND MODE READINGS	1 SECOND MODE READINGS	10 SECOND MODE READINGS
14.0	13.5	14.5	13.7
14.7	13.5	15.2	13.7
14.7	13.7	15.0	13.6
14.9	13.7	14.6	13.6
15.2	13.7	13.4	13.7
14.6	13.7	14.1	13.6
14.4	13.7	14.8	13.6
14.1	13.6	14.5	13.8
14.8	13.6	15.3	13.9
14.5	13.7	15.1	14.1
14.3	13.7	14.7	14.1
15.1	13.7	15.5	14.2
14.7	13.7		

1 second: Mean = 4.66
S.D. = 0.47
R.S.D. = 10.1%

10 second: Mean = 3.72
S.D. = .17
R.S.D. = 4.5%

TABLE 3

All readings presented as 3 least significant digits.

100 SECOND MODE READINGS		10 SECOND MODE READINGS	
Base Line	Difference	Base Line	Difference
681		774	
*738	-13	*774	+0.5
769		775	
*779	+1	*776	-0.5
791		776	
*791	-15	*776	-0.5
788		777	
*814	-4.5	*776	-1.0
831		777	
*832	-6.0	*777	0.0
821		777	

value of the peak; assess the base line after the peak; extrapolate the base-line value through the peak and calculate the desired peak parameter. Three distinct methods of carrying out this procedure may be defined: (i) point sample readings of the base-line and peak may be taken at suitable intervals using the one second mode; (ii) point-sample readings of the base-line and peak may be taken using a 10 second gating time, or longer gating time if desired; (iii) the peak area and base-line may be determined by continuous assessment, preferably using a gating time that can accommodate the entire peak area within a single count.

Maximum precision and accuracy of peak measurement can be attained by careful selection of the correct measuring method with respect to the following parameters: magnitude and stability of drift; peak height or peak area magnitude; peak length. Consider table 3, which sets out 10 consecutive results of 10 second gating time and the parallel 100 second gating time results from table 16. The difference column beside each asterisked number represents the value obtained by subtracting that number from the estimated value achieved by averaging the values of the two contiguous numbers. Suppose a four second sample of analyte had been introduced to the system to coincide with the asterisked count, and whose total peak area response had been 40 Hz. It can be seen that the variation superimposed on this value, from the estimation of the base-line which would not be directly accessible, would cause a much poorer precision for results obtained

using the 100 second gating period, than for results utilizing the ten second gating period.

Analogue Representation of the Signal.

Two oscillators were set up, one with a squalane coated crystal, the other with a "Carbowax 20M" coated crystal. Each crystal was located in a low volume impinger detector cell, oxygen-free nitrogen passed over the crystals at 12 mls per minute, and the cells thermostatted at 30°C. The frequency of the "Carbowax 20M" crystal was monitored by the digital counter, encoded in BCD and taken via a laboratory-built interface to the Hewlett Packard digital-analogue converter. The voltage signal was displayed on the "Servoscribe" chart-recorder. The converter was used to calibrate the recorder, by adjusting the full scale deflection of the recorder pen on the 100 mV scale, from the potentiometer on the converter. A selector on the converter was set to convert the last two digits of the frequency, so that each division on the chart recorder represented a one Hertz change in frequency. The frequency of the "Carbowax 20M" coated crystal was followed for a 16 hour period using this set up. See figure 24 a.

The inset on figure 24 shows the step-like type of output obtained with this system as a result of the one second gating time updating the converter with new information. At point x on the figure it can be seen that as the frequency decreased from 200 to 199 (for example), the converter immediately switched to the full scale deflection from the zero value. Effectively this

FIGURE 24a

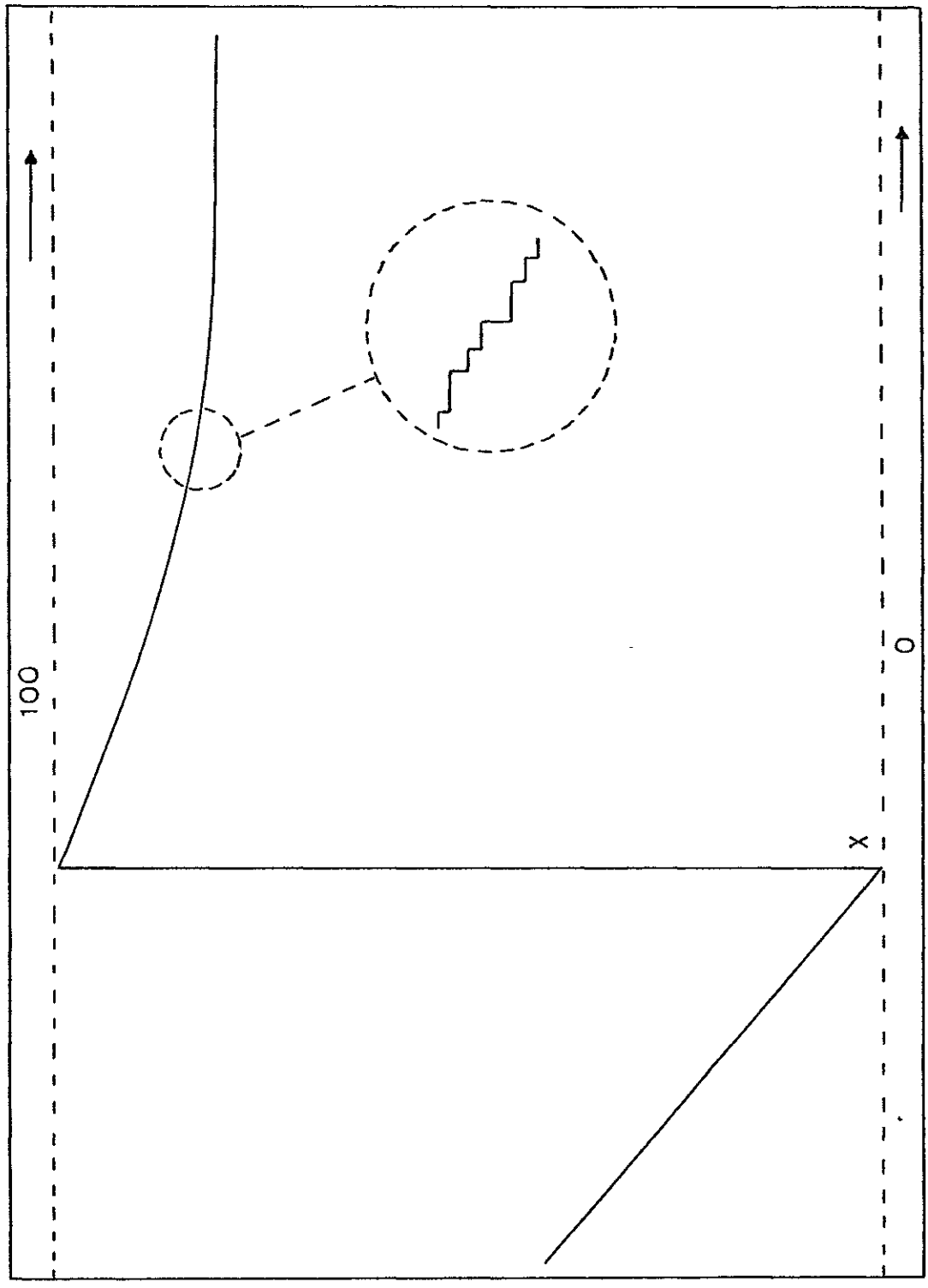

means that the output from the converter can never go off scale, providing that the 100 mV scale is used. Thus the frequency drift of a crystal can be monitored by this equipment for long periods of time, with the minimum of attention. The converter was found to be extremely useful for the rapid display of results, and for the creation of a permanent record of the behaviour of the piezoelectric detector. A digital data-logging system would have provided a more accurate method of recording the signals, as well as providing for a more rapid data manipulation by digital computing techniques. In the absence of this type of equipment the digital/analogue converter greatly assisted in data acquisition.

3.2 DETECTOR CELL DESIGN: GAS HANDLING: SAMPLE INTRODUCTION

3.2.1 Theory

The majority of coatings used to fabricate piezoelectric detectors in this study exhibited dissolution as the dominant analyte pick-up mode. The interactions of liquids and waxes with analyte gases could be estimated by the system's partition coefficient. It has been shown that these coatings respond rapidly and reversibly to analytes[88], and that the system for optimum use of these coatings employs a flowing gas stream, since static systems favour slow coating/analyte interactions[74]. The value of a flowing gas stream may be seen from the following consideration. In a piezoelectric detector, the two phase system, carrier gas and liquid coating, are in contact at

an interfacial boundary in an enclosed volume. Let the volume of gas be equal to the volume of liquid, and initially let there be x grms. of analyte present in the gas stream and zero grms. of analyte present in the liquid coating. K is the partition coefficient between the two phases, such that $K = \frac{\text{Mass of X in liquid/unit volume}}{\text{Mass of X in gas/unit volume}}$, for the equilibrium situation.

Thus, after equilibrium has been achieved in the case under consideration, the mass of analyte in the liquid, C_1 grms, and the residual analyte mass in the gas stream $x-C_1$ grms are related by: $K = \frac{C_1}{x - C_1}$.

That is: $$C_1 = \frac{Kx}{K + 1} \quad \ldots\ldots\ldots \quad 3.24$$

If the gas phase is now replaced by a fresh volume of gas containing x grms of analyte, a second equilibrium will occur, and a new mass of analyte C_2 grms will enter the liquid phase.

Then, $$\frac{C_1 + C_2}{x - C_2} = K$$

and $$C_2 = \frac{K^2 x}{(K + 1)^2} \quad \ldots\ldots\ldots \quad 3.25$$

Similarly it can be shown for the n^{th} equilibrium that:

$$C_n = \frac{K^n x}{(K + 1)^n} \quad \ldots\ldots\ldots \quad 3.26$$

After n equilibria the total analyte mass in the liquid is given by

$$C = \sum_1^n C_n = x\left(\frac{K}{K + 1} + \left(\frac{K}{K + 1}\right)^2 \ldots\ldots \left(\frac{K}{K + 1}\right)^n\right) \quad 3.27$$

Equation 3.27 is a geometric progression whose sum(s) may be calculated from:-

$$s = \frac{\left(\frac{K}{K+1}\right)\left(1-\left(\frac{K}{K+1}\right)^{n}\right)}{1-\frac{K}{K+1}} \qquad \ldots\ldots 3.28$$

Substituting 3.28 in 3.27 gives:

$$C = x\left[\frac{\left(\frac{K}{K+1}\right)\left(1-\left(\frac{K}{K+1}\right)^{n}\right)}{1-\frac{K}{K+1}}\right]$$

As $n \longrightarrow \infty$, $\left(\frac{K}{K+1}\right)^{n} \longrightarrow 0$

Thus $C = x\left[\frac{K/(K+1)}{1-(K/(K+1))}\right]$

Which simplifies to:

$$\underline{C = Kx} \qquad \ldots\ldots 3.29$$

Thus, in a situation where carrier gas bearing the analyte continually flushes the detector cell, the coating is gradually loaded with analyte to an equilibrium value, which cannot be exceeded. The number of cell flushes required to attain this value theoretically is infinite, in practice equilibrium is achieved by a finite number of equilibria. Consider the case where K = 80, and x = 1 grm, the maximum concentration in the coating = Kx = 80 grammes. Solution of equation 3.28 for values of n from 100 to 500 have been plotted as C against n in figure 24b. It can be seen from this figure that after 300 equilibria 97.5% of the equilibrium value has been reached, and that at 500 equilibria this value has become 99.75%

FIGURE 24 b

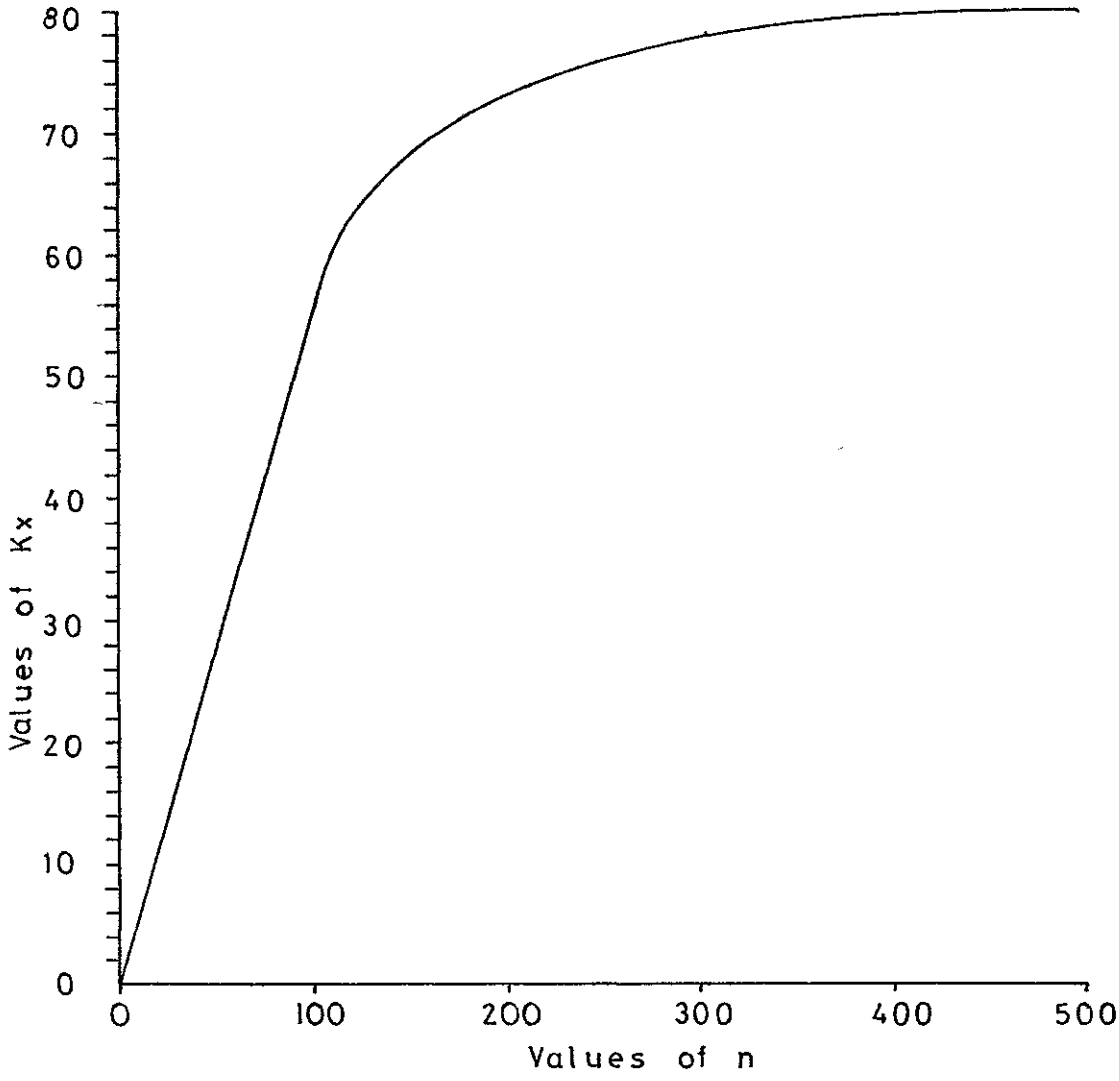
80
70
60
50
40
30
20
10
0
Values of Kx
0
100
200
300
400
500
Values of n

An important criterion for detector cell design may be seen from these results. The volume of the detector cell must be kept small in order to ensure rapid flushing of the cell, so that the maximum number of equilibria will occur for a sample of short duration in the carrier gas, and the resulting detector response will be optimal. Similarly, a low detector cell volume will be beneficial for analyte samples of longer duration, where the equilibrium value of analyte concentration in the gas coating has been reached, since rapid response to changes in the concentration of the analyte in the carrier gas stream can only take place where rapid flushing of the cell obtains. It could be argued that the detector volume could assume a fairly high value, and that rapid flushing of the volume could be achieved by using higher flow rates of the carrier gas. This approach is valid, only within limits, since the use of rapid carrier gas flow rates gives rise to problems of coating bleed from the detector. However, it should be noted that the increase of carrier gas flow rate for analyte slugs of similar duration and concentration will increase the response obtained providing that the equilibrium value has not been reached, and providing that the flushing rate is not so rapid that insufficient time is allowed for analyte/coating interaction.

The theory of the behaviour of the detector with respect to analyte mass, sample duration, coating liquid volume, partition coefficient and flow rate has been worked out by Janghorbani and Freund[88], for the situation

where equilibrium concentration of the analyte in the coating has been achieved.

Consider a simplified form of the equations relating ΔF to Δm developed in Chapter 2.

$$\Delta F = -B\ \Delta m \qquad \ldots\ldots\ldots\ldots \quad 3.30$$

where $$B = \frac{1}{\sqrt{A r_1 t}}$$

For a piezoelectric detector, where the total mass of analyte in the gas stream is W_T grms, length of analyte slug in gas stream is t seconds, volume of coating is V_c mls, volume of detector cell is V_g mls and partition coefficient is K, an expression may be derived from equations 3.29 and 3.30 thus:

$$\Delta f = -\frac{B\ K\ W_{T_i} V_c}{V_g} \qquad \ldots\ldots\ldots \quad 3.31$$

Where W_{T_i} = mass of analyte gas always present in the detector cell, and Δf = change in frequency of the detector. Consider a time interval Δt, in which one complete flush of the cell occurs.

Then $$\Delta t = \frac{V_g}{F} \qquad \ldots\ldots\ldots\ldots \quad 3.32$$

where F = flow rate of the carrier gas.

Multiply 3.31 and 3.32.

$$\Delta f \cdot \Delta t = -B \frac{K\ W_{T_i}}{V_g} \cdot V_c \cdot \frac{V_g}{F}$$

$$= \frac{-B\ K\ W_{T_i} V_c}{F} \qquad \ldots\ldots\ldots \quad 3.33$$

The total peak area $A = \sum \Delta f \cdot \Delta t$.

Thus: $$A = -\frac{B\ K\ V_c}{F} \sum W_{T_i},$$

but $$\sum W_{T_i} = W_T$$

Therefore $$A = -\frac{B\ K\ V_c\ W_T}{F} \qquad \ldots\ldots\ldots \quad 3.34$$

$$\text{Also,} \quad W_{T_i} = \frac{W_T}{t} \cdot \frac{V_g}{F} \qquad \ldots\ldots\ldots \quad 3.35$$

Substitute 3.35 in 3.31.

$$\Delta f = - \frac{B\ K\ W_T}{t.F} \cdot V_c \qquad \ldots\ldots\ldots \quad 3.36$$

Equations 3.34 and 3.36 illustrate a number of interesting facets of the behaviour of the piezoelectric detector operating under equilibrium conditions. Firstly, the volume of the cell V_g, does not directly affect the sensitivity of the detector in any way. However, if $\Delta t = \frac{V_g}{F} > t$, then dilution of the analyte slug will occur in the detector volume, and response will be lost. Secondly, both measures of the peak, peak area, and peak height, are proportional to W_T, the total mass of analyte introduced to the system, but the peak height may be expected to give less reproducible results since an extra experimental factor, t, enters into its value. Thirdly, A and Δf are proportional to the reciprocal of the flow rate. Finally Δf is proportional to the reciprocal of t. The last two considerations are logical extensions of the mechanics of sample introduction. Thus, an increase in the value of the flow rate, for a given sample introduction rate must cause a greater dilution of the sample and hence a reduction in the obtained response. Similarly, by increasing the time length in the gas stream of a sample of given mass in a constant gas flow rate, the concentration must be reduced.

An important parameter in an analytical system, is the extent of the linearity of the working curves. Equations 3.34 and 3.36 indicate that a continuous linear

relationship between A and W_T and Δf and W_t should be obtained. A graph of this relationship is shown in figure 25, where it may be seen that the y axis could be relabled partial pressure of analyte gas, and the system considered as an equilibrium of a solution with the partial pressures of its constituents. Then, consider the two laws of solution. Raoult's law states that, for an ideal solution of two components A and B, where the cohesive forces A-A, A-B and B-B, are all equal, the partial pressure above the solution due to the component A, P_A is given by: $P_A = X_A P_A^O$. Where P_A^O is the vapour pressure of the pure solution of A, and X_A is the mole fraction of A in the A/B solution. Henry's Law states that, for a dilute, non-ideal solution of a component B in A, where molecules of B can be considered as being surrounded entirely by A molecules, i.e., B is in a uniform environment, $P_B = X_B k$, where P_B is the vapour pressure due to B above, the solution, X_B is the mole fraction of B in the solution, and k is a constant peculiar to the system, and not equal to P_B^O, the vapour pressure above a pure B solution. Thus, for a dilute non-ideal solution of B in A, as $X_B \longrightarrow 0$, $P_B \longrightarrow X_B \cdot k$ (Henry's Law) and $X_A \longrightarrow 1$, $P_A \longrightarrow X_A P_A^O$. For the piezoelectric detector, where the analyte vapour (B) is dissolved in the coating (A), the value of X_B builds up linearly with P_B, until the conditions for Henry's Law break down, and the non-ideality of the system causes the working curve to cease being linear. A corollary of Raoult's Law, is that, for the coating A, the continued dissolution of B in A will lower P_B, and hence help to reduce the bleed rate of the coating.

FIGURE 25

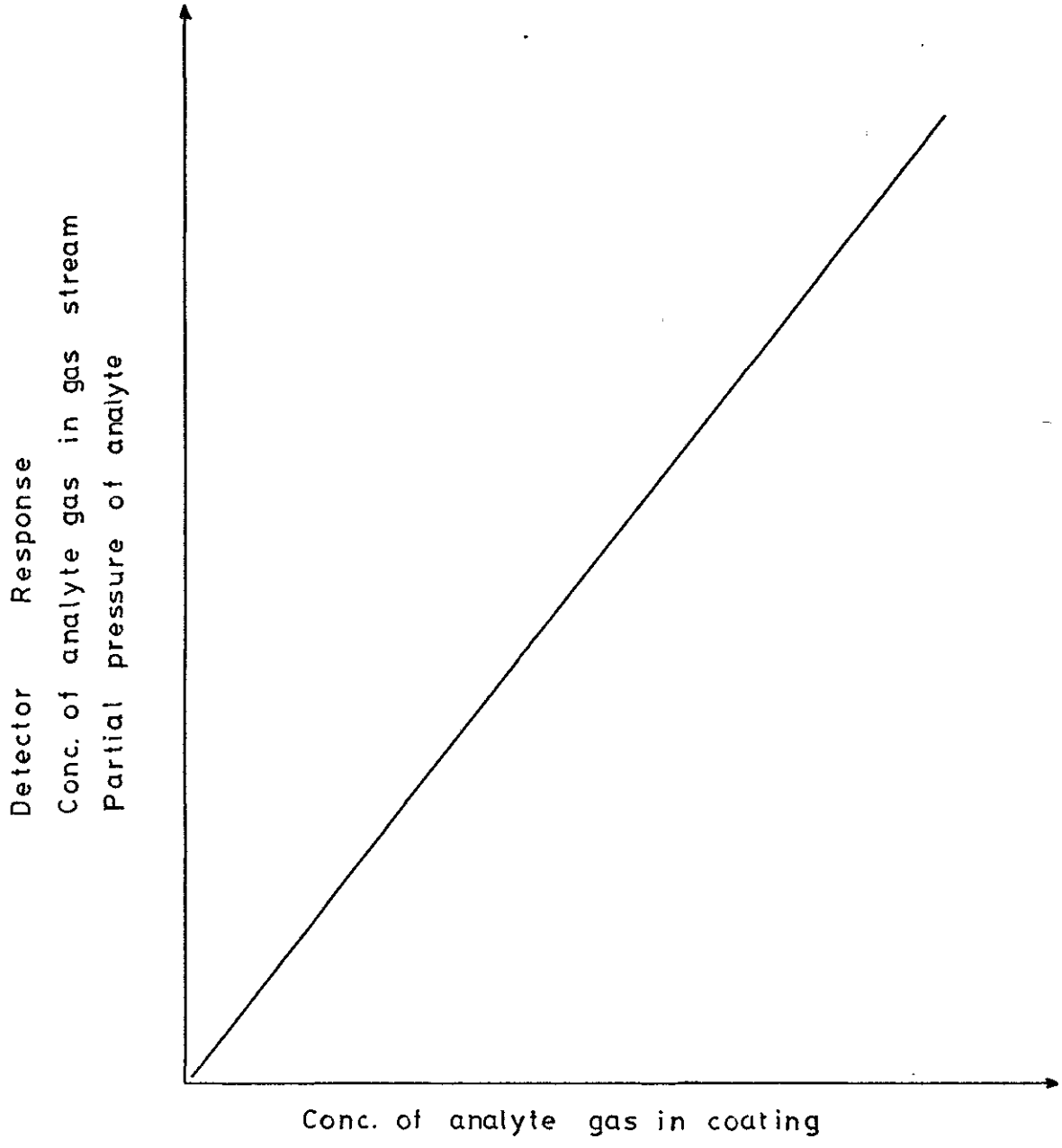
Detector Response
Conc. of analyte gas in gas stream
Partial pressure of analyte
Conc. of analyte gas in coating

Detector cell design.

Some of the parameters for detector cell design have already been discussed. These are:

(i) Cell volume must be kept as low as possible for rapid detector response.

(ii) Sensitivity of the detector to equilibrium attaining samples is not directly affected by cell volume. Other considerations may be added to these two.

(iii) The cell design must ensure that the coated crystal "sees" all of the analyte sample, and that none can pass through the cell without being presented to the coating.

(iv) The design must maintain a constant stable environment around the detector crystal.

(v) Memory effects should be eliminated to prevent undesirable "tailing" of peaks, and a general reduction in the speed of response of the detector to decreasing concentrations of analyte gas.

(vi) The cell should be gas and water tight to prevent loss of analyte vapour or an incursion by water from a water-bath.

(vii) The removal and replacing of crystals in the cell should be simple and reproducible, thus ensuring rapid changeover of detector crystals, with reproducible responses vis-à-vis cell geometry.

A design that satisfied many of these requirements was used by Bristow[79] in his mercury vapour detector. The detector cell was constructed from the metal cap that usually seals the crystal. Two holes, 0.0028 inch in

diameter were drilled through opposite faces of the cap, at points normal to the centre of the crystals gold electrodes, when located in the cell. The carrier gas was split into two streams and ducted through these holes to impinge directly onto the surface of the crystal, the gas exiting from a third hole drilled in the top of the cap. Bristow found that this cell design gave rise to an efficiency of 60% for the collection of mercury on the gold electrode. Two other practicable flowing gas stream detector cell designs have been reported in the literature. King has used a "spoiler" design[58,59] and Bonds[50], Karasak and Gibbins[89] and Janghorbani have described the use of a "sandwich" cell design. In the spoiler cell of King, the carrier gas stream was impinged on one edge of the crystal which acted as a spoiler, splitting the gas stream and passing it over the two faces of the crystal, after which it exited from a similarly placed hole in the opposite side of the detector cell. The sandwich cell (so called because of its method of construction) could be considered as a single jet impinger cell, with the carrier gas striking one face of the crystal before exiting from the second jet of the normal impinger cell. The three designs are depicted in figure 26a, b and c.

The design of the sandwich cell gave rise to some anomalous results. Bonds[50] found that with rapid gas flow rates (50 to 60 ml /minute) and short sample slugs, the difference in sensitivity between a crystal coated on one side, and a crystal coated on both sides was marginal. It will be shown in Section 3.3.2 that the

FIGURE 26a

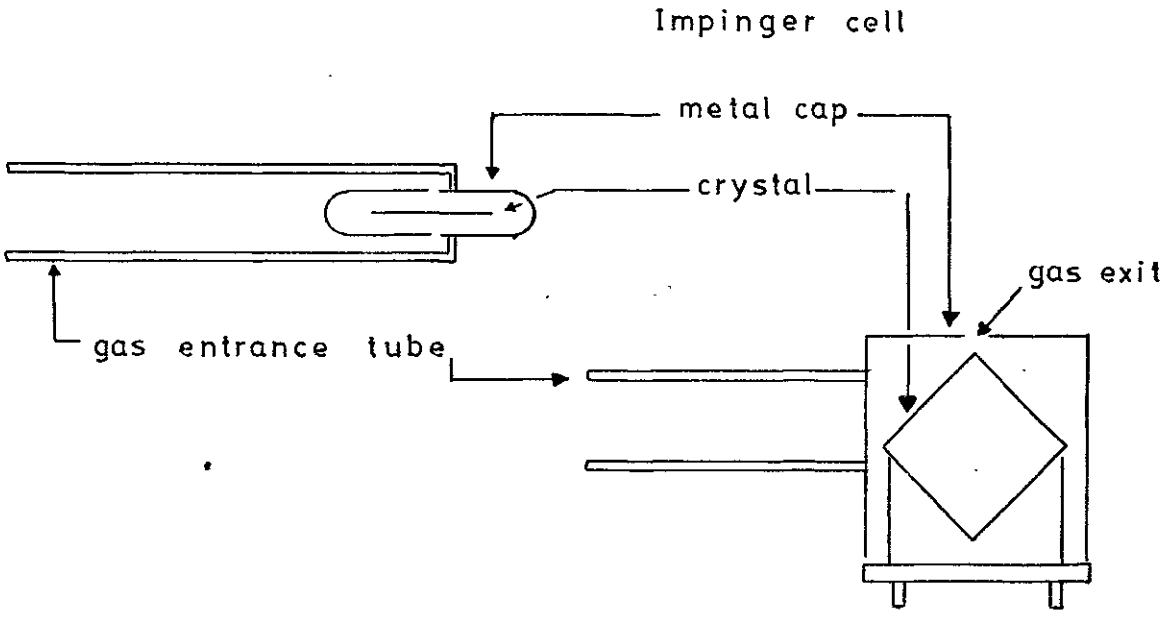

FIGURE 26b

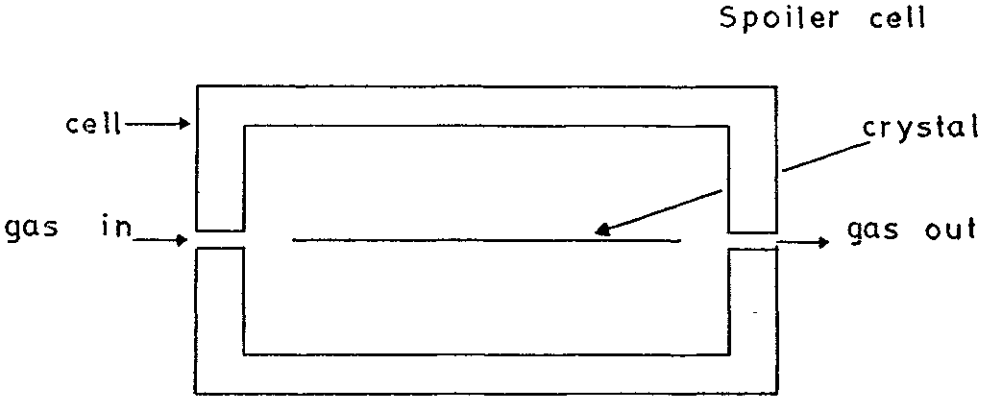

FIGURE 26c

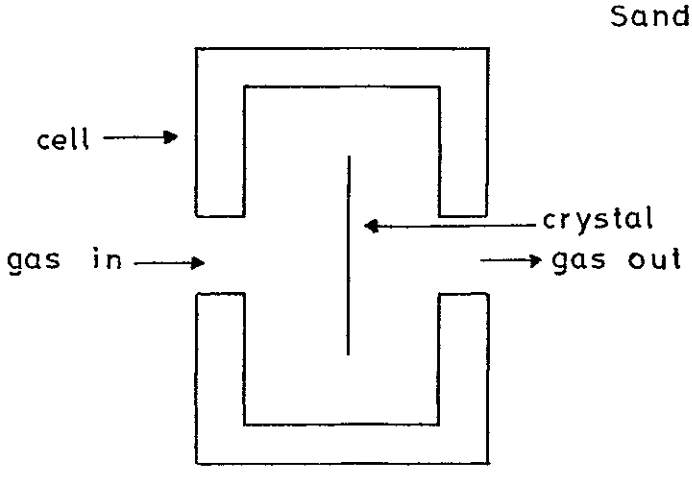

results normally achieved in this type of experiment, give a doubling of response for a two-sides-coated crystal. The unusual results from Bond's work were due to the lack of direct contact between the analyte in the carrier gas stream, and the face of the crystal away from the jet. The major method of sample approach was diffusion for this situation, and at a rapid flow rate the residence time of the analyte species was insufficient to permit diffusion to the reverse side of the crystal, and hence the coating on this side of the crystal was more or less redundant. It is interesting to note that Karasak and Guilbault[80] eventually abandoned the sandwich cell in favour of the impinger design.

The spoiler design requires accurate machining to ensure that the gas flow impinges directly on the edge of the crystal, thus dividing equally down the two sides. Similarly, the crystal must be accurately aligned in the cell to effect reproducible and equal splitting of the carrier gas stream. The geometry of these situations is indicated in figures 27 a, b and c. Incorrect machining, or inaccurate placing of the crystal in the cell, could lead to a situation analogous to the sandwich-cell problem.

Sampling Cell Design

All the compounds selected for general use in this study exist as liquids at room temperature, and develop a significant vapour pressure above the liquid. Expressing the concentrations of these vapours could be carried out in two different ways, depending on the type of unit selected. Volume ratios may be expressed as vapour parts

FIGURE 27a

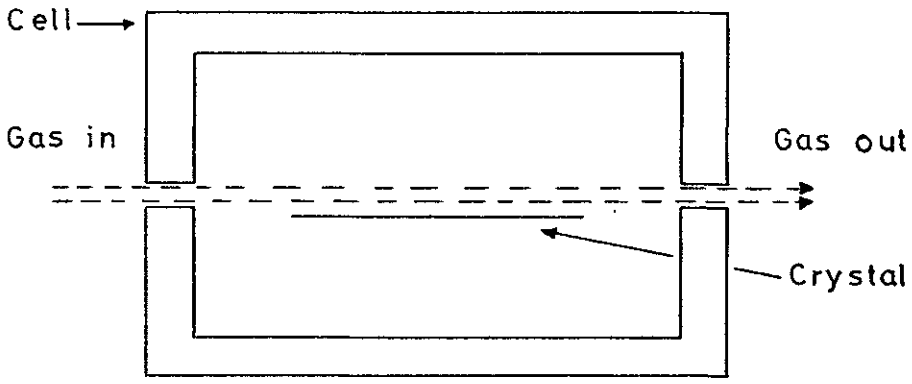

FIGURE 27 b

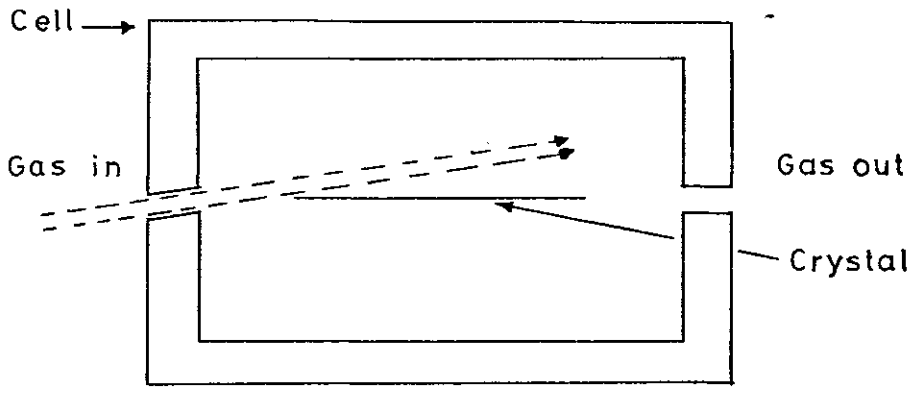

FIGURE 27 c

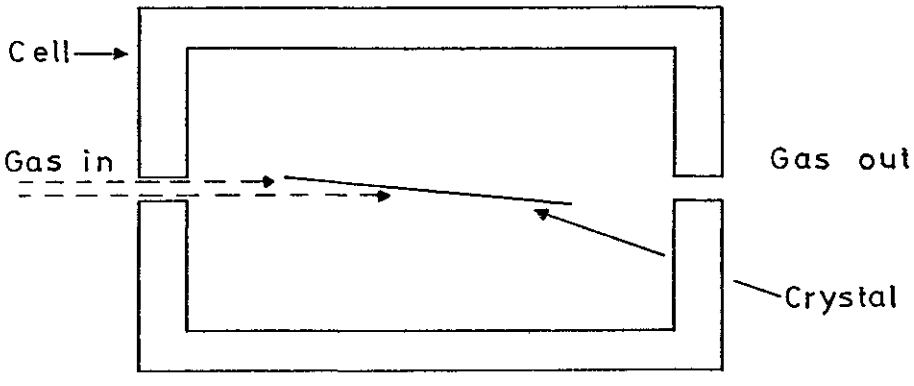

per million (vpm or occasionally ppm) at a given temperature and pressure, and may be derived from the partial pressure of the vapour in the atmosphere. Thus, for an analyte whose partial pressure is p torrs in the atmosphere, where total atmospheric pressure is P torrs, the vpm concentration will be $\frac{p}{P} \times 10^6$. This unit gives information regarding the volume, pressure or number of molecules of analyte present in a sample at a given pressure and temperature. The mass concentration unit, milligrams per cubic meter (mgs per m^3) is independant of pressure and temperature, and matches the type of detection effected by the piezoelectric detector, more aptly than vpm units. Hence mgs per m^3 will be adopted throughout this study.

The simplest sampling device used in this study consisted of an enclosed cell in which was placed a volume of the liquid of interest. The liquid was permitted to equilibrate with its vapour, and then a sample of the vapour withdrawn by gas-tight syringe. Appropriate dilutions of the vapour could be made by injecting a known volume of this vapour into a second enclosed cell, which contained only the diluent gas. Alternatively, a small aliquot of the liquid could be introduced to the cell and allowed to equilibrate completely as the vapour. Calculation of the saturated vapour pressure of a vapour above its pure liquid can be carried out using the following formula :-

$$\text{Log}_{10} P = (-0.2185\ A/K) + B$$

where P = partial pressure of vapour

K = temperature in ^{o}K.

A and B are constants that depend on the liquid under consideration. Values for A and B for a range of liquids are available in the literature.

Generation of sustained pulses of vapour was attempted by three methods: the use of a mercury reservoir; the use of a syringe pump; the use of a diffusion tube vapour generator. Calculation of the vapour concentrations delivered by the first two methods was straightforward: the vapour generator based on diffusion tubes required more complex calculation. This type of generator has been described by McKelvey and Hoelscher[103], Fortuin[104] and Altschuller and Cohen[105]. The vapour was contained in a small glass bulb, as the saturated vapour above a reservoir of liquid. The only exit from the bulb was along a narrow tube whose dimensions, length and cross-sectional area were known. The vapour diffused along this tube, to its exit, where it was carried away in the flow of the carrier gas. The rate of diffusion r grms per second was calculated by Fortuin[104]. The constraints on the calculation of r were that the concentration of vapour at the exit of the tube must be zero, and that the concentration at the entrance of the tube must be equal to the saturated vapour concentration of the liquid. Then:-

$$r = \frac{d\phi}{dt}$$

where ϕ = quantity of vapour diffused in time t.

That is, $$r = - A D \frac{C_t}{C_t - c} \cdot \frac{dc}{dx}$$

where A = cross sectional area of the tube.

D = diffusion rate in

C_t = total concentration of the gas mixture

c = concentration of diffusing vapour at distance x from the entrance of the tube.

Now, p = C.R.T.

and
$$r = -\frac{AD}{RT} \cdot \frac{Pt}{P_t - p} \cdot \frac{dp}{dx} \qquad \ldots\ldots\ldots \quad 3.36$$

Where P_t = total gas pressure of system

p = vapour pressure of gas at distance x from the entrance of the tube

R = gas constant

T = temperature (absolute).

In the stationary state r is constant, and 3.36 can be integrated to give

$$r = \frac{AD}{LRT} \cdot P_t \cdot \ln \frac{P_t - P_c}{P_t - P_o}$$

where P_o = saturated vapour pressure of the liquid

P_t = vapour pressure at tube exit

But $P_c = 0$

$$r = \frac{AD}{LRT} \cdot P \cdot \ln \pi$$

where $\pi = P/(P - p)$

P = Total pressure of the system

p = saturated vapour pressure of the liquid

3.2.2 Practice

Gas handling system.

The flow system for the piezoelectric detector requires: a source of clean, dry carrier gas; a flow meter; detector cells for the crystals; sample introduction area. In this study, oxygen-free nitrogen (OFN) supplied by the British Oxygen Company was used as the

carrier gas. King[55] has shown that the nature of the carrier gas does not affect the sensitivity of the detector: this statement is not completely true, in that differences in partition coefficients for various gases do occur. It would be of interest therefore to ascertain which particular carrier gas gave greatest sensitivity for a given analyte, but bearing in mind that the detector ultimately is to operate on air samples, a carrier gas resembling air, would be of more practical use. OFN was selected to fulfil this latter requirement, and for its uniformity from cylinder to cylinder. The cylinder was fitted with a two-stage regulator, and gas was delivered at 2.0×10^3 kgs per m^2 above atmospheric pressure. The gas was passed along $\frac{1}{4}$ inch O.D. nylon tubing and brass couplings were used throughout the system. A threaded plunger valve controlled the flow of gas through the detector cell, and the gas flow was measured by a laboratory-built capillary flow meter. The meter was constructed from a glass U-tube, part-filled with water, which was used as a manometer to measure the pressure drop across a short length of capillary tube through which the carrier gas flowed. The dimensions of the tube were calculated using Poiselle's equation, and the flow meter was calibrated against a bubble flow meter. Figure 28 gives a diagramatic account of the system.

Two conformations were possible if more than one detector cell was to be incorporated into the system of gas flow: the cells could be put parallel to one another and the gas stream split so that half went to each, or the

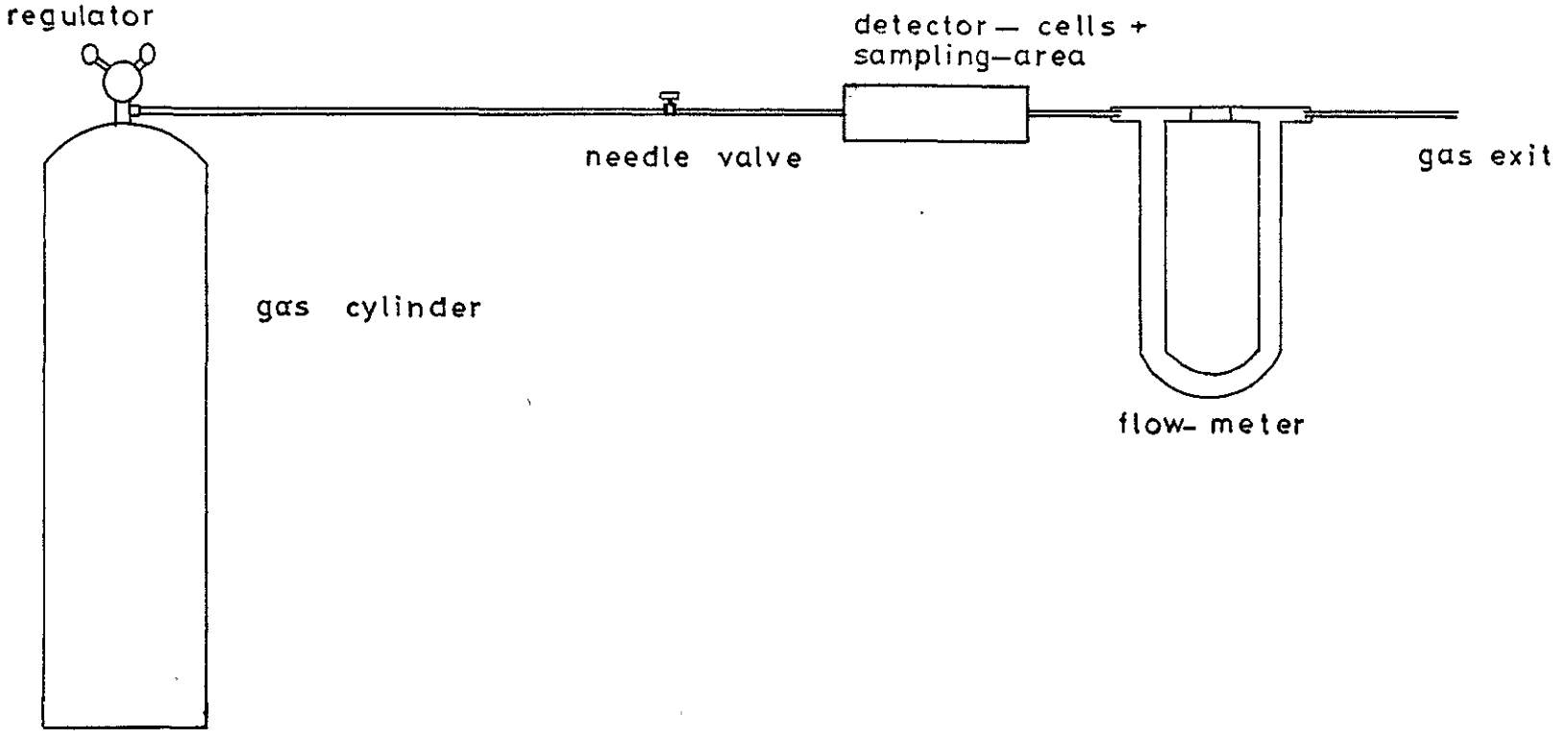

Gas system used in this study

FIGURE 28

cells could be put in series. The parallel conformation provided identical environments for the two detectors, whereas the downstream crystal in a serial system not only received any analyte after it had already reacted with one coating, but also was the recipient of any bleed from the upstream crystal.

Variation of uncoated crystal frecuency with gas flow.

An uncoated crystal was placed in the high volume impinger detector cell, and a gas flow of 50 mls per min was maintained through the cell. The frequency was recorded every five minutes for a given period. The experiment was carried out on three occasions, using the same crystal each time. The results were plotted as frequency change against time, and are depicted in figure 2 9.

Variation of frequency of a cleaned uncoated crystal with gas flow.

The crystal from the previous experiment was removed from the cell and thoroughly cleaned by first soaking the crystal in cold dilute nitric acid for two hours. The crystal was removed from the acid, rinsed in distilled water and dried in an oven at 70°C. The crystal was then soaked in chloroform, air-dried, and then set up in the same cell, using the same oscillator and identical conditions to the previous experiment. The frequency of the crystal was read every five minutes for three hours, when the crystal was removed and the cleaning procedure repeated. The crystal was set up again under the same conditions and the frequency monitored similarly. The results were plotted as frequence versus time, see Figures 30 a and b.

FIGURE 29 a

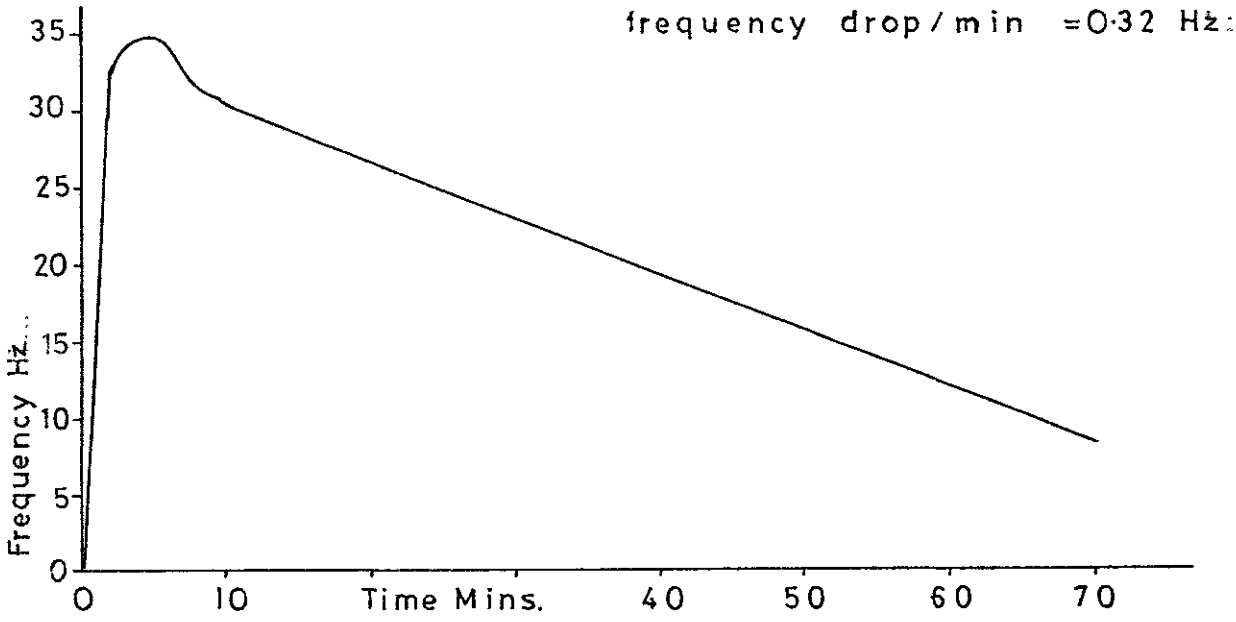

FIGURE 29 b

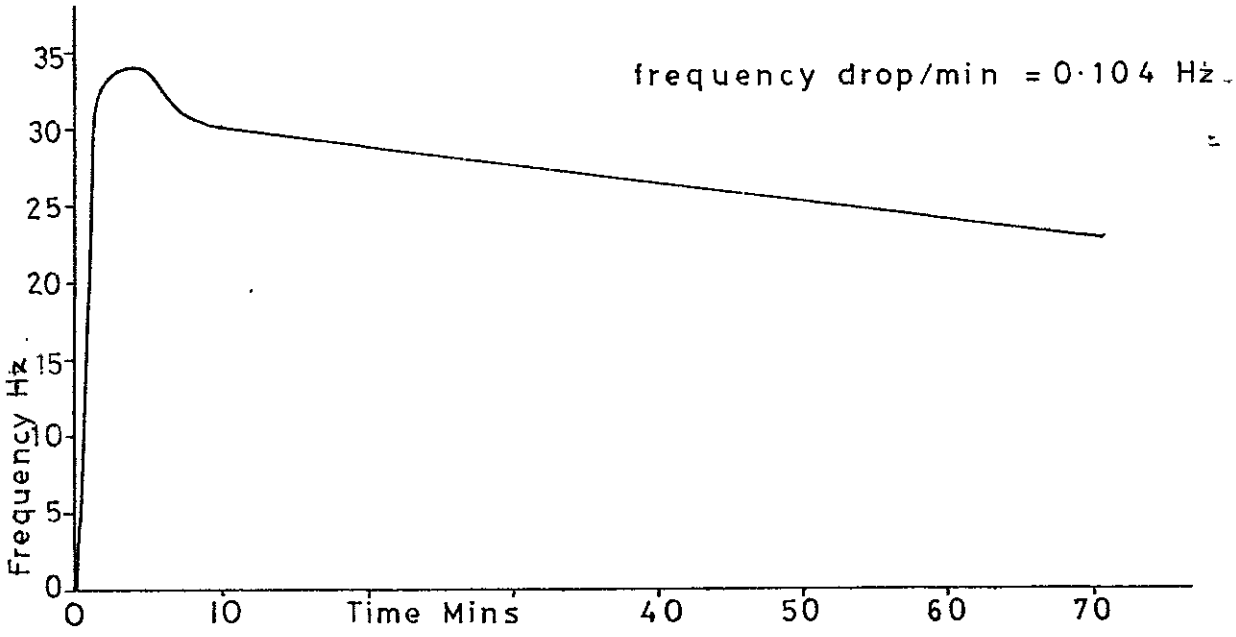

FIGURE 29 c

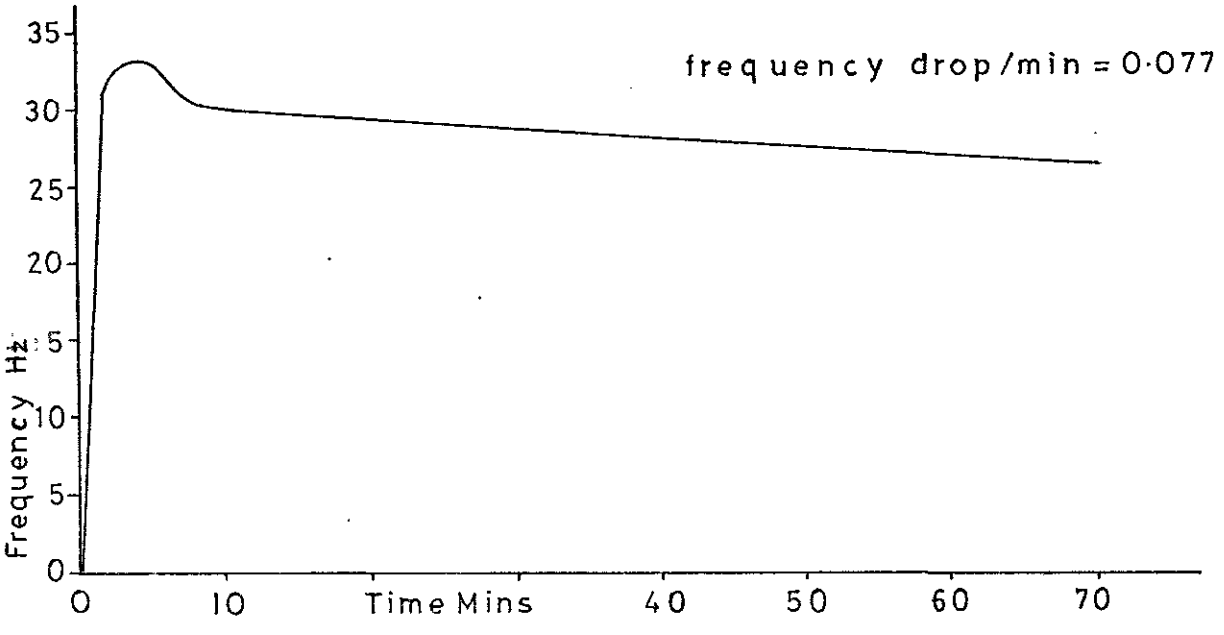

FIGURE 30 a

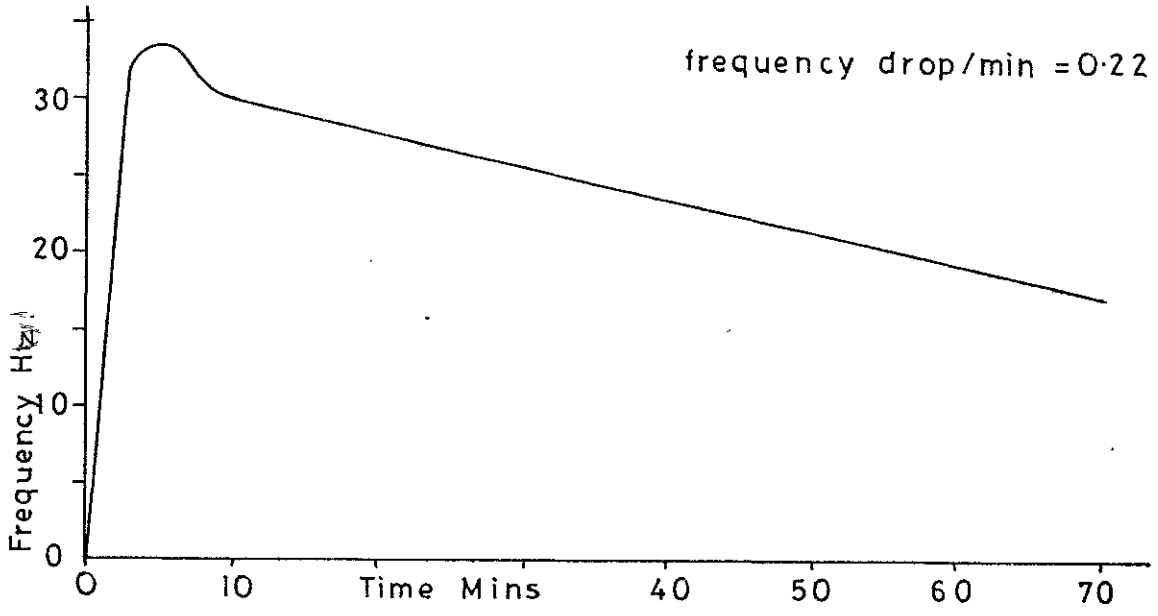

FIGURE 30 b

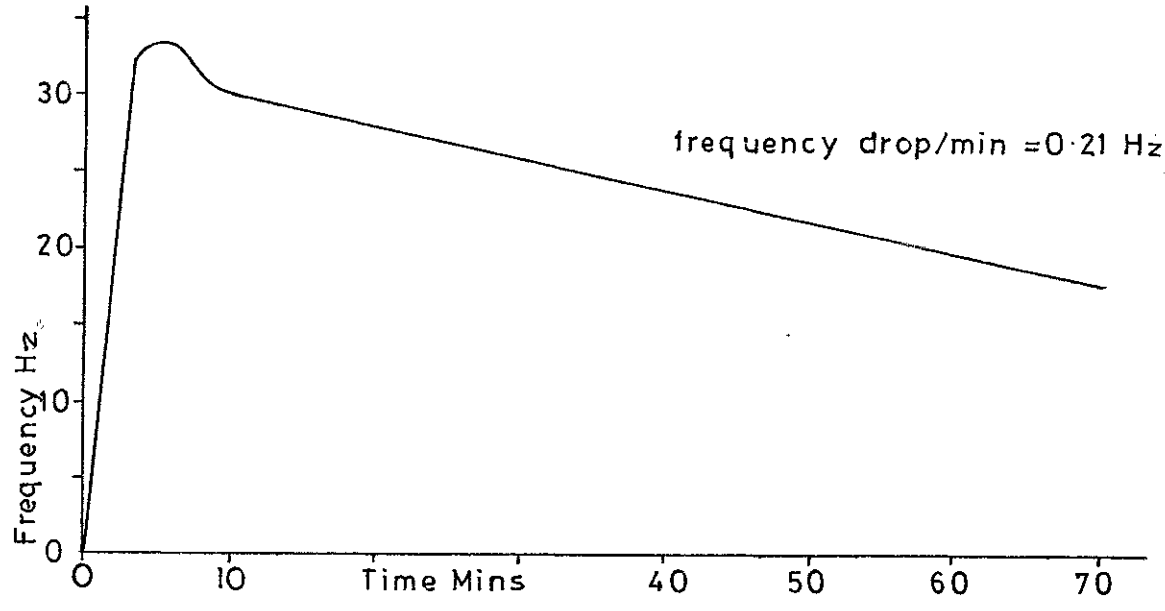

FIGURE 30 c

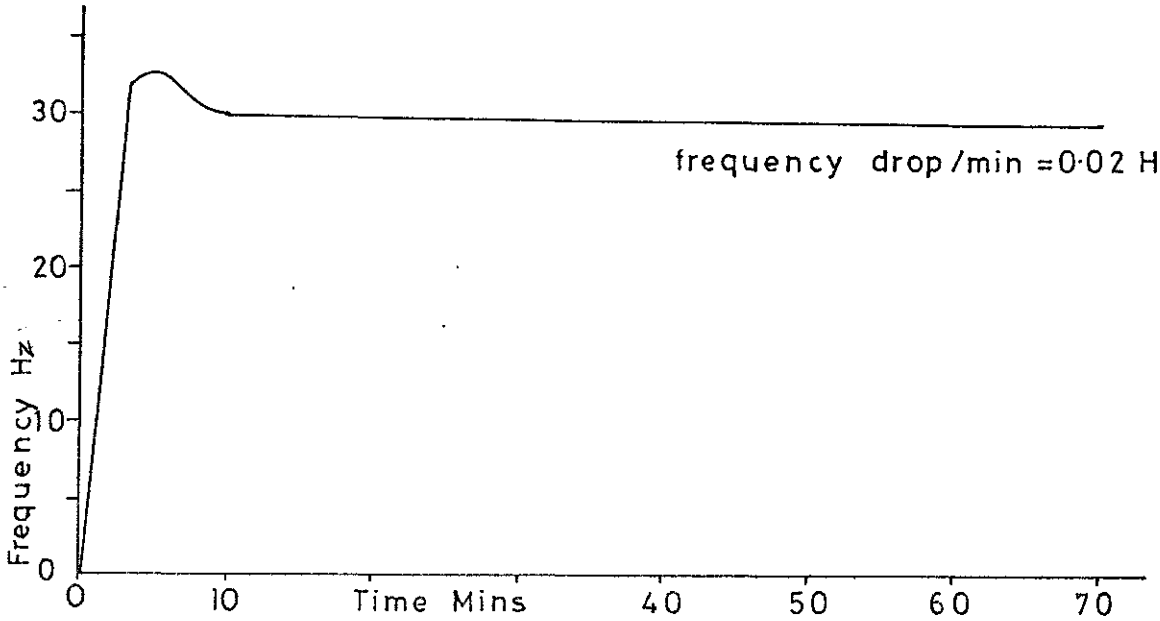

Variation of uncoated, cleaned crystal with gas flow: drying tube incorporated.

The crystal from the previous experiment was removed and cleaned using the recommended procedure. The crystal was located in the detector cell under the same conditions used in the previous experiment save that a magnesium perchlorate tube was included in the gas flow system, between the gas cylinder and detector cells. The frequency was monitored in the usual way, and a graph of the results obtained, depicted in figure 30 c.

Variation of frequency of a coated crystal with gas flow: no drying-tube incorporated.

A cleaned crystal was coated with two micrograms per side "Apiezon M", located in a high volume impinger detector cell and subjected to a 50 mls/minute gas glow. The frequency was monitored for two hours and the results plotted as frequency versus time. See figure 31 a.

Variation of frequency of a coated crystal with gas flow: drying tube incorporated.

The system from the previous experiment was left intact, and the magnesium perchlorate drying tube was reintroduced to the system. The frequency of the coated crystal was observed for two hours, and a graph plotted of frequency against time for the results. See figure 31 b.

The results from this experiment exhibited a number of points about the gas system and the crystals. The entire series of experiments was carried out in a situation where the detector cell temperature was in equilibrium with the ambient temperature. A close watch was

FIGURE 31a

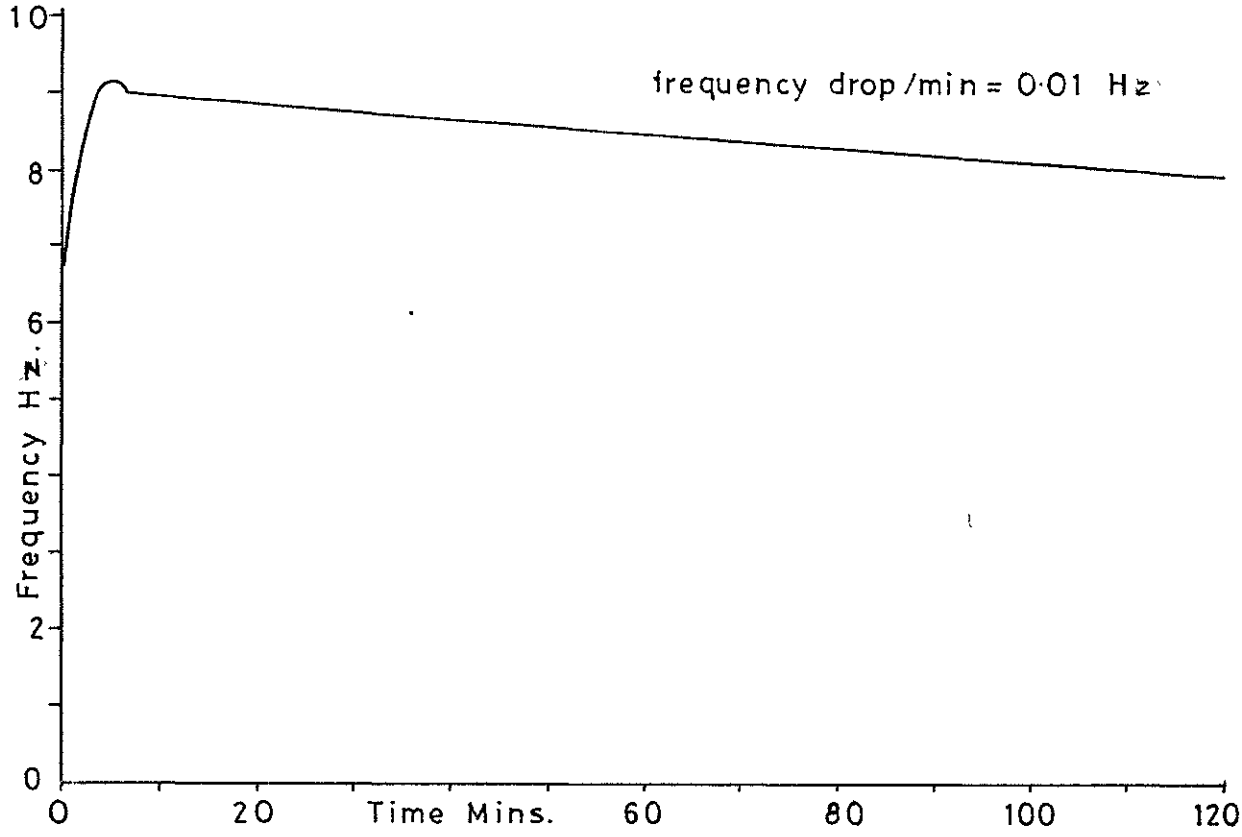

FIGURE 31b

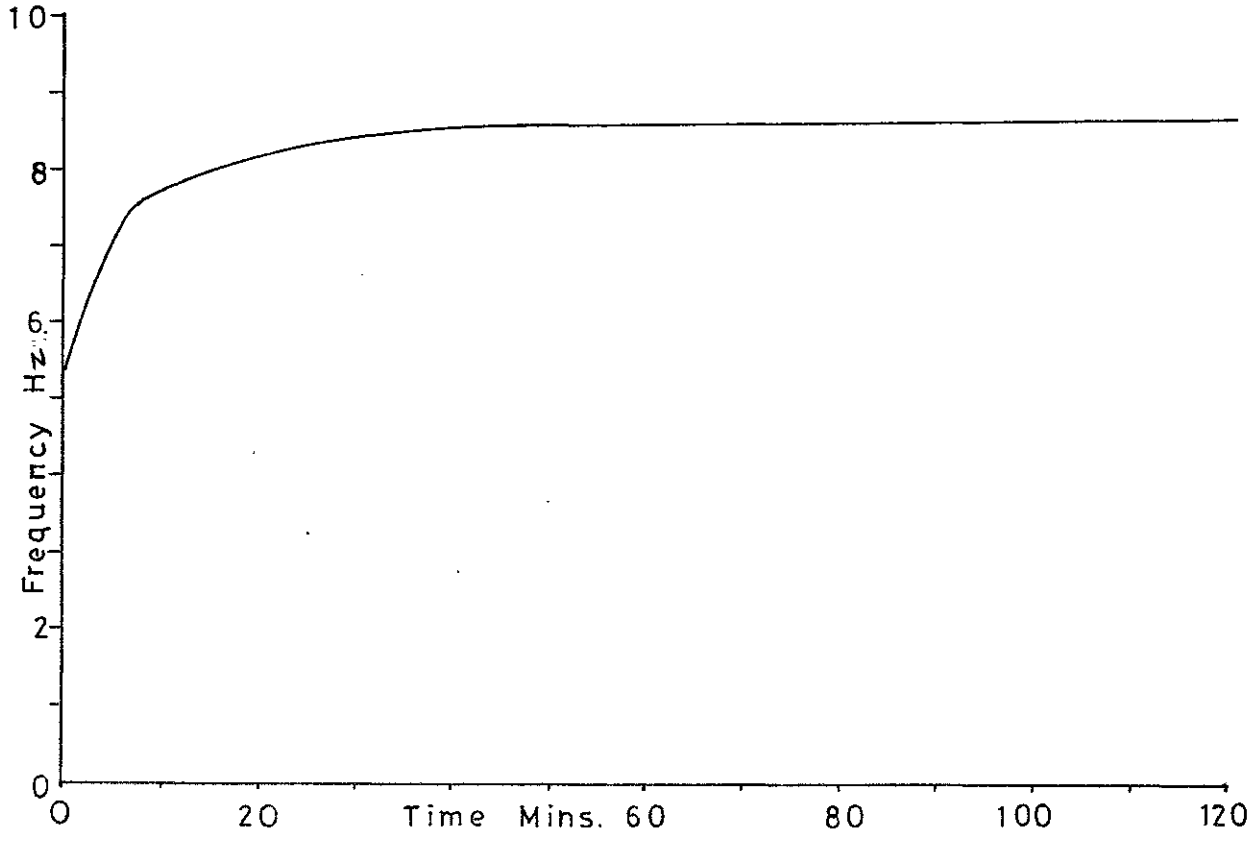

kept on the temperature, and the results here reported were achieved during periods of minimal temperature fluctuation (± 0.3°C). Thus alterations in the frequencies of the crystals were mainly due to sources of variation other than temperature. It can be seen from figure 29 a, b and c, that the exposure of a crystal to an OFN gas stream results in a gradual downward drift in the frequency with time: the slope of the decrease itself, decreases with time. The original rate of decrease was restored by cleaning the crystals (figure 30 a and b). It may be surmised that this decrease in frequency was due to the accretion of a contaminant on the surface of the crystal, hence as a point was reached where the available sites for adsorption decreased, the rate of mass accretion was restricted and the frequency decrease too was limited. Cleaning the crystal restored the number of active sites, and hence the rate of mass accretion. The introduction of a drying tube reduced the rate of frequency decrease, and it may be that water vapour was a significant contaminant. King[66,67] has reported the adsorption of water vapour onto the fresh gold electrodes of a crystal; older gold surfaces gave rise to a much lower rate of surface sorption. Similarly Stockbridge[41] has shown that the QCM can weigh partial monolayers of gas adsorbed onto the gold electrode at room temperature and atmospheric pressure. The effect of coating the crystal was to replace the gold surface with a surface of "Apiezon M", whose sorptive properties to water vapour would be expected to be different. Thus, from figure 31a,

it can be seen that the rate of frequency decrease (surface mass increase) was even lower than that for a "saturated" crystal, (see figure 29c). Drying the OFN prior to passing it over the coated crystal resulted in desorption of the moisture from the layer into the gas stream, until a steady state was reached (see figure 31b). The drying tube was incorporated into the gas flow system on a permanent basis, in order to reduce the drift in frequency of the detector due to OFN-contaminant pick-up.

Stockbridge[41] showed that gas pressure affected the QCM in three different ways. Firstly, an increase in pressure caused a linear increase in frequency due to alteration of the elastic modulus of quartz. Secondly, a frequency decrease was caused proportional to the square root of pressure due to the complex shear impedance of the gas which was considered as a viseo-elastic fluid. Thirdly, the frequency decreased due to sorption of gas by the crystal. The latter effect was thought to be insignificant compared with the first and second effect. In the previous experiments of this study, the effect of pressure was observed, when on switching on the gas flow a rapid increase in frequency was experienced. This increase was thought to be due to the sharp increase in pressure experienced in the cell as the fairly rapid gas flow was switched on. See figures 29 to 31.

Static sampling cells: saturated vapour method.

Static sampling cells for vapour generation were constructed from 25 mls glass sampling bottles. Snap-fit polyethylene tops were used to seal the bottles. Each top

was modified by the insertion of a ¼" brass straight coupling in order that a renewable rubber septum could be fixed into the top of the bottle. See figure 32. Generally, two mls of the liquid of interest were placed in the cell, the stopper firmly affixed, and the cell allowed to equilibrate at room temperature for five minutes. Samples of the vapour-impregnated air were withdrawn from the cell using a Scientific Glass Engineering Ltd., 100 microlitre gas-tight syringe. Sample introduction to the flow system took place via a rubber septum that was held in one arm of a ¼ inch brass T-piece, the gas stream passed through the other two arms. Sampling from this cell presented no problems, since effects such as vapour adsorption onto the walls of the cell could be ignored, due to the presence of excess liquid in the cell.

Static sampling cells: variation of vapour concentration with time in non-saturated situation.

Five microlitres of chloroform vapour were introduced into a static vapour sampling cell and allowed to completely vaporise at room temperature and pressure for different lengths of time. At the end of a given time period, 40 microlitres of the "spiked" air sample were withdrawn and injected at ten microlitres per second into a carrier gas stream of five mls per minute. The detector was a di-nonyl phthalate coated crystal located in the high volume impinger detector cell. The peak signal was recorded for each injection, and triplicate samples were run for each time interval. The results were plotted as frequency change versus time. See figure 33.

FIGURE 32

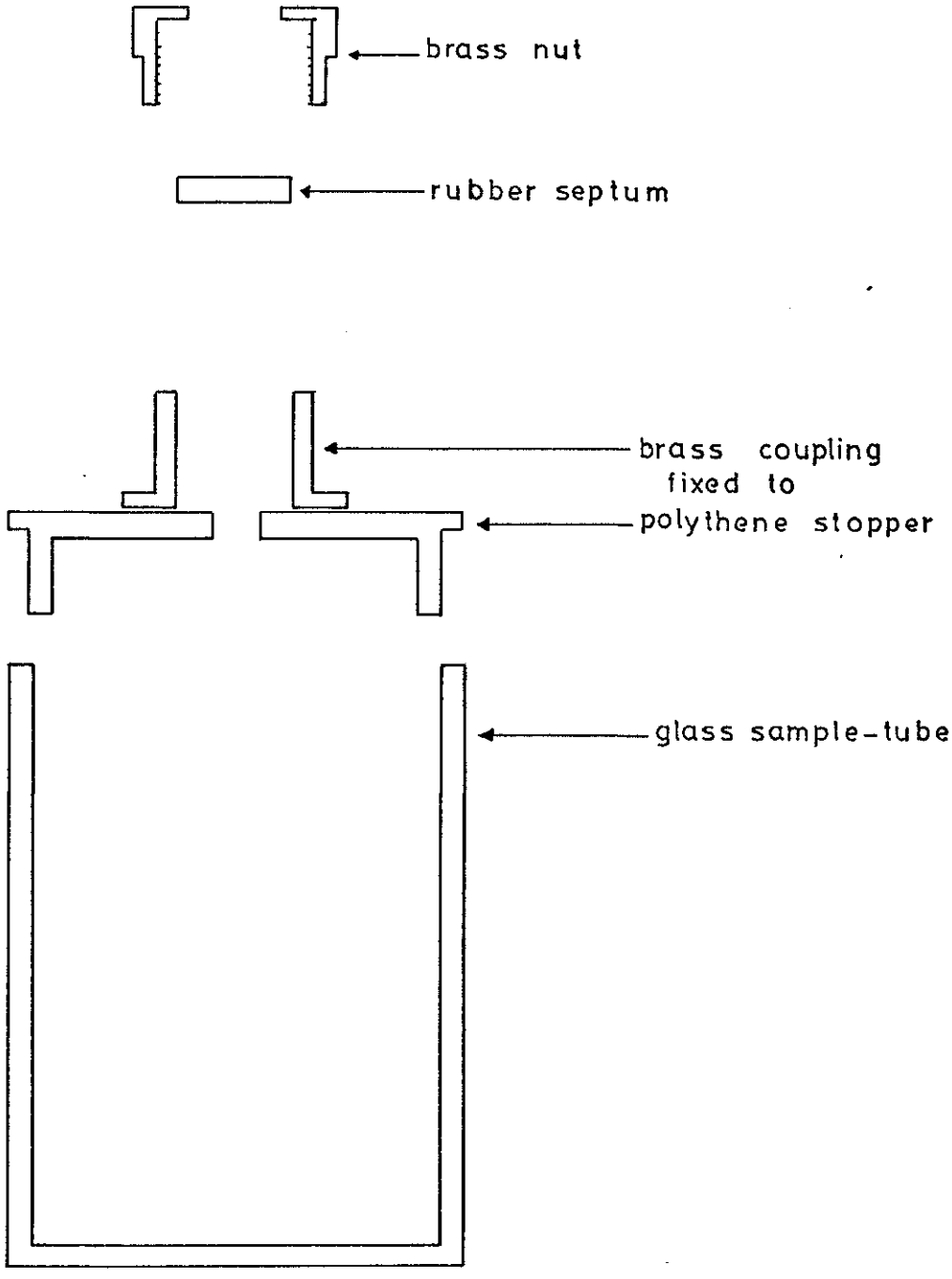
brass nut
rubber septum
brass coupling
fixed to
polythene stopper
glass sample-tube

FIGURE 33

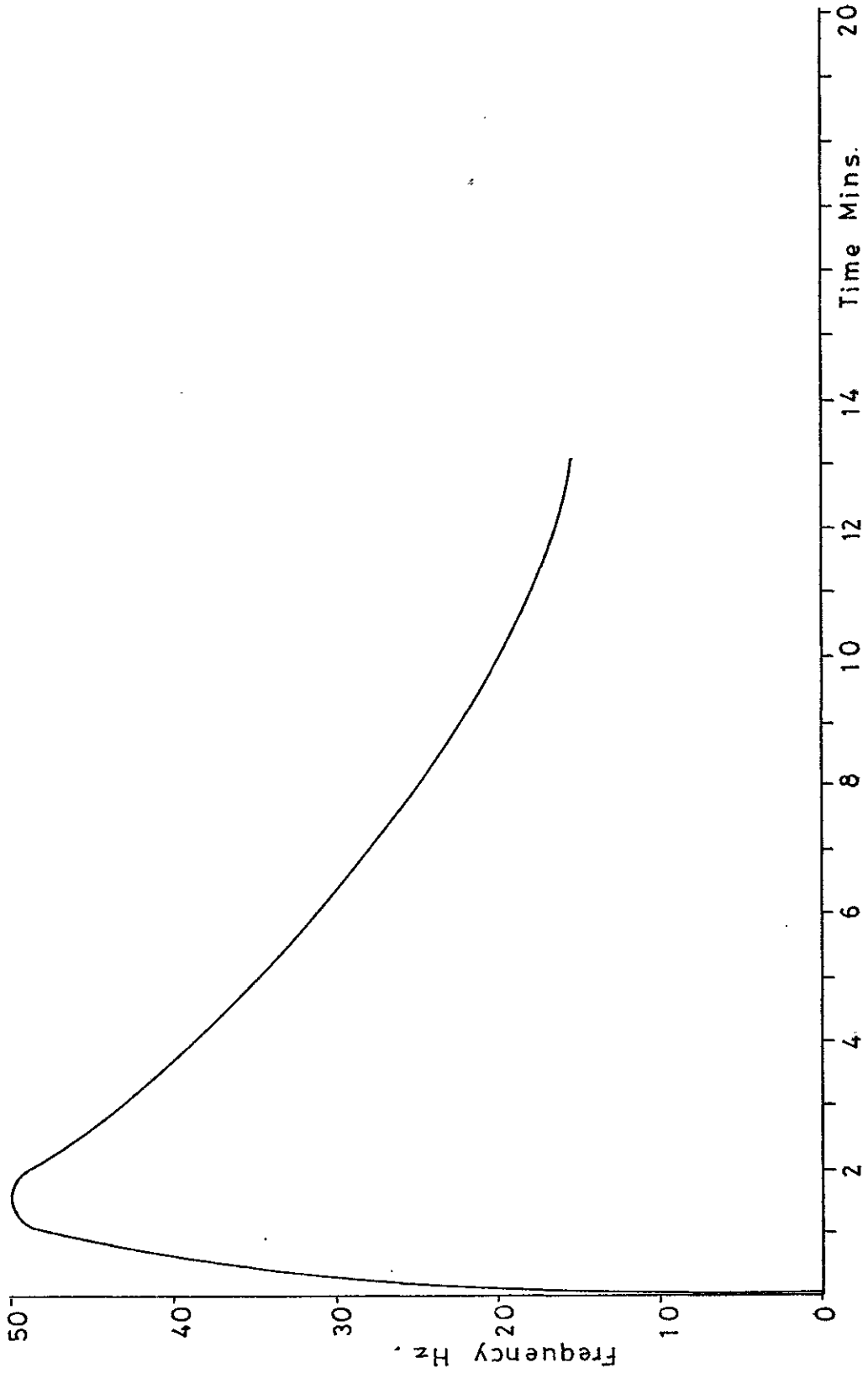

The results from this experiment indicated that a peak value for the response from the cell was obtained after a two minute interval from the liquid injection, followed by a decline in the response with time. It would seem that during the first two minutes, diffusion and convection establish the vapour concentration throughout the cell, and that subsequently the vapour commenced to adsorb onto the walls of the cell as it came in contact with them, thus reducing the concentration of the vapour in the cell. Thus, samples prepared from this cell were always withdrawn two minutes after the initial sample introduction.

Dynamic sampling cells: the mercury reservoir.

The mercury reservoir sampling cell was constructed from a thistle funnel that was connected to a long length of capillary tube by flexible rubber tubing. The flow of mercury from the thistle-funnel reservoir and along the horizontally held capillary tube was controlled by a thumbscrew clip placed over the interconnecting rubber tube. The air displaced from the tube was forced through a bubbler containing the liquid of interest. The flow rate of vapour-saturated air was calculated from the time taken for the mercury to move down a marked length of the capillary, whose diameter was known. The sampling procedure commenced with adjustment of the thumbscrew clip to give a smooth flow of mercury with the reservoir at a fixed height above the capillary: the reservoir was brought level with the capillary to cut the flow of mercury. The sampling system was connected via a piece of $\frac{1}{4}$ inch O.D.

nylon tube to a T-piece in the main gas flow system, the mercury reservoir raised to the required height, readings of the frequency taken at regular intervals, and the mercury flow measured between the two marks on the capillary tube. The type of signal arising from this sample input method may be seen in figure 34. An initial surge of air was created, as the mercury started to flow, followed by equilibration of the system. Periods during which steady flow was maintained in the sampling system varied from one to three minutes only, and this furnished a major reason for abandoning the use of this system in favour of a system using diffusion tubes. In addition to this drawback, the equipment was cumbersome, and a complete sampling procedure could take up to 15 minutes.

Dynamic sampling cells: the diffusion tubes.

The diffusion tubes used in this study were constricted from B 10/19 "Quickfit" cones, rounded-off and sealed at their parallel ends, and with a one cm length of two mm capillary tube fused into the tube about four cms from the open end. The cone fitted into a ground-glass socket fused into the by-pass system shown in figure 35. The bypass system permitted the carrier gas stream to be switched from the diffusion cell to a blank tube, with the minimum interruption of the gas flow. Eight diffusion tubes were made, the general mode of use involved, pipetting of an aliquot of the liquid of interest into the lower compartment of the tube, equilibration of the tube and contents in a thermostatted waterbath set at the desired temperature, then introduction of the tube into the gas flow system.

FIGURE 34

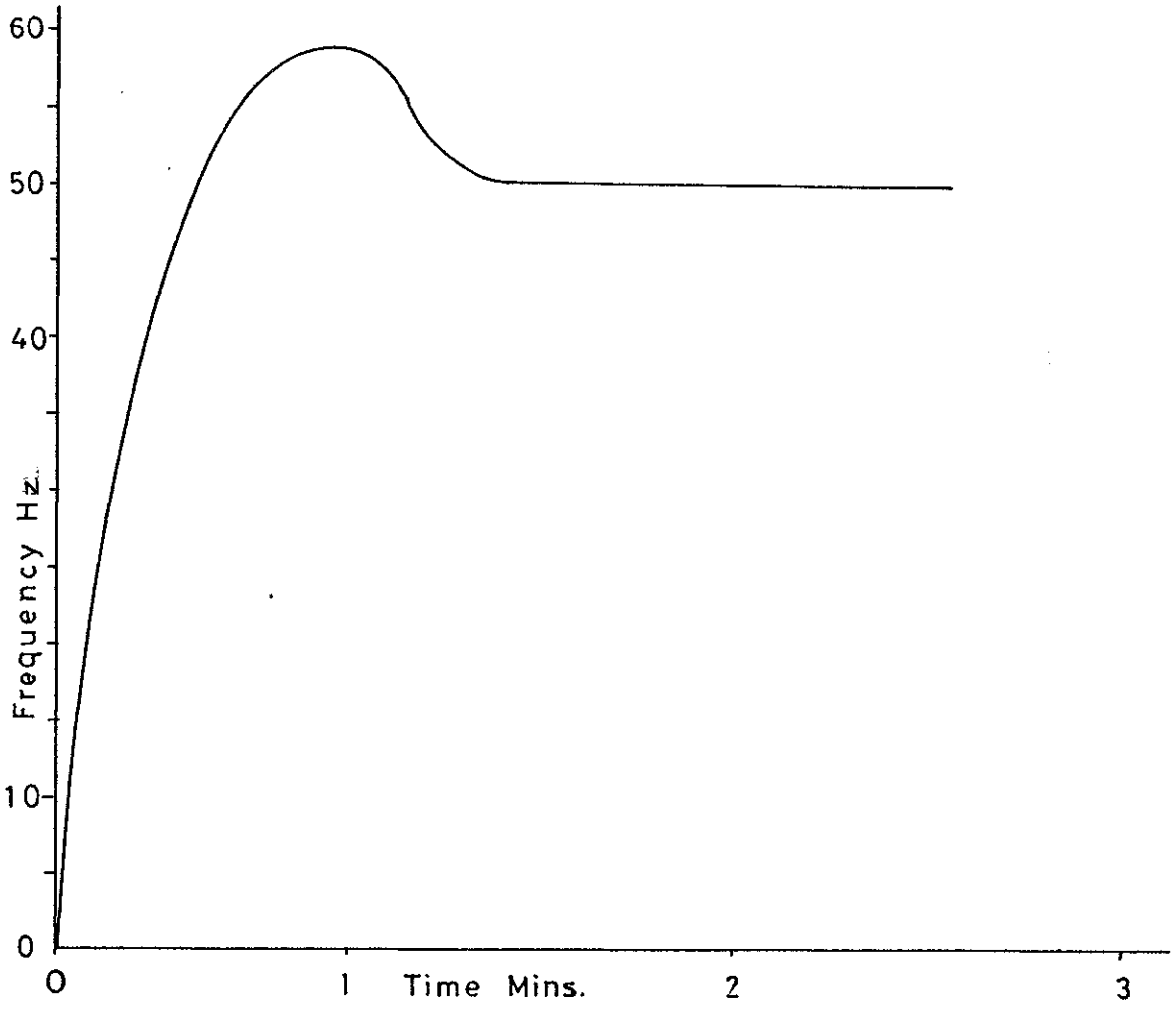

FIGURE 35

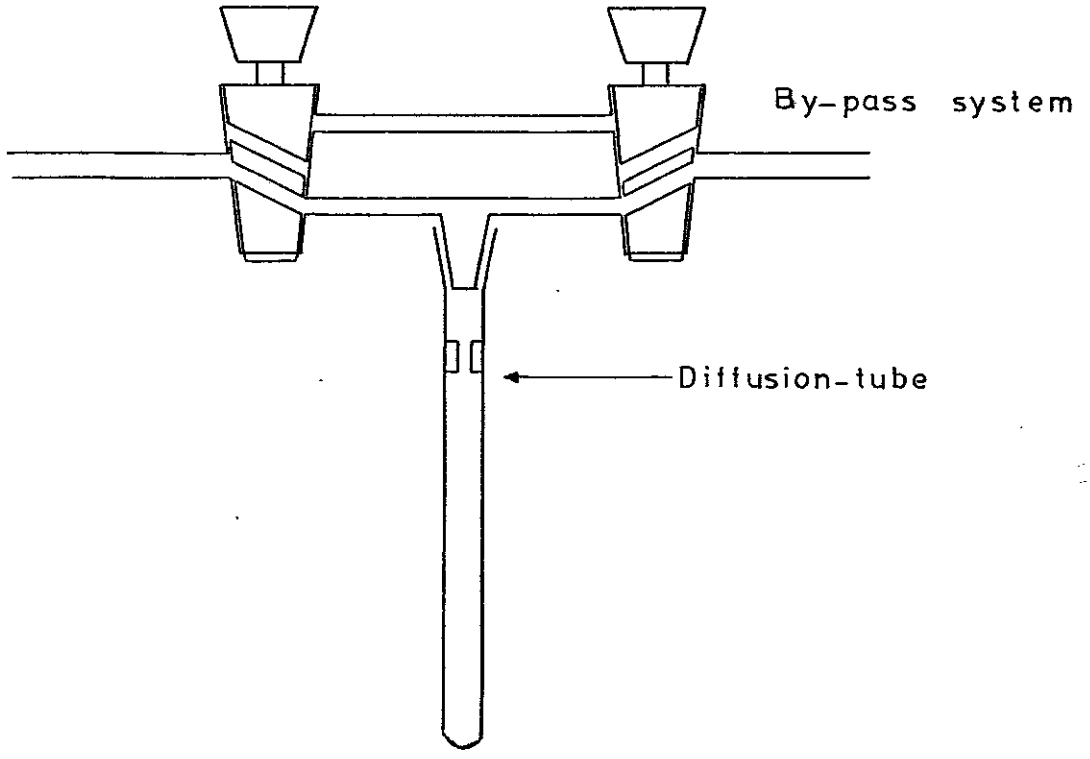

Dynamic sampling cells: performance and calibration of the diffusion tubes.

Two crystals were located in the low volume impinger detector cells, one crystal was coated with 200 microgrms per side "Carbowax 20M", the other with 10 microgrms per side di-nonyl phthalate. A gas flow of 12 mls per minute was maintained through the cells which were immersed in a water bath held at 30°C. The system was allowed to equilibrate: two digital counters were used to monitor the frequency of each crystal separately. A diffusion tube containing chloroform was equilibrated in a second water bath at 30°C, the tube had been located in position on the socket of the bypass system. On attainment of equilibrium, the tube was switched into the carrier gas flow by rotating the two stopcocks of the bypass system through 180°. The frequency of each crystal was recorded regularly for 25 minutes, after which the tube was switched out, and the frequencies permitted to return to their base-line values. The results were plotted as frequency versus time, see figure 36a. A similar sampling sequence was subsequently followed, save that the diffusion tube was located on the socket of the bypass system just prior to being switched into the carrier gas flow. See figure 36b.

Comparison of the two profiles of figure 36a and b, demonstrates a marked difference between the two initial phases. A large frequency depression was obtained in the first sample input, with a gradual increase in frequency to an equilibrium value: the second sample input

FIGURE 36

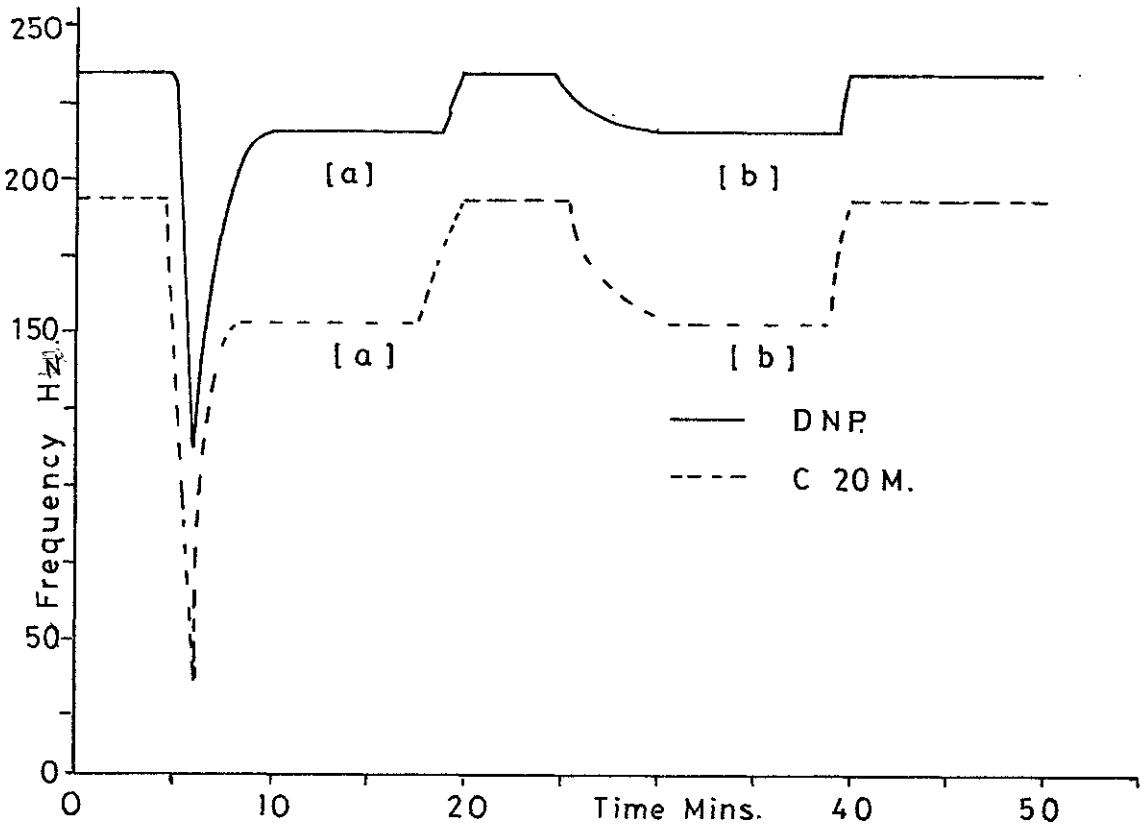
250
200
150
50
0
Frequency Hz.
[a]
[b]
[a]
[b]
DNP.
C 20 M.
0
10
20
Time Mins.
40
50

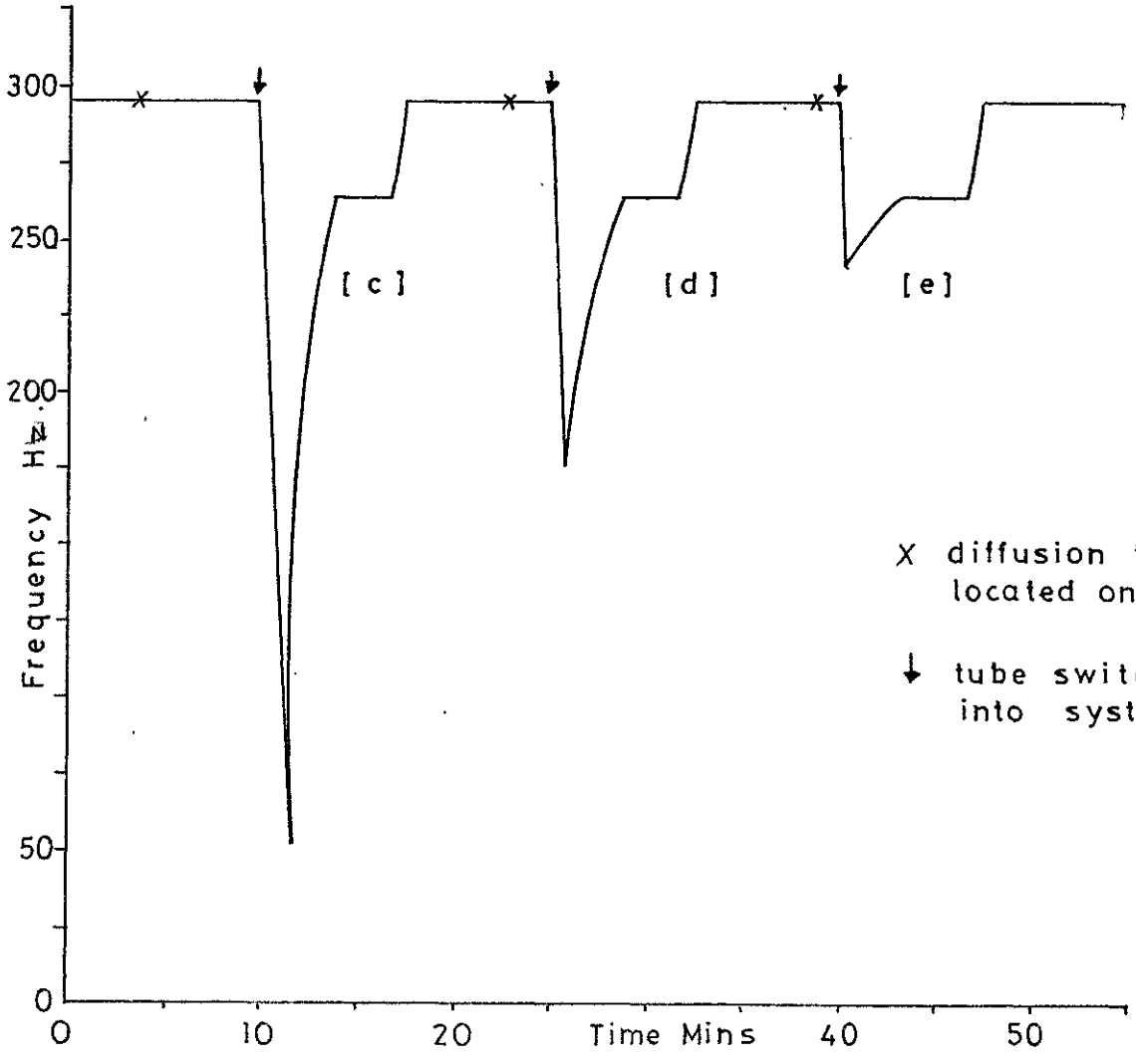
300
250
200
50
0
Frequency Hz.
[c]
[d]
[e]
X diffusion tube located on cone
tube switched into system
0
10
20
Time Mins
40
50

followed the shape predicted by equations 3.27 and 3.29. It was assumed that the initial frequency drop that arose from the first input was due to an accumulation of chloroform vapour in the enclosed diffusion tube side of the bypass system, which was swept through to the detectors when the stopcocks were turned. To test this hypothesis, the diffusion tube was located on the bypass socket for varying lengths of time, prior to switching in the sample generator, in an experimental set up otherwise identical to that described previously. See figure 36 c, d and e. The decrease in size of the initial frequency drop with decreasing interval between location of the diffuser tube and switching in the tube may clearly be seen. In all subsequent use of the diffuser tube, a 30 second interval was used. The characteristic shape of the response profile for this method of sample input may be seen from figure 37. The leading edge of the peak A to B resembles the curve drawn in figure 24b from data calculated by equation 3.27, whilst the flat portion from B to C indicates that equilibrium has been reached. The rapid decay from C to D on removal of the analyte vapour bodes well for a hysteresis-free system.

The stability of the diffusion tube vapour generator was investigated by following the frequency of the di-nonyl phthalate crystal, whilst chloroform vapour from the tube diffused into the gas flow for a 50 minute period. The experimental system was the same as that employed in previous experiments. The results were plotted as frequency versus time, see figure 38a. The reproducibility

FIGURE 37

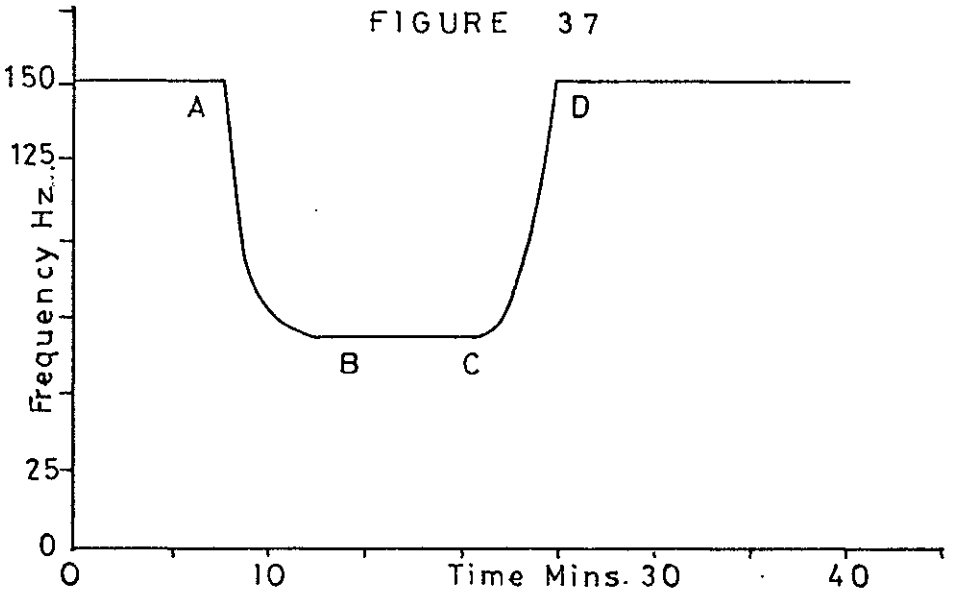

FIGURE 38a

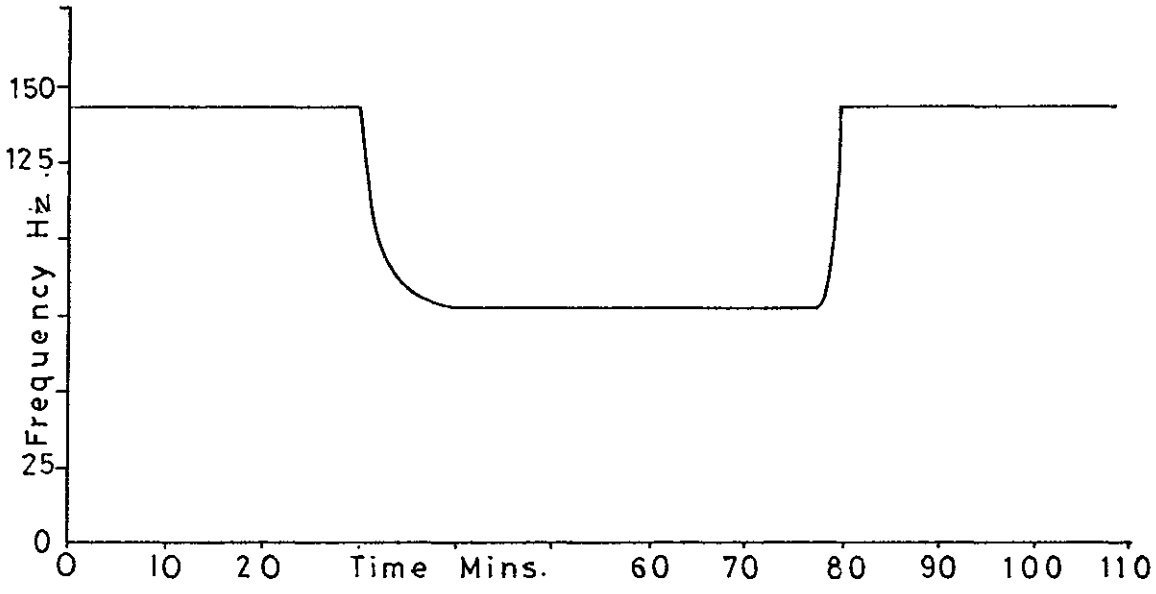

FIGURE 38b

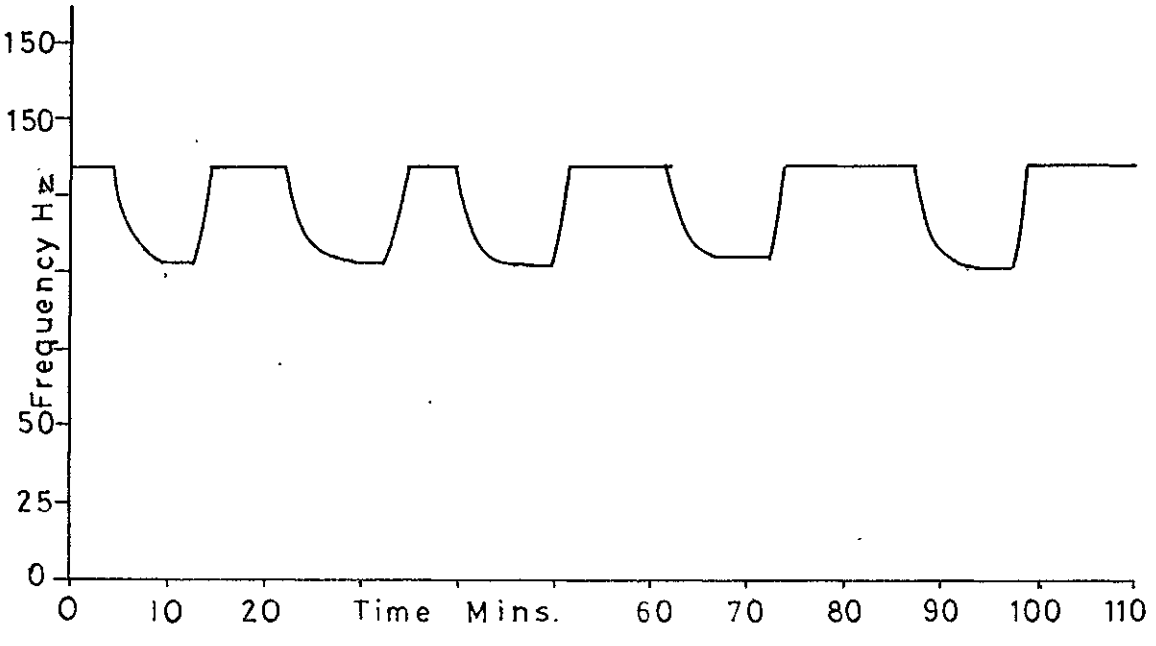

of the diffusion tube method of sample introduction may be seen from figure 38b, where the results of five consecutive, 13 minute sample introductions are plotted. Both figure 38a and 38b indicate favourable properties of the diffuser cell with respect to stability and reproducibility.

Calibration of the tubes was carried out in two distinct phases. First the tubes were calibrated one against the other. A crystal was coated with tri-cresyl phosphate, and located in the low volume impinger detector cell under a gas flow of 12 mls per minute. The system was equilibrated in a water bath at 30°C, and each of the eight diffusion tubes was in turn switched into the carrier gas system, for 15 minutes: a frequency reading was taken every five minutes. Each tube contained a two ml aliquot of chloroform, and was equilibrated in a water bath at 30°C prior to and during use for sample introduction. The results are recorded as frequency change against tube number in table 4.

The second phase of calibration involved introducing a two mls aliquot of each of the seven different liquids used in this study, into a separate diffusion tube: all eight tubes were used, two chloroform tubes were established. The stoppered tubes were each weighed on a double-pan balance to the nearest ten microgrms. The tubes were then unstoppered and placed in a waterbath for a given length of time. At the end of the period, the tubes were restoppered and reweighed, and the weight loss determined. The experiment was carried out for two different time periods, 21.5 and 47.5 hours. It was

TABLE 4

Tube No.	Freq. change (Hz.)
1	40
2	35.5
3	33
4	33.5
5	38.8
6	34.5
7	33.0
8	40.8

TABLE 5

Tube No.	Compound	Temp. °C	Weight loss per hour (mg.)		
			21.5 Hr. Expnt.	47.5 Hr. Expnt.	Ave.
1	Cyclohexane	30	4.1640	4.6800	4.4220
2	Xylene	60	1.0445	0.6454	0.8450
3	Ethylbenzene	60	0.9928	0.7042	0.8485
4	Acetone	30	8.8916	9.2663	9.0790
5	Heptene	30	2.4905	2.7941	2.6423
6	Hexane	30	6.5442	7.0120	6.7781
7	Chloroform	30	10.3126	-	10.3126
8	Chloroform	30	13.8191	13.6500	13.7346

found necessary to place the tubes containing ortho-xylene and ethyl-benzene in a water bath at 60°C in order to obtain a significant weight loss. The results are summarized in table 5. The last column of table 5 represents the averaged values of weight loss in mgs per hour obtained from the two different time periods. The discrepancies between the two sets of results were of the order 0.2 to 0.5 mgs per hour, representing errors of ± 23% of the average value at the worst, to ± 0.6% of the average value at the best. The results were regarded as acceptable, even for ortho-xylene, in the context of the small values undergoing determination. Replicate weighings of a blank tube undergoing the same procedure gave a scatter of results that would have accounted for about ± 1.5% of the error on the ortho-xylene weighings. The experimentally obtained values for diffusion were compared with values calculated from the equation derived from 3.36. Values of the diffusion coefficients were obtained from Lugg[106]. The cross sectional area of the capillary tube was known; the length of the tube was determined by travelling microscope; the saturated vapour pressure was calculated; the temperature was known; the atmospheric pressure was known; the gas constant was obtained from the literature.

RESULTS.

	Diffusion rate in mgs/min.		Difference Factor
Compound	Calculated	Experimental.	
Hexane	1.79×10^{-1}	1.13×10^{-1}	1.6
Acetone	2.76×10^{-1}	1.51×10^{-1}	1.8
Chloroform	4.0×10^{-1}	2.29×10^{-1}	1.7

The divergence between the calculated results and experimentally determined results involved a factor of about 1.7, the calculated results overestimating the diffusion. The source of this error lay with the measurement of the length of the capillary. The method used, was to measure the longest parallel section of the capillary, ignoring the sections at either end where some splaying had occurred due to the process of fusing the tube into the cone. This length was determined as 0.57 cms: the original length of capillary fused into the tube was one cm. The use of 0.57 in the calculation of the results, where a value of unity would be correct, would give rise to an overestimation of the diffusion by a factor of $\frac{1}{0.57}$. Now, $\frac{1}{0.57} = 1.75$, hence the assumption that the probable source of error lay in the capillary length measurement.

Dynamic sampling cells: Syringe Pump.

Sample introduction by the slow flushing of a syringe was accomplished by using a Sage Instruments model 355 syringe pump. This unit was furnished with a four-position selector switch which gave the full rated speed, 1/10th, 1/100th and 1/1000th of the full rated speed, and a rotating vernier dial for setting percentages of the speed from 4 to 100%. Thus, the flow rate of gas expelled from a syringe operated by this unit, was a function of the two instrumental settings and the volume of the syringe. Two types of syringe were used with this unit, a Chance 5.0 mls glass syringe with a ground glass plunger, and a Hamilton 50 mls gas-tight syringe with a "Teflon" ringed

plunger, luer tip and luer lock. Connection to the gas flow system for both syringes was made via a length of one mm bore "Teflon" tubing that entered the gas stream via a rubber septum inserted into one arm of a $\frac{1}{4}$ inch brass T-piece. The 5.0 mls syringes were used with an excess of the liquid of interest present in the barrel, so that the air in the syringe at all times was saturated with vapour. This arrangement meant that vapour losses due to sorption on the walls of the syringe, or onto the plunger, or loss of vapour past the plunger, could be ignored. The type of signal obtained from this system can be seen in figure 39a. The peak exhibited a great deal of noise due to the uneven movement of the plunger along the barrel. Lubrication of the plunger and barrel may have helped, but the liquids used in the syringe attacked the commonly used lubricants, such as paraffin wax. Smoother peaks were obtained with the Hamilton syringe, due no doubt to the self-lubricating "Teflon" washer around the plunger. See figure 39b.

Detector Cells: Fabrication

The cell design of Bristow[79] was favoured for this study. This choice was guided by the considerations of Section 3.21. The sandwich cell was felt to be inefficient, whereas the spoiler cell required accurate machining for a cell with reproducible properties. The major machining requirement of the impinger cell, was that the gas jets should strike the crystal surface approximately centrally.

FIGURE 39a

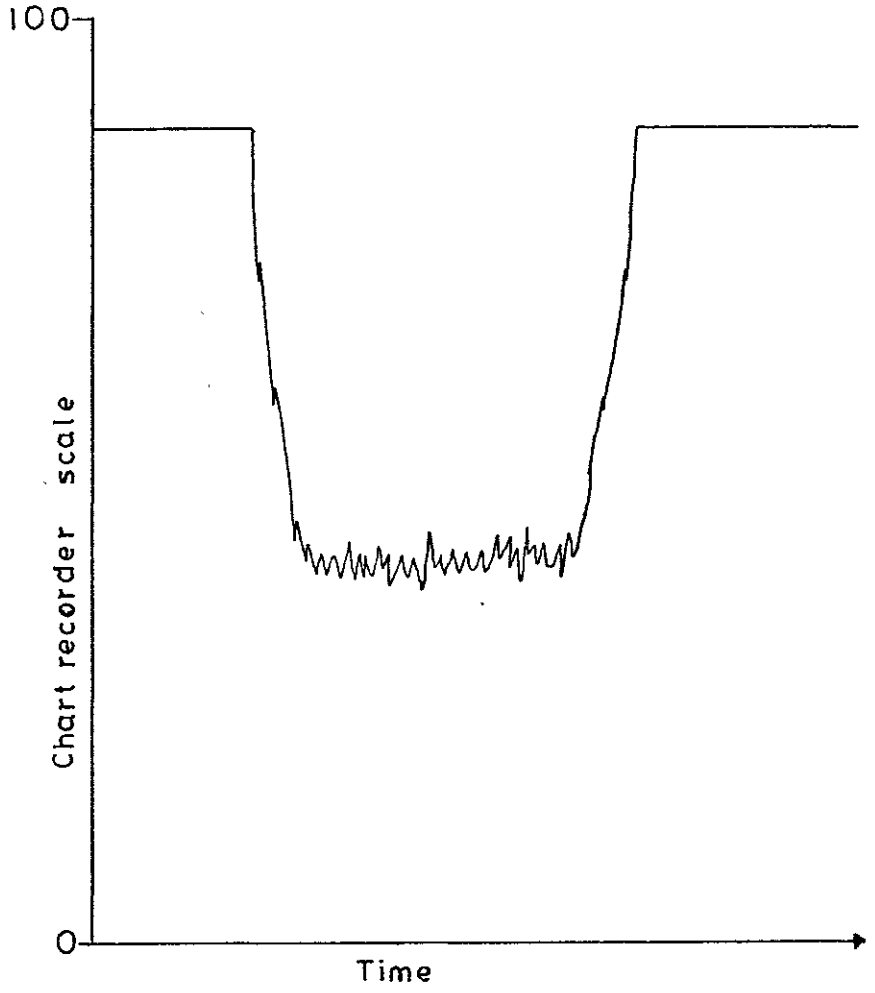

FIGURE 39 b

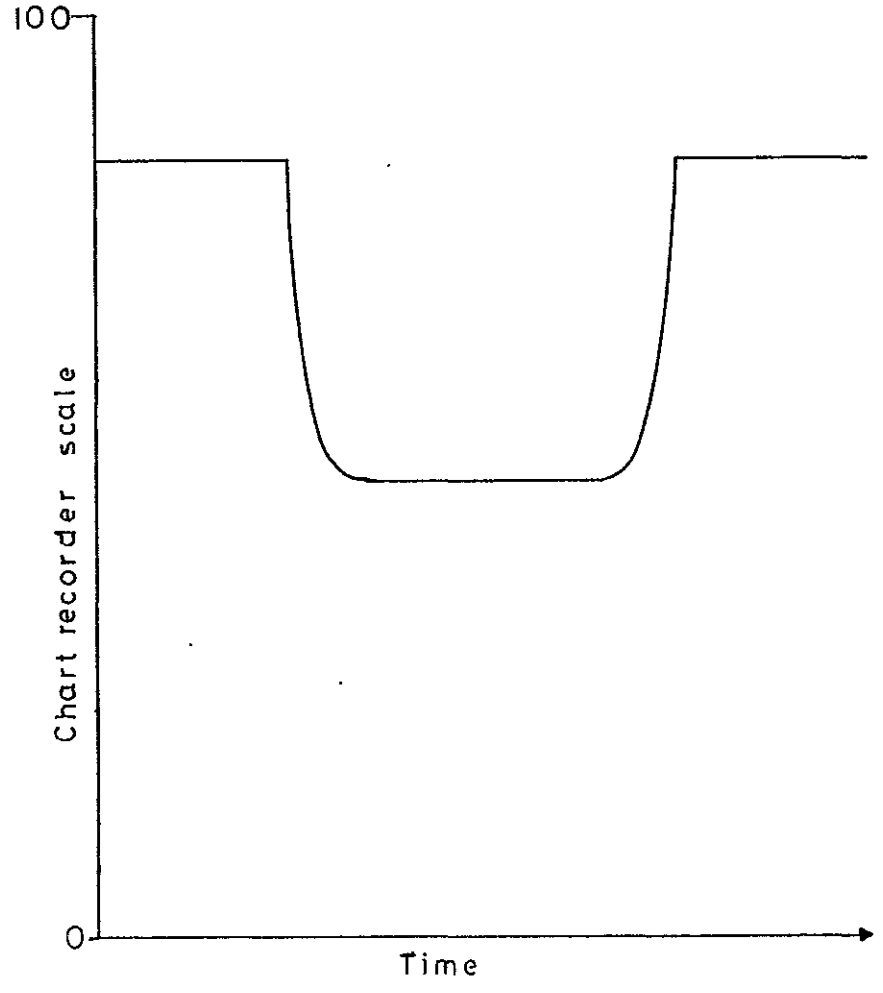

Two types of impinger cell were constructed. The first was similar to Bristow's design, in that the protective metal cap of the crystal was drilled in opposite faces with a 0.0028 inch hole. The holes were positioned in the flat side of the cap, so that gas passing through them impinged directly onto the centres of the gold electrodes of a quartz crystal when it was correctly positioned in the housing. A half inch diameter copper pipe was fitted over the cap to bring the gas to the holes, and a brass $\frac{1}{4}$ inch coupling fixed over a "$\frac{1}{8}$" hole in the top of the cap conducted the gas away. The crystal was located in the cell in the same manner as if the cell were simply a protective cap. A thin rubber gasket was placed between the cell and the base of the crystal holder in order to ensure a gas and watertight seal when the crystal was in position. See figure 40a. The cell volume was 2.5 mls.

A cell with smaller volume was made from two cast "Isopon" cylindrical blocks, four cms in diameter and four centimeters high. A slot was cut into one of the flat circular faces of the casting of sufficient width and depth to allow a crystal to just rest on the base of its holder when located in the slot. The block was drilled so that gas entering one side of the block was split into two equal streams and allowed to impinge through two 1/32 inch holes directly onto the centres of the two gold electrodes on the opposite faces of the quartz crystal. The gas exited via a $\frac{1}{8}$ inch hole that connected the deepest portion of the slot, with the opposite flat face of the

FIGURE 40 a

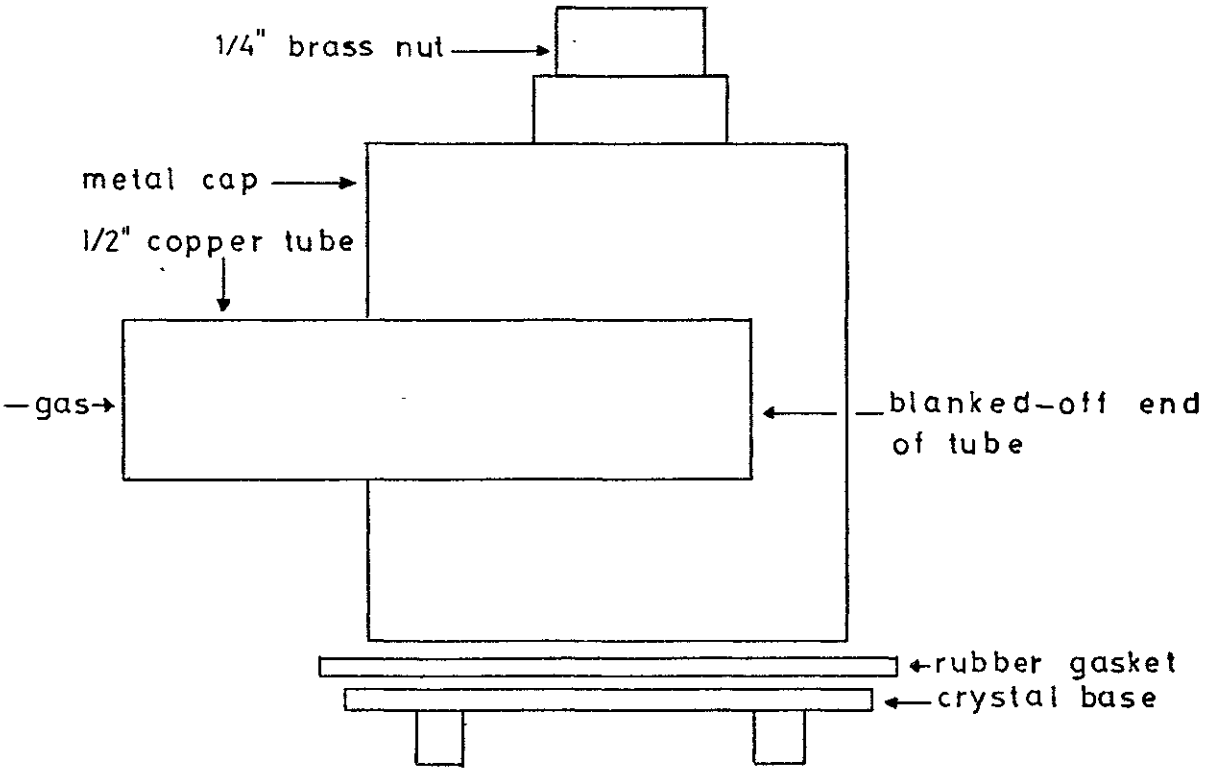

High Volume Impinger Detector Cell

FIGURE 40 b

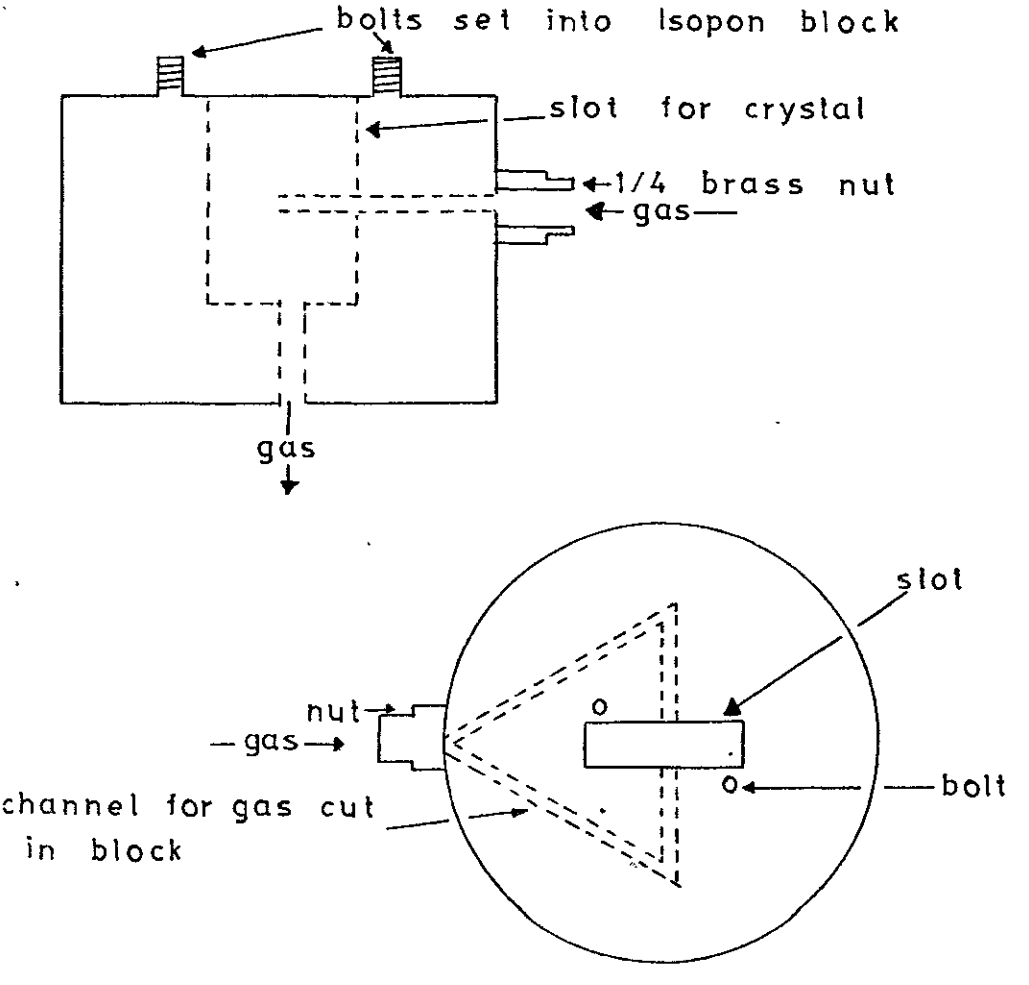

block. Connecting nuts for the ¼ inch brass couplings were set into the block at the gas entrance and exit points. Two small bolts were set into the flat face of the block at diametrically opposed corners of the slot for the crystal, so that a metal plate could be bolted down on top of the crystal, to hold it in place. A rubber gasket between the crystal base and the block provided a gas-tight and water-tight seal, whilst a second gasket between the base and the metal plate prevented damage to the base. See figure 40b. The volume of this cell was approximately 0.5 mls. Each of the two impinger cell designs was made in duplicate, so that various combinations of detector cells could be used.

Detector cells: comparison of the two designs.

A crystal was coated with 40 microgrms per side di-nonyl phthalate, and placed in turn in each of the two impinger detector cells, under a steady 12 mls/min stream of OFN. Three replicate samples of 40 microlitres of air saturated with chloroform vapour were withdrawn from a static sampling cell and injected at ten microlitres per second into the carrier gas stream. The peak height was recorded for each of the injections and the three results averaged for each cell. The responses obtained were: 143 Hz average peak response for the high volume impinger cell; 383 Hz for the low volume impinger cell. An spproximately 2.5 times increase in sensitivity was achieved for this size sample input by using the smaller volume cell. The result agrees with the predictions from section 3.21, regarding the implications for cell volume of equation

3.27, i.e.: a smaller volume cell permits a greater number of equilibria to be achieved for a given sample size and flow rate and provided that the limiting concentration of analyte in the coating has not been achieved, a greater response will be received from the detector.

Detector cells: efficiency of the low volume impinger cell.

The partition coefficient for cyclohexane between OFN and squalane was determined. A crystal was coated with 9×10^{-2} microlitres of squalane, entirely over each face of the crystal: the total volume of coating was hence 1.8×10^{-1} microlitres. The crystal was placed in a sealed glass cell of volume 18.5 mls, and was allowed to equilibrate in an atmosphere of OFN. A static sampling cell was prepared with liquid cyclohexane, and 250 microlitre samples of the vapour saturated air were withdrawn and injected into the glass cell. A 250 µl gastight syringe manufactured by the Scientific Glass Engineering Company was used. Sample introduction was effected through a rubber septum, and at a rate of 10 microlitres per second. The frequency of the crystal before injection was noted, as was the stable frequency achieved after injection. The cell was flushed out with OFN and the procedure repeated another four times. The five signals were averaged. A value of 13.4 Hz. was achieved.

Let the frequency constant of the coated crystal be χ Hz./grm, over the entire face of the crystal. Then, the mass of cyclohexane absorbed by the crystal is given by $\frac{13.4}{\chi}$ grms. Hence the concentration in the coating is

given by: $\frac{13.4}{1.8 \times 10^{-4} \cdot x}$ grms/ml. Now, the concentration of cyclohexane in the OFN is given by:

$$\frac{250 \times 10^{-3} \times 84}{22.4 \times 1000 \times 18.5} \cdot \% \text{ by Vol of vapour in the air.}$$

$$= \frac{250 \times 10^{-3} \times 84 \times 8.2}{22.4 \times 1000 \times 18.5 \times 100} \text{ grms/ml.}$$

The volume of the cell >> volume of the coating, then the partition coefficient K can simply be calculated from:

$$K = \frac{13.4 \cdot 22.4 \cdot 1000 \cdot 18.5 \cdot 100}{1.8 \times 10^{-4} \cdot x \cdot 8.2 \cdot 250 \cdot 10^{-3} \cdot 84}$$

$$= (17.915 \cdot 10^{9})/x .$$

The crystal was removed from the static cell, and placed in the low volume impinger cell, under a 16 mls per minute flow of OFN. The cell was thermostatted at 28°C, and on attainment of equilibrium, the diffusion tube containing cyclohexane was switched into the flow system. The frequency decrease was noted for the equilibrium concentration of analyte in the coating. A frequency drop of 15 Hz. was obtained.

Now, consider equation 3.36.

$$\Delta f = \frac{- B K. W_T. V_c}{t \cdot F.}$$

but $\Delta f = - B \Delta m$

Hence $\Delta m = \frac{\Delta f}{B}$

$$\Delta m = \frac{K. W_T \cdot V_c}{t \cdot F.}$$

Thus the mass change on the crystal surface due to the analyte can be calculated from two sources: (i) by the recorded frequency change Δf, i.e., experimentally;

(ii) by the calculation of Δm from K. V_c and the analyte concentration.

Hence for (i) $\underline{\Delta m_1 = \frac{15}{x}}$

for (ii), let t = 1 second

Then $W_T = \frac{4.422}{3600}$ grms. (See Table 5.)

Then $\Delta m_{ii} = \frac{17.915.10^9.60.4.422.1.8.10^4}{x.\ 16.\ 1000.\ 3600}$ grms

$\underline{\Delta m_{ii} = \frac{14.85}{x} \text{ grms.}}$

Now, bearing in mind that there will be sources of error in:- (a) the measurement of the coating volume on the crystal; (b) the measurement of the flow rate; (c) the determination of K; the results for the mass change agreed rather well, and it may be assumed that this impinger design efficiency for sample uptake was of the order of 100%.

Detector Cells: peak shapes obtained with the impinger cell under non-equilibrium conditions.

A crystal was coated with 20 microgrammes per side of "Apiezon M" wax, set up in the large volume impinger cell and allowed to equilibrate at room temperature under a steady flow of OFN. A 100 microlitre gas-tight syringe was used to introduce samples of air saturated with chloroform vapour into the gas flow system just prior to the crystal. First, 40 microlitre samples were introduced at two different rates, 10 and 5 microlitres per second into a gas flow rate of five mls per minute. The frequency of the crystal was recorded at one second intervals, and the results plotted as frequency versus time profiles.

See figure 41a. The same procedure was used to introduce a series of 50 microlitre injections at 25 μls per second into flow rates of 20, 30 and 40 mls per minute. See figure 41b. Finally, the injection port was moved two metres away from the detector cell, upstream, and 40 and 100 microlitre samples of chloroform saturated air were injected at 10 microlitres per second into a five mls per minute gas flow rate. See figure 41c.

The result of the preceding experiments make an interesting comparison with the theory. The theoretical pulse shapes would be symmetrical, as the analyte enters the coating, under conditions of analyte concentration in the gas stream, and then leaves the coating as gas, devoid of analyte, passes over the crystals. The profile of the peak would be a convolution of the curve given by equation 3.27, and the solution isotherm of the coating. For short duration slugs of analyte, in a situation where the limiting equilibrium concentration of analyte in the coating is not approached, the profile would approximately be linear, and a triangular peak would be produced. The peaks shown in figure 41a are more or less triangular, but both show a tendency to "tailing" on their trailing edges, BC and DE. There are two possible explanations for this: (i) the analyte/coating/carrier gas system exhibited hysteresis, due to an imperfectly reversible dissolution; (ii) diffusion of the slug in the gas stream occurred, distorting the trailing edge more than the leading edge. This latter situation is possible, since for a slug y seconds long, which takes x seconds for the leading

FIGURE 41a

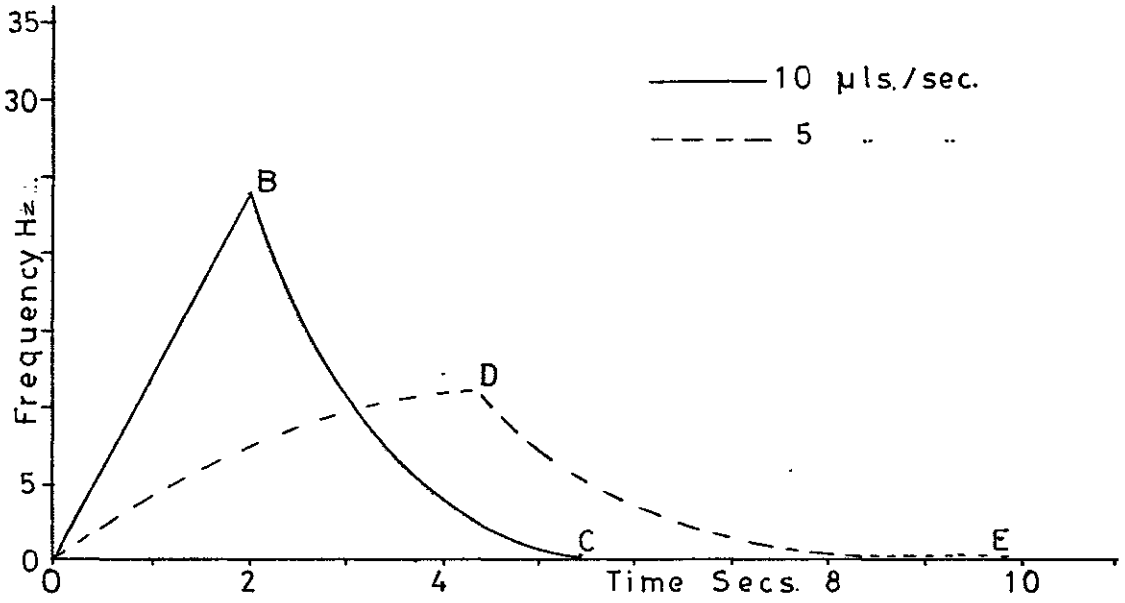

FIGURE 41b

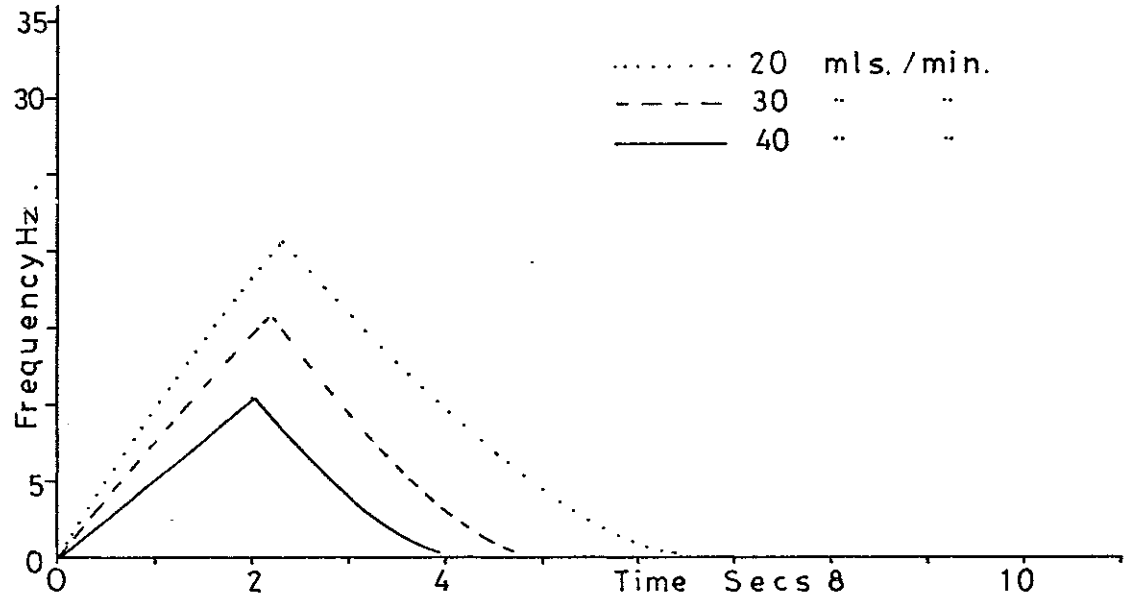

FIGURE 41c

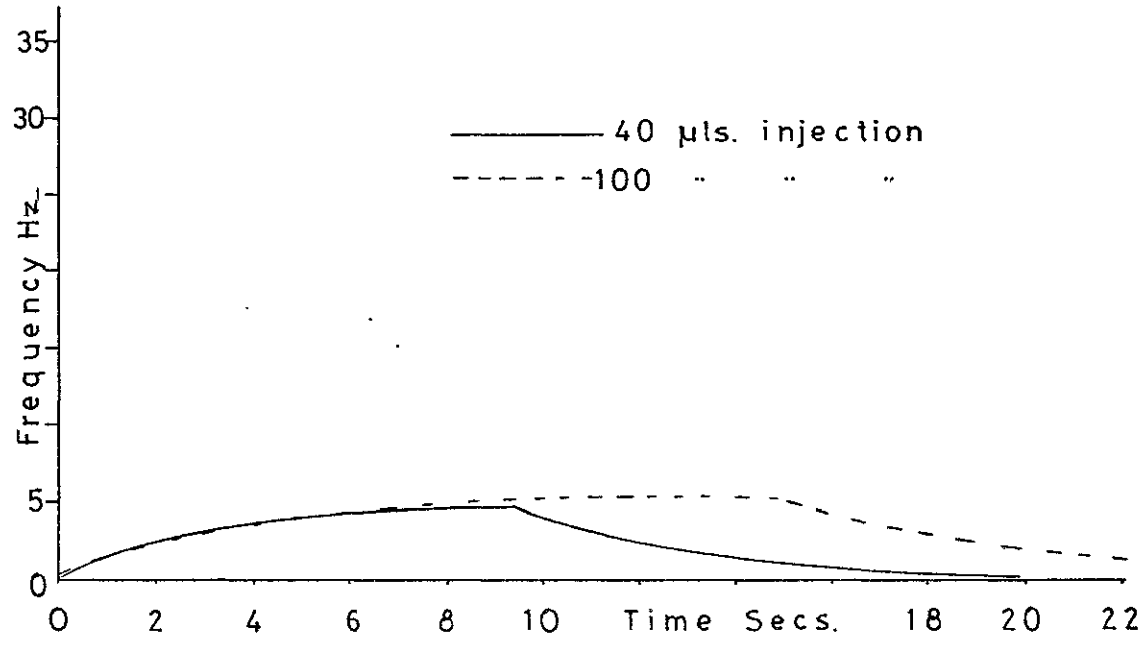

edge to reach the detector, the trailing edge will just pass the detector at x+y seconds. Thus more time is available for diffusion of the trailing edge of the slug, before the detector responds to it.

The second explanation was preferred for a number of reasons. Firstly, the frequency of the coated crystal both before and after the peaks was the same, indicating that no permanent analyte retention had taken place, thus the system was reversible. Secondly, both the leading and trailing edges of the eight second peak were more distorted than the comparable edges of the four second peak, indicating an increase in distortion with time, that would not obtain in a system showing hysteresis. The effect of considerable diffusion on the peak shapes may be seen by comparing figure 41c with 41a. The results from 41c, where the peaks took about three minutes to reach the detector, show the flattening and broadening of the peaks as a result of diffusion in the gas stream.

It would be expected from equation 3.27 that for fixed concentration of analyte of fixed slug length, increasing the flow rate of the carrier gas would increase the slope of the peak profile, and cause the peak height to increase. This effect was not observed in figure 41b, since the same sample size and input rate were used for each gas flow rate, resulting in a successive dilution of the analyte vapour. However, the results of figure 41b do demonstrate that as the flow rate was increased, the time taken for the peak to reach the detector decreased, less diffusion occurred, and the time at which peak

response was achieved, relative to the start of the peak, as the analyte initially reached the detector, approached the two second minimum to be expected from a two second sample input.

Detector cells: peak shapes obtained with the impinger cell under equilibrium conditions.

This subject has been dealt with in Section 3.2.2, under diffusion sampling cells. See figure 37.

Validity of equations 3.27, 3.34 and 3.36 under non-equilibrium conditions.

A crystal was coated on each side with 4×10^{-2} microlitres of di-nonyl phthalate, located in the large volume impinger detector cell and allowed to equilibrate at room temperature under a 12 mls per minute OFN gas flow. Samples of air saturated with chloroform vapour were withdrawn from a static sampling cell and introduced to the gas stream at a rate of 10 microlitres per second. A 100 microlitre gas tight syringe was used, and triplicate injections of 20, 40 and 80 microlitres of sample were introduced. The experiment was repeated for toluene vapour. The maximum frequency change for each sample was determined, the results for triplicates averaged, and the values plotted as frequency change versus slug time-length. See figure 42a and b.

These results may be interpreted as a solution of equation 3.27 for increasing values of n, for as the length of the slug increased, the number of cell flushes per sample increased. The concentration of the analyte vapour in the gas stream was kept constant. Hence the

FIGURE 42a

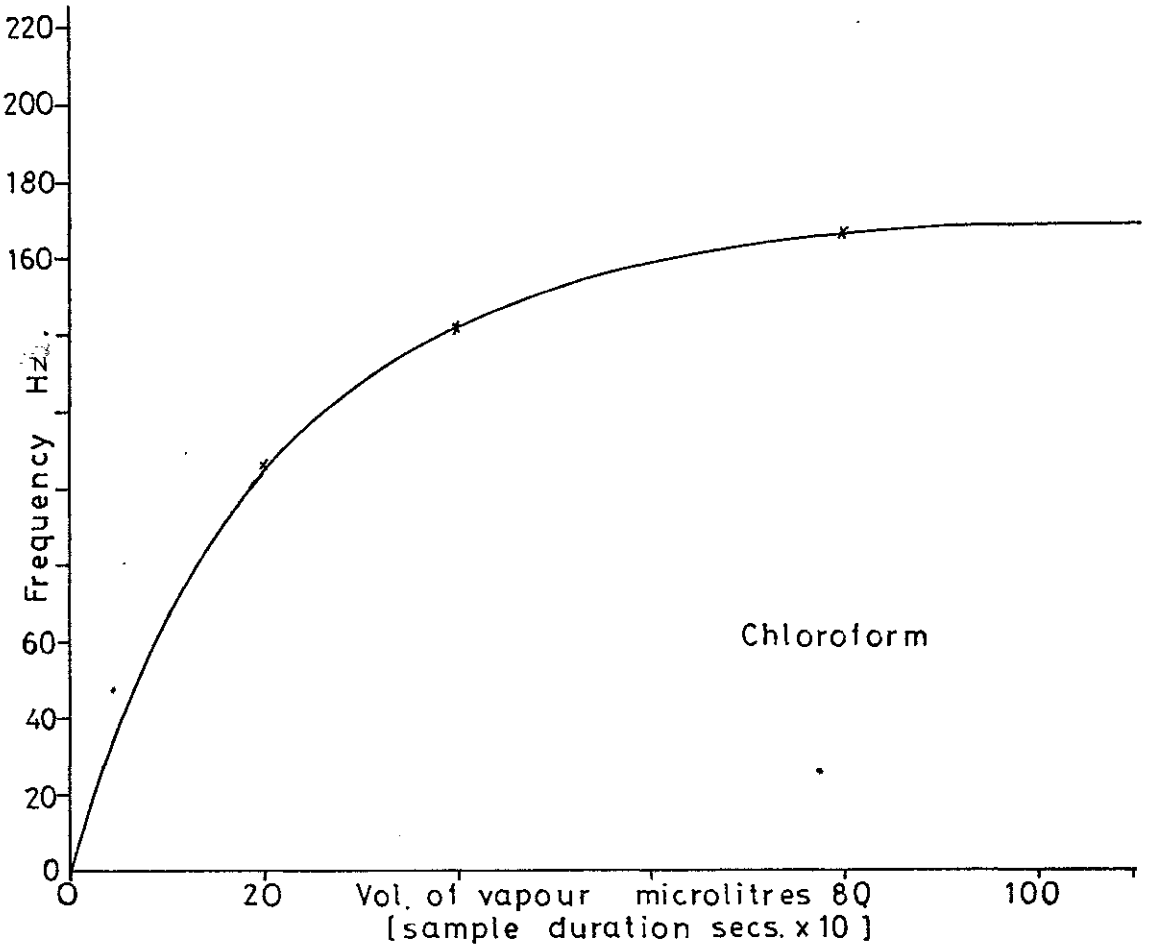

FIGURE 42 b

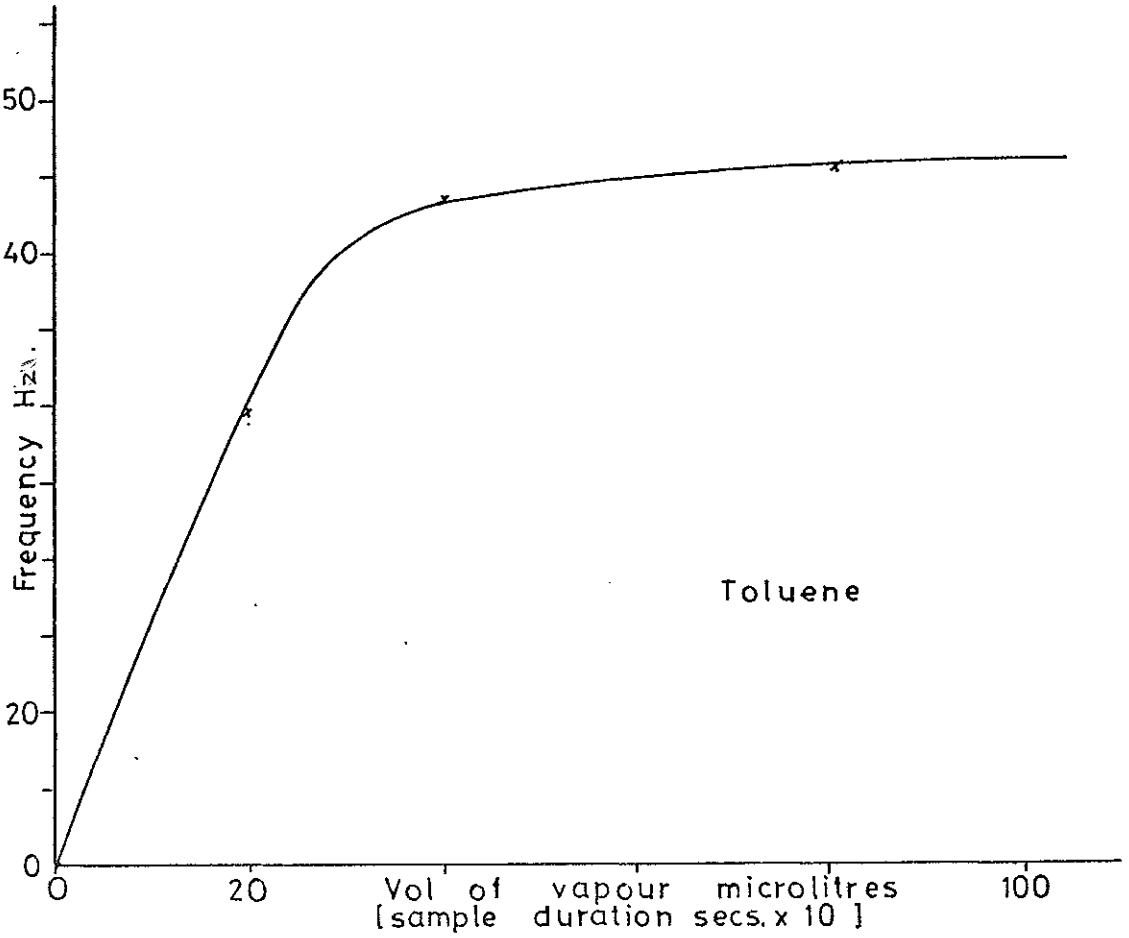

shape of the curves in figure 42a and b compares well, with the shape of the curve in figure 24b, that was obtained by solving 3.27 for arbitrary values of K, n and x.

Equations 3.34 and 3.36 predict that A and Δf are proportional to $\frac{1}{F}$, and that Δf is proportional to $\frac{1}{t}$. It is difficult to establish either of these relationships in the non-equilibrium situation, since any alteration of the flow rate F, for given values of W_T and t, will increase the value of Δf and A, since more cell flushes take place in a given time, and hence the concentration of analyte in the coating will be increased. Effectively the linear relationship between Δf or A and $\frac{1}{F}$ will be altered, causing a negative deviation (towards the 1/F axis) for large values of 1/F in a graph plotted of Δf or A <u>versus</u> $\frac{1}{F}$ and a positive deviation (away from the $\frac{1}{F}$ axis) for small values of $\frac{1}{F}$, as the response of the system is respectively reduced, then augmented by the increasing number of cell flushes with increasing flow rate.

Thus, a crystal was coated with six microgrms per side of "Apiezon M", located in the large volume impinger detector cell, and allowed to equilibrate at room temperature under a carrier gas flow rate of five mls per minute. Samples of air saturated with chloroform vapour were withdrawn from a static sampling cell, and the 40 microlitre volume injected into the carrier gas stream at three different input rates; 200 microlitres per second, 20 microlitres per second and 40 microlitres per second. Each injection was triplicated, and all

three input rates were used at each of five different carrier gas flow rates, 5 mls per minute, 10 mls per minute, 20 mls per minute, 40 mls per minute and 50 mls per minute. The maximum frequency depression for each injection was recorded, and the results averaged for the triplicate injections. The results were plotted for each injection rate as frequency change versus the reciprocal of the flow rate. See figure 43.

The graphs followed the predictions made earlier, in that for each injection rate, negative deviation may be observed at low flow rates, and positive deviation for high flow rates. It is also interesting to note, that at low flow rate values, $1/F = 0.1$ to 0.2, the greater response was achieved by the samples whose input rates were slower, and hence slug length longer. In other words response was principally determined by the number of cell flushes per sample, i.e.: equation 3.27 operated. At the highest flow rates, $1/F = 0.02$, the positions of the responses were reversed, thus equation 3.36 operated, and it may be assumed, that at this flow rate sufficient cell flushes had occurred, for the concentration of analyte in the coating to be little affected by further cell-flushes.

A further prediction from equations 3.34 and 3.36 was that the use of peak area for determination of W_T should give rise to more precise results than Δf values. This advantage should tell most obviously in a situation where manual injection of the sample occurs with a concomitant wide error in the value of t, the input time of the

FIGURE 43

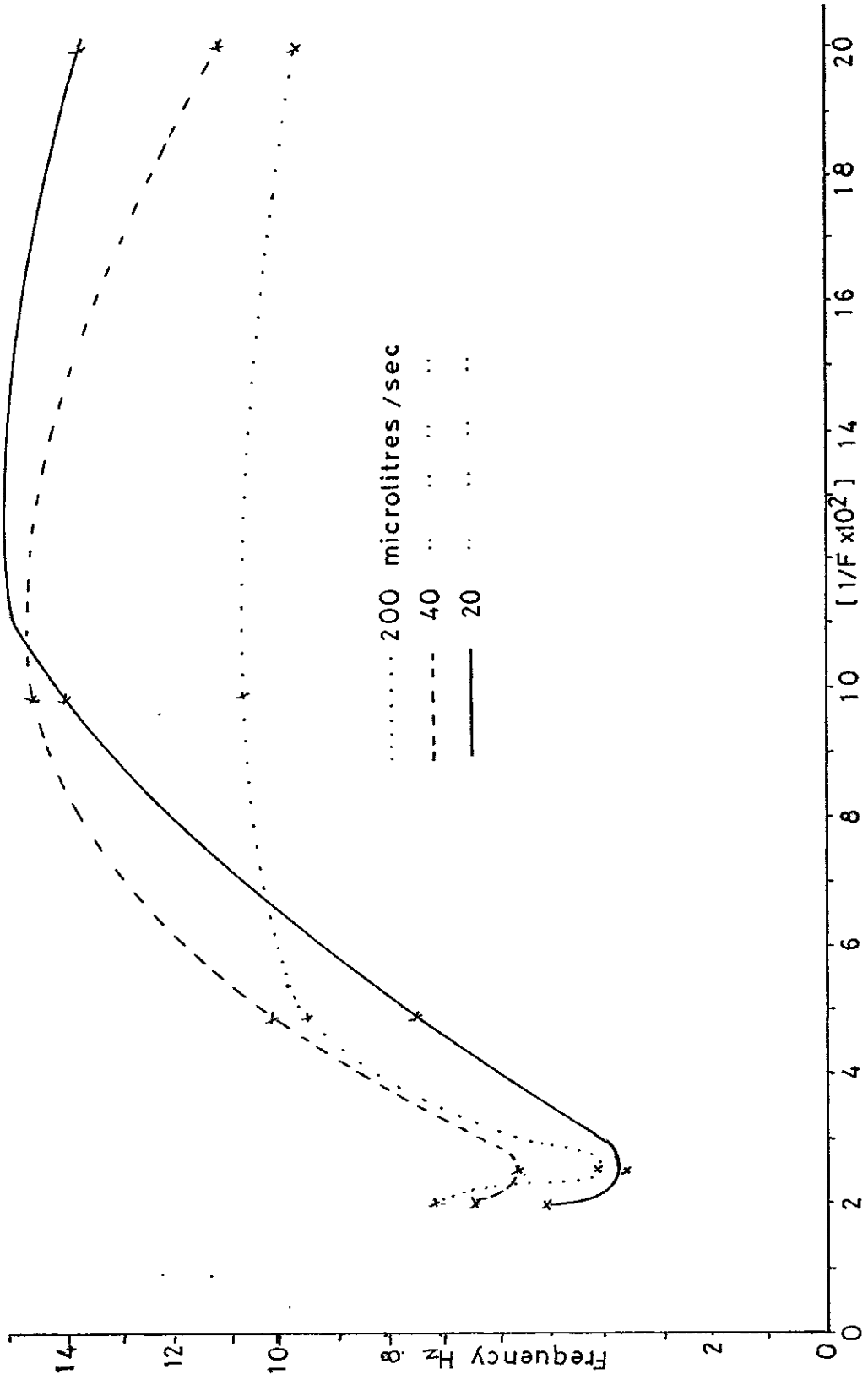
200 microlitres /sec
40
20
Frequency Hz
[1/F x10²]
0
2
4
6
8
10
12
14
16
18
20

sample. Hence, using the same set-up as was used in the previous experiment, replicate injections of 40 microlitres of air saturated with chloroform vapour were made, at an injection rate of 10 microlitres per second. Twenty injections were measured, using the maximum frequency depression Δf. A further twenty injections were measured by recording the frequency second by second throughout the peak, and calculating the total peak area from these measurements. The results are presented in Table 6, along with the statistical calculations. It can be seen that a greatly improved precision was obtained with the peak area results.

Validity of equations 3.27, 3.34 and 3.36 under equilibrium conditions.

Equation 3.27 predicts that on attainment of the equilibrium value for the concentration of analyte in the coating, no further mass accretion may occur, and hence the response versus time curve will reach a plateau region. This type of response may be seen from figure 38a, and the experimental details have been discussed earlier in the dynamic sampling cells section.

Equations 3.27 and 3.36 were tested simultaneously by one experiment. Two crystals were each located in a low volume impinger detector cell: one crystal was coated with 200 microgrms per side di-nonyl phthalate, the other with 10 micrograms per side "Carbowax 20M". The cells were equilibrated in a water bath at 30°C, with a carrier gas flow rate of 12 mls per minute. A thermostatted diffusion tube containing chloroform was switched into the

TABLE 6

Peak Height Hz	Peak Height Hz	Peak Area Hz	Peak Area Hz
16	15	128	124
19	13	117	137
17	14	123	117
19	15	127	129
16	19	136	132
19	21	127	118
17	15	113	124
20	14	124	127
16	12	123	127
15	12	116	128
Mean = 16.2 S.D. = 2.628 R.S.D. = 16.2%		Mean = 124.85 S.D. = 6.23 R.S.D. = 5.06%	

gas flow, and the frequency of each crystal recorded at regular intervals from separate digital counters. The flow rate was varied in steps, from a meter reading of 11 divisions, down to 9, then 5 divisions, back up again to 10 divisions: sufficient time was allowed between each step for the system to reach equilibrium for the new concentration of analyte. The frequency versus time profile for the experiment may be seen in figure 44.

The diffusion tube method of sample introduction provided a constant rate of analyte flow into the carrier gas, provided that the temperature and pressure in the sampler was kept constant. Let this rate of introduction be x grams per second. Equation 3.36 may then be re-written:

$$\Delta f = \frac{B K V_c}{F} \cdot x \qquad \ldots\ldots\ldots \quad 3.37$$

$$\text{i.e. } \Delta f \propto \frac{1}{F}$$

Thus a plot of the response values from figure 44, against $\frac{1}{F}$, should give a linear graph. This procedure has been carried out for both coatings, and the graphs are depicted in figure 45a. It can be seen that the relationship $\Delta f \propto \frac{1}{F}$ is well supported by the previous experiment.

The time taken at each flow rate for the detector response to reach an equilibrium value was obtained from figure 44, for the di-nonyl phthalate coated crystal, and plotted against $\frac{1}{F}$. See figure 45b. The results indicated a linear relationship between the two quantities.

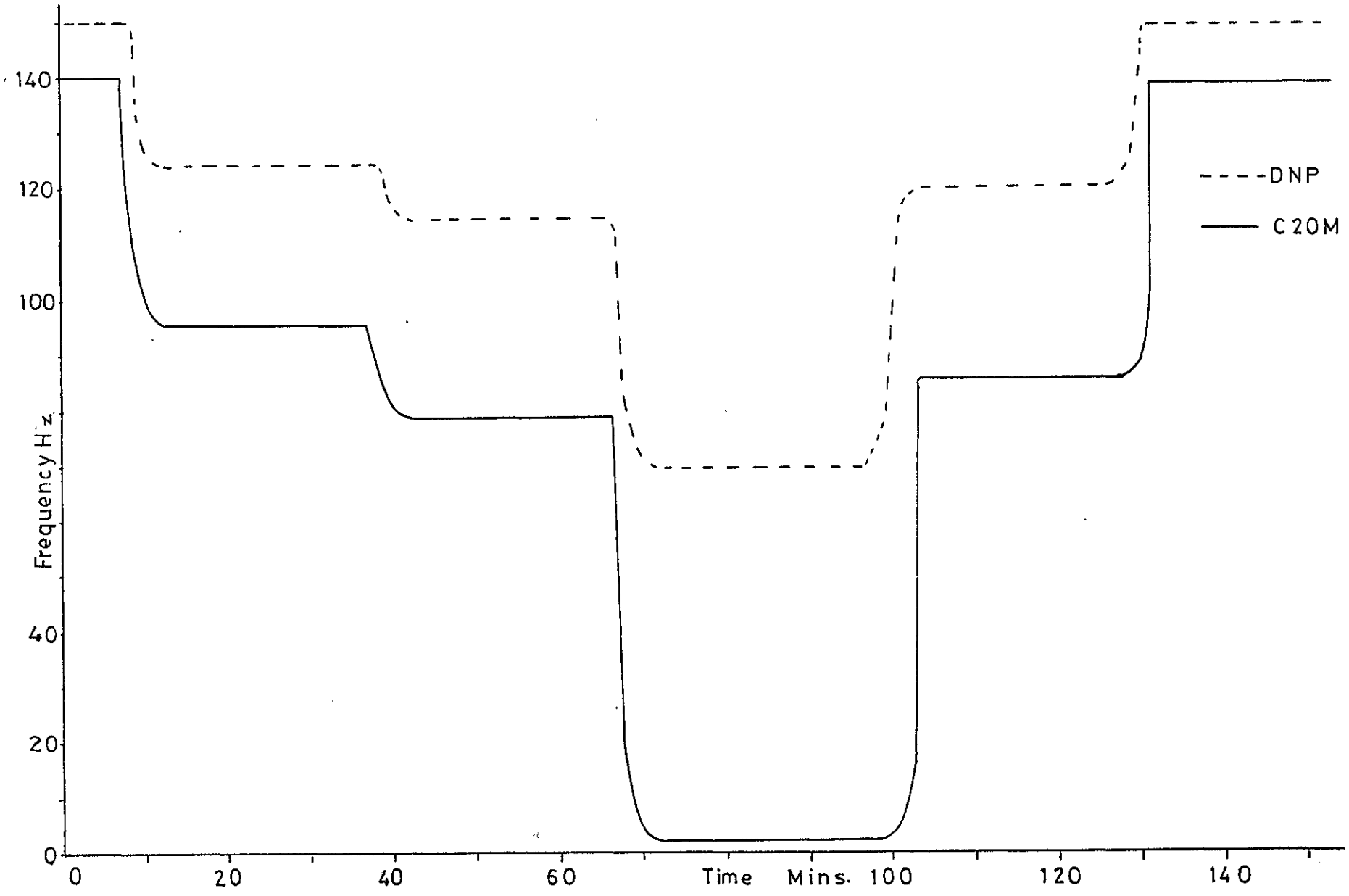
140
120
100
40
20
0
Frequency Hz
0
20
40
60
Time Mins.
100
120
140
----DNP
—— C20M

FIGURE 44

FIGURE 45a

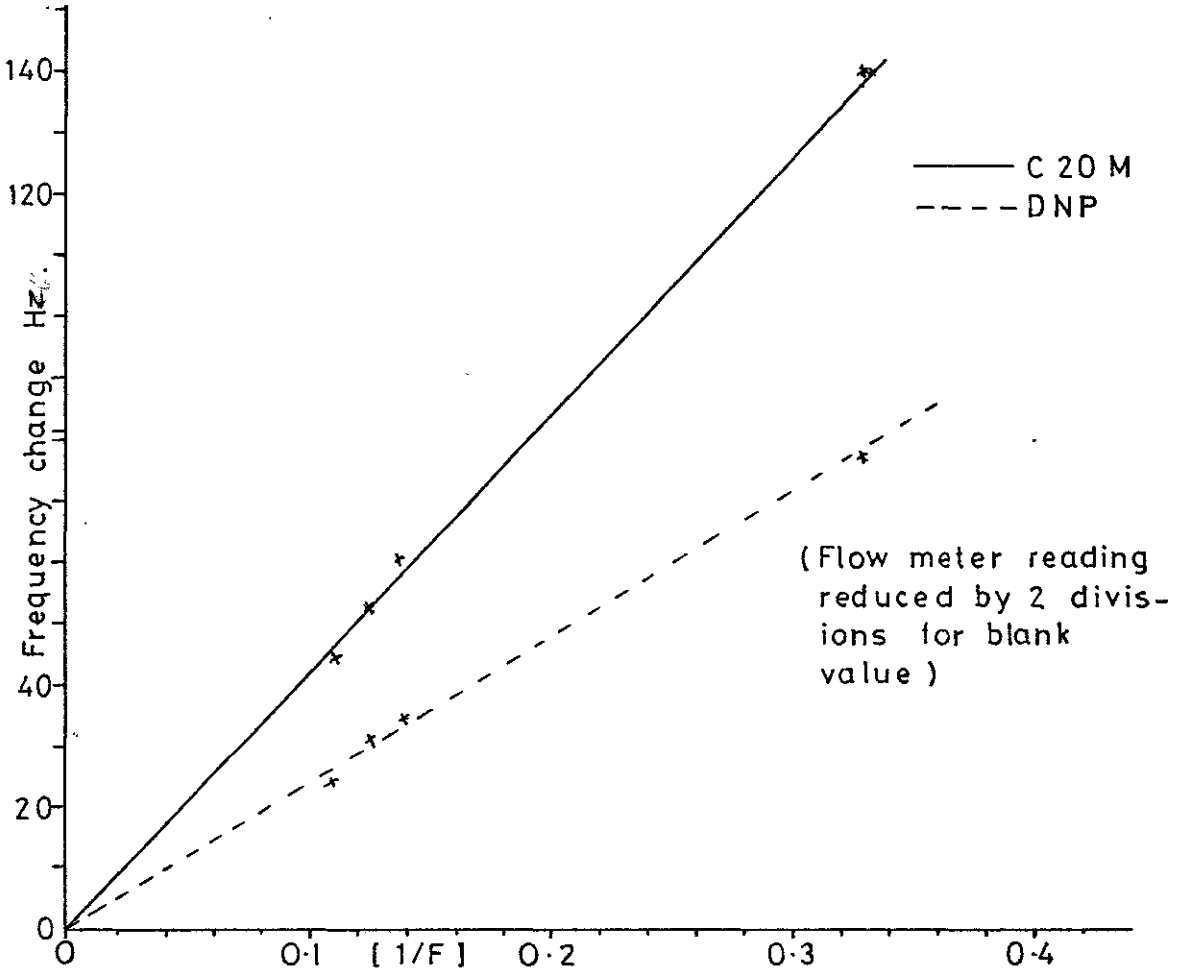

FIGURE 45 b

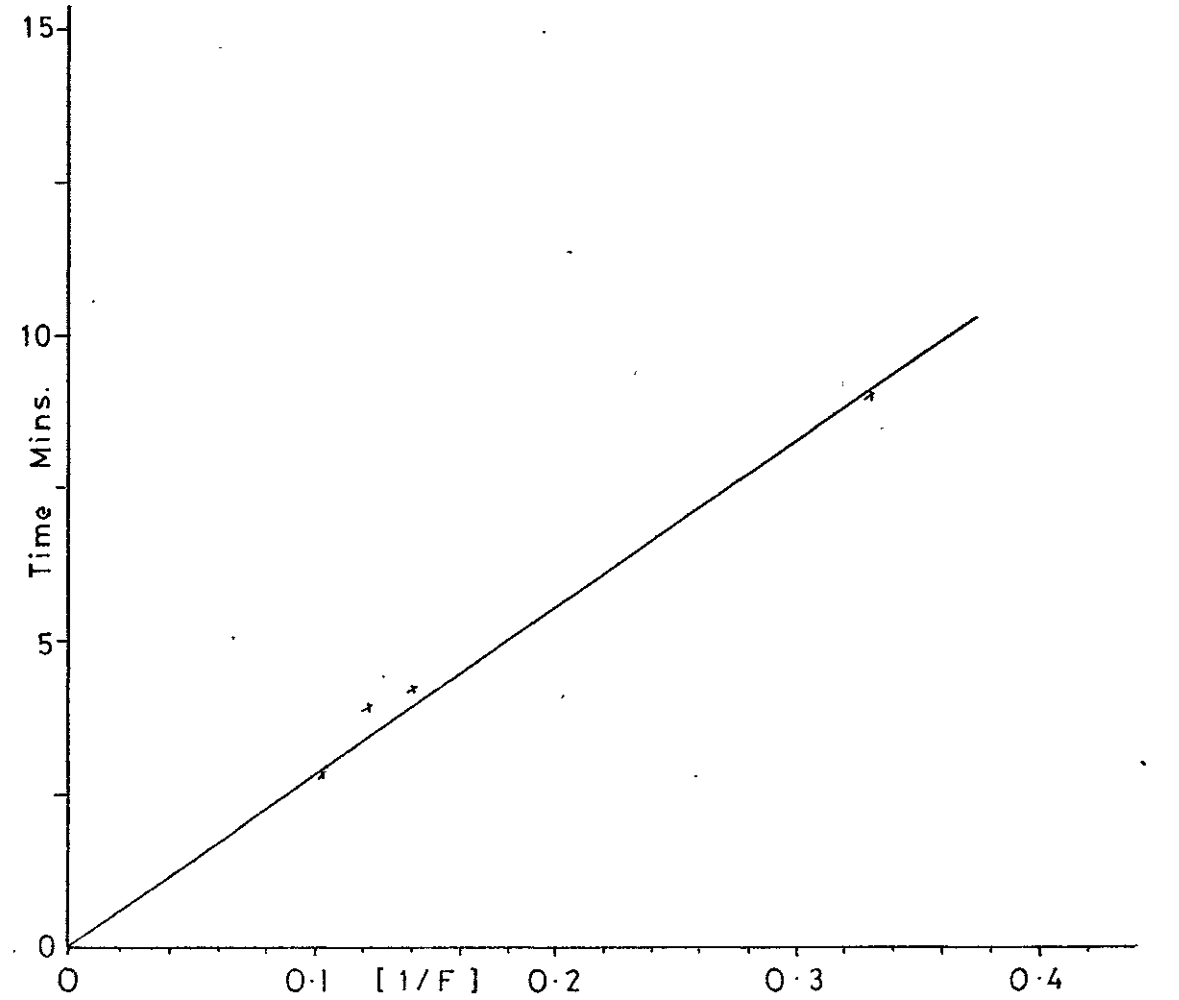

It may be seen from equation 3.27, that for a given coating/analyte system, the same number of cell flushes must occur for the sample to reach equilibrium irrespective of analyte concentration in the gas phase. If this is so, then for a given cell system, the number of cell flushes per second will be proportional to the carrier gas flow rate. In other words the time taken for a sample to reach equilibrium concentration in the coating, will be proportional to $\frac{1}{F}$. The results of the experiment illustrated in figure 45b validated these assumptions.

Validity of equations 3.34 and 3.36: independence of response on cell design for an equilibrium situation.

To test this idea, a completely different cell design was used. The cell consisted of a protective metal cap from a crystal, with a $\frac{1}{8}$ inch hole drilled in one face only, in the centre. A piece of $\frac{1}{4}$ inch nylon tubing 10 cms long was cut with a slot in the centre portion, and was affixed to the metal cap with epoxy resin adhesive. See figure 46. The crystal was located in the cell in a manner identical to the location of a crystal in the large volume impinger cell. The gas stream in the former cell then flowed past the crystal, and at a little distance from it. The only method of analyte gas transport to the crystal was diffusion and probably eddy-currents. A crystal was coated with β-β-oxydipropionitrile, placed in the cell and equilibrated at 30°C in a water bath, with a 12 mls per minute carrier gas flow. The diffusion tube containing chloroform was switched into the carrier gas stream, the response allowed to reach its

FIGURE 46

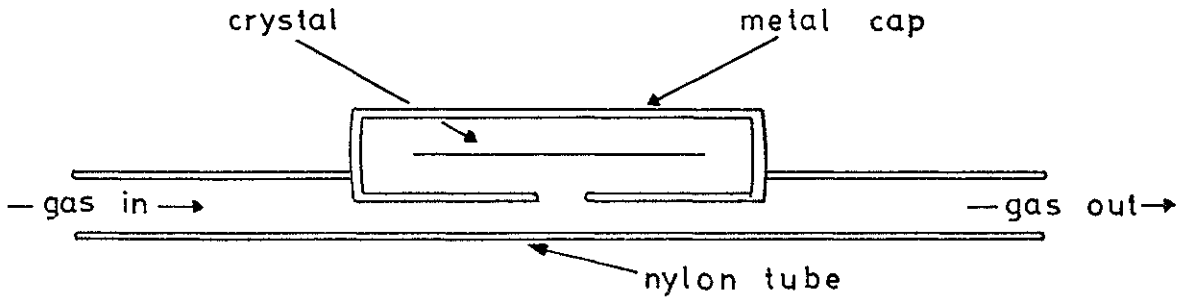

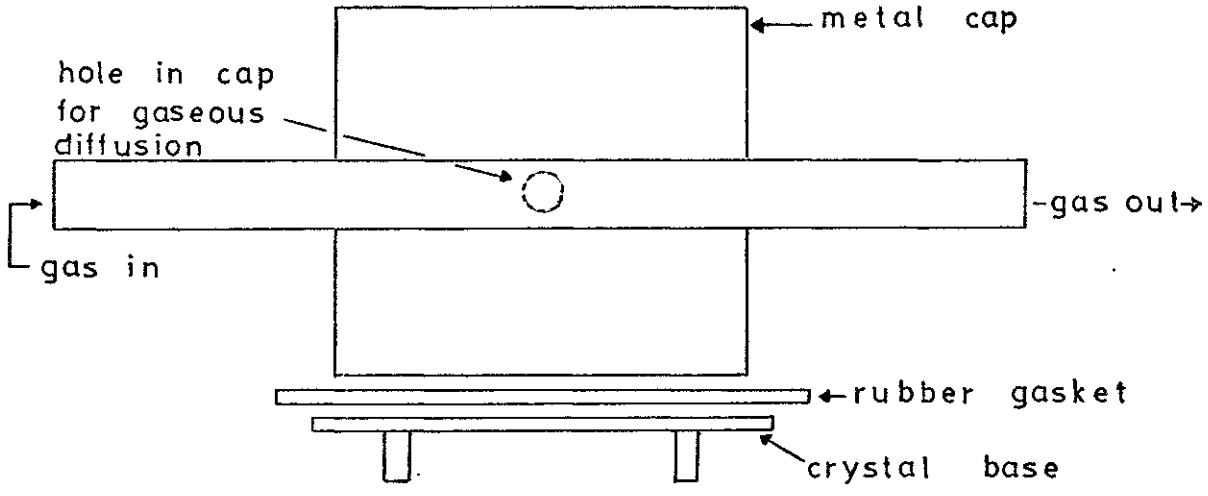

Diffusion Detector Cell

equilibrium value, and the frequency change noted. Three replicate samples were used and the readings averaged. A frequency change of 11.5 Hz was obtained with the diffuser detector cell, compared with 11.0 Hz achieved with the low volume impinger cell under identical conditions.

3.3 DETECTOR COATINGS: COATING METHODS AND PARAMETERS FOR OPTIMUM SENSITIVITY.

The coating parameters discussed in this section are extrinsic properties, related to the method of coating application, volume of coating used, etc. Intrinsic properties of the coatings will be discussed in Chapter 4.

3.3.1 Theory.

There are three parameters to be considered when coating a crystal to ensure maximum response to the analyte. Firstly, the area of coating is important. Equations 2.21, 2.26 and 2.31 all indicate that $\Delta f = B\frac{\Delta m}{A}$, where B is a constant and A is the area of coating. Thus, by restricting the coating to a small area, the mass increase due to analyte dissolution will be localized, and a higher response will be obtained from the detector. Secondly, the location of the coating is critical: Sauerbrey[94] has shown that the maximum shear amplitude of an AT cut quartz crystal occurs in the centre of the plate. In effect, this means that the most mass sensitive area will be located in the centre. Finally, the volume of the coating will determine the response, since equations 3.34 and 3.36, show a linear relationship between response and coating volume.

The method selected for applying the coating to the crystal must ensure that a thin even film is deposited. The importance of this technique lies not only in the fact that the basic assumptions behind the derivations of equations 2.21 to 2.31 depend on the presence of a thin even film on the crystal surface, but also because uneven films may give rise to results that are irreproducible from coating to coating. Another problem with uneven coatings has been pointed out by King[66,67]. Thus irregular coatings caused vibrations in the Z and Y axis, as well as the X axis of the plate, preventing the establishment of a stable resonating condition. Finally, the presence of uneven layers on the crystal may either alter the electrical value of the crystal, so that it no longer matches the circuit, and resonance ceases, or the mechanical quality of the crystal may be altered, causing coupling to other modes of motion, and resulting in anomalous frequency changes.

In the literature on piezoelectric detectors three main techniques for coating crystals with liquids have been employed. The liquid is usually held in a solution of a volatile solvent, and then either sprayed onto the crystal, or dropped onto the crystal from a syringe, or the crystal is dipped into the solution. These processes are followed by evaporation of the solvent at a suitable temperature. Solid coatings have been applied using all three techniques, and in addition some workers have attempted to glue the coating on. Thus King[55,60] has described the use of poly vinyl alcohol and

other light glues for attaching solids to crystals. King suggested that metals could be coated by electroplating, and oxides prepared chemically from metals so deposited. Guilbault[73] used a dipping technique to coat halides of mercury onto crystals. In a later paper Guilbault and Lopez-Roman found that the application of sodium tetrachlormercuriate coatings proceeded better when a spray method was used, a smoother coating was produced, and the dipping method was abandoned. The spray method was also preferred by Guilbault, Lopez-Roman and Billedeau[78] for the application of other metal halides.

The application of undiluted liquid coatings to the crystal has been described by King[58,59] who used a camel-hair brush to spread the liquid. Karasak and Gibbins[89] and Shackleford and Guilbault[77] used 5% solutions of the liquid coatings. A small aliquot of the solution was dropped onto the crystal and allowed to spread; evaporation of the solvent left a thin smooth coating. Similar techniques have been used by King[55,60] and Bonds[50]. Liquid coatings have been sprayed onto the crystal in a similar manner to solid coatings[69].

3.3.2 PRACTICE

Coating Methods

Three types of GC coating were used (with respect to relative viscosity): liquids, such as di-nonyl phthalate and squalane; waxes and rubbers such as "Carbowax" and silicone gum rubber; solids, such as ethylene glycol

succinate. The most frequently used method of coating was to dissolve the coating in a suitable solvent to give a 1 to 5% solution by weight. The solution was applied to each side of the crystal, the desired volume being delivered by a Scientific Glass Engineering 10 microlitre syringe. The solvent was evaporated at room temperature, and then the crystal was placed in an oven at 80 - 110°C for 1 to 4 hours, depending on the nature of the coating. The heating smoothed the wax and rubber type of coatings, eliminating the concentric rings caused by solvent evaporation. The more liquid coatings were spread over the entire crystal surface by the heating step. A list of the solvents used and heating times for the various coatings is presented in table 7.

The method described gave smooth reproducible coatings of known volume. Thus, three separate crystals were coated using the described technique. A one microgrm per microlitre solution of "Apiezon M" was prepared in chloroform, and 20 micrograms per side coated onto the crystals. Each crystal in turn was located in the high-volume impinger detector cell, equilibrated at room temperature and 12 mls per minute gas flow, and then triplicate 40 microlitres samples of air saturated with chloroform vapour were injected into the system at 10 microlitres per second. The maximum frequency change was recorded for each injection, and the results for triplicate injections averaged.

TABLE 7

Coating	Solvent	Oven Temperature °C	Time in Oven Mins.
"Apiezon M"	C	80	30-60
B-B-oxydipropionitrile	M	Room Temp.	60
"Carbowax 20M"	C	140	10-15
Di-nonyl Phthalate	A	100	50-70
Ethylene Glycol Succinate		80	50
Pluronic L64	M	80	30-60
Rubber Solution	H	80	60-120
Silicone Gum Rubber	T	150	120-240
Squalane	T	100	45-60
Tri-cresyl Phosphate	M	95	45-60

A = Acetone
C = Chloroform
H = Hexane
M = Methanol
T = Toluene

RESULTS.

Crystal Number	Δf on coating	Response to Chloroform
1	9.6 KHz	40 Hz
2	9.4 KHz	42 Hz
3	9.7 KHz	42 Hz

An alternative method for coating the crystals involved dropping a very small aliquot of the undissolved coating onto the crystal surface. The liquid was spread over the entire crystal area with a glass rod, and then tested in an oscillator circuit to see if it would resonate. If resonance was not achieved the crystal surfaces were rubbed gently with a "non-fluffy" tissue, and the crystal tested again. The procedure was repeated until the crystal resonated. Thus, two separate crystals were coated using the method described above. Squalane was used as the coating, the initial aliquot was 0.5 microlitres. The coated crystals were placed in turn in the low volume impinger detector cell, and equilibrated at 30°C under a gas flow of 12 mls per minute. A diffusion tube containing hexane was switched into the carrier gas stream, and the frequency change recorded for the equilibrium signal.

RESULTS.

Crystal Number	Δf on coating	Response to Hexane
1	12.2 KHz	8 Hz
2	14.3 KHz	11 Hz

This coating method was extremely rapid, but was generally found to be less reproducible than the original method. The choice of coating method depended therefore on the precise application of the detector.

Two coatings that required specialised coating techniques were ethylene glycol succinate (EGS) and "Carbowax 20M" (abbreviated to "Carbowax"). EGS was a white crystalline solid at room temperature which was soluble in chloroform. When applied to the crystal in solution from a microsyringe, the evaporation of the solvent left a series of concentric rings of the coating. Attempts to smooth the coating by heating the crystal so that the EGS melted (at about 80°C) failed, and even a small deposited mass prevented the crystal from resonating. It was found that by placing a small crystal of the EGS onto the centre of the gold electrode, and then heating the quartz crystal at 80°C for 50 minutes, a smooth thin coating was obtained that permitted the quartz crystal to resonate.

Two crystals were coated with "Carbowax" using identical technique. The "Carbowax" was dissolved in chloroform, and aliquots of the solution were placed on either side of the crystal. The solvent was allowed to evaporate off at room temperature, and then the crystal was placed in an oven at 200°C for 40 minutes. Coatings of 200 microgrms per side were applied to each crystal using this method. Each crystal was located in turn in the low volume impinger detector cell under identical conditions (30°C water bath and 12 mls/min gas flow).

Triplicate 40 microlitres injections were made of chloroform vapour saturated air at 10 microlitres per second over each crystal. The maximum frequency depressions were recorded and averaged.

RESULTS.

Crystal Number	Δf on coating	Response to Chloroform
1	28.4 KHz	490 Hz
2	30.0 KHz	230 Hz

Thus, for an otherwise reliable method of coating, two crystals had been prepared with similar coatings and widely differing sensitivities. Checking the history of the crystals showed that number 1 was brand new, whereas number 2 had been previously coated and cleaned. It was also noticed that the solution used to prepare crystal number one's coating was freshly prepared, whereas the other coating had been prepared from an older solution. Crystal 2 was checked with other coatings to ascertain whether the decreased response was due to an inferior mass sensitivity. The crystal was found to be as mass sensitive as most other crystals. Next, the coating technique was thoroughly investigated, each parameter was altered in order to find out how it affected the sensitivity of the coating. From these experiments four important criteria were established for the production of high-sensitivity "Carbowax" coated crystals.

(i) Brand-new or thoroughly cleaned old crystals must be used.

(ii) Freshly prepared solutions of "Carbowax" in chloroform should be used.

(iii) The heat spreading process was best carried out at 140°C for 10 to 15 minutes, and the crystal, in its protective metal cap, removed from the oven after the temperature had gradually been lowered to 80°C.

(iv) Care must be taken to prevent any dust or particle from entering the coating prior to the cooling process.

A visible difference was discernible between the two coatings: low sensitivity coatings were hard, non-viscous and translucent; high sensitivity coatings were transparent, viscous and tacky to the touch. High sensitivity coatings could be converted to low sensitivity coatings by rapid heating and cooling. The high sensitivity coatings were stable in the normal detector cell environment, even under conditions of high analyte concentrations for the two months that they were studied.

A reasonable explanation for these phenomena would be that the two different forms of the coating are physically different. The low sensitivity coating is the typical waxy solid that "Carbowax" normally assumes, the high sensitivity coating is a liquid, which, because it is extant at a temperature well below the freezing point of "Carbowax" (60°C), should be identified with the supercooled liquid state. Pryde[107] considered that a liquid that demonstrated a very high viscosity in the vicinity

of its freezing point could quite readily be cooled below this temperature without solidifying, providing that the process of nucleation could be sufficiently hindered. This situation occurs for compounds with complicated molecular shapes and strongly directed intermolecular forces. This process of supercooling takes place more readily on clean, dust and particle free smooth surfaces, when the cooling rate is not too rapid. "Carbowax" is a polyethylene glycol, which exhibits all the favourable features for supercooling; high viscosity, complex molecular geometry and strong inter-molecular H-bonding. The conditions that give rise to supercooling are those that favour formation of high-sensitivity coatings.

The final piece of evidence for the super-cooled "Carbowax" coating comes from the work of Fiddler and Doerr[108]. These workers followed the alteration of retention coefficients with temperature for a "Carbowax 20M" packed column. A discontinuity occurred at 60°C, the retention coefficients, which had been increasing in value with decreasing temperature, displayed a sudden decrease. The retention coefficients were two to two and a half times lower for a range of compounds. This discontinuity could be reversed by increasing the temperature above 60°C, and reproduced by cooling the column to below 60°C. The authors pointed out that at 60°C the "Carbowax" passed from its liquid to its solid form. At temperatures below 60°C gas-solid chromatography was undertaken, above 60°C gas-liquid chromatography was carried out. The difference in sensitivity between the two types of "Carbowax" coating

produced in this study, was usually 2.1 to 2.3, which accords well with the retention coefficient alterations found by Fiddler and Doerr.

Coating factors affecting sensitivity

Sauerbrey's work[94] on the variation of mass sensitivity with position of coating location was checked by the following experiment. A solution of "Apiezon M" in chloroform was deposited on a selected area of the gold electrode. Small discrete coatings were made, three microgrms by weight and two mms in diameter. Three areas of the gold electrode were chosen, one was central, the other midway between centre and top, and the third at the top. See figure 47. Eight replicate coatings were made at each point, and the frequency change on coating recorded for each one. See table 8 for the results. The means and standard deviations were calculated for each location, and statistical tests applied to these results showed that there was a significant difference between the frequency changes for area B, when compared with areas A and C. Hence the most sensitive portion of the crystal would seem to be a little above the centre of the electrode.

Variation of response with area of coating.

The validity of equations 2.21, 2.26 and 2.31 is difficult to establish by experiment for two reasons. Firstly, the effect of spreading a coating over a larger area, reduces the $\Delta m/A$ value, and hence the frequency, but at the same time, the location of the coating moves outward from a small area in the centre of the crystal's

FIGURE 47

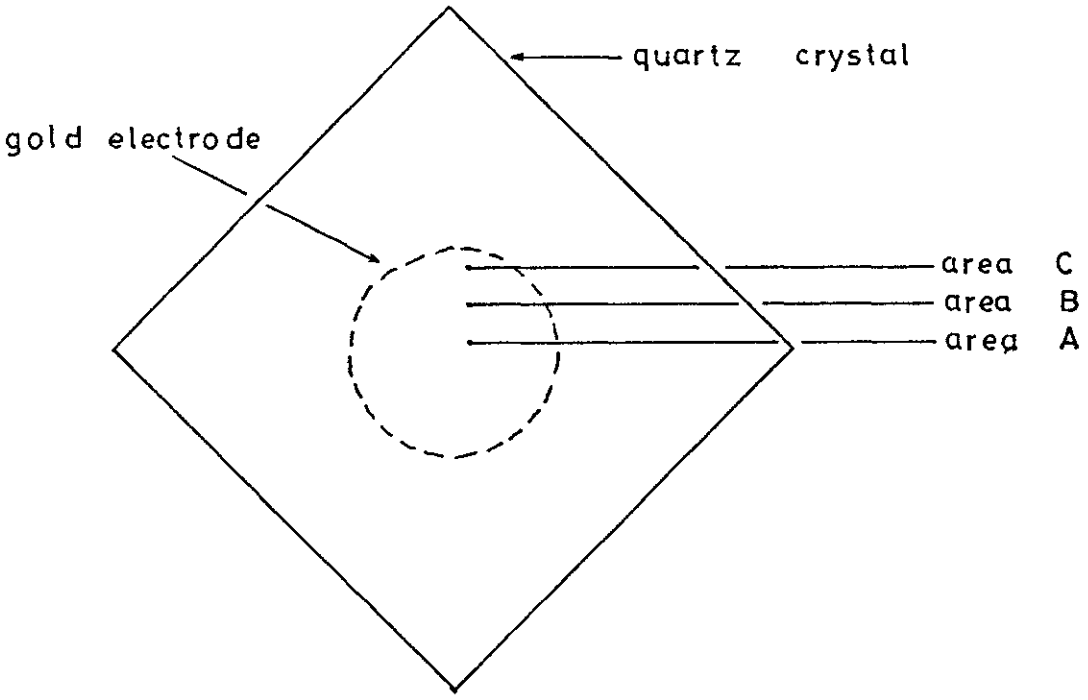

TABLE 8

	Position of Coating (See Diagram 47)		
	A	B	C
Frequency Change For Coating	2229	4212	2922
	2683	6168	2864
	2604	4103	2381
	1751	4126	3931
	2393	3975	3573
	2077	3401	2902
	1793	4348	3594
	3273	4002	3875

electrode. It has been demonstrated that the mass sensitivity is not constant over the entire plate area. Hence, the total frequency change on coating is not only reduced because of an increase in the area, but also by a decrease in the overall mass sensitivity of the portion of the plate covered by the deposit. Secondly, the simplest way to spread a coating on a crystal, was to use a heating method; inevitably this caused some vaporisation of the coating, thus reducing the total volume. Equations 3.34 and 3.36 indicate that A and Δf are proportional to the coating volume, and hence the variation in response of the detector is yet again a function of two variables.

One method of overcoming the variable mass sensitivity with coating location, would be to consider the frequency change on coating as a guide to the alteration of mass sensitivity. Thus, if two coatings of the same mass are spread over different areas, the $\Delta m/A$ value assumed from the frequency change, contains an inbuilt correction for the variation of mass sensitivity with coating location. The problem of coating-loss on heat spreading may be overcome by selecting a coating with low volatility, and employing a low spreading temperature.

Thus, four crystals were coated with five microgrms per side of rubber solution. The coating substance was dissolved in hexane, and applied to the crystal with a microsyringe. The area of the deposit was controlled at this stage, by constantly moving the syringe around the desired area whilst pipetting the solution. The hexane was allowed to evaporate, and then all four crystals were placed

in an oven at 60°C for 20 minutes to obtain a smooth surface. The frequency change on coating was noted. Each crystal was located in turn in the low volume impinger detector cell under a gas flow of 12 mls per minute and at a temperature of 30°C. The frequency change obtained for the equilibrium signal produced by chloroform vapour in the gas stream was recorded for each crystal. The chloroform was introduced to the gas stream from a diffusion tube. Each crystal was exposed to triplicate samples of the chloroform, and the frequency changes averaged. The results were plotted as response to chloroform against frequency change on coating, and response to chloroform against the reciprocal of the area. See figure 48. It may be seen that the former plot gives a straight line, as expected, whereas the latter contains a negative deviation for high area values, due to the reduction of overall mass-sensitivity of the plate.

Similarly equations 3.34 and 3.36 are difficult to prove, since any increase in volume of a mobile coating necessitates an increase in the area covered by that coating, as the liquid spreads. The solution to this problem is to spread the liquid coating, whatever the volume, over the entire surface of the crystal, thus preventing any further increase in the area covered by that coating.

Thus, a crystal was coated with 2×10^{-2} microlitre of squalane on each side, and the coating was spread over the entire crystal surface be gently heating the crystal in an oven at 40°C. The coated crystal was located in the large volume impinger detector cell under

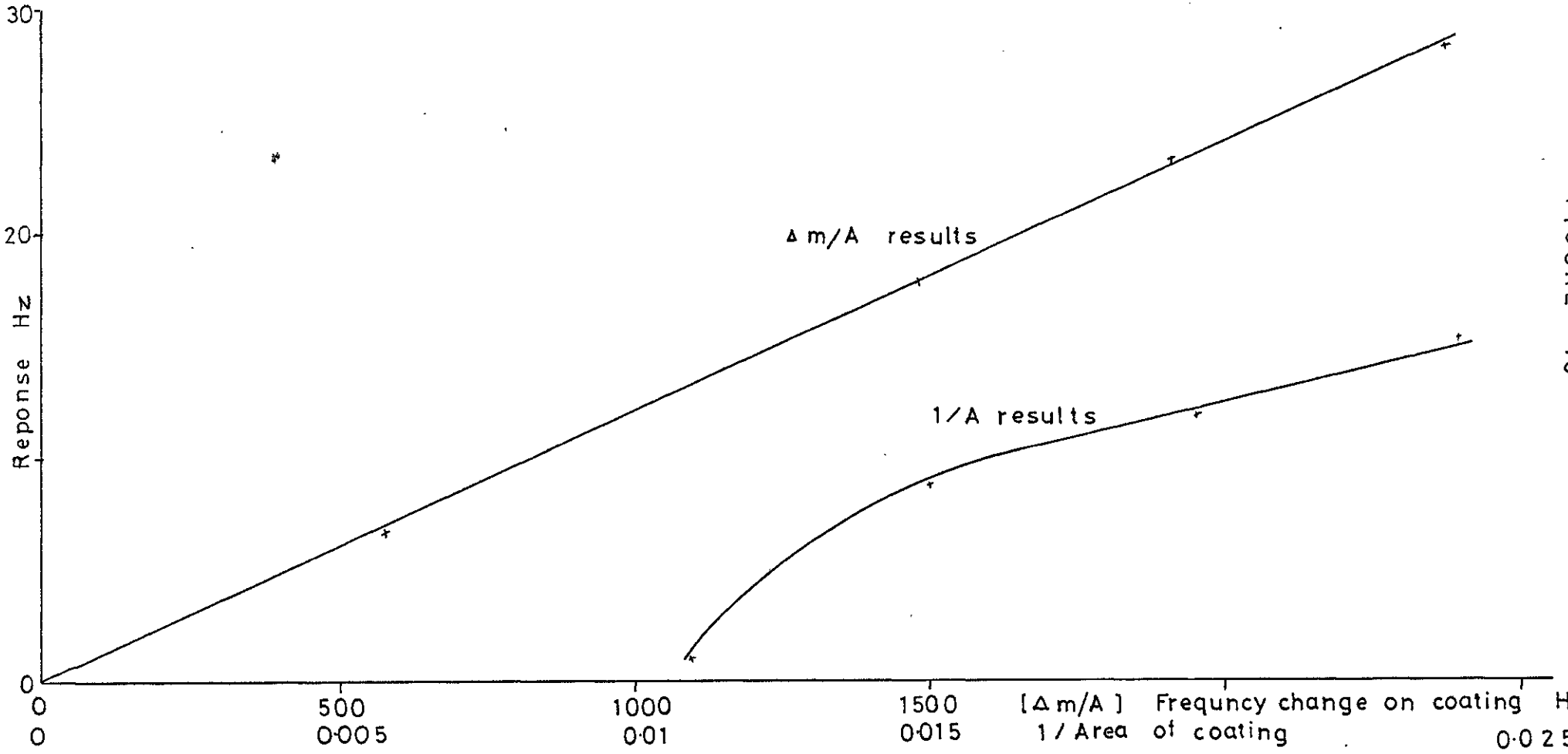
30
20
0
Reponse Hz
Δ m/A results
1/A results
0
0
500
0·005
1000
0·01
1500
0·015
[Δ m/A] Frequncy change on coating Htz.
1/Area of coating
0·025

FIGURE 48

a gas flow of 12 mls per minute, and allowed to equilibrate at room temperature. Three 40 microlitres samples of chloroform vapour were passed over the crystal, and the peak frequency change for each sample recorded. The three results were averaged. The entire procedure was repeated for 4, 6 and 8 x 10^{-2} microlitres per side of coating. The results were plotted as response to chloroform versus volume of coating. See figure 49a. The results support the relationship between Δf and Vc shown in equation 3.36.

In the preceding experiment, the value of A, the area of coating was kept constant, and the added mass Δm gradually increased. Equations 2.21, 2.26 and 2.31 indicated that a linear relationship should exist between the change in frequency and Δm for this situation. Reference to figure 49b, where these values have been plotted against one another for the experiment, demonstrates the validity of these equations.

An interesting feature of the piezoelectric crystal as a mass detector is that each side of the crystal operates independently. Thus, when 40 microgrms of squalane were coated onto one side of a crystal, covering the entire plate area, frequency drop of 4900 Hz was obtained. Coating the other side in exactly the same manner caused a further frequency drop of 4900 Hz . The total value of $\Delta m/A$ for the entire crystal did not change, whether one or both sides were coated. Hence, if the two sides of the crystal did not act independently, there should be no further frequency change on coating the

FIGURE 49 a

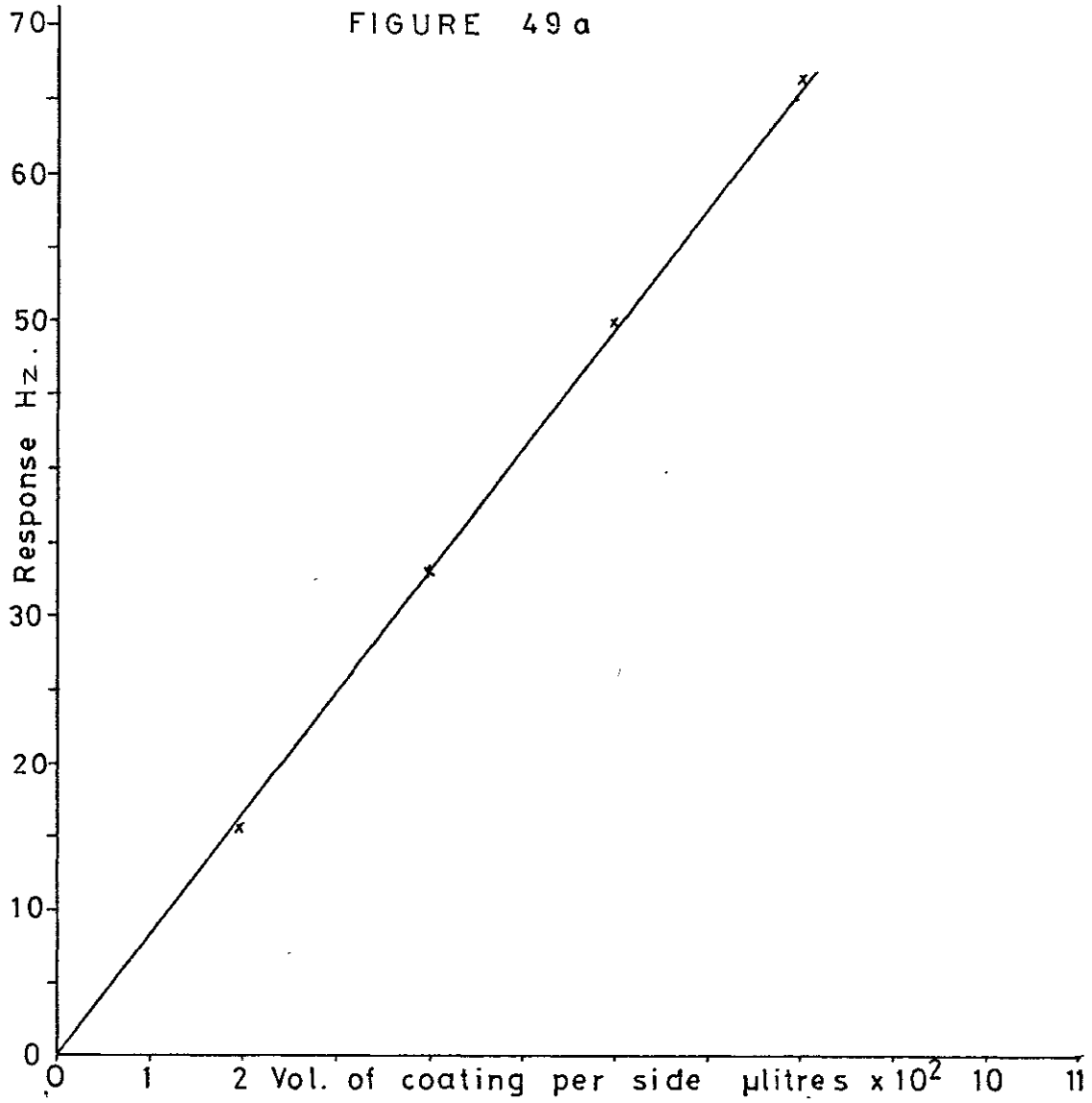

FIGURE 49 b

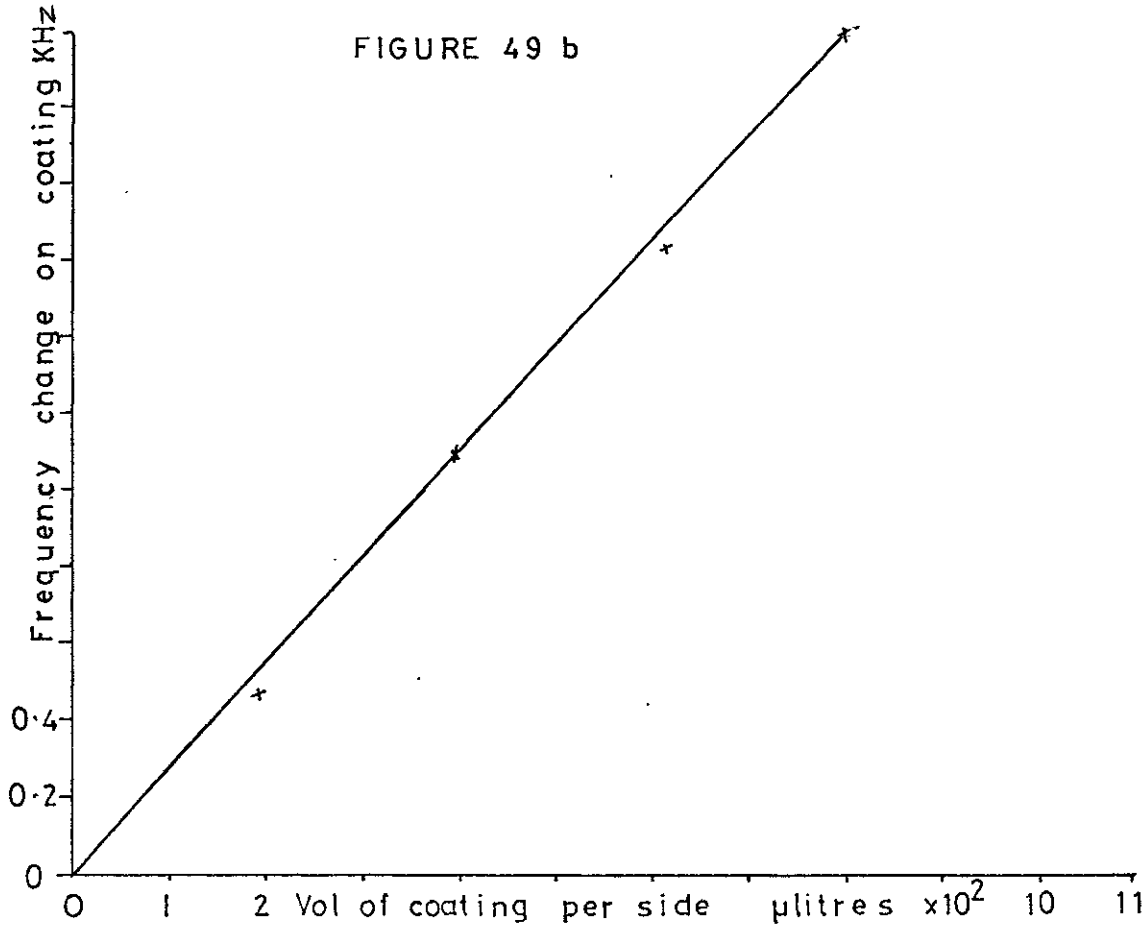

opposite side. This was obviously not the case for the experiment under discussion, and it may be assumed that the two sides of the crystal operated independently.

For maximum sensitivity, a coating must be kept to a limited area. This criterion may be established when using coatings like silicone gum rubber, rubber solution and ethylene glycol succinate. The liquid coatings could not be localized in this way, and it was preferred to spread these coatings over the entire crystal surface, thus losing some sensitivity, but gaining base-line stability due to the absence of drift caused by the gradual creep of the liquid over the plate surface.

Stability of crystal coatings.

The stability of a coated crystal has already received some attention in an earlier section (3.1.2). For a crystal coated with a relatively volatile coating, the major cause of frequency drift in a thermostatted system is due to bleed of the coating from the crystal surface. Figure 50a illustrates the frequency change versus time graph for a crystal coated with β-β-oxydipropionitrile, located in the low volume impinger detector cell. The carrier gas flow was 12 mls per minute and the water bath temperature 30°C. The coating bleed rate was sufficient to ensure total coating removal within three hours. Two possible mechanisms could be postulated for this phenomenon: (i) the coating's small, but significant vapour pressure was sufficient to cause evaporation of the coating into the carrier gas stream; (ii) the jet effect of the impinger cell was physically blowing material from the

FIGURE 50 a

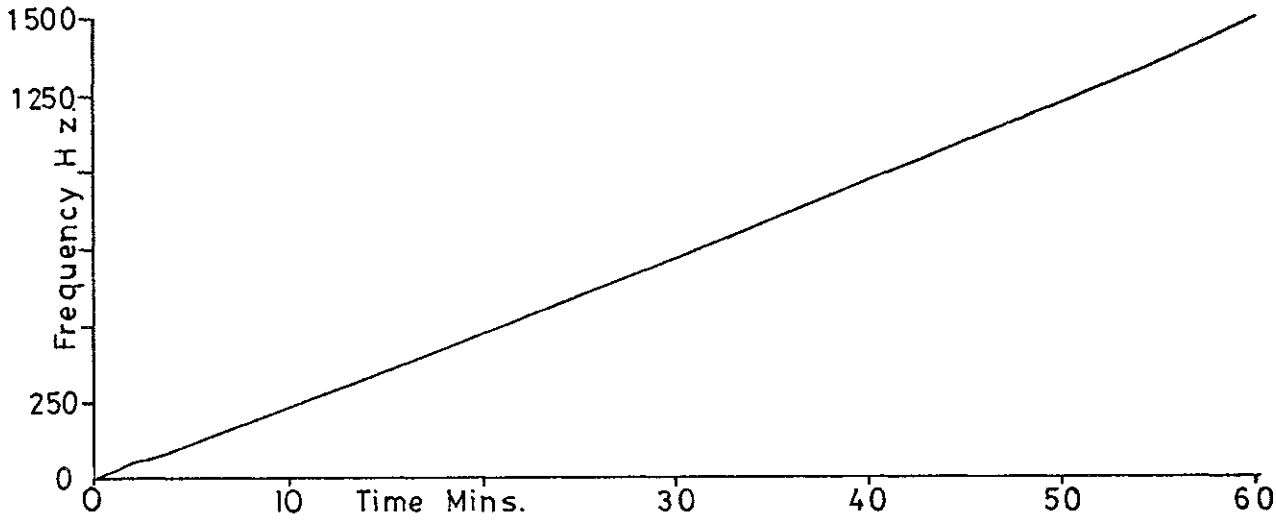

FIGURE 50 b

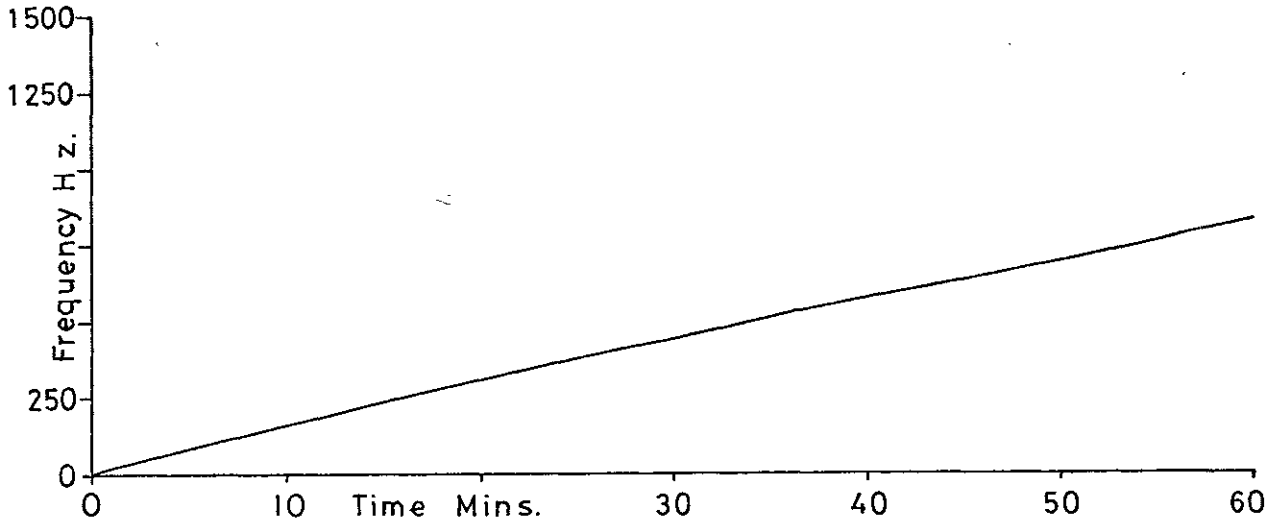

FIGURE 50 c

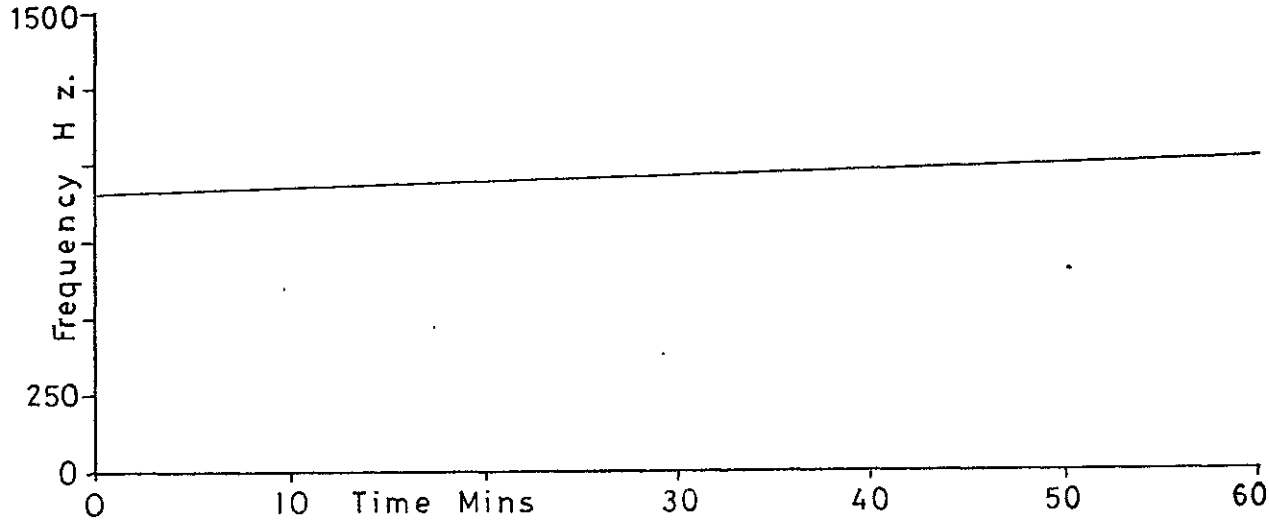

surface of the coating. In order to distinguish the main cause of the bleed, a bubbler containing the liquid coating of interest was placed in the gas stream just prior to the detector cell. The effect of this bubbler, and its various modifications on the bleed rate, was negligible, hence it was assumed that material ablation was responsible for the bleed.

The possibility of decreasing the bleed rate by inserting foil shields into the detector cell was investigated. The shields were designed to deflect the jet of gas arising in the impinger cell away from the crystal surface. A β-β-oxydipropionitrile crystal was located in this modified cell under identical conditions to those used in the first experiment. A graph of the frequency change with time is depicted in figure 50b. It can be seen that the foil shield modification reduced the bleed rate. A considerably more effective cell design for bleed-rate reduction has been described in Section 3.2.3 and is depicted in figure 46. A β-β-oxydipropionitrile coated crystal was located in the diffuser detector cell, and subjected to conditions identical to those described in the previous two experiments. The frequency change versus time graph for this cell may be seen from figure 50c.

The results from these three experiments are tabulated below:

Cell Design	Frequency Change per hour
Impinger Cell	1500 Hz .
Shielded Impinger Cell	700 Hz .
Diffusion Cell	100 Hz .

The coating used for this work exhibited the most drastic bleed rate of all the coatings used, by an order of magnitude. It has been shown in Section 3.2.3 that this cell design operated as efficiently as the impinger detector cell for equilibrium samples. Hence in analytical situations where equilibrium concentration of the analyte in the gas phase can occur, the diffusion cell is to be preferred.

CHAPTER IV DETECTION AND DETERMINATION OF ORGANIC GASES

The application of the piezoelectric detector to the measurement of organic gases in the atmosphere is subject to two important design considerations. Firstly, a coating must be found with desirable properties, such as sensitivity and selectivity towards the analyte gas. Secondly, the detector must be capable of determining that gas in a real sample. The intrinsic properties of detector coatings that affect the detector sensitivity will be discussed in the first section of this chapter, and latterly the examination of the detector behaviour towards real samples.

4.1 ANALYTICAL BEHAVIOUR OF DETECTOR COATINGS

4.1.1 Theory

The separation of organic gases by GC stationary phases relies on the interaction between the analyte gas and the column's coating. One method of measuring this interaction between the gas and coating, that is often employed in GC literature is the retention volume V_r. This is the volume of gas emerging from the system during the time taken from sample introduction to the emergence of half that sample plug from the GC column.

It has been shown that:

$$V_r = n(V_g + K V_L) \quad \ldots\ldots\ldots \quad 4.1$$

Where: n = number of theoretical plates

V_g = volume of gas in system

V_L = volume of liquid in system

K = partition coefficient.

King[55] has shown that for the piezoelectric detector, a plot of log area of response versus solute boiling point is linear, and is parallel with a plot of log retention time versus solute boiling point. Thus, log area is proportional to log retention time.

Thus $\log A \propto \log V_r$

$A \propto V_T$

but $V_T \propto V_R$

$\therefore A \propto V_R$

From equation 4.1 it can be seen that $V_R \propto K$, for a given system. Similarly equations 3.34 and 3.36 demonstrated a relationship between Δf and K, and A and K. Thus whichever method is used to characterize an analyte/stationary phase interaction, the relative effect of two analytes on a detector coating may be determined directly, providing that the same units are used for each analyte. Expression of the interaction of the analytes in differing units, requires that the experimental conditions of the GC systems used to derive the values be known, so that interconversion may be carried out.

The analytes selected for investigation in this study were: acetone; chloroform; cyclohexane; ethylbenzene; heptene; hexane; ortho-xylene. On one occasion

phenol was used. Nine GC stationary phases were investigated as detector coatings: β-β-oxydipropionitrile; "Carbowax 20M"; di-nonyl phthalate; ethylene glycol succinate; "Pluronic L 64"; rubber solution; silicone gum rubber E350; squalane; tri-cresyl phosphate. The vapours were all derived from "Analar" liquids: the majority of the coatings were supplied by Phasesep Ltd. The vapours were selected as examples of classes of compounds that commonly occur in atmospheric pollution. Thus: aliphatic hydrocarbons, hexane and heptene; chlorinated hydrocarbons, chloroform; substituted aromatic hydrocarbons, ethyl-benzene, ortho-xylene; cyclic hydrocarbons, cyclo-hexane; oxygenated aliphatic compounds, acetone. The inclusion of ethylbenzene and ortho-xylene furnished information on the determination of isomers. The majority of these vapours are toxic when inhaled or imbibed[109], with narcotic or irritant effects at sub-lethal doses. Exposure to concentrations of these vapours above certain levels for a length of time can cause chronic illness, and habituation is possible with chloroform. These compounds occur industrially mainly as solvents, or in mixtures of solvents: cyclohexane is a starting material for some man-made materials.

There are many GC stationary phases exhibiting a wide range of interactions with many analyte vapours. Littlewood[110] has developed a classification scheme for these coatings that greatly clarifies their individual behaviour. Four distinct types of stationary phase were recognized. (i) Paraffinic. These coatings contained

no polarizable groups, not even aromatic nuclei. Retention occurred by dispersion forces, and the polarity of an analyte in no way affected its retention by the coating. Examples of this type of coating are the paraffins and their mixtures, and alkyl silicones. (ii) Polar: Dilute. In these coatings the majority of the molecular volume was occupied by non-polar groups, although some polar groups were present. Coatings of this type are the organic esters, alkanols and ethers. (iii) Polar: Concentrated. A large proportion of the molecular volume of these coatings was occupied by polarizable groups, e.g. low molecular weight polyethylene glycols. (iv) Specific. The coating contained or consisted of a specific chemical reagent that reacted with a class of solute in a chemical manner. Thus, silver nitrate dissolved in a stationary liquid gives a reaction with alkenes and dienes.

Sections (ii) and (iii) may be further subdivided. Thus: (a) polar, the molecules contained essentially polarizable groups such as nitriles, and large retention volumes occurred for polarized analytes apart from molecules with hydroxyl or H-bonding donors; (b) hydroxyl, the presence of this group in the coating increased the retention of OH-containing analytes, as well as favouring H-bond donors; (c) H-bond donors, large retention volumes were demonstrated for solutes with H-bonds available for donation.

The coatings used in this study have been grouped into the Littlewood classification in table 9. Included in this table are the suggested analytes that give optimum

TABLE 9

Coating	Suggested Analytes			Littlewood Class
	CH	CHO	CHON	
Squalane	✓	X	X	1
Silicone Gum Rubber	X	✓	X	1
Rubber Solution	-	-	-	1
Tri-cresyl Phosphate	✓	✓	✓	2.a.
Pluronic L64	-	-	-	2.c.
Di-nonyl Phthalate	✓	✓	X	2.c.
"Carbowax 20M"	X	✓	X	2.b.
β-β-oxydipropionitrile	✓	✓	✓	3.a.
Ethylene Glycol Succinate	-	-	-	3.c.

retention volumes from Kaiser[111]. The allocation of a coating to a Littlewood class may help in understanding its behaviour towards different analytes. Thus consider the data obtained from reference[112].

Relative Retention Coefficient Pentane = 1.00 at 100°C	COATING		Temperature at which Compound boils
	Silicone DC 200	Polyethylene Glycol	
Hexane	2.29	2.54	69°C
Isopentane	0.84	1.0	28°C
n-pentane	1.0	1.0	36°C
Benzene	3.66	26.1	80°C
Toluene	7.75	49.0	111°C
Tert-Butanol	3.57	111.0	118°C
Methanol	0.34	23.4	64.5°C
Ethanol	0.69	31.5	78.3°C

Silicone DC 200 is a non-polar paraffinic coating of type 1, polyethylene glycol (PEG) is a hydroxylated concentrated polar coating of type 3.b. The retention volume data demonstrate the difference between these coatings. Thus PEG has a strong preference for hydroxylated molecules, hence the retention coefficient for hexane is about nine times lower than that for methanol, yet these two compounds have similar boiling points. On the type 1 coating the hydrocarbons are selected virtually by boiling point, so that a plot of retention volume versus boiling point gives a shallow curve, diverging little from

the linear. The PEG coating however shows a marked preference for the aromatic compounds, the similar graph giving a sharp increase in slope for these. See figure 51. The polarizable nature of the aromatic nuclei causes this discontinuity in retention data for the type 3b coating.

The coatings used in this study have been classified into the Littlewood groupings. Squalane is a typical paraffinic coating of type 1. It is a saturated hydrocarbon, 2, 6, 10, 15, 19, 23 hexamethyl tetracosane. Kaiser[111] has recommended this coating for the separation of hydrocarbons. Smith et al.[113] determined retention coefficients for 112 hydrocarbons on this coating at 25°C. Results for hexane, cyclohexane and heptene were 3.2, 5.91, 9.08 respectively.

The silicone gum rubber coating used was a high melting point stationary phase of type 1. The compound is a methyl-phenyl-silicone gum, non-polar, and with rather specialized applications. Thus Kaiser[111] recommended that this coating be used for the separation of oxygenated hydrocarbons and steroids.

Ordinary rubber solution has been shown by Karasak and Tiernay(90) to be a sensitive coating for the low molecular weight alkanes, and this fact, coupled with its hydrocarbon structure indicated that it should be considered as a type 1 stationary phase.

A representative of the type 2 coatings was tricresyl phosphate, a polar molecule, whose molecular formula $(C_6H_4CH_3O)_3PO$ indicated that it should be considered a type 2.b. compound. Kaiser[111] suggested that hydrocarbons,

FIGURE 51

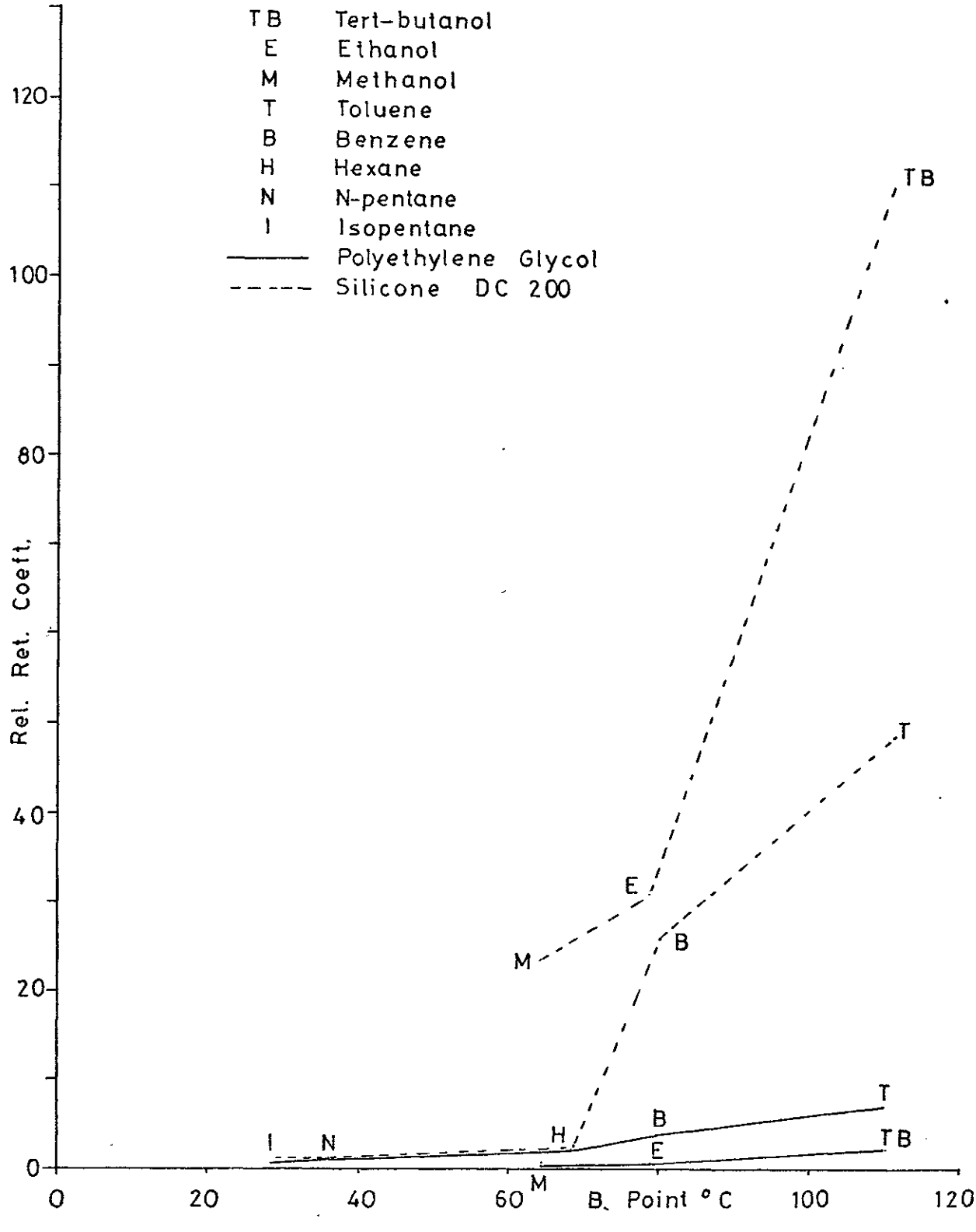
TB Tert-butanol
E Ethanol
M Methanol
T Toluene
B Benzene
H Hexane
N N-pentane
I Isopentane
Polyethylene Glycol
Silicone DC 200
Rel. Ret. Coeff.
B. Point °C
0
20
40
60
80
100
120
TB
T
E
M
B
H
N
I

oxygenated hydrocarbons, and molecules containing both nitrogen and oxygen atoms could be separated on this coating. West et al.[114] have used this liquid phase for the determination of a large number of probable air pollutants. Retention times for compounds used in this study were: hexane, 0.329; acetone, 0.63; cyclohexane, 0.63; heptene, 0.808; chloroform,1.28; ethylbenzene, 4.36; ortho-xylene, 6.11. All these data were determined at 93°C.

Di-nonyl phthalate is a type 2 stationary phase of general applicability. Kaiser[111] recommended the separation of hydrocarbons and oxygenated compounds on this stationary phase. Its molecular formula is 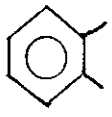 ,and it can be considered as a type 2.c coating.

"Carbowax 20M" is a polyethylene glycol, molecular weight 20,000. This high molecular weight renders the compound a suitable candidate for type 2.b, since the effect of the -OH group is "diluted" by the size of the molecule. Separation of oxygen-containing compounds was advised by Kaiser[111], and the molecular structure would certainly uphold this advice, the coating probably showing selectivity towards polar compounds as well.

"Pluronic L64" is a surfactant liquid, a block copolymer of ethylene oxide and propylene oxide, with a high molecular weight. This coating has a polar nature, and sites available for H-bonding. In the Littlewood classification it would fit into type 2.c.

Two coatings were selected which belonged to the third Littlewood class. Ethylene glycol succinate was shown by Brown et al.[115] to demonstrate a specific retention volume of 3200 for phenol, compared with 69.4, 18.0 and 18.8 for chlorobenzene, benzene and chloroform respectively. The powerful H-bonding nature of the coating puts it in type 3.c. Another relatively small molecule is β-β-oxydipropionitrile; $\begin{matrix} CN - CH_2 - CH_2 \\ CN - CH_2 - CH_2 \end{matrix}\!\!>\!O$.

Smith et al.[113] have determined the relative retention coefficients for a large number of hydrocarbons on this coating, including: hexane, 2.15; cyclohexane, 6.45; heptene, 9.2. West et al.[114] used β-β-oxydipropionitrile as a stationary phase for the determination of putative air pollutants by GC at 53°C. Results of interest for this study were: hexane, 0.254; cyclohexane, 0.397; heptene, 0.538; acetone, 2.42; chloroform, 2.64; ethylbenzene, 6.3; ortho-xylene, 10.65. β-β-oxydipropionitrile is a type 3.a. coating.

Coatings from the first three Littlewood groups have been selected in order to study their interactions with the vapours used in this work. The information already available about the coatings' performance with the various vapours must be circumspectly interpreted in the light of the differing conditions used to obtain these data, and the conditions under which they are to be applied.

4.1.2 Practice

The investigation of detector response to the various coating and analyte combinations was carried out

using the low volume impinger detector cell and diffusion tube sampler. Generally, the coating under investigation was applied to four crystals using a rapid coating method. Each crystal was tested under identical conditions for its response to the chloroform diffusion tube, and the most sensitive crystal retained for the subsequent tests. Ethylene glycol succinate and "Carbowax 20M" were applied to the crystals using the coating techniques described in Section 3.3.2.

A sensitive crystal having been prepared, it was located in the low volume impinger detector cell, a gas flow of 12 mls per minute passed, and a water-bath temperature of 30°C established. The entire system was allowed to equilibrate, the diffusion tubes switched into the system in turn, and the frequency change for the equilibrium concentration of analyte in the system obtained for each vapour. The results for each coating were corrected for the differing diffusion rates due to the various vapours present in the tubes, and then compared with the value due to chloroform. This was accomplished by multiplying the frequency change value for a given analyte by its diffusion rate in grms. per minute, and then dividing by the diffusion rate for the chloroform tube. The diffusion rate values that were used were those obtained is Section 3.2.2. Finally, this modified frequency change value was divided by the frequency change value obtained for chloroform. The results for this series of calculations are displayed in table 10.

TABLE 10

Coating	Relative Response ($CHCl_3$ = 1.00) to: $CHCl_3$	E-B	O-X	Acet.	Hex.	O Hex.	Hept.	ΔF $CHCl_3$
T.C.P.	1.00	3.23	3.20	0.41	0.06	0.36	0.48	35.0
C.20M	1.00	3.20	3.53	0.42	0.09	0.21	0.34	162.5
S.G.R.	1.00	0	0	0	0	0	0	12.0
B.B.O.	1.00	2.61	3.10	0.71	0.52	0.26	0.34	21.0
Squa.	1.00	9.18	9.48	0.38	0.77	1.55	1.65	30.0
D.N.P.	1.00	4.51	5.47	0.18	0.21	0.43	0.45	61.0
Plu.L64	1.00	3.57	3.85	0.15	0.15	0.17	0.26	158.5
R.S.	1.00	13.84	9.34	0	0.35	1.5	0.91	27.0
E.G.S.	1.00	3.37	2.70	1.3	0.66	-	-	24.0
Boiling Point	61.3°C	136.1°C	144.1°C	56.5°C	69°C	81.4°C	98.0°C	61.3°

T.C.P. = Tri-cresyl Phosphate
C.20M = "Carbowax 20M"
S.G.R. = Silicone Gum Rubber
B.B.O. = β-β-oxydipropionitrile
Squa. = Squalane
D.N.P. = Di-nonyl Phthalate
Plu.L64 = "Pluronic L64"
R.S. = Rubber Solution
E.G.S. = Ethylene glycol succinate
E-B = Ethylbenzene
O-X = Ortho-xylene
Acet. = Acetone
Hex. = Hexane
O Hex. = Cyclohexane
Hept. = Heptene
$CHCl_3$ = Chloroform

In the experiment, two chloroform tubes were used, one at the beginning of a run of vapour introduction, the other at the end, to check that the sensitivity had remained constant. During a complete vapour run, all parameters were frequently checked, and reset if necessary, e.g. carrier gas flow rate; water bath temperature; oscillator supply voltage. The accuracy of the results obtained varied according to the coating and vapour. Obviously better accuracy would be associated with results where large frequency changes were observed, and the relative values of reading errors were reduced.

The results of this experiment are discussed below, coating by coating.

Squalane.

The approximately 2 to 1 ratio for the cyclohexane/hexane retention times found by Smith et al[113] also was obtained in this experiment. Thus Smith et al's value for the ratio was 1.85, here it was 2.01. The larger retention time obtained for heptene in reference[113] (about thrice the hexane value) was not obtained, although the relative response was higher, thus: hexane, 0.77; cyclohexane, 1.55; heptene 1.65. The series acetone, hexane, cyclohexane and heptene, gave responses that increased in concert with the increase in boiling point, thus giving a more or less linear graph, see figure 52a. Ethylbenzene and ortho-xylene did not form part of this graph, although they did give responses relative to their boiling point. Chloroform too gave an anomalously high response, and it may be that squalane exhibited some

FIGURE 52 a

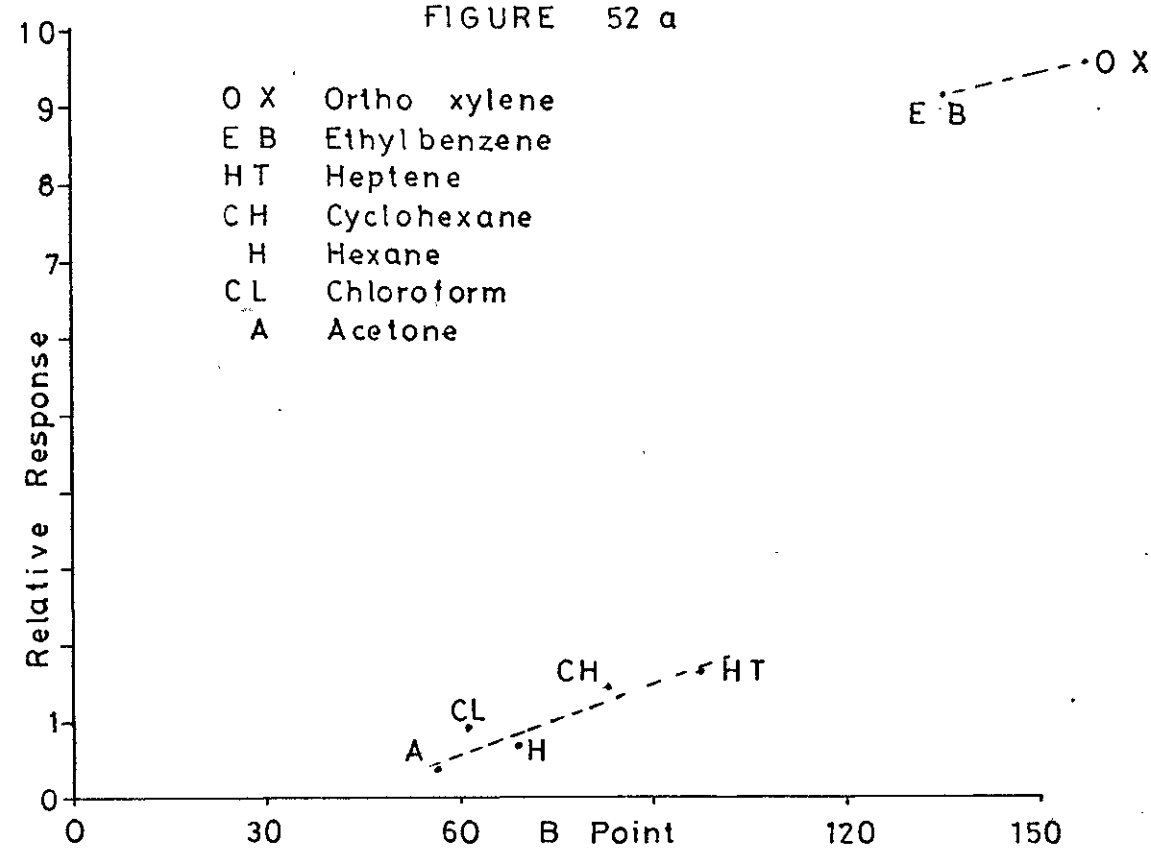

FIGURE 52 b

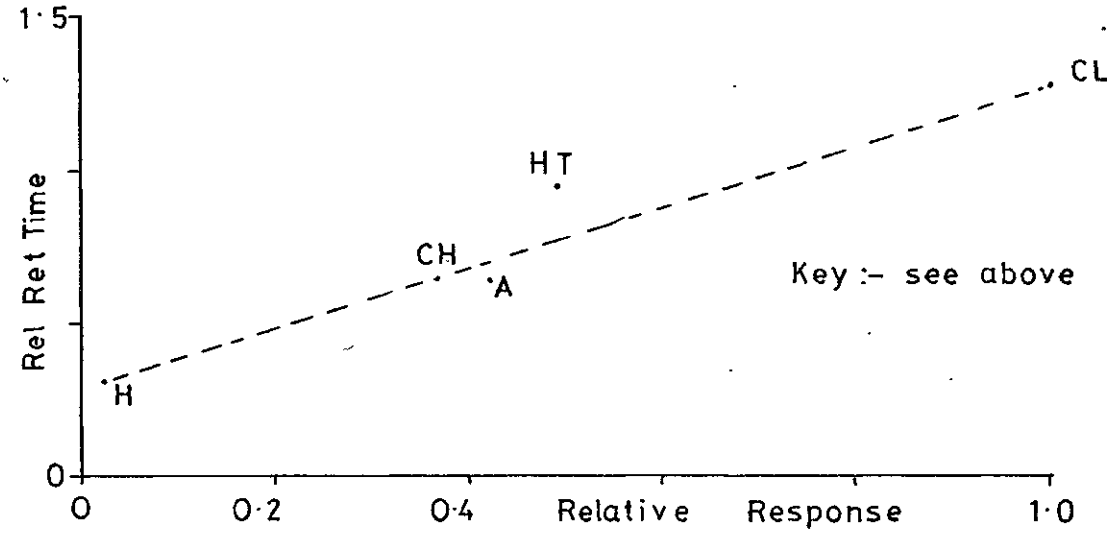

FIGURE 52 c

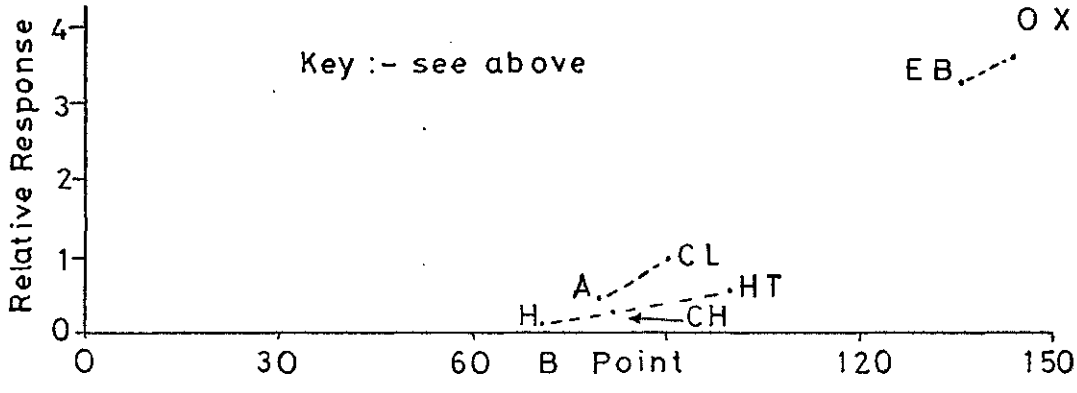

selectivity with respect to polarization.

Silicone Gum Rubber

This coating gave no discernable frequency drop for any of the compounds examined, save chloroform. The diffusion tubes were all run at 60°C in order to increase the diffusion rate, but again no response was obtained. This lack of reactivity probably is due to the low temperature (30°C) at which the coating was used. A typical GC utilization would employ a temperature of 100 to 300°C, where the coating is in its liquid state.

Rubber Solution

The range of responses experienced with this coating was similar to those of squalane. The increase in response for hexane discussed in Karasak and Tiernay's paper[45] did not materialize. A probable cause of this was that these authors compared the "enhanced" response of rubber solution, with the response of "Carbowax 400", a low molecular weight polyethylene glycol. This coating is a type 3.b. compound, and would be expected to favour more polar solutes. Thus the rubber solution would be expected to show a greater sensitivity toward alkanes when compared with this type of stationary phase. The rubber solution used in this experiment was obtained from a commercial supplier, and was unlikely to be a pure chemical, since its primary purpose was the repair of punctures in rubber inner tubes. This may explain the rather unusual results obtained. Thus, no response occurred for acetone, yet chloroform's response exceeded that of hexane and that of heptene. Similarly ethylbenzene and

ortho-xylene gave responses that were not in concert with their boiling points. It is possible that these effects were due to other compounds present in the rubber solution, such as fillers.

Tri-cresyl Phosphate

The following order of increasing response was obtained for this coating: hexane, cyclohexane, acetone, heptene, chloroform, ortho-xylene and ethylbenzene. This is similar to the order determined by West et al.[114] for the same coating at 93°C. There are two major differences: firstly the cyclohexane and acetone retention data from West et al. were identical; secondly the ethylbenzene ortho-xylene results are reversed. The first five compounds in the series gave responses in rough proportion to the retention times, hence a plot of the response against retention time for these compounds is approximately linear. See figure 52b. The lack of correlation between the ethylbenzene, ortho-xylene results could either be due to alteration of the retention time order, as the coating passes from 93°C to 30°C, the operating temperature of the detector, or to inaccuracies in the determination of the frequency changes for these compounds.

"Carbowax 20M"

This stationary phase behaved a little like the previous coating, in that the responses to the various compounds showed a marginal increase in selectivity towards the more polar molecules such as chloroform and acetone. Hence the relative response to cyclohexane and heptene decreased, and the acetone relative response increased

with respect to the results obtained for the tri-cresyl phosphate coatings. Boiling point versus response plots for each of the three different series, aliphatics, polar aliphatics, aromatics, gave positive slopes. See figure 52c.

Di-nonyl Phthalate

This polar molecule was considered a type 2c compound, that is the polar function was dilute in the molecule, with a preference for hydrogen bonding. The results from table 10 certainly validate this argument since the response order followed boiling point increase for all the analytes except chloroform. The relationship between response and boiling point is not completely linear; a discontinuity occurs between the aromatics and the aliphatics. The probable cause of the high response to chloroform lies in the preference of the coating for the slightly positive hydrogen of the chloroform molecule.

"Pluronic L64"

The hydrogen bonding effect of this coating is even more pronounced than for the previous coating. Thus the relative responses of hexane, cyclohexane and heptene were reduced, as the chloroform demonstrated a preferential dissolution.

B-B-oxydipropionitrile

West et al.[114] and Smith et al.[113] have determined the order of elution from a β-β-oxydipropionitrile column of hexane, cyclohexane and heptene at 53°C and 25°C respectively. On both occasions the order was: hexane; cyclohexane and heptene. The results from table 10 indicate

FIGURE 53

Relative response versus b. point for Di-nonyl phthalate coating (see preceding page)

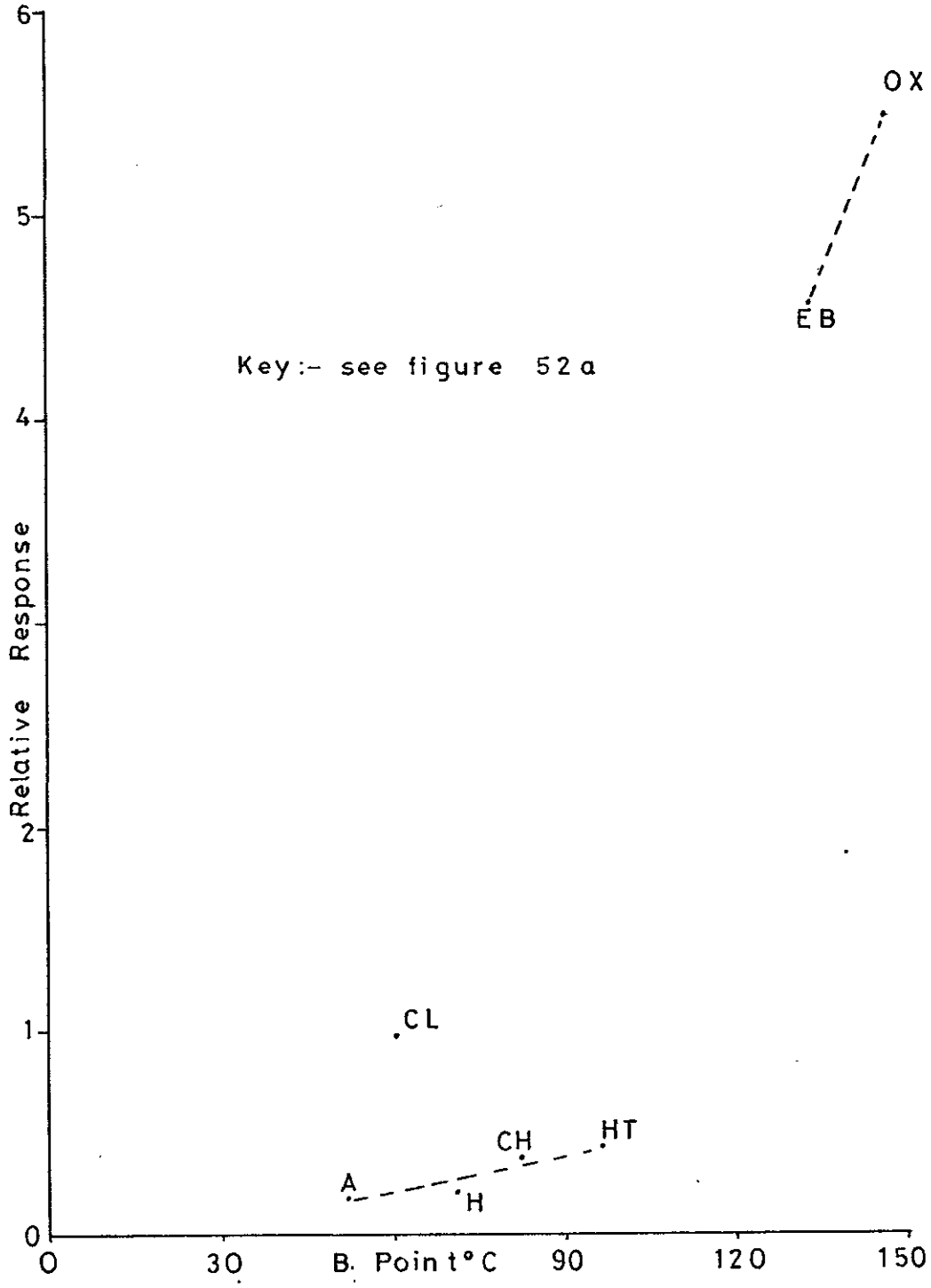

that the response order obtained in this study was: cyclohexane; heptene; hexane. The entire elution sequence determined by West et al. for the vapours used in this study, was followed by the relative responses with the exception of hexane. The anomalous behaviour of the aliphatic hydrocarbons may well be caused by errors that have arisen in the determination of their small frequency changes. The high relative responses obtained for acetone and chloroform were expected within the context of the properties of the type 3.a. stationary phase.

Ethylene Glycol Succinate

Ethylene glycol succinate was selected for investigation due to the extremely high retention volume of 3200 reported by Brown et al[115]. The frequency changes were significant for all the vapours used in this study, but a blank value had to be subtracted due to the high affinity of this coating to water vapour. The signal from a blank tube was used to assess this blank value. The result for cyclohexane and heptene fell below the blank value, and hence the zero results in table 10. The use of phenol as an analyte was tried. The phenol was placed in the diffusion tube, and run at temperatures between 30°C to 100°C. An alternative method was to lodge a few crystals above the necked portion of the diffusion tube, and the tube was run at 35°C (melting point of phenol, 40°C). None of these approaches gave a phenol vapour concentration of sufficient magnitude to cause a significant response from the detector. Again,

the problem of results obtained for a coating in its liquid form being non-representative of the coating behaviour as a solid, was encountered.

Modification of coating response

The modification of stationary phases by the addition of other substances is a well established technique in GC. A brief study was carried out to determine whether the mixing technique could be used for a liquid/porous solid system on a piezoelectric crystal.

A clean crystal was held in a clamp, so that the faces of the crystal were in a horizontal plane. A small quantity of "Porasil A" (37-75 micron bead) was placed on the centre of the electrode, and then a concentrated solution of squalane in chloroform dropped onto the beads and allowed to spread and evaporated. Differing amounts of the "Porasil" bead were used for each coating. The crystal was located in a high volume impinger detector cell and equilibrated under 12 mls per minute carrier gas at room temperature. Triplicate 40 microlitre samples of air saturated with chloroform vapour and air saturated with benzene vapour were injected into the system at 10 microlitres per second. The frequency decreases were averaged for each trio of injections, and a ratio determined for chloroform/benzene.

RESULTS:

Coating	$CHCl_3$/Benz.
(i) Squalane	1/0.555
(ii) Squalane + "Porasil A"	1/0.571
(iii) Squalane + "Porasil A"	1/0.675

Crystal (iii) received more "Porasil A" than crystal (ii), and the effect was observed as an increase in the relative response of benzene.

4.2 APPLICATION TO REAL SAMPLES

4.2.1 Theory

The application of the piezoelectric detector to real samples demands certain requirements from the system, one of which is that the detector should display sufficient sensitivity for the vapour under consideration. The normal mode of operation of the detector would be the measurement of the continuous level of a pollutant in the atmosphere, in order to determine its concentration with reference to the TLV. The detector must operate linearly in this range, and with a reasonable degree of certainty in the measured value, i.e. it must operate above its detection limit.

The vapours used in this study have, with the exception of heptene, been allocated TLV's commensurate with their toxicity and ability to cause chronic illness. Thus Gerarde[116] has given the TLV's for ortho-xylene, ethylbenzene, hexane and cyclohexane, as 200 ppm, 200 ppm, 500 ppm and 400 ppm respectively. These values may be expressed as mgrms per m^3 thus, 870, 870, 1760 and 1376. Rowe and Wolfe[117] indicated that acetone's TLV should be 1000 ppm (2400 mgs per m^3), and Irish[118] that the TLV for chloroform should be 50 ppm or 240 mgs per m^3.

The determination of analytes in air samples with the piezoelectric detector may be carried out in two distinct ways: the air may serve as a continuous stream of carrier gas; the air may be introduced with another carrier gas. The latter approach may be further subdivided thus: the air may be continuously bled into a stream of carrier gas, thus diluting the sample; the air may be introduced as pulses into the carrier gas; the air may be switched over the crystal instead of the carrier gas, so that the crystal "sees" alternate slugs of carrier gas and air sample. The effect of bleeding the air into the carrier gas stream or introducing pulses of air into the stream, is to dilute the sample, which may render some analytes indistinguishable. Using air as a continuous carrier stream, or for interrupting the carrier gas flow preserves the concentration of the sample. A further advantage of the interrupted flow method, is that re-establishment of the base-line value may be achieved. The relative durations of carrier gas and air sample will depend on the drift in the system, the sensitivity of the coating and the concentration of the analyte to be measured.

The use of air as a carrier gas, either in the continuous stream, or the interrupted stream method, may give rise to some problems due to undesirable atmospheric constituents. The two constituents most likely to cause trouble are dust and water-vapour. Dust is a component of the atmosphere in most situations: over the sea it may consist mainly of salt particles; in rural areas pollen and finely powdered vegetable matter and soil may

be present; in urban areas, soot and fly ash are major constituents of dust. The piezoelectric detector is a sensitive mass detector, and the presence of viscous liquid coatings on the crystal surfaces renders the device an efficient dust collector and measurer; the piezoelectric crystal device for measuring particulates in the atmosphere, due to Chuan[82], consisted essentially of these components. Water vapour in the air, even when diluted, has been shown to affect ethylene glycol succinate (section 4.1.2), and probably the effect of the undiluted atmospheric moisture would be felt on most of the detector coatings employed. Evidently the need exists to filter out both particulate matter and water vapour from the atmospheric sample.

The technology of filters is quite complex and lies outside the scope of this work; however, some consideration of filter design would be appropriate. Richards[119] has defined two types of filter: absolute filters, made of ceramic, sintered glass or metal, present a pore size smaller than the particulate to be collected, and cause a 100% hold-up; fibrous filters are made of beds or pads of materials such as paper, cotton wool, or glass wool. These latter filters are not absolute, since the pore size is usually many times larger than the smallest dimension of the particulate it is desired to trap.

The risk with any type of filter is that the substance of interest may be partially or wholly removed, along with the interferent. This problem has been mentioned earlier in connection with freeze-out traps (section 1.2.1), but it may also occur with dust filters and drying tubes.

4.2.2 Practice

The applicability of the various coatings to the detection of the selected vapours may be seen from table 11. This table has been prepared from table 10 by first calculating the concentration of chloroform present in the gas stream. Thus:

Gas flow rate = 12 mls per minute

$CHCl_3$ diffusion rate = 2.29×10^{-1} mgs per minute.

Hence concentration of $CHCl_3$

$$= \frac{2.29 \cdot 10^{-1} \cdot 10^{6}}{12} \text{ mgs per } m^3$$

$$= \underline{1.9 \cdot 10^{4} \text{ mgs per } m^3}$$

The sensitivity for chloroform on each coating was calculated next. Thus:

Response of coating "n"

to $CHCl_3$ = R_n Hertz

Sensitivity = $\frac{1.9 \cdot 10^{4}}{R_n}$ mgs/m^3/Hz

The sensitivity for the other compounds was obtained by dividing the chloroform sensitivity by the ratioed response from table 10.

The results indicated that for the vapours under consideration, coatings of sufficient sensitivity were available to determine each one below its TLV. See Table 12. Ethylbenzene, orthoxylene and acetone may all be determined fairly easily, since the signal size at the TLV will be of reasonable dimensions. Thus consider acetone on "Carbowax 20M". In the low volume impinger detector cell, the time taken by a sample in reaching its equilibrium coating concentration value was five minutes

TABLE 11

	Sensitivity in mgrms/m^3/Hz for:						
	$CHCl_3$	E-B	O-X	Acet.	Hex.	O Hex	Hept.
T.C.P.	545.2	168.8	180.5	1330	9086	1514.4	1136
C.20M	117.4	36.7	33.26	279.5	1304.4	559	345.3
S.G.R.	1590	-	-	-	-	-	-
B.B.O.	908.7	348.2	293.1	1280	1747.5	3495	2673
Squa.	636.1	69.3	67.1	1674	826.1	410.4	385.5
D.N.P.	312.8	69.4	57.2	1738	1490	727.4	695.1
Plu.L64	120.4	33.7	31.3	802.7	802.7	708.2	463.1
E.G.S.	795.1	235.9	294.5	611.6	1205	-	-
R.S.	706.8	51.07	75.7	0	2019	471.2	776.7

Legend: See Table 10

TABLE 12

Compound	TLV mgs/m^3	Most Sensitive Coating	Sensitivity mgs/m^3
E-B	870	Plu.L64	33.73
O-X	870	Plu.L64	31.27
Acet.	2400	C.20M	279.5
Hex.	1760	Plu.L64	826.1
O Hex.	1376	Squa.	410.4
$CHCl_3$	240	C.20M	117.4

for a gas flow of 12 mls per minute. Uncertainty in the frequency reading for this period was the ± 1 value associated with the counting technique. Hence, for the signal size of 8.5 Hertz required to measure the TLV, the signal to noise (S/N) ratio was greater than 4:1, i.e. twice times that of the detection limit. This would be sufficient for the determination of the TLV.

Chloroform, hexane and cyclohexane present a greater problem, since the S/N ratios for the TLV signals of these compounds would be of the same order as the 2:1 ratio associated with the detection limit. In order to measure these signals, the simple recording of the frequency change would not be sufficiently certain a method: a pulse type of method would prove more fruitful, along the lines of those discussed in Section 3.1.2 and Section 4.2.1. The principal feature is that the base line may be time-averaged to give more reproducible results, and the entire peak area can be read, thus increasing the size of the signal.

The use of a pulse method would give rise to the type of signal seen in figure 36b. Measurement of this type of signal has been described in Section 3.12. A computer program was developed to determine the area of this type of signal using the following algorithm. Consider a consecutive series of frequency readings taken from a piezoelectric detector thus:-

$$a_1, a_2, a_3, a_4 \ldots\ldots\ldots a_x$$

The readings may be taken using the one second mode, the ten second mode, or over any convenient sampling

period, but the mode must be kept constant throughout a series of readings which must be taken consecutively, with no intervals between them.

Suppose that the frequency drifted linearly with time during this period, such that

$$a_1 = a_x + |n| \quad \ldots\ldots\ldots \quad 4.2$$

If a_k is any reading between a_1 and a_x, then from 4.2

$$a_k = a_1 + \frac{|n|\ (k-1)}{(x-1)} \quad \ldots\ldots\ldots \quad 4.3$$

Suppose a second series of readings were obtained:-

$$b_1,\ b_2,\ b_3,\ b_4,\ b_5,\ b_6,\ b_7$$

and that during these readings a sample of analyte had been introduced in the time interval covered by b_3, b_4, b_5. The true base line values of b_3 to b_5, could be determined by using equation 4.3, with readings b_1 and b_7 to construct a complete base line:-

$$b_1,\ c_2,\ c_3,\ c_4,\ c_5,\ c_6,\ b_7$$

Subtraction of the calculated base line from the original series of results, element by element should give:-

$$0,\ 0,\ b_3 - c_3,\ b_4 - c_4,\ b_5 - c_5,\ 0,\ 0$$

These results may be added to give the area of the peak.

In practice the computer program could be designed to cope with non-linear base-line drifts, provided that this drift could be expressed as a function of time.

The use of real samples with the piezoelectric detector was investigated by the following experiments. Two crystals were located in low volume impinger detector cells. One crystal was coated with squalane, the other with "Carbowax 20M". The two cells were set up in a parallel configuration, and a carrier gas flow of five mls per minute maintained through each cell (10 mls per minute total flow). The system was allowed to equilibrate under this flow of gas at a temperature of 30°C. The frequency from each crystal was counted on a separate digital counter; the frequency of the "Carbowax 20M" crystal was taken through the interface unit to the D/A converter, and the voltage analogue of the two least significant digits displayed on the 100mV scale of the chart-recorder. Samples were introduced to the system using the 50 mls Hamilton gas-tight syringe, and the syringe pump unit. The pump was adjusted so that 10 mls per minute were delivered from the syringe to the flow system via a length of narrow bore "Teflon" tubing. The initial sequence of operations to effect sample introduction was: (i) take sample of air into syringe after a preliminary flush of the syringe; (ii) place the syringe in the syringe pump unit, and connect the "Teflon" tube to the carrier gas flow system; (iii) record the frequency of the crystals prior to sample introduction and mark the point on the chart recorder; (iv) divert the OFN to a by-pass, and switch in the syringe pump; (v) take regular readings for the duration of the sample; (vi) on termination of the syringe pump flow, reintroduce

the carrier gas and remove the syringe; (vii) mark this point on the chart-recorder and take readings of the re-established base-line.

The above technique was used to introduce samples of OFN that had been collected in the syringe. No discernible frequency change on either crystal was detected for the sample. The introduction technique was used again, for triplicate injections of laboratory air. The results for the two crystals are depicted in figure 54a. It can be seen that the chart recorder trace from crystal 2 furnished more detailed information than the frequency readings from crystal 1, hence the former will be used for the subsequent presentation of results. The effect of passing air over the crystals can be seen to have caused a major peak a short while after sample introduction, and another peak on sample termination. The initial flat portion of the signal arose because of the time taken to flush the air through the interconnecting "Teflon" tube. The two peaks were caused by the surges that occurred in the syringe pump as a result of switching it on, and by the carrier gas as a result of reintroduction. The slow recovery of the crystal indicated the high concentration of the interferent giving rise to the peaks. Removal of the first peak was effected by switching on the syringe pump just prior to its connection to the carrier gas flow, so that the initial surge was vented into the atmosphere. See figure 54b.

The syringe was fitted with a magnesium perchlorate filter, which was fabricated from a five cms length of

FIGURE 54 a

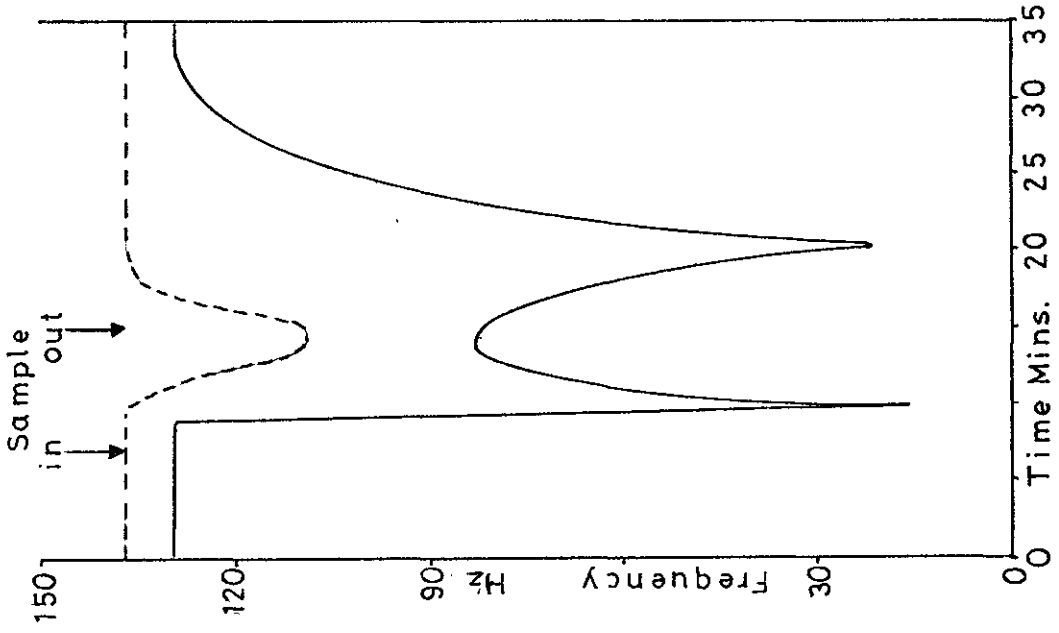

FIGURE 54 b

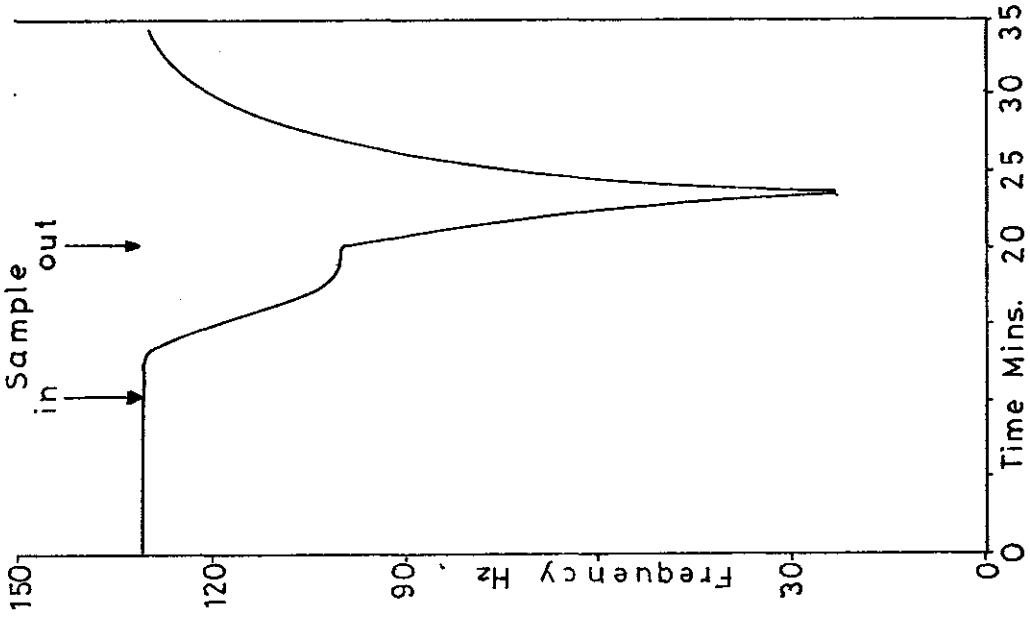

FIGURE 54 c

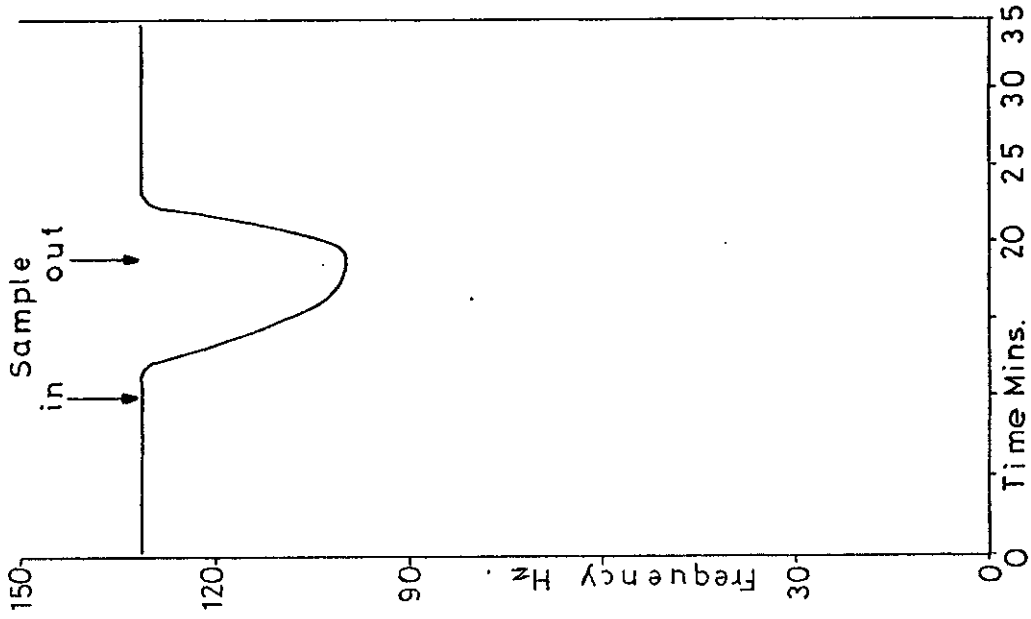

¼ inch O.D. nylon tubing, packed with the drying agent. The magnesium perchlorate was prevented from falling out of the tube by a small piece of glass-fibre wool. The filter was connected to the syringe by a stainless steel needle which passed through a rubber septum mounted at one end of the filter. Triplicate samples of laboratory air were drawn into the syringe, with the filter in place, and were introduced to the flow-system in the usual way. Figure 52c illustrates the type of signal achieved with the filter-type sampling. Both of the large peaks have been removed, and the only peak left, is one that shows the typical equilibration type of profile predicted by equation 3.27 and depicted in figure 24b. The average frequency change for this type of sample input was 16.6 Hz. A silica-gel filter was constructed and used in the same way, to give a signal of 16.5 Hz.

Finally, using the syringe with the magnesium perchlorate filter, air saturated with ortho-xylene vapour was sampled. Duplicate injections were made using the prescribed technique, and an average peak, height of 19 Hz was obtained. Corrected for the blank value, a net frequency change of 2.5 Hz was calculated. Since the expected value for this type of concentration should have been at least two orders of magnitude higher, it was assumed that the majority of the vapour was not reaching the detector. The system was tested to see if memory effects were operating, i.e. the vapour had been sorbed onto the surface of the syringe, or elsewhere in the system. These tests were negative, and it was assumed that the vapour was being removed by the filter.

These experiments demonstrated the type of problem that occurs in the analysis of real samples. Determination of chloroform and hexane vapour, introduced to the syringe after the sampling of laboratory air, gave results that agreed well with calculated values. Thus, once the air has been dried and filtered the determination of these vapours may proceed. The problem lies in selecting a specific dust and water vapour filter.

CHAPTER V METHODS OF ACHIEVING SELECTIVITY

The results of the work carried out in Chapters 3 and 4 have indicated the feasibility of using the piezoelectric detector as a monitor for air pollution. An obvious problem is that, although the detector is rapid and sensitive, it is not very selective: one coating may give significant responses for several analytes. This chapter will subsequently investigate methods of overcoming this problem.

5.1 MULTIPLEXING

5.1.1 Theory

Multiplexing is a term used to describe the coupling of a series of detectors or measuring instruments in such a way that the pooled information of the devices may be correctly interpreted and handled. The multiplexing may be carried out completely automatically, or manually, but in either case some form of data processing is required to extract the desired information. In the case of the piezoelectric detector a system of n detectors may be used, each one of which responds to n components, whose mixture may be determined by the correct processing of the n signals arising from the detectors. Two methods have been investigated for the data processing: the signal ratio method, (SRM); the simultaneous equation method, (SEM).

The signal ratioing method.

Ostojik[120] has described a method for the separation of signals at a detector due to the components of an

unresolved (in the GC sense) mixture: the basic experimental values required are the signal ratios of the individual components, and the signal ratio of the mixture. The signal ratio is the ratio of the signals for a component or mixture from two different detectors. In fact, a single detector operating under different conditions may be used.

Thus:-

$$\text{Signal Ratio} = {}^{K}R_{ij} = \frac{K_{Y_i}}{K_{Y_j}} \qquad \ldots\ldots\ldots \quad 5.1$$

Where:

R = ratio

Y = signal

i = detector i

j = detector j

K = compound K.

The general procedure is: (a) for a mixture of qualitatively known components, determine the signal ratios for the mixture at each pair of detectors; (b) determine the signal ratio for each pure component of the mixture at each pair of detectors. If the qualitative nature of the mixture is unknown, some component resolution will be required. This case will be dealt with in Section 5.2.3.

Now, consider the signal ratio R_{ij} for an N component mixture:

$$R_{ij} = \frac{A_{Y_i} + B_{Y_i} + C_{Y_i} \ldots\ldots N_{Y_i}}{A_{Y_j} + B_{Y_j} + C_{Y_j} \ldots\ldots N_{Y_j}} \qquad \ldots\ldots \quad 5.2$$

For an N component mixture, substitute in the characteristic signal ratios for the pure compounds as defined in equation 5.1.

$$R_{ij} = \frac{{}^{A}R_{ij} \cdot {}^{A}Y_j + {}^{B}R_{ij} \cdot {}^{B}Y_j + \ldots {}^{N}R_{ij} \cdot {}^{N}Y_j}{{}^{A}Y_j + {}^{B}Y_j + {}^{C}Y_j \ldots\ldots\ldots\ldots\ldots {}^{N}Y_j} \qquad 5.3$$

Rearrange 5.3

$$R_{ij} = \frac{{}^{A}R_{ij} + {}^{B}R_{ij} \cdot {}^{B}X + \ldots\ldots {}^{N}R_{ij} \cdot {}^{N}X}{1 + {}^{B}X + {}^{C}X + \ldots\ldots\ldots\ldots {}^{N}X} \qquad 5.4$$

Where $${}^{K}X = \frac{{}^{K}Y_j}{{}^{A}Y_j} \qquad \ldots\ldots\ldots \qquad 5.5$$

Rearrange 5.4

$${}^{B}X({}^{B}R_{ij} - R_{ij}) + {}^{C}X({}^{C}R_{ij} - R_{ij}) + \ldots\ldots {}^{N}X({}^{N}R_{ij} - R_{ij})$$

$$= R_{ij} - {}^{A}R_{ij} \qquad \ldots\ldots\ldots \qquad 5.6$$

Equation 5.6 contains the experimentally measured quantities, viz: the signal ratio for the mixture R_{ij} and the signal ratios for the pure components ${}^{N}R_{ij}$. Hence, using n detectors for n unknowns, n equations like 5.6 can be constructed for the unknowns ${}^{B}X \ldots\ldots {}^{N}X$. The solution of these may be carried out by matrices, and the values ${}^{B}X \ldots\ldots {}^{N}X$ determined.

Then $${}^{A}Y_n = \frac{Y_n}{1 + X^{B} + X^{C} \ldots . X^{N}}$$

where Y_n = signal from detector n for mixture

${}^{A}Y_n$ = signal from detector n for compound A.

Other values of ${}^{K}Y_n$ may be determined from equation 5.5

For a simple two component system, compounds A + B, with detectors 1 + 2 :

$$ {}^{A}Y_1 = Y_1 \cdot \frac{R_{2,1} - {}^{B}R_{2,1}}{{}^{A}R_{2,1} - {}^{B}R_{2,1}} \qquad \ldots\ldots\ldots \quad 5.7 $$

$$ {}^{B}Y_1 = Y_1 \frac{{}^{A}R_{2,1} - R_{2,1}}{{}^{A}R_{2,1} - {}^{B}R_{2,1}} \qquad \ldots\ldots\ldots \quad 5.8 $$

The requirements on the system for this type of analysis are:-

(i) The number of detectors $\geqslant$ the number of unknowns.

(ii) All detectors must be operating in their linear range.

(iii) The system of equations which resemble 5.6 must have a non-zero determinant. For a two component system this requires that the two characteristic signal ratios must be different. For a system of n equations the zero-determinant is avoided if:-

(a) for every detector pair at least one characteristic signal ratio should be different from the others.

(b) the number of characteristic signal ratios of any two detector pairs which can be mutually proportional, must be at least one less than the number of components of the mixture.

(c) for every component at least one of the signal ratios should be different from the others.

(d) the ratios of the differences between the characteristic signal ratios of one component and any other two compounds on the same detector pair, must not equal the similar value for any of the detector pairs, i.e.:

$$ \frac{i_{R_{1,n}} - k_{R_{1,n}}}{j_{R_{1,n}} - k_{R_{1,n}}} \neq \frac{i_{R_{2,n}} - k_{R_{2,n}}}{j_{R_{2,n}} - k_{R_{2,n}}} \neq \ldots\ldots \frac{i_{R_{n-1,n}} - k_{R_{n-1,n}}}{j_{R_{n-1,n}} - k_{R_{n-1,n}}} $$

The method will work for signal ratios determined at any time during the passage of the mixture through the detectors, provided that the same time is used for the determination of the characteristic signal ratios of the pure compounds. The entire signal area could also be used.

Precision may be achieved by the use of configurations furthest away from the forbidden cases: accuracy will depend on the linearity and additivity of the system. The signal handling must be carefully controlled in this system particularly with respect to base-line correction and peak characterization. Identical dynamic properties must be maintained in all the detectors. One of the benefits of SRM is that the characteristic signal ratios obtained are a function of the physical and chemical properties of the analyte, and as such may be of help in the identification of unknown species.

Simultaneous equation method.

In this method, the values to be determined are the slopes of the response versus concentration curves for each of the components on each of the coatings. Let ${}^{k}S_{n}$ be the slope of the graph for component k on coating n. For a system of n detectors and k components, n.k. such slopes must be determined. Thus, if the response of the detector n to a mixture of k components is Y_n, an equation may be written thus:

$$Y_n = {}^{1}S_{n} \cdot [1] + {}^{2}S_{n} [2] + \ldots\ldots {}^{k}S_{n} [k]$$

where [k] is the concentration of the k^{th} component. For each detector a similar equation may be written, relating the signal at the detector for the mixture, to

the concentration of the components of the mixture. The solution may be found by the use of matrices.

Consider the following set of simultaneous equations.

$$x + 2y + 3z = 12 \quad \ldots . \quad (1)$$
$$2x - y + 2z = 2 \quad \ldots . \quad (2)$$
$$3x + 4y - z = 2 \quad \ldots . \quad (3)$$

These may be used to write an augmented coefficient matrix.

$$\begin{matrix} 1 & 2 & 3 & 12 \\ 2 & -1 & 2 & 2 \\ 3 & 4 & -1 & 2 \end{matrix}$$

For the generalized case it is desirable to reduce the matrix thus:

$$\begin{matrix} ax & & & = & d \\ & by & & = & e \\ & & cz & = & f \end{matrix}$$

Elimination of the off-diagonal elements occurs by the multiplication and division of both sides of the equation. The method is formalized in the pivotal condensation of matrices.

Hence: The Pivot Element $\equiv$ the number which is to be the operand.

The Pivot Row $\equiv$ the matrix row containing the pivot element.

The Elimination Row $\equiv$ the row on which the operation is being carried out, in order to eliminate the coefficients. Thus to solve (1), (2) and (3), let: Row 1 be the pivot row, element 1,1 the pivot element.

Then $-2 \times ① + ② \longrightarrow ②$ elimination row.

$-3 \times ① + ③ \longrightarrow ③$ elimination row.

$$\begin{aligned} x + 2y + 3z &= 12 && ① \\ -5y - 4z &= -22 && ② \\ -2y - 10z &= -34 && ③ \end{aligned}$$

Similarly let Row 2 be the pivot row and element 2,2 the pivot element.

Then $2/5 \times ② + ① \longrightarrow ①$ elimination row.

$-2/5 \times ② + ③ \longrightarrow ③$ elimination row.

$$\begin{aligned} x + 7/5 &= + 16/5 && ① \\ -5y - 4z &= - 22 && ② \\ -\tfrac{42}{5}z &= -\tfrac{126}{5} && ③ \end{aligned}$$

Similarly eliminate rows ① and ② to give:-

$$\begin{aligned} x &= - 1 && ① \\ -5y &= -10 && ② \\ -\tfrac{42}{5}z &= \tfrac{-126}{5} && ③ \end{aligned}$$

and $x = -1$, $y = 2$, $z = 3$.

For the generalized matrix

$$\begin{matrix} a_{11} & \cdots & a_{1k} \\ \vdots & & \vdots \\ a_{j1} & \cdots & a_{jk} \end{matrix}$$

If the elimination row is d, and the pivot row is e, row d is altered element by element thus:-

$$^{1}a_{dg} = a_{dg} + M_d \cdot a_{eg} \text{ for } g = 1,k.$$

Where M_d is the multiplying factor

$$= - \frac{a_{de}}{a_{dd}}$$

The solution may be carried out manually for a small number of equations, but a larger number will require the use of a computer programme.

The requirements for the successful application of the SEM are:

(i) for n compounds, n detectors must be used to generate n equations;

(ii) there must be a unique solution to the matrix;

(iii) linearity and additivity must obtain in all the detectors;

(iv) the coefficients must be known with accuracy, as it is essential to avoid the generation of wildly inaccurate results.

The subject of simultaneous equation solution by matrices is dealt with by Noble[121]. The problems of "ill-conditioned" matrices, which can cause the errors mentioned in (iv) is fully discussed, as is the production of unique solutions to non-homogenous equations by matrix methods (ii). The condition that a set of non-homogeneous simultaneous equations has a unique solution is that the rank of the coefficient's matrix be the same as the rank of the augmented coefficient matrix, and that this equals n, the number of unknowns. The rank of a matrix, is the order of the largest possible determinant that can be formed from the matrix by striking out rows and columns,

whose sum is non-zero. A determinant has a zero value if: (a) all elements in one column or row are zero; (b) if two rows or columns are identical, element by element. The best precision is achieved by configurations well away from the forbidden cases.

5.1.2 Practice

Several different coatings, analytes and system configurations were used to test the system for multiplex operation. In all cases a two component mixture was used in order to provide a simple analysis. The first experiment checked that linear curves and additive dissolution could be obtained for a number of different coatings. Thus, a crystal was coated using the rapid coating technique, and located in the low volume impinger detector cell under a gas flow of 3 mls per minute at room temperature. Samples of vapour, 80 microlitres in size were injected over the crystal at 10 microlitres per second. The vapour samples were obtained from static sampling cells. A small volume of the liquid or liquids of interest was introduced into the cell and allowed to completely vaporise. The use of these cells has been described in section 3.2.2. Each sample was introduced in triplicate, for a range of chloroform and benzene concentrations as shown in table 13. This entire procedure was carried out for di-nonyl phthalate, squalane, β-β-oxydipropionitrile and "Carbowax 20M". In each case the maximum frequency depression obtained on sample introduction was recorded, and a family of curves plotted for

TABLE 13

		No. of microlitres of benzene in sampling cell.					
		0	1	2	3	4	5
No. of microlitres of Chloroform in Sampling Cell.	0	1	7	13	19	25	31
	1	2	8	14	20	26	32
	2	3	9	15	21	27	33
	3	4	10	16	22	28	34
	4	5	11	17	23	29	35
	5	6	12	18	24	30	36

The body of the table gives the sample numbers, the legends give the constitution of the sample.

each of the two analytes, as Δf versus analyte concentration, for each coating. See figures 55 to 58.

Thus the concentration of analyte in the gas stream for a one microlitre introduction of liquid in the sample cell can be calculated:

1 microlitre of benzene weighs 0.9 mgrms) present in
1 " " $CHCl_3$ " 1.48 mgrms) 21.5 mls.

$\therefore$ conc in mgrms/m^3 = $4.186_{\Lambda}^{\times 10^4}$ for benzene

$6.884_{\Lambda}^{\times 10^4}$ for chloroform

80 microlitres of this vapour put into 3 mls/minute at 10 microlitres per second.

Hence concentration in gas stream of analyte

$$= \frac{60 \times 80}{3 \times 8 \times 1000} \times \text{concentration of vapour in cell.}$$

$= 8.372 \times 10^3$ mgrms/m^3 for benzene

$= 1.377 \times 10^4$ mgrms/m^3 for $CHCl_3$

The results from figures 55 to 58 demonstrate a linear increase in the frequency response for an increase in the chloroform vapour concentration. The addition of successive increments of benzene caused additive response at first, but higher concentrations ceased to be additive, and the response graphs curved towards the concentration axis. A similar set of results arose from the benzene graphs, save that here, it can be seen that the linear portion of the curve is shorter, and that increments of chloroform produced additive response for a smaller range. The useful range of concentrations for the two analytes extended up to approximately, 5.0×10^4 mgrms per m^3 for chloroform and 1.7×10^4 mgrms per m^3 for benzene.

FIGURE 55

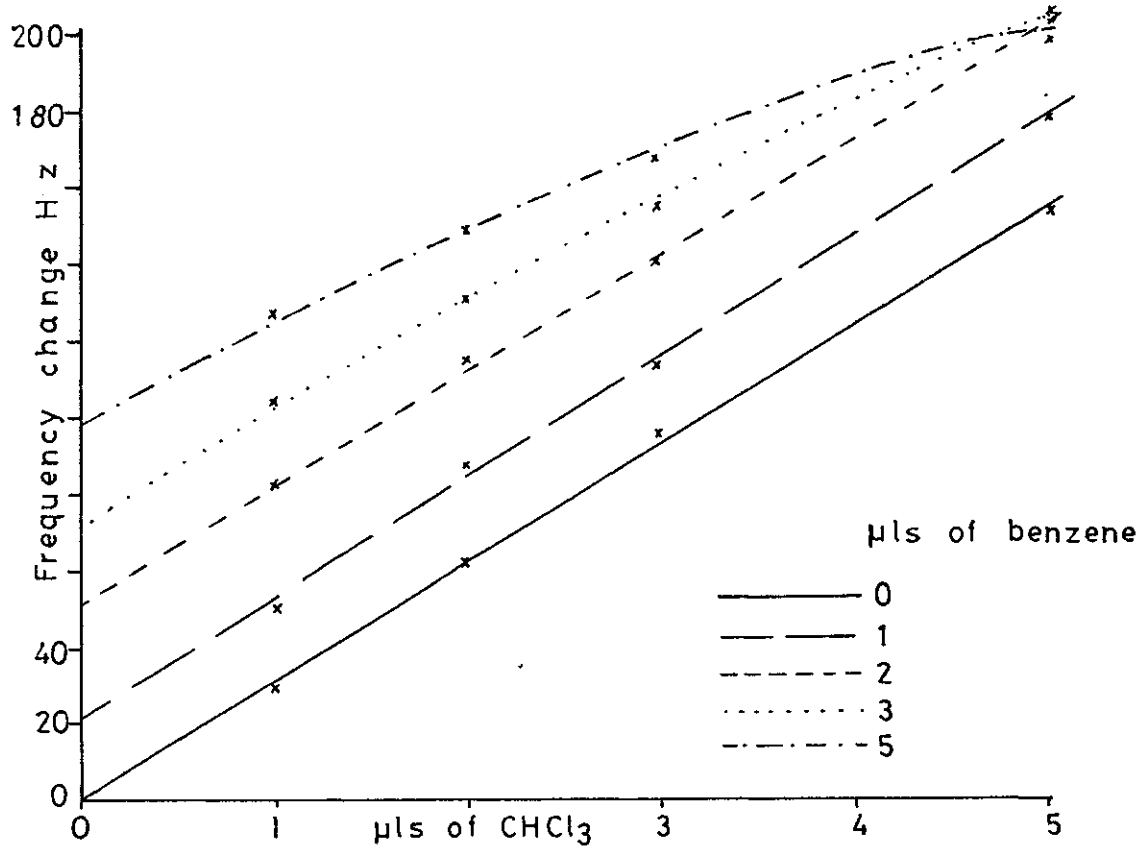

Di-nonyl phthalate

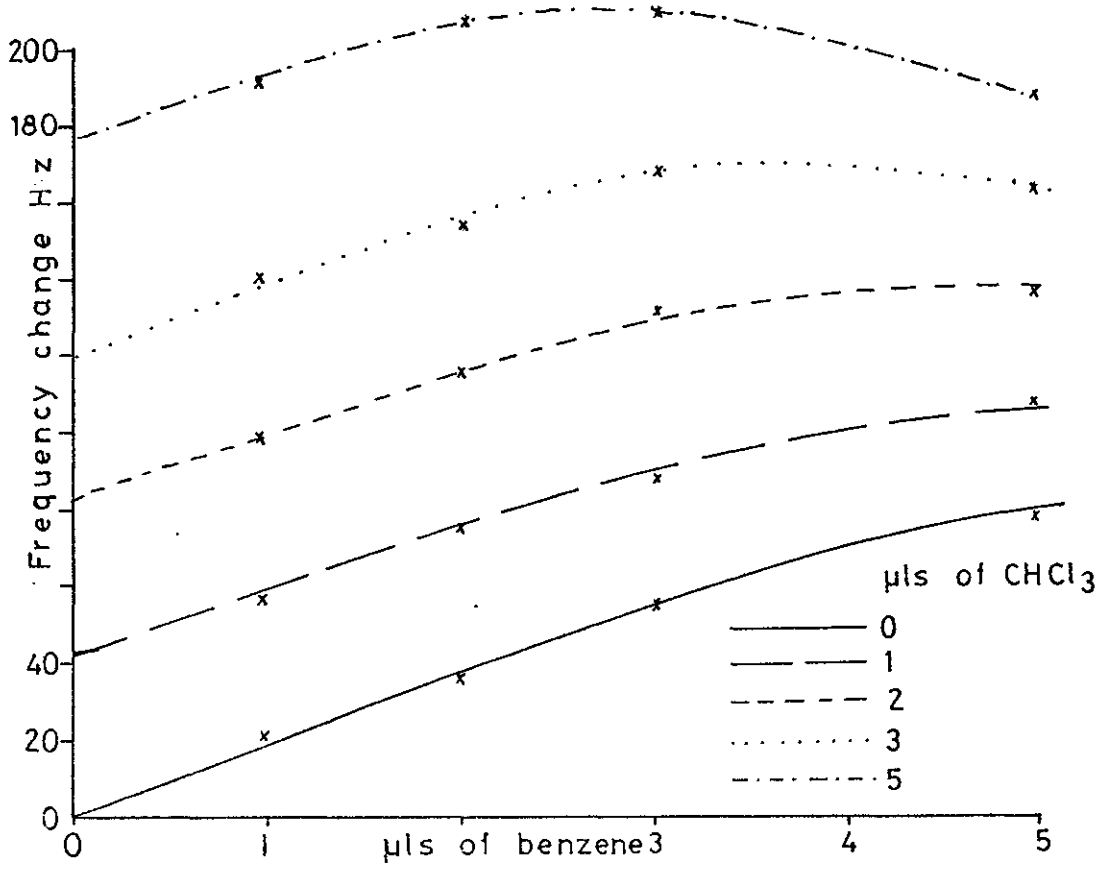

FIGURE 56

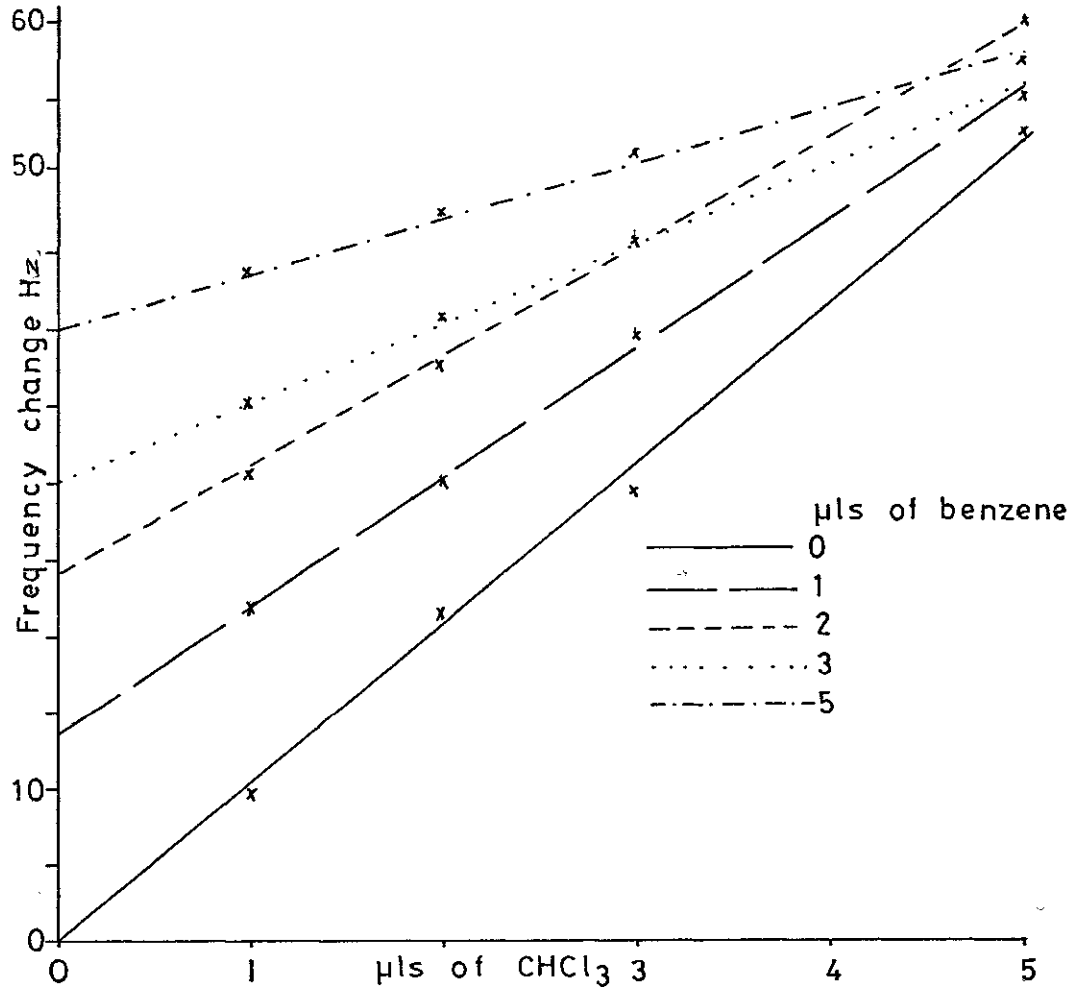

Squalane

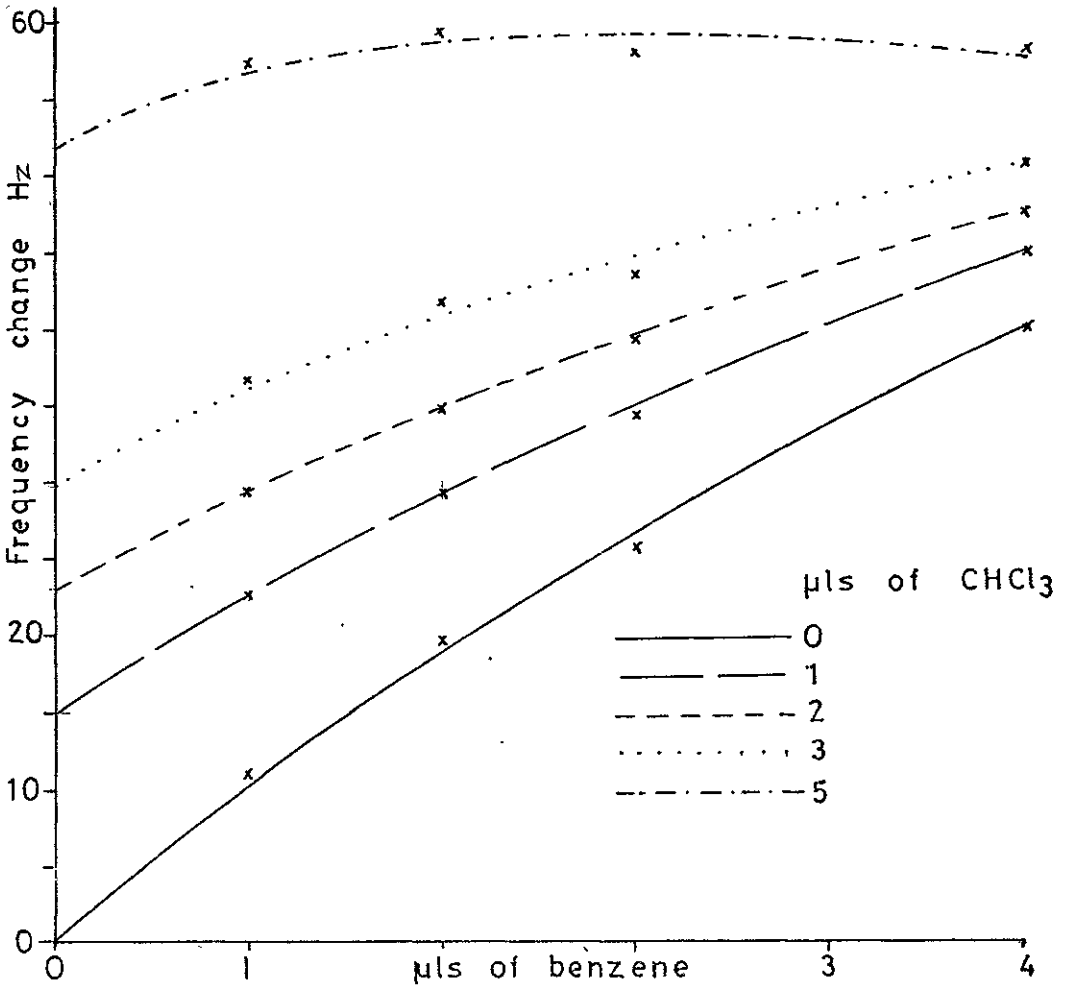

FIGURE 57

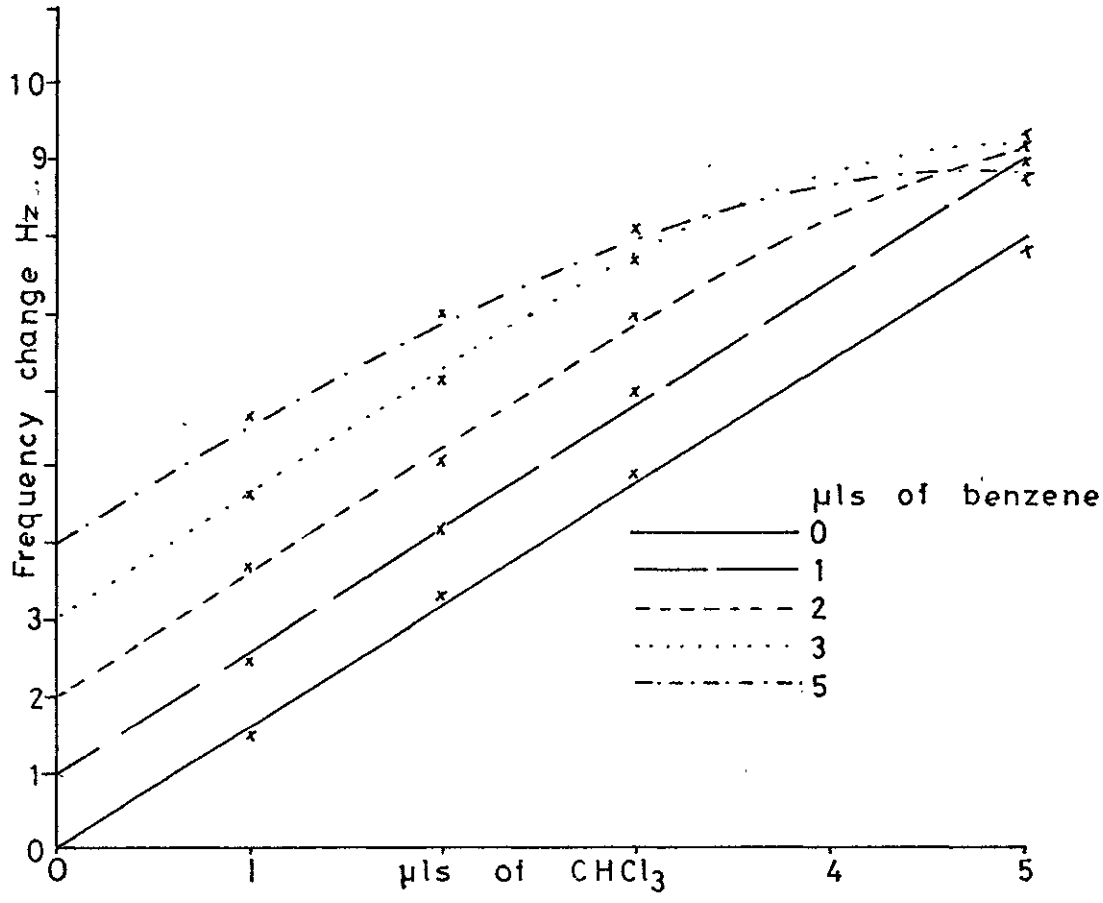

β-β— Oxydipropionitrile

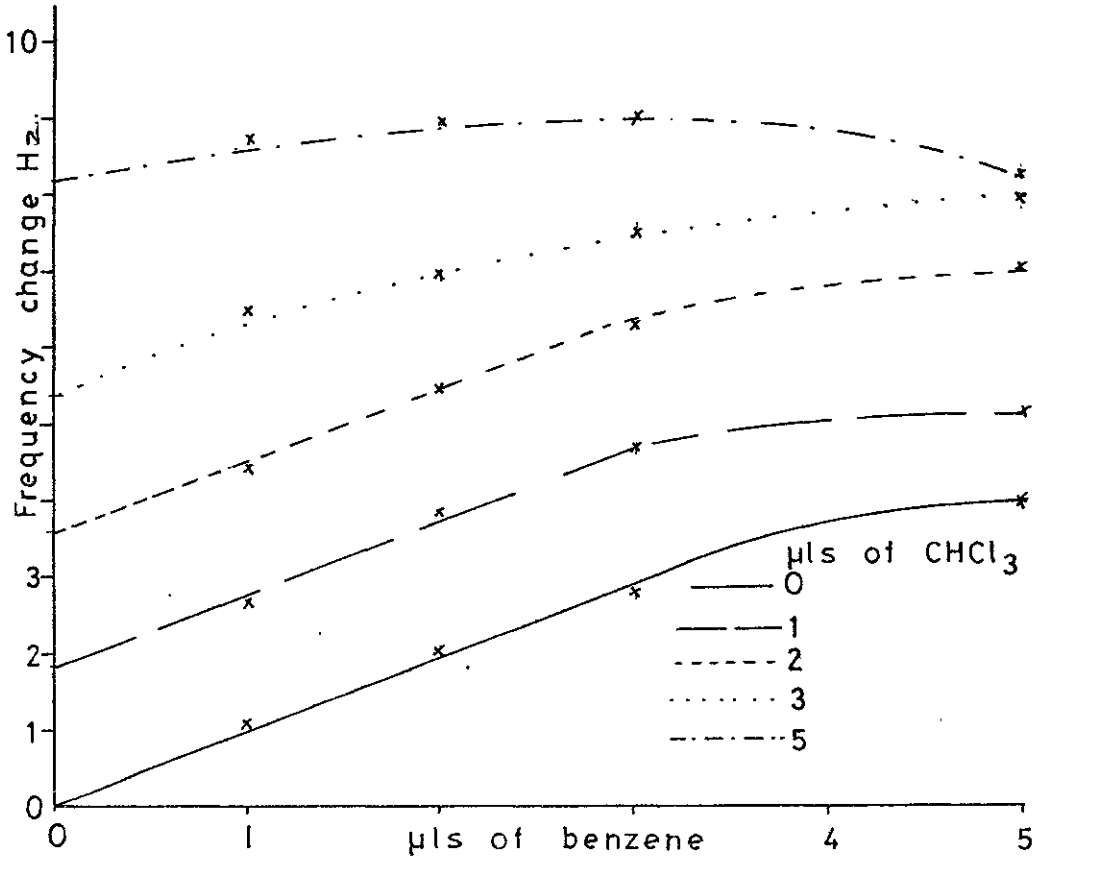

FIGURE 58

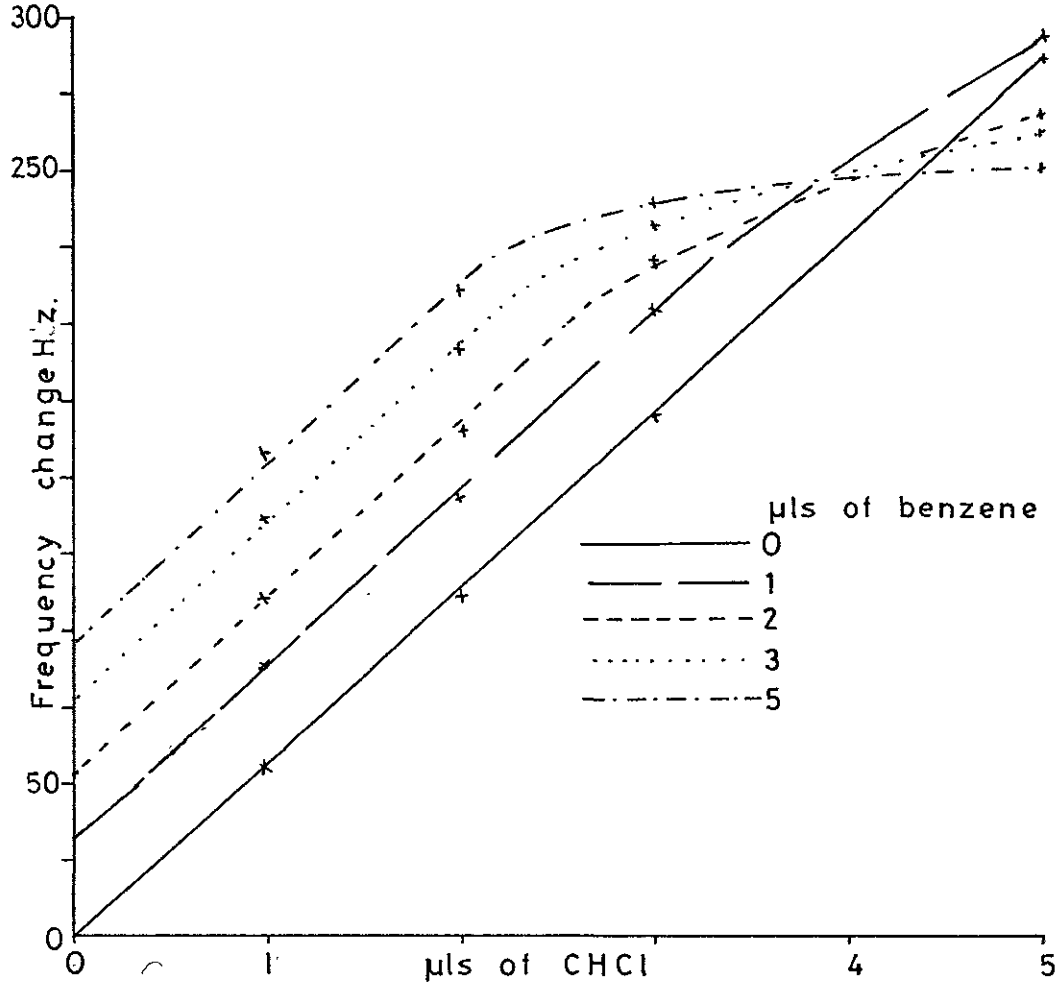

"Carbowax 20 M"

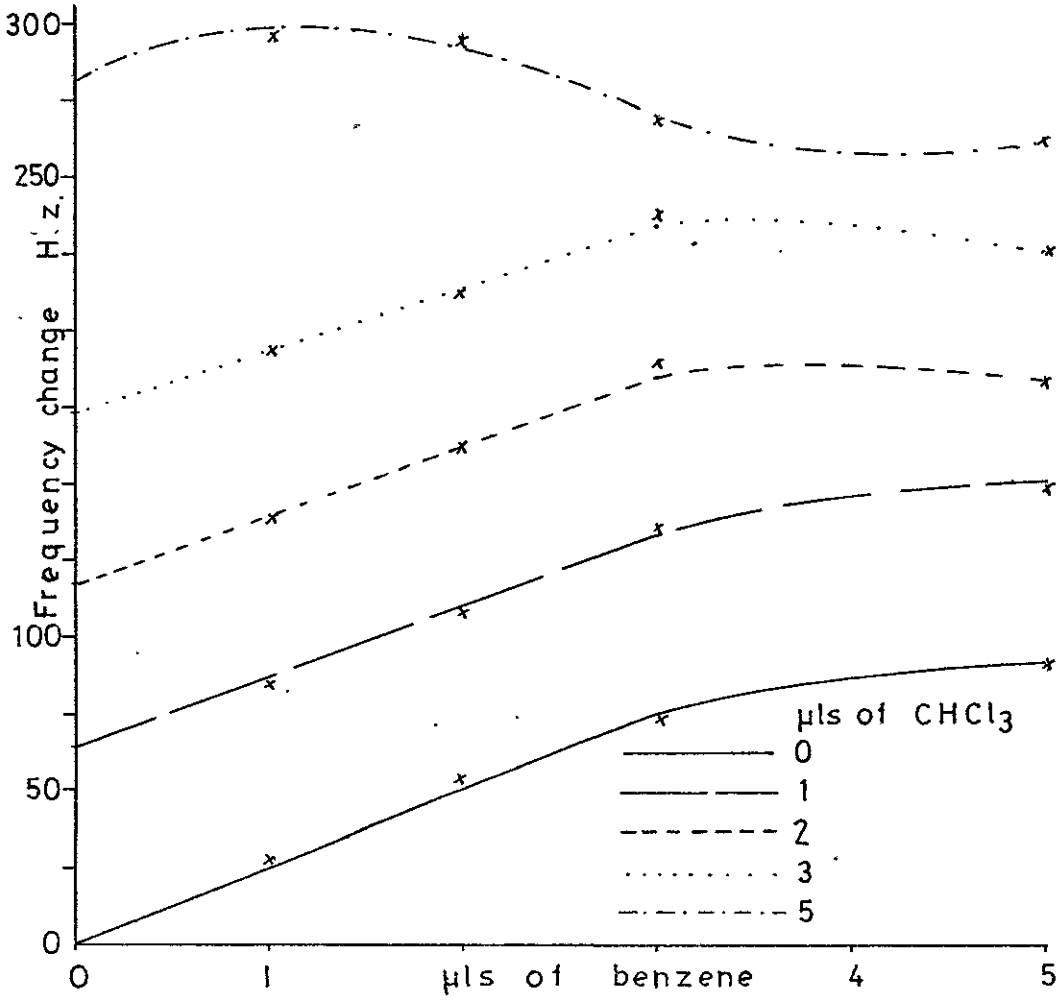

In the non-equilibrium conditions employed, the full concentration of analyte in the coating would not be obtained. The curved response graph is a function of conditions in the coating (see Section 3.2.1) hence, the use of vapour concentrations that do not cause the analyte concentration in the coating to exceed those that obtained for the linear and additive sections of the graphs, should be used. In other words, the frequency changes obtained for these optimum regions of linearity and additivity should not be exceeded.

The first experiment to attempt the determination of a binary mixture of chloroform and benzene, employed di-nonyl phthalate and "Carbowax 20M" coated crystals. Each crystal was located in a low-volume impinger detector cell under a gas flow of three mls per minute at room temperature: the cells were placed in a series configuration. Triplicate injections of 80 microlitres samples of various vapours were made using the technique described for the preliminary experiment in this section. The injections were made at septa placed just before each cell. Results were recorded as the maximum frequency change produced by the given sample.

RESULTS:

Sample mixture in static cell	Di-nonyl Phthalate coated crystal, response. Hz	"Carbowax 20M" coated crystal, response. Hz
1 microlitre $CHCl_3$	40	58
1 microlitre Benzene	17	29
1+1 $CHCl_3$/Benzene	53	85
2.5+1.5 $CHCl_3$/Benzene	138	188
0.5+0.5 $CHCl_3$/Benzene	38	52

SRM was used to analyse the results; the calculations were simplified by leaving the concentrations as the volumes of liquid introduced to the cell. The response for each component on each coating was calculated by SRM and compared with the response that would be expected on the basis of the responses for the pure components.

Mixture		Expected $CHCl_3$/Benzene		Found. $CHCl_3$/Benzene	
$CHCl_3$	Benzene	Di-nonyl Phthalate	"Carbowax 20M"	Di-nonyl Phthalate	"Carbowax 20M"
1	1	37/16	57/28	21/53	31/54
0.5	0.5	27/11	35/28	50/-12	73/-21
2.5	1.5	110/28	134/51	185/-47	81/107

The calculated results did not agree with the expected results, and in three cases, were trivial. The analysis was kept within the limits of linearity and additivity, hence the problem must lie within the actual values of the responses. Consider evaluation of equation 5.7, for the 1+1 mixture, di-nonyl phthalate coating, and the response ^{A}Y is sought for chloroform.

$$53. \quad \frac{(1.60377 - 1.70588)}{(1.45000 - 1.70588} = 21$$

Suppose the value of ^{A}Y altered by one, thus 53 becomes 54. The result of the calculation goes from 21 to 23. A unit change in the value ^{B}Y (result for pure benzene on the di-nonyl phthalate crystal) from 17 to 18 alters the calculation result from 21 to 2.4.

The next experiment introduced refinements in the system, designed to provide more accurate determinations of the signal ratios. The two crystals were located in the low volume impinger detector cells, which were arranged in a parallel configuration. Thus samples introduced to the system were split, and passed to each cell, causing a simultaneous change in the two detectors, thus permitting the determination of the signal ratio for a single injection. A gas flow rate of 5 mls per minute was maintained in the system, and sample volumes of 10 microlitres were introduced into the system, using the sampling technique described for the previous experiments. The frequency of each crystal was read using the 10 second gating time, and a computer program used to determine the entire peak area for each signal.

RESULTS.

Mixture in sample cell		Crystal Coating	
		Di-nonyl Phthalate	"Carbowax 20M"
$CHCl_3$	Benzene		
1	0	256.3 Hz.	299.2 Hz.
0	1	65.2 Hz.	63.3 Hz.
1	1	130.5 Hz.	158.25 Hz.
2	3	123 Hz.	156.7 Hz.
3	2	147.8 Hz.	186.0 Hz.
4	1	194.7 Hz.	236.2 Hz.
1	4	93.7 Hz.	111.2 Hz.

The data were analysed using the SRM: the concentrations were left in their simplified form. The results obtained were all trivial, with negative values for many calculated responses. Again, the ratios selected, gave results that were extremely sensitive to small alterations in a signal value. In fact these ratios were close to one of the forbidden cases described in section 5.1.1 (case no (iii)).

The SEM method was also used to analyse the results, again trivial values for the concentrations were obtained. The SEM required less calculation than the SRM, but failed to give good results for a similar reason. The sensitivities of the components were so similar, (256.3 Hz obtained for chloroform on di-nonyl phthalate and 299.2 Hz for chloroform on "Carbowax 20M": 65.2 Hz for benzene on di-nonyl phthalate and 63.3 Hz for benzene on "Carbowax 20M") that the forbidden case in section 5.1.1 was approached, where the rank number was less than the number of components.

The third system used to test the multiplexing method utilized "Carbowax 20M" and squalane coatings. The crystals were located in the low volume impinger detector cell, under a carrier gas flow of 12 mls per minute. A parallel configuration was used for the cells, which were immersed in a water bath at 30°C. Samples were introduced, using the diffusion tubes: binary mixtures were obtained from tubes containing a mixture of the two liquid phases of the analytes of interest. The liquids used were cyclohexane and acetone. The vapours

were admitted to the carrier gas, and allowed to reach an equilibrium concentration in the detector coating, at which point the frequency depression was measured. Triplicate samples were used, and the results averaged for each sample. SRM was used to determine the responses of the components of the mixtures, on each detector.

RESULTS:

Tube Number	Mls. of Acetone	Mls. of Hexane	Response on Squalane	Response on "Carbowax 20M"
1	1	1	6.5	55.5
2	1.5	0.5	2.5	42
3	0.5	1.5	2.8	28
4	1	0	1.5	40.8
5	1	2	4.0	7.7
6	0	1	2.9	8.1
8	2	1	5.7	47.7

The proportions of liquid in the tubes was used to calculate a relative diffusion rate for the mixtures, using equation 3.36. From these diffusion rates, the expected responses for each component in each mixture on each detector was calculated, employing the results for the pure liquids.

SQUALANE DETECTOR.

Tube Number	Expected Response		Observed Response	
	Hexane	Acetone	Hexane	Acetone
1	1.390	0.704	4.970	1.530
2	0.678	1.09	1.065	1.435
3	2.126	.342	2.007	0.823
5	1.874	.460	3.733	0.267
8	0.910	.959	4.398	1.302

"CARBOWAX 20M" DETECTOR.

Tube Number	Expected Response		Observed Response	
	Hexane	Acetone	Hexane	Acetone
1	3.88	19.16	13.88	41.62
2	1.89	29.65	2.97	39.0
3	2.88	9.3	5.60	22.4
5	5.23	12.52	10.42	7.28
8	2.54	26.07	12.28	35.42

The results obtained from this experiment were more meaningful, than previous attempts, since all the signals determined had positive values. The agreement with the expected results was poor, and the most probable reason was the determination of the very small frequency changes from the squalane detector. It should be noted,

however, that although the uncertainty of these readings was high, compared with the error on the readings in the second experiment, the use of a system whose ratios were well away from the forbidden case gave rise to results that were far less trivial, in spite of the more significant uncertainty in the fundamental values.

The final experiment employed a system identical to the previous work. The replicate samples of the hexane and chloroform analytes, were introduced to the system by diffusion tube and syringe pump respectively. The diffusion tube was used at temperatures of 40°C and 50°C to provide different vapour concentrations for the binary mixture. The syringe pump employed a Chance five mls glass syringe. The syringe contained an excess of chloroform liquid and the saturated vapour was introduced to the carrier gas at three different flow rates, to provide a range of concentrations of vapour for the mixture. Digital counters monitored the frequency of each crystal, and results from the "Carbowax 20M" crystal were displayed on a chart-recorder after digital-analogue conversion.

RESULTS.

Sample Number	Concentration		Response	
	Hexane mgs/m^3	$CHCl_3$ mgs/m^3	"Carbowax 20M"	Squalane
1	988.6	-	24.0 Hz	7.5 Hz
2	1100	-	25.5 "	8.0 "
3	-	3775	58.0 "	5.5 "
4	-	2265	43.5 "	4.0 "
5	-	4530	76.0 "	7.0 "
6	988.6	3775	81.0 "	13.0 "
7	1100	2265	69.0 "	11.5 "
8	1100	4530	101.0 "	15.0 "

The calculations for the mixtures were carried out using both SRM and SEM. Hence results due to SRM:

Tube Number	Response on "Carbowax 20"				Response on Squalane			
	Hexane		Chloroform		Hexane		Chloroform	
	Calc-ulated	Ex-pected	Calc-ulated	Ex-pected	Calc-ulated	Ex-pected	Calc-ulated	Ex-pected
6	24.8	23.7	56.2	58.3	7.8	7.5	5.2	5.5
7	23.1	25.5	45.9	43.5	7.2	7.7	4.3	4.3
8	25.5	24.9	75.5	76.6	8.0	8.0	7.0	7.0

Results due to SEM.

Sample Number	Calculated Concentration		Known Concentration	
	Hexane mgs/m^3	$CHCl_3$ mgs/m^3	Hexane mgs/m^3	$CHCl_3$ mgs/m^3
6	1048	3279	988.6	3775
7	974	2681	1100	2265
8	1075	4410	1100	4530

The results from both methods of calculation correlated well with the known values. Sample 8 demonstrated close agreement, within 2% of the expected values. The results for 6 and 7 were less accurate, with a maximum error of 18%.

This series of experiments has demonstrated and underlined some of the criteria discussed in section 5.1.1 for the operation of a multiplexing system. (i) The system must be stable and predictable. This ensures that

the signals are determined with the minimum of error. Thus the use of temperature controlled systems with equilibrium signals from long sample inputs would be recommended.

(ii) The dynamic performance of the detector must be maintained for samples and mixtures, in order that accurate results may be obtained. Hence the use of parallel detector cell systems, and replicate determinations of all signals, in order to provide, or compensate for a lack of, dynamic stability.

(iii) The fundamental signal ratios must be determined with maximum certainty, i.e. suitable samples sizes and sensitive detectors must be used in order to obtain large values for the signals.

(iv) Forbidden configurations for both augmented coefficient matrices, and detector ratios must be avoided.

By following these criteria, both SRM and SEM may successfully be used for the analysis of multicomponent mixtures.

5.2 OTHER METHODS

5.2.1 Equilibrium profile method

Equation 3.29 indicates that the equilibrium concentration of an analyte in a crystal's coating is given by: Kx, where x is the concentration of the analyte in the carrier gas stream, and K the partition coefficient for the particular system. This result, is the limit of the following equation as $n \longrightarrow \infty$

$$C = x\left[\frac{\left(\frac{K}{K+1}\right)\left(1-\left(\frac{K}{K+1}\right)^{n}\right)}{1-\left(\frac{K}{K+1}\right)}\right] \quad \ldots\ldots\ldots 5.9$$

Thus the number of equilibria to attain C, or a fraction of C is independent *of* x, but dependent on K.

Consider the C versus n profile obtained using the results from solving equation 5.9, for three distinct hypothetical cases: K = 80; K = 160; K = 320.

Value of n	Value of C if x = 1		
	K = 80	K = 160	K = 320
100	56	74.2	85.8
200	73.3	114	148.5
300	78	135.3	194.5
400	79.4	146.8	228.1
500	79.8	152.9	252.8
600	79.95	156.2	270.8

Figure 59 depicts the curves obtained by plotting the graphs of C versus n, for the three values of K. It can be seen that the growth rates (profiles) of the curves are different for each analyte. Now, suppose that analyte a, partition coefficient = k, is present in an atmospheric sample at x_a concentration units in the gas stream, and a second analyte b an interferent is similarly present at x_b concentration units, and its partition coefficient = K. The carrier gas is passed

FIGURE 59

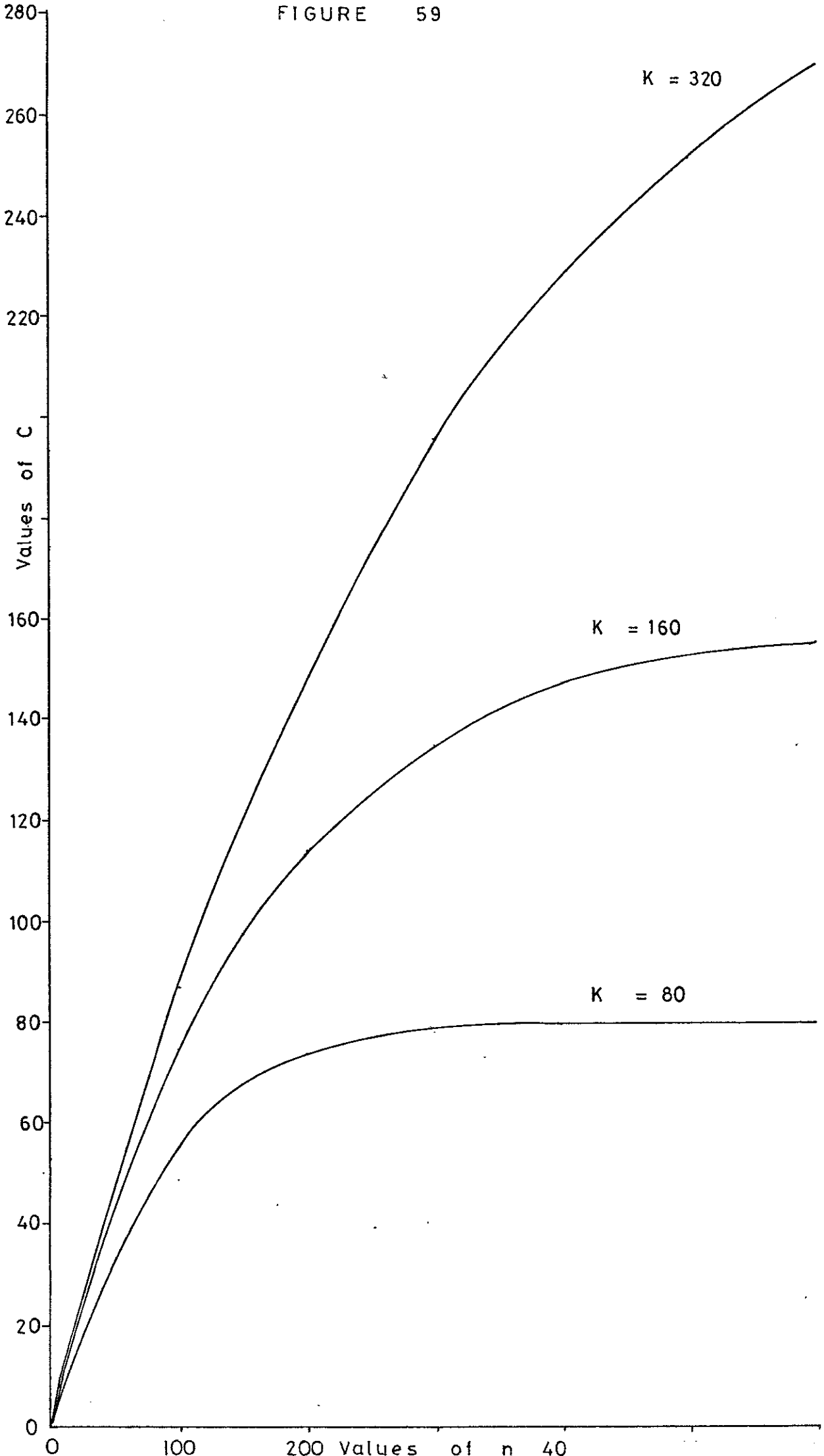
280
260
240
220
160
140
120
100
80
60
40
20
0
Values of C
K = 320
K = 160
K = 80
0
100
200 Values of n 40

over the crystals such that equilibrium occurs. A growth curve of the profile could be obtained from the detector for this mixture.

Consider at time t, at any point on the growth curve prior to equilibrium. The total concentration of the two compounds in the coating ${}^1C_t$ is given by:

$$ {}^1C_t = c_a + c_b $$

Where c_a = concentration of a in coating

c_b = concentration of b in coating.

Now, from equation 5.9

$$ c_a = (k_e^n)\, x_a $$

$$ c_b = (K_e^n)\, x_b $$

where k = partition coefficient for a

K = partition coefficient for b

and (k_e^n) = solution of equation 5.9 for k and n (no. of equilibria in time t_1).

At time t_1, the response of the detector ${}^1R_t$ is given by:

$$ {}^1R_t = c_a.d + c_b.f $$

$$ = (k_e^n)x_a.d + (K_e^n)x_b.f \quad \ldots\ldots\ldots \quad 5.10 $$

Where d and f are proportionality constants for a and b respectively.

Similarly at time t_2

$$ {}^2R_t = (k_e^m)x_a.d + (K_e^m)x_b.f \quad \ldots\ldots\ldots \quad 5.11 $$

where m = no. of equilibria occurring in time t_2.

Let $$ R_m = \frac{{}^1R_t \,.\, (k_e^m)}{(k_e^n)} $$

$$ {}^2R_t - R_m = x_b f\left((K_e^m) - \left(\frac{(K_e^n)\,.\,(k_e^m)}{(k_e^n)}\right)\right) $$

$$ = R_{diff} $$

Let $Z = (K_e^m) - \left(\frac{(K_e^n) \cdot (k_e^m)}{(k_e^n)} \right)$

Then $x_b f = \frac{R\ diff}{Z}$

Since all the values that make up Z may be determined for a given pair of vapours and a given flow system, and R diff may also be determined from these values and the experimental results, $x_b f$ may be determined. This value can be back-substituted in 5.10 and 5.11 to give the corrected value for R, as if no interferent were present.

For a given profile, several estimations of $x_b f$ may be made, thus improving the accuracy of the evaluation of this quantity.

It is essential that the value of Z be non-zero, i.e.

$$(K_e^m) \neq \frac{(K_e^n)(k_e^m)}{(k_e^n)}$$

Thus, the selection of values K, k, n and m furthest away from the forbidden case will give greatest accuracy for the determination of $x_b f$.

This system could be extended to cover the analyses of profiles that arise from multiple component systems, but in all cases, the dynamic behaviour of the system must be rigorously controlled, in order to provide a reproducible system for the measurement of the profiles.

5.2.2 Diffusion detector cell method

The use of a detector cell that relies on the diffusion of the analyte from the main gas stream to the detector has been described in sections 3.22 and 3.32, and has been illustrated in figure 46. This type of cell

could be a method of introducing selectivity into the system. The construction of a mathematical model for the diffusion situation would be extremely complex.

The number of gaseous molecules diffusing per second per unit area along the x axis of a volume wherein exists a concentration gradient of the gas of interest, has been shown by Fick (see Kennard [122]) to be:-

$$\frac{dn_1}{dt} = D \frac{d^2n}{dx^2}$$

Where n_1 = the number of moles of gas diffusing/unit volume

D = diffusion coefficient

x = distance along the x-axis

t = time.

Consider the situation shown in figure 60, where n_o analyte molecules are present at the end of a cylinder of nitrogen. The value of n_o is maintained constant throughout the diffusion. The boundary conditions are:

$n_1 = n_o$ where $x \leqslant 0$ at any time t.

$n_1 = 0$ where $0 < x < H$ at $t = 0$.

$n_1 \rightarrow n_o$ where $0 < x \leqslant H$ at $t \rightarrow \infty$.

For this case, Partington[123] has demonstrated that the solution to the integration of Fick's equation is:

$$n_1 = \frac{n_o h}{H} + \frac{2n_o}{\pi} \sum_1^{\infty} \frac{1}{m} \sin \frac{m\pi h}{H} \cos \frac{m\pi x}{H} \cdot e^{-(m\pi/H)^2} \cdot Dt$$

Where m takes integral values from 1 to infinity.

FIGURE 60

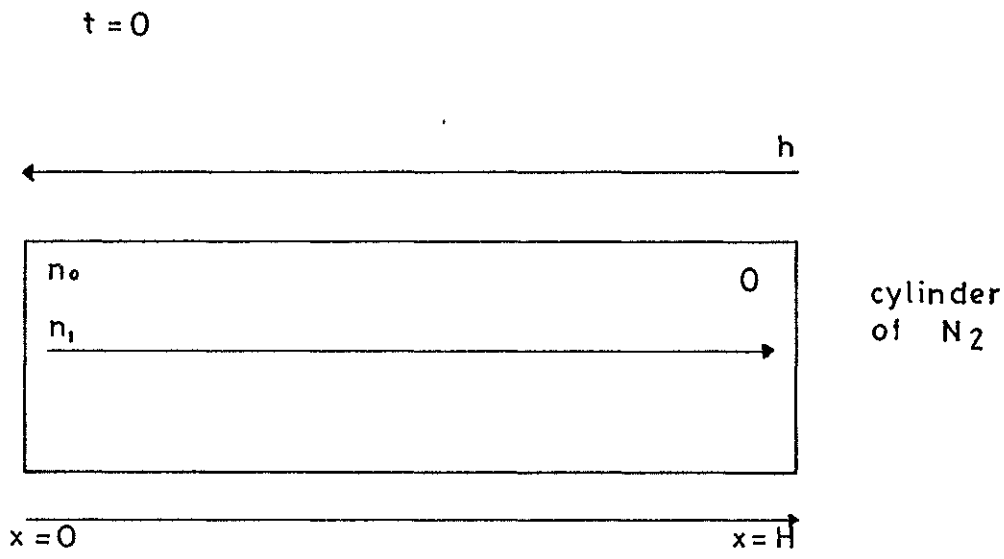

It may be seen that for a situation where a gas stream contains two analytes, the effect of placing the detector at one end of a tube down which the analytes must diffuse in order to interact with the coating, will be to partially separate them, if the difference in diffusion coefficients is sufficient. Thus the effect of an analyte may be reduced, for a given slug duration, because the diffusion rate may be so low, that insufficient equilibria take place in the detector coating for a significant response to be observed.

This suppression of interference is not as flexible as the method described in section 5.2.1,since the diffusion rate not only depends on the diffusion coefficient of the analyte, but also on the analytes' concentration. Thus the relative suppression will depend on the concentration of the two components, the interferent, and the analyte of interest. This approach will be most effective in a situation where the interferent concentration varies little, and where the value of the concentration, and diffusion coefficient of the analyte of interest ensures a relatively rapid diffusion rate.

5.2.3 Gas chromatography column method

The work of Karasak and Gibbins[89] and Karasak and Tiernay[90] indicated the value of the piezoelectric detector as a detector for GC. Application of this work could improve the selectivity of the detector for use in atmospheric pollution determination. The style of analysis and desired output would affect the type and

length of the GC column used. For example, analysis of a gaseous pollutant in a well-defined sample, where several interferents were present, would require a column of sufficient length only to separate the pollutant of interest, all the other components could remain unresolved. Alternatively the column may be quite long, in order to resolve a number of analytes in the atmosphere which the analyst wishes to determine. Finally, the column by itself, or in conjunction with a number of detectors, could be employed to determine the qualitative and quantitative composition of an "unknown" atmosphere.

The SRM of Ostojic[120] may be applied to partially resolved peaks from a chromatograph, where the identities of the individual components are unknown. The use of the SRM described in section 5.1.1, could be regarded as the determination of a completely unresolved GC peak, where the identity of all the components is known. In the case of a partially resolved peak, the effluent of the GC column is fed simultaneously to each detector. If there are n detectors, then n different partially resolved chromatograms will be produced. To obtain the characteristic signal ratios for the pure compounds from these data a different procedure from the one described in section 5.1.1 must be followed. For a system of "n" chromatograms, n-1 chromatograms are divided by the n'th. Division is carried out throughout the chromatogram to give n-1 signal ratio curves as a function of time. The signal ratio curves are differentiated, and the derivatives divided as for the first step. This process of differentiation and

division is repeated, until the signal ratio curves for every detector pair have been achieved. If n=2, only the first step is carried out; if n=3 only the first two steps are carried out. The analysis then proceeds in the manner described previously. (See Section 5.1.1.)

This technique could render the piezoelectric detector a powerful and rapid method for the qualitative and quantitative determination of atmospheric pollutants. Thus a system consisting of a GC column and detector array, linked to a micro-computer, could be used to assess an atmosphere qualitatively, by characteristic signal ratios and retention data, and quantitatively, by SRM.

CHAPTER VI CONCLUSIONS

In a recent review, O'Keefe[124] stressed that the future of air pollution monitoring lay in the development of chemoelectric transducers, and in systems whose basic design rationale included these devices. Chemoelectric transducers are solid-state devices whose electrical properties respond rapidly and reversibly to alteration in the composition of their environment. The ion-selective electrode is an example of a chemoelectric transducer, and the piezoelectric detector may also be included in this category.

The application of the piezoelectric detector as an analytical device for gas vapour measurement depends on three factors: the predictability of the detector; the stability of the detector; the reliability of the detector. The detector's predictability is a measure of the degree to which the detector's performance may be characterized in mathematical terms. A well characterized system can be adjusted, by the alteration of the correct parameters to suit a range of analytical situations, and to provide the analyst with a useful output. The piezoelectric detector has been demonstrated to be such a system. In sections 3.2.1 and 3.2.2 the basic equations that described the system's performance were discussed and illustrated, so that the full implications on the detector response were realized of such parameters as sample size, sample concentration, gas flow rate and cell

design, in both equilibrium and non-equilibrium situations. In section 3.3.1 and 3.3.2, the alteration of detector response was related to alterations in the volume, area and method of application of coatings. Thus, the response of the detector may be determined, given the basic values of: coating volume; system partition coefficient; frequency constant of the crystal; frequency of the crystal; carrier gas flow rate; sample duration; total sample mass or concentration. For general analytical use, it may be desirable to keep the system's parameters as constant unknowns, and to use calibration methods to determine the value of an unknown sample.

The stability of the system is a function of the short term noise and long term drift. In section 3.1.2, the major source of short-term noise has been demonstrated to be due to the uncertainty of measuring the least-significant digit of a given number of pulses fed to the digital counter. In the longer term, drift of the base-line frequency has been shown to be the major source of instability. Employment of a $\pm$ 0.1^{o}C thermostatted water bath was shown to significantly reduce drift for a crystal covered with a non-bleeding coating: for crystals coated with liquids that bled at significant rates, this source of drift could be reduced by suitable cell design. The correct choice of sample duration, signal handling and peak measurement technique has been discussed in chapters 3 and 4, for the attainment of optimum detection limits.

The reliability of the system, in a mechanical and electrical sense was found to be excellent. The

detector crystal, although fragile when unprotected, was found to be rugged and durable when located in a detector cell. The entire system was operated more or less continuously, for two years, during which time no mechanical breakdowns occurred, and very few electrical breakdowns. The electrical breakdowns that occurred were due to the separation of soldered joints between connecting wires and terminals, as a result of excessive handling incurred in the frequent alterations that were made to the system. The reliability of the majority of the coatings may be gauged from the fact that they could be continuously operated for six to twelve weeks with very little change in sensitivity. The coatings that were subject to more rapid bleed rates showed serious sensitivity decrease after a few hours (for β-β-oxydipropionitrile) or a few days (for tri-cresyl phosphate).

The suitability of the piezoelectric detector for monitoring atmospheric pollution depends a great deal on the exact concept of a monitor. If a pollution monitor is regarded as a device that measures the concentration of an environmental contaminant, *in situ*, and on a continuous basis, with rapid output of a pollutant concentration *versus* time profile, then the piezoelectric detector has several useful attributes that recommend its use as a monitor. Firstly, its stability and reliability, which have been discussed previously, are advantageous, in the situation where it is desirable for a system to operate continuously with little attention or maintenance on a day-to-day basis. Similarly the simplicity of the system

lends itself to monitoring applications. The basic detector could consist of: a coated crystal; a detector cell to house and protect the crystal; a battery-powered oscillator to drive the crystal. This detector could be placed in the environment to be monitored, and the alteration of pollutant levels would be registered as changes in the frequency output, as the pollutant entered and left the coating. It is more likely that a more sophisticated system would be used, with facilities for maintaining a flow of gas over the detector, a temperature compensating device, and sampling and filtering attachments. However, the simplicity of the detector remains, since the majority of the more complex procedures described in this work relate to signal handling and data manipulation, rather than alterations in the detector characteristics. Thus, the detector could be placed in a relatively hostile or inaccessible place, whilst the signal could be relayed back via landlines to a more suitable location for signal handling. The digital nature of the signal from the detector is suitable for rapid data acquisition and logging as well as manipulation by computers. Finally, the detector can be used on a continuous basis, with rapid output of results. Thus, the system could either be operated with a continuous stream of the polluted air passing over the crystals, or alternatively the base-line of the detector could be periodically re-established by using a pulse-type of sample input, with a standard atmosphere interrupting the sample pulses. Janghorbani and Freund[88] have demonstrated that the speed of response of

the piezoelectric detector to the presence of analyte in the detector cell is of the order of 100 milliseconds. In sections 3.2.1 and 3.2.2, the time taken for a sample to reach an equilibrium value in a given coating, was shown to depend linearly on the carrier gas flow rate, and inversely on the detector cell volume: for the flow rates and cell volumes used in this study, this value was found to be of the order of a few minutes. Hence, the piezoelectric monitor could produce its equilibrium results within a few minutes of change in pollutant level.

The ability of the piezoelectric detector to successfully monitor air pollution will depend on whether sufficient sensitivity and selectivity can be achieved. The mass sensitivity of the quartz crystal microbalance has been estimated by Warner and Stockbridge[22] to be one to ten picogrms, in a system where frequency changes of the order of one part in 10^{10} could be detected. The system used in this present study could distinguish frequency changes of the order of one part per 10^{7}, hence a mass sensitivity of 1 to 10 nanogrms could be expected. The mass sensitivity of this system may be estimated from the figures of table 8, where, for the most sensitive area of the crystal, the following value was obtained: 499.5 Hz/microgrm/cm^2. For a frequency change of one Hertz, 2.2 nanogrms must be added. In section 3.2.1 data for squalane coatings may be used to derive the mass sensitivity for a crystal coated over the entire face. Thus, 40 microgrms gave a Δf of 4900 Hz, hence for a one Hertz frequency change, 8.16 nanogrms must be added to the

crystal surface. This less sensitive value is to be expected in view of the use of less sensitive areas of the crystal. Suppose "typical" values are now selected for an analytical system, the expected sensitivity of the system could be calculated from equations 3.36. Let the concentration of the pollutant be x mgs/m^3, a response of one Hz achieved from this in a system where 1.0×10^{-1} microlitre of coating are present on each side of the crystal, whose K value is 200. Then, the mass of analyte in the coating at equilibrium will be $\frac{200.\ 20.\ 10^{-2}.\ x}{10^9}$ mgs.

Since the mass sensitivity is 8.16×10^{-6} nanogrms/Hz :

$$8.16 \times 10^{-6} = \frac{200.\ 20.\ 10^{-2}.\ x}{10^9}$$

Then $$x = 2.04 \times 10^2 \text{ mgs/m}^3\text{/Hz}.$$

This value compares well with those obtained in table 12, indicating that the detector used in this study performed within reasonable agreement of its theoretical sensitivity. Littlewood[110] has indicated that partition coefficients of 100 - 1000 may be expected at the normal operating temperatures of GC columns. This temperature is usually between 2 to 5 times higher than the temperature at which the piezoelectric detector is operated, hence a maximum value of 2000 for the partition coefficient may be more realistic. In this case, the sensitivity of the detector in the hypothetical situation described earlier would be of the order of 20 mgs/m^3/Hz . Further improvements in sensitivity could be made by increasing the volume of coating liquid on the crystal, or by using crystals of

higher frequency, thus increasing the value of the frequency constant. It has been demonstrated (see table 12) that the sensitivity of the piezoelectric detector was sufficient for the measurement of all the vapours discussed in this study, at or below the vapour's TLV. For a monitoring system in which precise values of contaminant concentrations are not needed, less strain is put on the detection limits, sensitivity and stability of a system. This approach to monitoring has been discussed by West[125], and applies to many situations, where the only output requisite is, whether the concentration value of an analyte is above or below a certain level, e.g.: a TLV. The piezoelectric detector could be operated using extremely simple equipment for this type of application.

The selectivity of the detector has been shown to be poor, since most of the vapours used dissolved in most of the coatings. This situation was foreseen by O'Keefe[124] who felt that solid-state chemoelectric transducers were unlikely to provide truly selective detectors. The solution proposed by O'Keefe was to use an array of detectors, each one responding to a different degree to a range of analytes. The signals from these detectors could be decoded by a simple computer. This approach has been studied with the piezoelectric detector, for a binary mixture, using SRM and SEM to calculate the concentrations of the individual components. In addition to multiplexing other methods of improving selectivity have been discussed in Chapter 5.

It may be that strenuous attempts to achieve selectivity are not always valid. In many analytical situations, the problem is well defined: the type and level of pollutant to be measured is known, as are the other atmospheric components. In such a case, the monitor only need be non-selective towards the extraneous components of that particular environment. Thus the problem reduces to finding a coating for the crystal that demonstrates significant sensitivity for the contaminant of interest, and little or no sensitivity to the other constituents of the atmosphere. The concept of high selectivity is redundant, in its place is contextual selectivity, and pollution monitors must be designed to provide this. The piezoelectric detector is particularly well suited to this type of application, since many hundreds of different GC stationary phases exist, with varying partition coefficients towards different analytes. In Ghapter 4, some of these phases were investigated, and their performance related to GC data obtained by other workers, and to their classification on a structural basis into one of the Littlewood classes. It was demonstrated that, in general, GC data and coating structure could be extrapolated to the piezoelectric detector situation, and the type of response obtained in this situation predicted. Thus, monitor-design should start with a consideration of the type of pollutant to be measured, and the sort of interferent to be avoided. Thence a literature search should be carried out and a range of suitable phases selected. Finally experimentation with the detector

should be used to prove the best coating. The search may include not only the common stationary phases, but also those with highly specific properties such as liquid crystals[126].

The piezoelectric detector can be seen to be a suitable device for use as an atmospheric organic-pollutant monitor. A wide range of analytical determinations are available on simple equipment, with adequate sensitivity. Compared to the other detectors used for monitoring organic contaminants in the air, NDIR and the FID, the piezoelectric detector is capable of a wider range of analyses, with the facility of tailoring the detector to the situation to be analysed. The hardware required is much cheaper than that involved in laser fluorescence techniques, and it is quite possible for many detectors at various locations to be "read" at one data acquisition point. The detector responds rapidly and reversibly to analyte concentration, with a simple mathematical relationship between these two values. The output of the detector is ideal for data-processing.

Future work should include: testing the detector more thoroughly with "real" samples; examining the various methods of obtaining selectivity; investigation of electronic methods of compensating for drift; interfacing the detector with a small digital computer for complex data manipulation; continuous research into new coatings in order to optimize detector performance.

BIBLIOGRAPHY

1. J. EVELYN, "Fumifugium" 1661.
2. D.L. COFFIN, Adv. in Environmtl. Sci. and Technol., 1971, 2, 1.
3. E.R. HENDRICKSON, in, Air Pollution, Vol. II, Editor, A.C. Stern, Academic Press, 1968.
4. M. SHEPHARD, S.M. ROCK, R. HOWARD, J. STORMES, Anal. Chem., 1951, 23, 1431.
5. F.G. ROUNDS, P.A. BENNETT, G.J. NEBEL, J. Air Poll. Control Assoc., 1955, 5, 109.
6. A.J. ANDREATCH, R. FEINLAND, Anal. Chem., 1960, 33, 1021.
7. C. NARRAIN, P.J. MARRON, J.H. GLOVER, Gas Chromatog. Proc. Int. Symp. (Europe) 1972, 9, 1.
8. J.H. SIMMONS, in, Gas Chromatog., Vol. XVII. Editor, S.G. Perry, Applied Science Publishers, 1972.
9. H.M. CHIEF INSPECTOR OF FACTORIES, ANNUAL REPORT, H.M.S.O., London, 1973.
10. H.N.M. STEWART, in, Automatic Air Quality Monitoring Systems, Editor, T. Schneider, Elsevier, 1974.
11. PHILLIPS COMPANY commercial literature.
12. H. SIEVERING, Adv. in Environmtl. Sci. and Technol., 1971, 2, 278.
13. J.W. ROBINSON, J.D. DAKE, Anal.Chim.Acta., 1974, 71, 277.
14. J.W. ROBINSON, Seminar delivered at I.C.S.T., 1975.
15. R.A. SPEARS, J. Brit. Inst. Radio Engnrs., 1946, 6, 50.
16. R.A. SYKES, Proc. Inst. Radio Engnrs., 1948, 36, 4.
17. W. PARRISH, Phillips Techn. Rev., 1950, 12, 166.

18. M. LOSTIS, Thesis presented at Faculty of Science, University of Paris, 1958.
19. idem J. Phys. Rad. 1959, 20, 255.
20. G. SAUERBREY, Z. Fur Physik, 1959, 155, 206.
21. J.C. BRUYERE, J. Phys. Rad., 1960, 21, 222A.
22. A.W. WARNER, C.D. STOCKBRIDGE, Vac. Microbal. Techn., 1962, 2, 71.
23. idem ibid. 1963, 3, 55.
24. I. HALLER, P. WHITE, Rev. Sci. Instr., 1963, 34, 677.
25. C.D. STOCKBRIDGE, Vac. Microbal. Tech., 1966, 5, 193.
26. G.M. KHAN, Rev. Sci. Instr., 1972, 43, 117.
27. P. OBERG, J. LINGENSJO, ibid., 1959, 30, 1053.
28. K.H. BEHRNDT, R.W. LOVE, Vac. Symp. Trans., Pergamon Press, 1960.
29. T.E. HARTMAN, J. Vac. Sci. and Tech., 1965, 2, 239.
30. R.P. RIEGERT, Vac. Microbal. Tech., 1965, 4, 99.
31. A. LANGER, J.T. PATTON, ibid., 1966, 5, 231.
32. S.J. LINS, H.S. KUKUK, Vac. Symp. Trans., Pergamon Press, 1960.
33. H.T. PULKER, Z. Angew. Phy., 1966, 20, 537.
34. D. HILLECKE, R. NIEDERMAYER, Vakuum-Technik, 1965, 14, 69.
35. R. NIEDERMAYER, N. GLADKICH, D. HILLECKE, Vac. Microbal. Tech., 1966, 5, 217.
36. H.L. ESCHBACK, E.W. KRUIDHOF, ibid., 1966, 5, 207.
37. J. EDGECUMBE, J. Vac. Sci. Tech., 1966, 3, 28.
38. A.R. WOLTER, J. Appl. Phys., 1965, 36, 2377.
39. L.J. SLUTSKY, W.H. WADE, J. Chem. Phys., 1962, 36,2688.
40. idem., Vac. Microbal. Tech., 1962, 2, 115.

41. C.D. STOCKBRIDGE, ibid., 1966, 5, 147.

42. idem., ibid., 1966, 5, 175.

43. W.H. WADE, R.C. ALLEN, J. Colloid and Interface Sci., 1968, 27, 722.

44. J.P. MIEURE, Ph.D. Dissertation, Texas A. and M. University, 1968.

45. J.P. MIEURE, J.L. JONES, Talanta, 1969, 16, 149.

46. idem. Anal.Chem., 1969, 41, 484.

47. D. McKEOWN, Rev. Sci. Instr., 1961, 32, 133.

48. R.L. LITTLER, U.S.A. Patent 3, 253, 219.

49. W.F. FISCHER, W.H. KING, Anal. Chem., 1967, 39, 1265.

50. J.D. BONDS, Ph.D. Thesis, University of Alabama, 1969.

51. D. HILLECKE, H. MAYER, Vac. Microbal. Tech., 1970, 7, 135.

52. K.S. VAN DYKE, U.S.A. Patent 2,571,171.

53. idem. ibid 2,536,111.

54. W.H. KING in International Symposium on Humidity and Moisture, Vol. I, Editor, A. Wexler, Washington D.C. 1963.

55. idem. Anal. Chem. 1964, 36, 1735.

56. W.H. KING, C.T. CAMILLI, A.F. FINDEIS, ibid., 1968, 40, 1330.

57. W.H. KING, L.W. CORBETT, ibid., 1969, 41, 580.

58. W.H. KING, U.S.A. Patent 3,164,004.

59. idem. ibid. 3,260,104.

60. idem. ibid. 3,427,864.

61. ESSO RESEARCH AND ENGINEERING CO., British Patent 986,011.

62. idem. ibid. 1,049,742.

63. H.M. CRAWFORD, J.J. HEIGL, W.H. KING, T.J. MESH, Analysis Instrum., 1964, p.105.

64. J.A. WILLIAMSON, D.W. JANZEN, ibid., 1972, 10, 175.

65. W.H. KING, Environmtl. Sci. and Tech., 1970, 4, 1136.

66. idem., Res. Dev., 1969, 20(4), 28.

67. idem., ibid., 1969, 20(5), 28.

68. M.J. HARTIGAN, Ph.D. Thesis, University Rhode Island, 1970.

69. G.G. GUILBAULT, A. LOPEZ-ROMAN, Environmtl. Lettr., 1971, 2, 35.

70. A. LOPEZ-ROMAN, G.G. GUILBAULT, Analyt. Lettr., 1972, 5, 225.

71. M.W. FRECHETTE, J.L. FASCHING, D.M. ROSIE, Anal.Chem., 1973, 45, 1765.

72. K.H. KARMARKAR, B. GUILBAULT, Anal.Chim.Acta. 1974, 71, 419.

73. G. GUILBAULT, Anal.Chim.Acta., 1967, 39, 260.

74. E.P. SCHEIDE, Ph.D. Thesis, Louisiana State University in New Orleans.

75. W.G. CADY, Proc. I.R.E., 1922, 10, 85.

76. E.P. SCHEIDE, G.G. GUILBAULT, Anal.Chem., 1972, 44,1764.

77. W.M. SHACKLEFORD, G.G. GUILBAULT, Anal.Chim.Acta, 1974, 73, 383.

78. G.G. GUILBAULT, A. LOPEZ-ROMAN, S.M. BILLEDEAU, Anal. Chim. Acta, 1972, 58, 421.

79. Q. BRISTOW, J. of Geochem. Expltn., 1972, 1, 55.

80. K.H. KARMARKAR, G.G. GUILBAULT, Anal. Chim. Acta, 1975, 75, 111.

81. P.K. MUELLER, E.L. KOTHNY, Anal. Chem., 1973, 45, 1R.

82. R.L. CHUAN, Joint Conference on Sensing of Environmental Pollutants, California 1971, Preprint AIAA, 71-1099.

83. J.G. OLIN, G.J. SEM, Atmosph. Environ., 1971, 5, 653.

84. J.G. OLIN, G.J. SEM, L. CHRISTENSON, Amer.Ind.Hyg. Ass.J., 1971, 32, 209.

85. J.G. OLIN, Adv. in Instrum., 1971, 26, 558.

86. R.B.W. Earp, Ph.D. Thesis, University of Alabama, 1966.

87. M. JANGHORBANI, Ph.D. Thesis, Oregon State University, 1972.

88. M. JANGHORBANI, H. FREUND, Anal.Chem., 1973, 45, 325.

89. F.W. KARASAK, K.R. GIBBINS, J. Chromat. Sci., 1971,9,535.

90. F.W. KARASAK, J.M. TIERNAY, J. of Chromatog., 1974, 89,31.

91. W.A. MARRISON, Proc. I.R.E., 1929, 17, 1103.

92. F.R. LACK, G.W. WILLARD, I.E. FAIR, B.S.T.J., 1934, 13, 453.

93. W.G. CADY, Piezoelectricity, McGraw Hill, 1946.

94. G. SAUERBREY, Z. Fur Physik, 1964, 178, 457.

95. W.P. MASON, piezoelectric Crystals and their Applications to Ultrasonics. Van Nostrand, 1950.

96. H.J. McSKIMMIN in, Quartz Crystals For Electrical Circuits, Editor R.A. Heising, Van Nostrand, 1947.

97. R.A. SYKES ibid.

98. W.H. LAWSON, J. Sci. Instrum., 1967, 44, 917.

99. LORD R. RAYLEIGH, The Theory of Sound, Revised edition. Dover Publications 1945.

100. D.C. STREET, T.S. WEST, Unpublished work.

101. K.S. VAN DYKE, Phys. Rev., 1925, 25, 895.

102. F. BUTLER, Wireless World, 1965, 71(7), 356.

103. J.M. McKELVEY, H.E. HOELSCHER, Anal. Chem., 1957, 29, 123.

104. J.M.H. FORTUIN, Anal. Chim. Acta, 1956, 15, 521.

105. A.P. ALTSHULLER, I.R. COHEN, Anal.Chem., 1960, 32, 7.

106. G.A. LUGG, Anal. Chem., 1968, 40, 1072.

107. J.A. PRYDE, The Liquid State, Hutchinson University Library, London, 1969.

108. W. FIDDLER, R.C. DOERR, J. Chromatog., 1966, 22, 481.

109. P. COOPER, Poisoning by Drugs and Chemicals, Alchemists Publishers, London 1974.

110. A.B. LITTLEWOOD, Gas Chromatography, Academic Press, 1970.

111. R. KAISER, Gas Phase Chromatography, Vol. III, Butterworths, 1963.

112. CHROMATOGRAPHIC DATA, J. of Chromatog., 1959, 2, B 10.

113. B. SMITH, R. OHLSON, G. LARSON, Acta Chemica Scanda, 1963, 17, 436.

114. P.W. WEST, BUDDHADEV SEN, BHARAT R. SANT, K.L. MALLIK, J.G. SEN GUPTA, J. of Chromatog., 1961, 6, 220.

115. I. BROWN, I.L. CHAPMAN, G.J. NICHOLSON, Aust. J. Chem., 1968, 21, 1125.

116. H.W. GERARDE in Industrial Hygiene and Toxicology, Vol. II, Editor, Patty, F.A., Interscience Publishers 1967.

117. V.K. ROWE, WOLFE, M.A., ibid.

118. D.D. IRISH, ibid.

119. J.W. RICHARDS, Introduction to Industrial Sterilization, Academic Press 1968.

120. N. OSTOJIK, Anal. Chem., 1974, 46, 1653.

121. B. NOBLE, Applied Linear Algebra, Prentice Hall 1969.

122. E.M. KENNARD, Kinetic Theory of Gases, McGraw Hill 1938.

123. J.B. PARTINGTON, Physical Chemistry, Vol. I, Longmans 1949.

124. A. O'KEEFE, 16th. National Symposium, Anal. Instr. Div. of Instr. Soc. of Amer., Pittsburgh 1970, Vol. 8.

125. T.S. WEST, Lab. Pract., 1971, 20, 71.

126. G.H. BROWN, Anal. Chem., 1969, 41, 26A.